OPTIMAL DESIGN AND OPERATION OF DIESEL COGENERATION SYSTEMS

by

John Holmes, MA

June, 1980

A thesis submitted for the degree of Doctor of Philosophy of the University of London and for the Diploma of Membership of the Imperial College

Mechanical Engineering Department,
Imperial College,
London, S.W.7.

ABSTRACT

Cogeneration of heat and power in diesel engines converts a high fraction of fuel input energy to electricity, gives high overall energy recovery, and therefore a high value added to the fuel. However the diesel engine has traditionally been designed only as a power unit: in this thesis the design parameters of engine and heat recovery equipment have been re-examined further with the aim of optimising performance for cogeneration.

Most diesel cogeneration schemes are presently constrained to meet the local power demand; removal of this constraint could significantly improve scheme economics, but requires that electricity be traded at a 'fair' price. The proper valuation of CHP electricity and the consequent optimisation of scheme operation is developed here. Maximum benefit from diesel cogeneration may be derived from this optimisation of both design and operation.

Computer simulations of both engine and waste heat boiler were developed and used to investigate a number of options for improving exhaust heat recovery. Heat recovery from the engine cooling circuits was also studied. Reduction of valve overlap and higher pressure drops across the waste heat boiler were found significantly to increase exhaust heat recovery: the necessary design changes and their value are discussed.

The 'fair' price for CHP electricity is shown to be the electricity supply industry's marginal generating costs. These costs were calculated by a probabilistic simulation model, and together with models developed to simulate site operation, and methods for calculating displaced capacity, used to evaluate the economics of diesel cogeneration at two sites. The economic returns on diesel cogeneration are found to be strongly dependent on the rate of increase of the oil to coal price ratio.

The potential contribution of diesel cogeneration is therefore limited by the depletion of oil reserves rather than the availability of suitable sites.

ACKNOWLEDGEMENTS

I should first like to thank my supervisor, Dr. Nigel Lucas, for his advice and the enthusiasm he has shown throughout the project.

The work would not have been possible without the co-operation of the diesel and boiler manufacturers who provided much needed information. Many thanks are due to them, and in particular to Mr. Don Sinha of Ruston Diesels for his help and interest in the project.

I am also grateful to Professor Murgatroyd and Dr. Niel Watson for their advice, and to Tony Rockingham for his participation in the system analysis work.

The Science Research Council are to be thanked for their financial support during my three years at Imperial College.

Thanks also to my family and friends for their encouragement during the sometimes arduous hours of study, and finally to Jane Robinson who typed the thesis despite the standard of my handwriting.

CONTENTS

LIST OF FIGURES

LIST OF TABLES

CHAPTER 7

7.1 Total Industrial Heat Base for CHP in 1976

7.2 Costs and Characteristics of CHP Prime Movers

CHAPTER 1

INTRODUCTION

Cogeneration is the complementary generation of heat and power. The term combined heat and power, abbreviated CHP, will be used synonymously. The method of cogeneration considered is that in which the prime mover produces electricity, and rejects heat for process or space heating. This is sometimes referred to as a 'topping' cycle, as distinct from a 'bottoming' cycle, in which waste heat from another process is used to generate electricity.

By maximising the conversion of heat energy to work in thermodynamic cycles, modern central power stations may generate electricity at up to 40% efficiency, but in so doing reject the remaining 60% as heat at too low a temperature to be of significant use. Cogeneration, by meeting needs for both heat and power, can convert around 80% of fuel energy input to useful energy.

This introductory chapter gives some background information, firstly on the energy situation and secondly, more specifically on CHP. It then identifies the need for the research, and describes the format of the thesis.

1.1 THE ENERGY SITUATION

The 20th century has seen a very rapid rise in the rate of energy demand in industrialised countries. A wide range of forecasts and scenarios of future energy demand exists. Many 'conventional' forecasts assume a continuation of economic growth and with it, rising energy consumption, typically in the UK at a growth rate around 1-3% per annum (eg. Ref.21). The scenario of Leach (Ref.50) postulates economic growth with steady energy consumption in the UK. More extreme scenarios question the need for continued economic growth in the industrialised world, and can show falling rates of energy demand.

Readily available supplies of fossil fuels; initially of coal and more recently of oil, have permitted this rapid increase in consumption. Fossil fuel resources are however finite: in the UK indigenous supplies of oil and gas are likely to be on the decline at the turn of the century, supplies of coal will last somewhat longer. Energy supply replacements are generally considered to be nuclear power and the renewable energy sources. These are capital intensive technologies whose rate of introduction is limited. The result in many of the conventional energy growth scenarios is a conceptual 'gap' between supply and demand.

Energy conservation, as a moderator of demand, has therefore recently assumed increasing importance in all future scenarios, although there is again a wide range of opinion on the possible

savings and the vigour with which it should be pursued. Cogeneration saves fuel and hence there is considerable interest in its potential as an integral part of energy conservation programmes. Recent UK reports on energy conservation (Refs. 65 and 12), and the 1978 Green Paper, 'Energy Policy' (Ref.21), have all mentioned cogeneration in this context.

1.2 THE COGENERATION SITUATION

Two types of cogeneration may be identified: that associated with a district heating load, district heating/CHP, and that serving an industrial process or space heating load, industrial cogeneration. The dividing line between them is indistinct, as for example in the heating of industrial or commercial offices, but is generally the difference between a local, concentrated heat requirement in industry, and a more dispersed heat load for district heating.

At present around 15-20% of the UK's industrial electricity requirement is self-generated: of this, 70% is in CHP schemes having an average heat to power ratio of 7.7:1 (Refs. 17,27). Figures for European countries, compiled from another source (Ref.37), show industrial self-generation as a percentage of total national electricity generation in 1975 to be almost the lowest in the UK at approximately 8%, and ranging up to 20.8% in West Germany, 71.4% in Luxembourg. The ratio of private to total electricity generation in the UK has declined steadily over the last 20 years,

although the absolute quantity of industrially generated electricity has increased (Ref.5). This decline in the percentage contribution of industrial self-generation (and by inference, industrial CHP) is paralleled in the US where as a fraction of the total US electricity consumption it has declined from 22% in 1920 to 4% in 1976 (Ref.92).

A survey of industrial cogeneration schemes contemplated or implemented in the UK in the past shows one fairly common trait: that interaction with the grid is reduced to a minimum. The electricity supply industry operates almost no schemes in the UK. Only rarely is electricity exported from the private schemes, and hence the heat and power requirements of industry have usually resulted in the high heat to power ratio steam or gas turbines being chosen. The constraint of meeting both the local heat and power demands is frequently cited as being a severe impedement to the economics of industrial cogeneration.

District heating/CHP is widely used in the communist countries of Eastern Europe (Ref.26). Denmark and Sweden are two countries of Western Europe notable for their use of district heating/CHP, other countries have smaller but not insignificant amounts, but there is very little in the UK. Low density dwelling patterns in the US are less suitable for district heating/CHP but renewed interest is now being shown in district heating for city centres.

The situation in the UK is therefore that heat and power demands are generally met separately. Electricity is generated in large power stations, usually situated conveniently for their fuel source, remote from the load. Fuel is burnt locally to meet individual heat

demands. It is interesting to examine the factors whereby this situation may have arisen.

In the UK a monopolistic electricity supply industry (ESI) has been set up to rationalise the supply of electricity, and whose purpose is to provide the Nation with electricity cheaply and reliably. The ESI has essentially approached this objective by developing larger, more efficient power stations (the economies of scale), and by constructing a national grid by which the operational advantages of diverse supply and demand can be gained. The trend then has been to larger, remotely sited plants with lower manning levels, and centrally planned expansion programmes and system operation. To adopt cogeneration, particularly based on industrial heat loads but also for district heating, would reverse these trends: plant would be smaller, sited on heat loads and might require higher manning levels. System expansion planning would be subject to further local influences and constraints, and system operation would be complicated by the requirement to meet the additional non-electrical loads.

Therefore although the ESI in the UK has the statutory duty to investigate methods of using 'waste' heat from electricity generation, it is not entirely surprising that they have avoided any significant involvement with CHP. The marketing of CHP heat, a peripheral duty, would involve a disproportionate amount of management effort from the view of the ESI's main concern.

In a period of falling real price of electricity and increasing reliability and quality of the public supply, the decline in privately cogenerated electricity could be expected. The extent to which private electricity generation has been discouraged by the ESI as policy is the subject of some debate (eg. Ref.54). The situation

in other countries is rather different as already explained. The local economic and institutional conditions that have determined these differences are discussed in refs. 17,54,51.

It is important at this stage to consider whether events may have changed the situation for CHP. Fossil fuel prices and hence the cost of electricity generated from fossil fuels have risen sharply in real terms since the large oil price rises of 1973, discontinuing the previous trend of decreasing real prices. The capital/fuel cost ratio of energy produced from fossil fuels that is so important in capital investment decisions has therefore generally decreased, and is likely to continue to do so in future.

It is feasible that the balance on CHP investment decisions in the private sector has changed, or will soon do so. The utilities may be spurred to reconsider the path of economy of scale and power station siting policies, and to consider the effort of CHP and the marketing of heat worthwhile. This incentive will be reinforced by the diseconomics of scale, for example high outage rates and long construction times, that are becoming apparent. Governments faced with absolute shortages of energy or crippling balance of payments problems to purchase it, may feel justified in distorting industrial investment decisions in favour of energy conservation, or in widening the formal objectives of the utilities to include the marketing of heat.

As a result of the 'energy crisis' of 1973 and the recognition of the need to conserve finite fossil fuel resources, much attention has recently been given to CHP. In particular three reports have resulted in the UK: Kendall (Ref.47), Fells (Ref.5), and the combined

heat and power group under the chairmanship of Dr. W. Marshall (Refs. 19,17). Kendall concentrates on industrial cogeneration, surveying industrialists' decision making processes on cogeneration, and concludes that under industrialists' perceptions of present economic and institutional conditions, industrially owned cogeneration is unlikely to make much impact. The report of Fells, et al also concentrates on industrial cogeneration, and while presenting some interesting studies on the interaction between privately owned schemes and the electricity supply industry, does not attempt any comprehensive analysis of the potential for CHP.

Probably the most influential report is that of the combined heat and power group, representing as it does, the findings of a distinguished group acting under the auspices of the Department of Energy. The emphasis is on district heating/CHP and despite low economic returns at present day prices, it is recommended that long lead times and the need to preserve a future option justify the initiation of a large, subsidised demonstration CHP/district heating scheme. They conclude that most of the industrial heat load suitable for CHP is already supplied in this way. Thinking on the type of prime mover and integration with the grid is inconsistent: while praising the merits of a scheme having a high electrical generating efficiency and being fully integrated with the grid, examples presented assume the need to meet locally the heat and power demands and use high heat to power ratio prime movers. A lack of suitable sites and the high rates of return required by industrialists are held to severely limit the potential for industrial cogeneration, although a cautious recommendation is made for industrialists' investment decisions to be distorted more into line with the nationalised energy supply industries'

investment criteria.

1.3 THE NEED FOR RESEARCH

Steam cycles for conventional electricity generation have been highly optimised, resulting in the high present day design generating efficiencies. On the other hand the items of plant constituting a cogeneration scheme, particularly the prime-movers, are usually designed separately and for purposes other than cogeneration. It is therefore likely that there is potential for design modification to cogeneration plant, to optimise the cogeneration system.

The ratio of values of power to heat is usually around 2 or 3 to 1. The 'best practice' for separate production of heat and power gives efficiencies around 80% for heat and 40% for power. Therefore to maximise both the value added to the fuel and the energy saved, a cogeneration technology must not only have high overall rates of energy recovery from the fuel input, but also convert a high proportion to electricity.

The diesel engine is a developed and readily available technology having a high electrical generating efficiency, and giving up to 80% energy recovery in cogeneration schemes. The diesel engine has traditionally been designed as a power only unit, not as a cogeneration prime-mover. An opportunity was therefore perceived for the re-examination of the design parameters of engine and heat recovery

equipment, to optimise the design of the diesel cogeneration system.

High electrical generating efficiencies in cogeneration schemes may frequently result in more electricity being produced than can be consumed locally. Electricity is more readily transportable over long distances than heat, and so whereas demands for heat must be met locally, electricity production need not be so constrained. The existence of a national distribution network for electricity in the UK means that in principle advantage may be taken of the diversity of electrical loads.

This added degree of freedom for cogeneration operation, not frequently used in the past, requires that a value be attached to the exported electricity. Discussion of the value to all parties of independent or utility CHP when connected to the grid, has had little theoretical foundation. A method of valuation of CHP electricity and capacity to the interested parties is therefore needed. In this way the optimal operation of cogeneration schemes may be determined. The resulting cogeneration economics may then be compared to other electricity supply options, and cogeneration potential assessed.

The higher physical concentration of heat loads in industry, gives reduced costs for heat distribution over those for district heating. District heating/CHP costs are strongly dependent on the heat load density, and so any domestic conservation measures will be unfavourable to district heating economics. Heat distribution networks already exist in industry, and conservation measures if planned in conjunction with cogeneration design should have small but perhaps even beneficial effects on industrial CHP economics. The association

of process and space heating loads will in many cases give higher annual load factors for industrial cogeneration than district heating/CHP.

These advantages of the industrial heat load over the district heating load, were felt to make it the more favourable option, and this thesis therefore concentrates on industrial cogeneration. The design considerations for diesel cogeneration and the method of analysis of operational value, will however also be applicable to district heating/CHP. The study concentrates on the UK situation, but many of the analyses will be applicable elsewhere. Although interest in CHP arises out of its conservation of energy, economic returns are used as the measure of benefit. Value is allocated over time by discounted cash flow methods.

1.4 THESIS FORMAT

The thesis is divided into eight chapters in all: 2 to 4 are broadly concerned with system design, 5 to 7 with operation, the first is the introduction, the last, the conclusion. Chapter 2 gives some engine development history, and describes the engine and boiler models developed for the study. Chapter 3 then presents the design modifications considered for cogeneration and some limiting criteria on engine alterations. Chapter 4 concludes the first part of the work by presenting the results and conclusions on design modification. The study on cogeneration operation commences with chapter 5: a description of the valuation methods for the electricity

and capacity of the marginal CHP scheme. Chapter 6 then presents industrial case studies, some incorporating the design modifications of chapter 4, of the operation of diesel cogeneration schemes, using the methods of analysis given in chapter 5. In chapter 7 the results and conclusions of the previous chapters are drawn together with information on the industrial heat load, to give some indication of diesel CHP potential.

The sequence of the chapters is therefore such that the perspective of the study opens out from the detail of design modification of the scheme components, to the broader considerations of the operation of the scheme, and finally to the possible role of diesel CHP schemes in the UK energy supply system as a whole.

In addition to the main chapters there are 5 appendices. More detailed theory of the models and their descriptions are given in appendices 1 to 4, in order not to obscure the development of the analysis in the main text. Certain symbols find common use throughout the main text and hence a list of these together with a list of abbreviations used are given in appendix 5. Other symbols are just used locally and hence are defined in the text as they occur. Figures and tables for each chapter are presented at appropriate points in the text. Systeme Internationale units, or close approximations thereto, are used throughout.

CHAPTER 2

DESIGN METHODS AND DEVELOPMENT TRENDS

2.1 INTRODUCTION

Chapter 2 serves as an introduction to the more detailed design optimisation of diesel cogeneration systems presented in chapters 3 and 4. The past development trends and philosophies are reviewed, and the present and possible future development paths surveyed. The reasons for the choice of engine and boiler types studied in the succeeding two chapters are then presented. The methods of analysis of engine and waste heat boiler are described here, and in more detail in appendices 1 and 2.

2.2 ENGINE DEVELOPMENT HISTORY

The modern diesel engine is the result of over 50 years of research and development: figure 2.1 shows the development trends (represented by some important parameters) over the last 30 years (Ref.44). The increasing pace of progress over the past 15 years, evident from this figure, has been facilitated by the adoption of

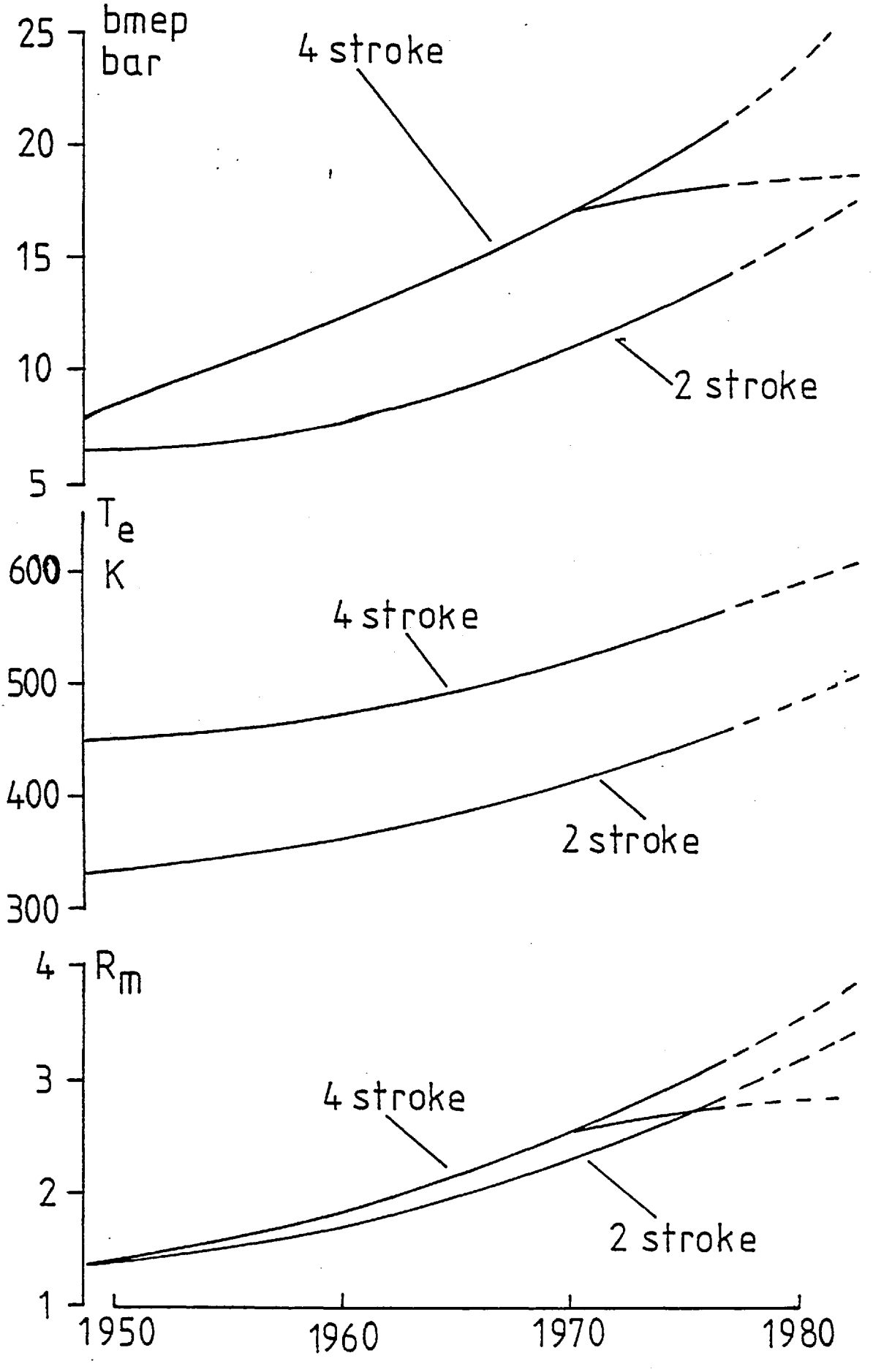

Fig. 2.1 Diesel Engine Development Trends 1950-1980 (Ref. 44)

more sophisticated development techniques, and in particular by the advent of the computer in the early 1960's.

In the context of this thesis it is important to realise that the diesel engine has been developed exclusively as a power producing unit, i.e. to produce motive power as cheaply and reliably as possible. Hence to the engine designer the enthalpy of the exhaust gas and engine cooling circuits is implicitly regarded as having no value, other than to enhance the power producing capability of the engine, for example by turbocharging. When heat is recovered it is regarded as 'an additional bonus'.

The main aims of development have been to reduce the capital cost per kW of maximum power output, to increase the brake efficiency, and to improve reliability on a wide range of fuels.

Reduction in specific capital cost has been achieved by increasing the output from a given size of engine. This may be done by increases to speed or brake mean effective pressure (abbreviated bmep). The potential for increasing engine speed is limited by the inertia of the reciprocating parts, and decreases in combustion and brake efficiency. Hence the increase in speed over the last 20 years has not been great. Most of the increase in specific output has come from increases in bmep, which have largely resulted from the application of turbocharging to the engine. The introduction of turbocharging gave rapid increases in bmep, and for example between 1950 and 1960 the real specific cost of engines dropped by 26%; the specific volume and weight were reduced by 20-40% and 40-50% respectively, during the same period (Ref.70).

Significant increases in brake efficiency came with turbo-charging, but the efficiency is now reaching a peak, and may actually decline at higher bmep's (figure 2.2, ref.70). Engine reliability has also improved, and the range of acceptable fuels widened.

The thermal and mechanical limits of the 4-stroke engine have not yet been reached, but those of its single stage turbocharger have. This has led to the recent divergence in development trends shown in figure 2.1. Some manufacturers have gone for increased reliability using normal turbochargers, others have used two stage or high pressure ratio single stage turbochargers to achieve higher bmep's and hence still lower specific weight, volume and, possibly, cost. 2-stroke engines are less highly rated than 4-strokes, and limitations have not yet been reached on turbochargers.

2.3 PRESENT DAY DIESEL TECHNOLOGY

It is informative to see where the development paths have led at the present. Tables 2.1 and 2.2 have therefore been included to show the type of engines available in the late 1970's, and some of their important design parameters.

Table 2.1 shows the results of a comprehensive survey (Ref.22) of diesel engines sold by manufacturers from the non-communist sector for power generation, in the year ending May 1978 and in the 10 years

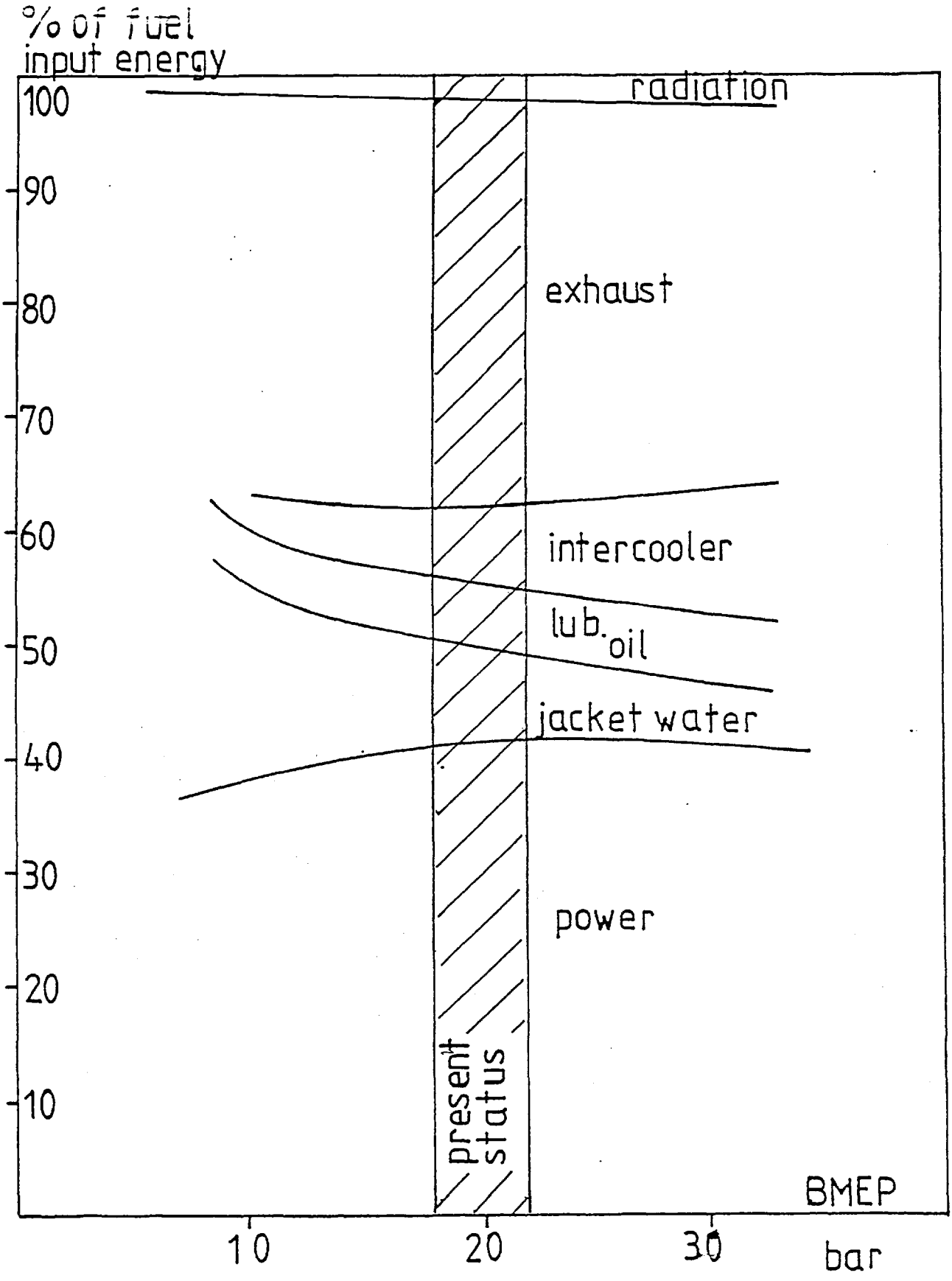

Fig. 2.2 Heat Balance: Medium Speed 4-stroke Engines (Ref. 70)

TABLE 2.1

Diesel Engine New Orders June 1977 - May 1978

Range MW	Number	%	%			%		
			Standby	Peaking	Continuous	Diesel	HFO	Dual
1-2	572	56.6	24.3	6.1	69.6	87.4	11.4	1.2
2-3.5	232	23.0	40.5	4.3	55.2	81.9	15.5	2.6
3.5-5	61	6.1	23.0	11.5	65.5	67.2	31.1	1.7
5-7.5	54	5.4	20.4	13.0	66.6	63.0	37.0	
7.5-10	48	4.8	41.7		58.3	83.3	14.6	2.1
10-15	25	2.5			100.0	56.0	44.0	
15-20	12	1.2			100.0		100.0	
20-30								
30-60	4	0.4	50.0	25.0	25.0	100.0		
Totals	1008		27.8	6.0	66.2	81.6	16.9	1.5

Installed or ordered 10 years prior to 1977 spring 1MW

	Number	%		Diesel	HFO	Dual
1-2	1772	35.9		84.4	12.5	3.1
2-3.5	1799	36.5		81.8	15.0	3.2
3.5-5	481	9.7		50.1	39.9	10.0
5-7.5	619	12.5		33.1	58.5	8.4
7.5-10	159	3.2		42.1	57.2	0.7
10-15	83	1.7		33.7	66.3	
15-20	21	0.5		19.0	81.0	
20-30						
30-60						
Totals	4934			71.2	24.5	4.3

TABLE 2.2

Survey of Medium Speed 4-Stroke Engines: Some Important Parameters

Manufacturers Name	Allen		MAN	Mirrlees	Mitsui	Ruston		Semt-Pielstick		Sulzer		
Engine Name	S-12	S-37&370	52/55	K-Major	42M	RKC	AT350	PA	PC	A	Z40/48	65/65
1. Output Range (MW)	0.3-2	1-3	4.5-13.4	1.1-8	3.35-10	1-2.8	2.1-6.5	0.5-4.4	2.9-20	0.62-3.6	3-9.9	8-15.9
2. Speed (rpm)	750	600	430	500/600	530	750/1000	600	900-1500	375-514	1000	500-600	400
3. Pulse/constant pressure turbo charging	Pulse	Pulse	Pulse		Pulse	Pulse	Pulse			Pulse	Pulse	Constant Pressure
4. Boost Pressure Ratio at full load			2.5 bar	2.4	2.8	2.7	3	2.3-2.5		2.7	2.8-3.1	3.1
5. bmep (bar)	12.6	12-15	17.9	17	20.4	19.7 at 750 rpm	20.4	16.8-17.6	19.7-21.3	16.3	20	18.4
6. T_e full T_o load			500°C 370°C	426°C	550 360	540	480 370	430-480	400-425	530	530-550	490
7. η_b full load	0.40	0.41	0.42	0.41	0.42	0.40	0.40	0.37-0.39	0.41	0.40	0.42-0.43	0.41
8. Fuel viscosity limit (SRI)	1500	1500	3500	3500	3500	1500 at 750 rpm	3500	1500	3500	1000	3500	3500
9. Weight/power ratio (Kg/kW)	16-20	16-17	11.4-12.2	14-26					9.4-12			
10. Valve overlap °CA	>120°	120°		120°		140	168					

previous to May 1977. No attempt is made to categorise the engines as 2 or 4-strokes, but it does show the size distribution to be heavily weighted in numbers to the 1-3.5 MW range. A large proportion (around 66%) are used for continuous generation, and the percentage burning heavy fuel oils (abbreviated HFO) increases with size.

Many of the major European engine manufacturers were contacted at the commencement of this project to obtain information on their product ranges. Table 2.2 shows the result of this survey, together with information on one Japanese manufacturer (Mitsui). The table is limited to medium speed (400-1000 rpm), 4-stroke engines, as the study will concentrate on this type, for reasons explained more fully in section 2.5. Of particular note is the narrow range of boost pressure ratio, exhaust temperatures and brake efficiencies at full load, and the long valve overlap periods. This uniformity will be important in generalising the conclusions drawn about the particular engines studied.

2.4 POSSIBILITIES FOR FUTURE DEVELOPMENTS

It is worth first reviewing the present situation in engine development:

1. The engine brake efficiency has settled at a peak of around 0.4-0.42 (table 2), and the medium term ($\lesssim$10 years) prospects for substantial improvements are not good. Longer term ($\gtrsim$10 years)

the 'adiabatic' engine, in which the cylinder is not cooled, may have significantly higher brake efficiency.

2. The divergence in trends of boost pressure shown in figure 2.1 is an indication that the reduction in specific engine cost by higher turbocharging levels has reached a limit imposed by turbo-charger technology, and that the economics of going to higher boost levels may be marginal.

The future for diesel engine manufacturers in a period of declining oil resources is uncertain. It is realistic to assume however that the price of fuel will rise relative to the capital cost of the engine. Traditional markets, for example the marine market, have recently contracted, and as a result manufacturers are exploring new fields, of which one is CHP.

Past trends in development, have reached a period of diminishing returns; new markets are being sought for output. An example will now serve to show the potential economic benefit of a re-optimisation of diesel engines for CHP applications.

A design change is considered which increases the heat recoverable from the engine by 5% of the fuel input energy, at little increased capital cost. At a load factor of 0.75, a brake efficiency of 40% and a heat value of 0.64 p/kWh (corresponding to a 1979 HFO cost of £60/tonne burnt at 80% efficiency), this extra heat is worth £5.25 per installed kW per year. Between 1950 and 1960, by intensive development, the real capital cost per kW was reduced by 26%, corresponding to a reduction in the annual charge on a £100/kW engine, at 10% discount rate over a 20 year life, by £3.1/kW.

The benefit of the increased heat recovery is therefore comparable to the reduction in capital charges resulting from 10 years of development. If a straightforward method for enhancing the heat recovery can be found, the economics of the diesel engine as a CHP prime mover could be improved very quickly relative to its economics as a power only generator. The incentive for the study is therefore evident, but before proceeding to the presentation of results, the reasons for the choice of engine type and the methodology adopted must be given.

2.5 THE CHOICE OF ENGINE TYPE

Three diesel engine types might be considered for diesel cogeneration: slow or medium speed 2-stroke, medium speed 4-stroke, and dual fuel engines. High speed engines are not suitable for continuous duties.

2-stroke engines are at a disadvantage with respect to 4-stroke engines for the following reasons:

1. Figure 2.1 shows that the bmep of the 2-stroke engine is less than that of the 4-stroke, resulting in a higher specific cost for the 2-stroke engine. The price of the 2-stroke may be as much as 50% higher than the 4-stroke (Ref.2).

2. The cost of civil works forms a significant fraction of a CHP system: civil works for the more massive 2-strokes may be 60% higher than those for the 4-stroke (Ref.2).

3. The alternator required for the slow speed 2-stroke engine is more expensive than that for the 4-stroke.

4. The advantage that the 2-stroke used to possess in being able to burn poorer quality fuel has been eroded by developments to the 4-stroke engine.

5. A smaller fraction of the exhaust heat may be recovered from the lower temperature exhaust gases of the 2-stroke (Fig. 2.1). The low exhaust temperatures result from the high excess air ratios necessary for the operation of the 2-stroke cycle.

2-stroke engines will therefore not be specifically considered further. However some of the conclusions pertaining to the 4-stroke engines will be applicable to the 2-strokes. The comparison with dual fuel engines is not as clear, the economic balance being determined by the relative prices of gas and oil.

Figure 2.3 shows the performance of the Mirrlees K-Major 4-stroke engine in normal and dual fuel forms. The dual fuel engine has the disadvantage of higher capital costs as it is less highly rated, but the advantages of lower maintenance and lubricating oil costs, and a higher rate of heat recovery from the sulphur free exhaust (when burning natural gas) which may be cooled to 120°C. Low temperature corrosion problems normally limit stack temperatures to 200°C on HFO burning engines. Total generating costs for a range of fuel prices were calculated, assuming a load factor of 0.75, a discount rate of 10% and a life of 20 years, and including maintenance and lubricating oil costs. The results are presented in figure 2.4 for the dual fuel engine with the exhaust cooled to 120°C and 200°C, and for the oil burning engine.

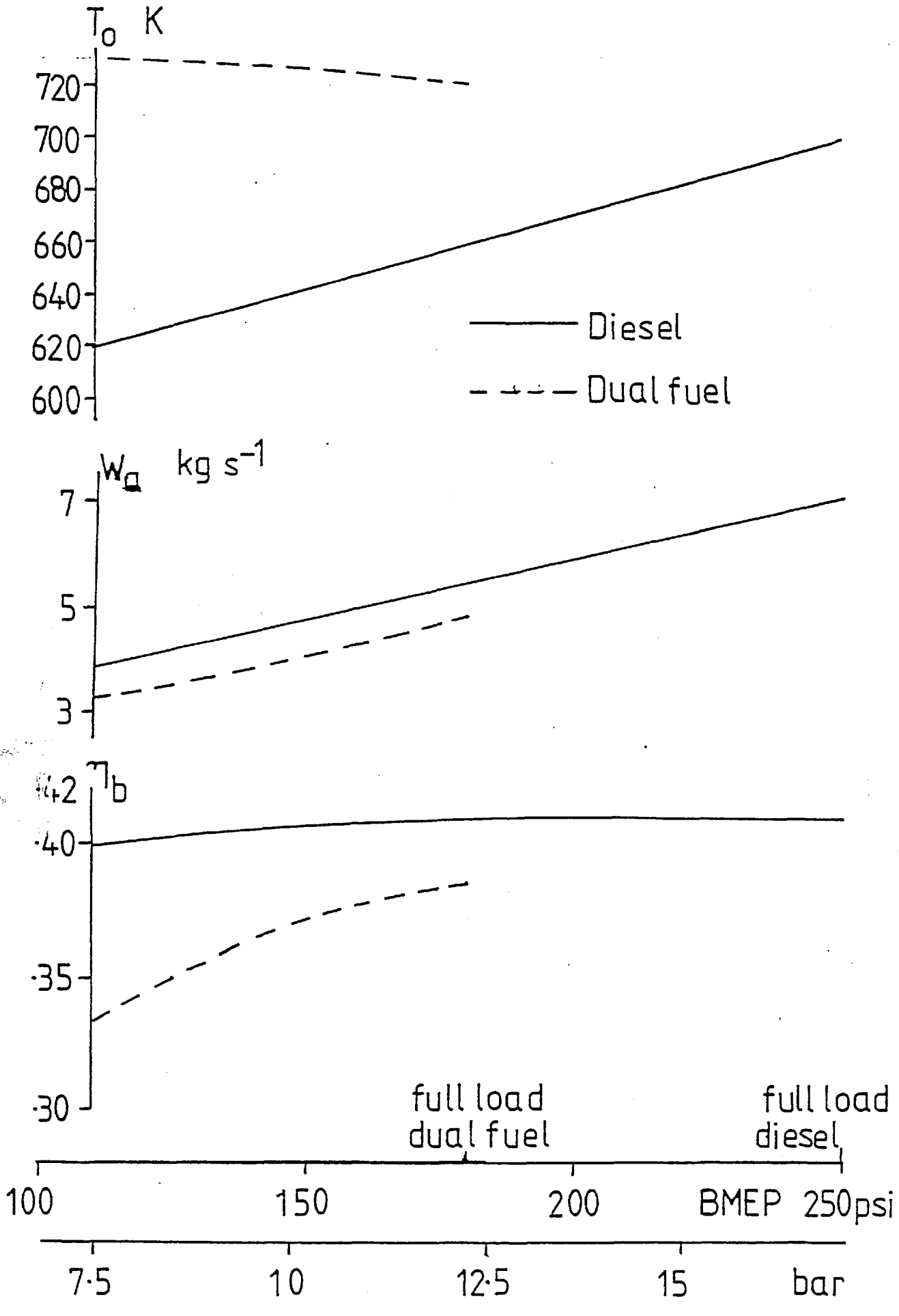

Fig. 2.3 Performance Parameters : Mirrlees K-Major

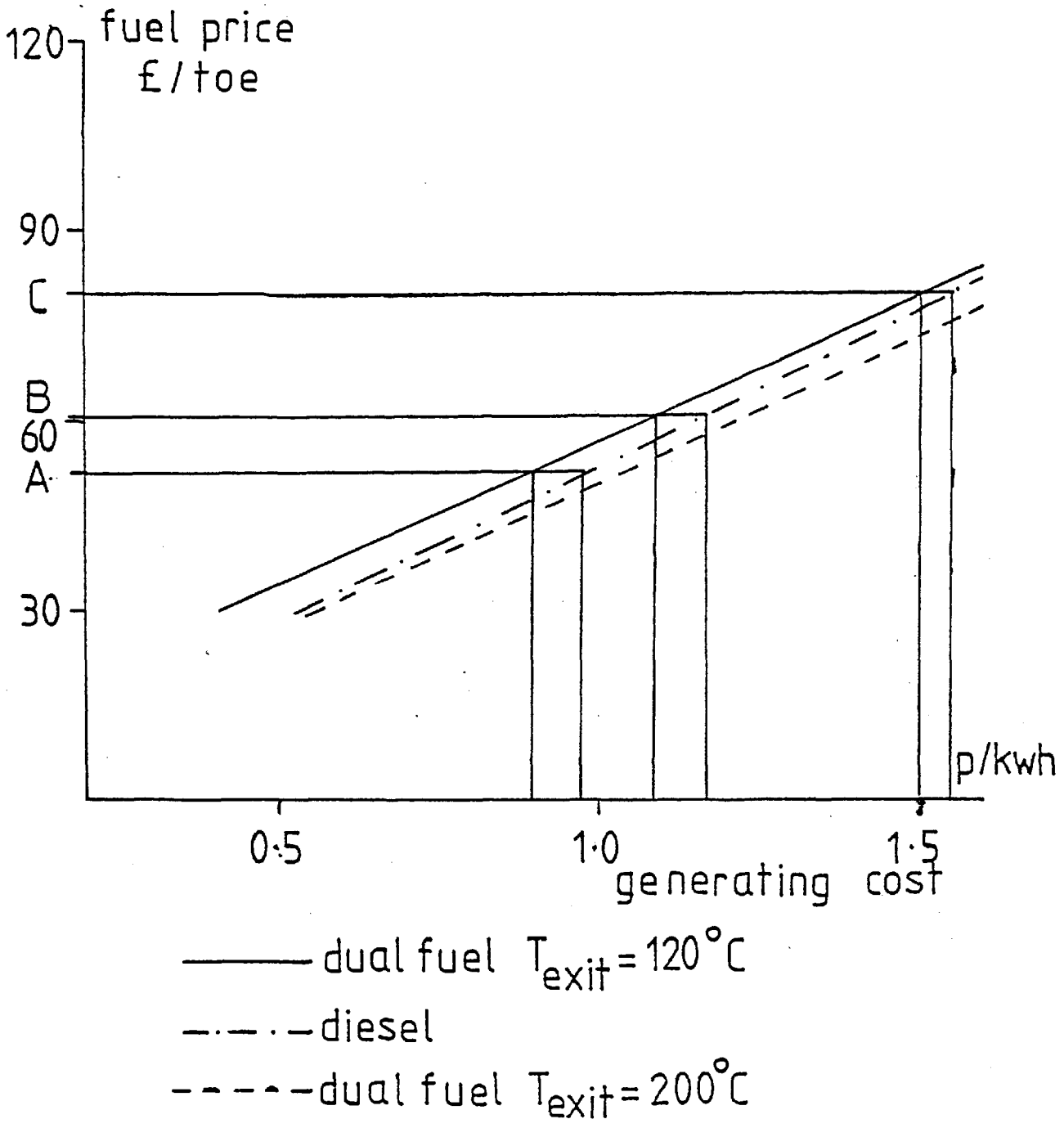

Fig. 2.4 Dual Fuel /HFO Generating Cost Comparisons

If gas were to be sold at the heavy fuel oil (HFO) price (A), the dual fuel engine with its exhaust temperature reduced to 120°C has the advantage. However the situation is reversed when the gas is sold at the average price for new gas supply contracts (B), and even more so if the gas is at the gas-oil price (C), as is likely to be the case with the British Gas marketing policy. The heavy fuel oil burning engine is therefore on the whole the better option and is the engine studied in depth in the following 2 chapters. The special problems that burning HFO incurs will be treated in depth in chapter 3.

2.6 THE APPROACH ADOPTED

The process of engine improvement is a continuous one, improvements being made to the existing technology, using the experience gained from past development. The approach then has not been to design a cogeneration engine from first principles, but to look for improvements to present day engines. Wherever possible simple design modifications have been sought.

Engine reliability is regarded as an important factor, influencing both the economics and acceptability of schemes. Emphasis is therefore placed on maintaining this reliability. Similarly environmental acceptability, for example the condition of the exhaust and the noise generated by the scheme, is assumed to be necessary.

As yet nothing has been said about the method of analysis employed in these studies. The condition of the gases in the volumes of the engine undergoes rapid changes over the course of the diesel cycle. The thermodynamic link with the turbocharger is also of critical importance. Any change to one engine operating parameter will affect other parameters in a way that is not easily determined. The thermodynamic equations governing these inter-relationships cannot be solved analytically, and hence the results of design change must be found by experiment or by computer simulation.

The high cost of engine testing has meant that it is now only used at the final stage, after extensive computer studies have been carried out. An aim of this project was to develop a model of a diesel cogeneration system, suited to the requirements of the study. As such it consumed a significant portion of the research efforts; the development of the engine model is therefore described in more detail in the next section.

2.7 DIESEL ENGINE SIMULATION

2.7.1 Background

Diesel engine analysis was first programmed for computers in the 1950's. Since then the scope, complexity and utility of diesel engine simulations has grown with the development of the computer.

Initial attempts just transferred the existing simple cycle and graphical techniques to the computer, so saving some manual labour, but not significantly advancing the thermodynamic analysis of the engine. More sophisticated models appeared in the early 1960's (eg. Ref.91), in the form of step-by-step models of diesel cycles, in which the engine cycle is analysed by splitting it into a large number of small steps.

By the mid-1960's diesel simulation was well established, as the proceedings of the conference of Ref. 42 indicate. The step-by-step models predominate for the cycle analysis, some covering just the closed cycle (the in-cylinder processes), others the open cycle (the gas exchange process), a further set covering both. There are also programs dealing with specific aspects of engine design such as thermal and mechanical loading, combustion and heat transfer.

More recently programs to predict the performance of more complex engine-turbocharger arrangements, eg. 2-stage turbocharging (Ref.3), and transient performance (Refs. 89,33,7), have been written. In some cases moving away from step-by-step calculations and reverting to matching procedures using experimental or simple cycle data (Refs. 3,33,7).

2.7.2 The Advantages of Simulation

The various types of cycle analysis programs have proved to be of great value in diesel research and development. This statement is supported by the wide use of simulation techniques, both by engine manufacturers and in research institutions.

The advantages of systematic simulation studies over the traditional methods of experiment plus intuition may be enumerated as follows:

1. A program can give a better understanding of the effects of particular variables on engine performance it being sometimes difficult to isolate the effects of a change to just one parameter on the test bed.

2. Design parameters can be optimised before the engine is built, and hence the number of tests needed is greatly reduced, resulting in substantial financial savings.

3. More accurate knowledge of the thermodynamic processes obtained from simulation leads to a better interpretation of test results.

4. The range of parameters that it is financially feasible to investigate is extended.

5. Enables studies to be made where experimental facilities are not available (as with this project).

The computer programs do not completely eliminate the need for testing: before a new design is used commercially, final testing will always take place. The wide variety of simulation techniques has been emphasised. It is important to adopt the one most suited to the needs of the project.

2.7.3 Classification

Before classifying the program types that might be considered, some of the requirements on the program will be stated. Parameters

influencing the possible heat recovery include the valve timings, the level of turbocharging and the interaction with the waste heat boiler. The results of changes to these parameters must therefore be simulated. Table 2.2 reveals that most modern 4-stroke engines use the pulse turbocharging method, i.e. the exhaust blowdown energy is utilised to drive the turbine, and hence to be realistic the program must treat time varying pressure in the exhaust manifold. It is not required to look at transient performance, and hence steady state conditions will suffice.

Simulation methods are broadly classified into three groups according to their level of complexity: a procedure suggested by Freeman and Walsham (Ref.29).

1. Simple Matching Techniques

Good examples are those given in references 85 and 86. Performance maps for engine, compressor and turbine are formulated in terms of a set of operating variables. A stable operating point of the unit is then found by balancing mass flows and turbocharger power. Operating values being found by interpolation within data arrays. Data for turbine and compressor are experimental. Data for the engine may be generated by some sort of simple cycle calculation, or from experiment. Exhaust and inlet manifold pressures are cycle averaged, valve timings not specifically included.

The simplified techniques therefore attempt to make use of available experimental data; if this is not available they must resort to simple cycle calculations. The more experimental data is available, the more accurate these techniques may be, but in general

they can only give a 'first-order' answer. Their advantages are that little input data is needed, the demands on computing resources are small, and that they are fast and easy to use. Their principle faults are as follows:

1. The averaged exhaust pressures and temperatures do not give an accurate prediction of turbine energy. An experimentally determined 'apparent pulse turbine efficiency factor' must be introduced, which will vary with load and pulse shape. The calculation of airflows must also be approximate.

2. Valve timings and effective flow areas for the gas exchanges are not included. Flows are calculated from arbitrarily defined discharge coefficients and averaged flow areas and pressures. It is not possible therefore to investigate valve timing changes.

The simplified techniques are therefore limited to:

1. Getting an approximate first match between an engine and turbocharger.

2. To find for example, the dependance of the exhaust temperature on the scavenge ratio or trapped air-fuel ratio, without relating these parameters to the valve timings or boost pressures needed.

2. Hybrid Techniques

Their name being derived from their having facets of methods 1 and 3. An example is that given in reference 87. The aim is to retain the computational speed and simplicity of the simple matching techniques, but to move towards the confidence and accuracy afforded by the step-by-step models, especially at points of the engine cycle relevant to the particular study. They have the following features:

1. Critical parts of the cycle may be divided into a number of small steps.

2. More realistic models of the physical processes are used.

3. Parameters such as valve and fuel injection timing can be included.

These methods can be used for systematic investigations of a larger number of parameters over a wider range of loads than may be possible with full step-by-step models. It does not afford quite the accuracy of the step-by-step models, but by concentrating on the physical processes controlled by the parameters being investigated, sufficient accuracy can be assured.

3. Step-by-step models

Step-by-step models are well documented in the literature (eg. Ref.42), and only a few salient points are mentioned here:

1. The analysis follows the detailed fluid mechanical and thermodynamic changes that the working fluid is subjected to.

2. Quasi-steady flow is assumed: the engine is divided into a number of control volumes throughout each of which conditions are assumed uniform at any one time. The cycle is divided into a large number of short steps: flows are assumed steady over each step.

3. Numerous approximations are still made. Empirical correlations relating heat release and transfer, to cycle parameters may be used.

4. A reasonably accurate estimate of conditions in all control volumes at one point in the cycle must be made.

5. Running times are typically much longer than for either of the previous methods discussed. Data preparation is more detailed and hence time consuming.

6. Unlike methods 1 and 2, this method calculates accurate maximum cylinder pressures for stress analysis, and may be extended to calculate component temperatures for studies of thermal loading.

A mention should be given to the more sophisticated 'method of characteristics', which deals with the unsteady pulse interaction in the exhaust manifold. However the increase in accuracy of the turbine energy calculation is not normally required.

To give some feel for the running times of the three methods, they would typically take 2, 10 and 120 seconds for one stable operating point on a CDC 6600 computer. Typical accuracies are 10% for method 1, 7% method 2, 5% for method 3 without any experimental data but 3% if some experimental results are available for calibration. Thus by adopting the more sophisticated model a small increase in accuracy is achieved, and the scope of information extended, at the expense of much higher computing costs. It was decided therefore that the level of accuracy required for this project could be met by a method 2 type program, and this would not restrict the range of parameters investigated. The development of the programming method is described in the next section.

2.7.4 The 'Match 8' Simulation

It was not the original intention to develop a new diesel engine model; rather to modify existing programs to suit the requirements of the study. A start was therefore made with the simple cycle techniques of Wallace described in references 85 and 86. These proved to be inadequate for the reasons outlined in the previous section. Consult-

ation with Professor Wallace of Bath University revealed a more sophisticated model (Ref.87), that would be classified under method 2. This became the foundation for the 'Match 8' program eventually used in the study.

Wallace's method is not described here, but certain features that have been modified for Match 8 are given. Changes envisaged to the closed cycle conditions should not significantly affect the combustion characteristics, and hence the closed cycle calculation of Wallace is substantially retained. The gas exchange processes are however much more important, and the following inadequacies were identified:

1. The scavenge airflow is based on incompressible flow through a single orifice, from a steady inlet to a steady exhaust manifold pressure. An average valve diameter and a time averaged valve lift are used. Valve timings are not explicitly used.

2. The turbine energy is calculated by a simple pulse model. At evo the exhaust manifold is assumed to contain gas at the pressure and temperature used for the scavenge calculation. The contents of 2 cylinders is then assumed to mix instantaneously with the exhaust manifold mixture, and subsequently flow through the turbine in units of $^1/_{10}$ the combined contents at evo. The energy extraction by the turbine is calculated for each step from the turbine map, and then summed. It should be noted that no attempt is made to equalise conditions at the end of the pulse with those at the start, and that the exhaust volume required for realistic turbine energies is much larger than the actual volume.

The scavenge airflow and the turbine energy calculation are critical to the parameters to be investigated, and it is therefore unsatisfactory that they should be based on different, and both rather approximate,

models. The program was developed for high speed engines for which the valve overlaps and hence scavenge airflows are much smaller than for slow and medium speed engines.

The 'Match 8' program was therefore developed from the Wallace method, essentially by incorporating a more sophisticated model of the gas exchange process. The program is described in some detail in Appendix 1. The open cycle calculation is similar to that of the step-by-step programs, but longer step sizes, around 4° crank angle instead of 1°, are used.

The open cycle calculation therefore approaches the sophistication of the step-by-step models, and hence the accuracy of the results of the changes investigated rival that obtained from the step-by-step methods. 'Match 8' can treat constant pressure or pulse turbocharged 4-stroke engines, having 1, 2, 3 or 4 cylinders per exhaust manifold. Although not used on 2-strokes the adaptation would be a simple one.

2.8 THE EXHAUST HEAT-RECOVERY BOILER

The attention so far has been devoted exclusively to the engine, the central item of equipment in a diesel cogeneration scheme. However the exhaust heat-recovery boiler is also an integral part of the system, and hence it too is studied, although in somewhat less detail than the engine. The exhaust boiler cannot be treated independently of the engine, as the two interact via the back-pressure imposed on the engine exhaust by the boiler.

The important design criteria for the exhaust heat-recovery boiler are:

1. The gas pressure drop across the boiler.
2. The fraction of the exhaust heat that it must recover.
3. Its capital cost: this being largely determined, for given steam conditions, by the first two criteria.

Requirements for high rates of heat transfer, and hence lower capital costs, and a low gas pressure drop, are in opposition. This 'trade-off' between the parameters is an important subject, and is studied in the next two chapters; this section will just describe the method adopted.

Waste heat boilers may be divided into watertube and firetube types. In the watertube boiler the water or steam is contained within tubes over which the gases pass. The reverse situation pertains to the firetube boiler. Within both types many tube designs and arrangements, steam separation and pumping methods may be used.

Enquiries were made to most of the major UK waste heat boiler manufacturers, for information on the boilers they supply for heat recovery from diesel engines. Approximately eight useful replies were received and in these the balance in terms of boiler type was found to be slightly in favour of watertube boilers. Watertube boilers are most suitable for large sizes and high steam pressures; they can accept dry running conditions, and forced circulation types offer great flexibility in design (ref.81). Their disadvantage compared to firetube boilers is a somewhat higher capital cost, although commercial secrecy prevented this being checked or any value to be assigned to the differential. On balance a decision was made to concentrate in the boiler studies on the watertube type.

Neither experimental facilities nor computer program were available, and hence a computer simulation of a watertube boiler was developed, in order to investigate the interaction of the parameters mentioned above. This program is described in appendix 2. It is able to simulate a wide variety of tube arrangements and fluid conditions, and was tailored to the needs of the project. The input to this program is compatible with the output from the diesel engine program. Computer simulation does not appear to be widely used within the waste heat boiler manufacturing industry, and it is felt that this program or similar ones would be a useful tool to the boiler manufacturers.

2.9 SUMMARY AND CONCLUSIONS - CHAPTER 2

A re-optimisation of diesel engines for cogeneration applications is likely to give better returns than traditional avenues of engine development. The 4-stroke engine and watertube boiler have been chosen as being most suitable for this re-optimisation. Computer simulation models of engine and exhaust heat recovery boiler have been developed for the needs of the study.

CHAPTER 3

DESIGN OPTIONS AND LIMITATIONS

3.1 INTRODUCTION

The design parameters that are to be investigated are presented. The limitations on engine design are then explained, as a precursor to the results of the next chapter.

Energy balances for some modern 4-stroke diesels are shown in figure 3.1. Approximately 60% of the energy in the fuel appears as heat; the exhaust heat is typically at 450°C; heat in the jacket water, lubricating oil cooler and intercooler is at 120°C or less. Heat recovery can therefore be conveniently treated in two parts: high temperature heat of the exhaust, around 35% of fuel input energy, and low temperature heat of the engine, lubricating oil and charge air coolers, totalling 25% of fuel input energy.

The engine working fluid is in an open cycle, hence some exhaust energy will inevitably be lost: the computer simulation work is devoted to minimising this loss. The low temperature heat is recovered from closed circuits and all the heat is theoretically recoverable. The problem is that it is low quality heat and the low temperature work is therefore a qualitative examination of methods of upgrading this heat.

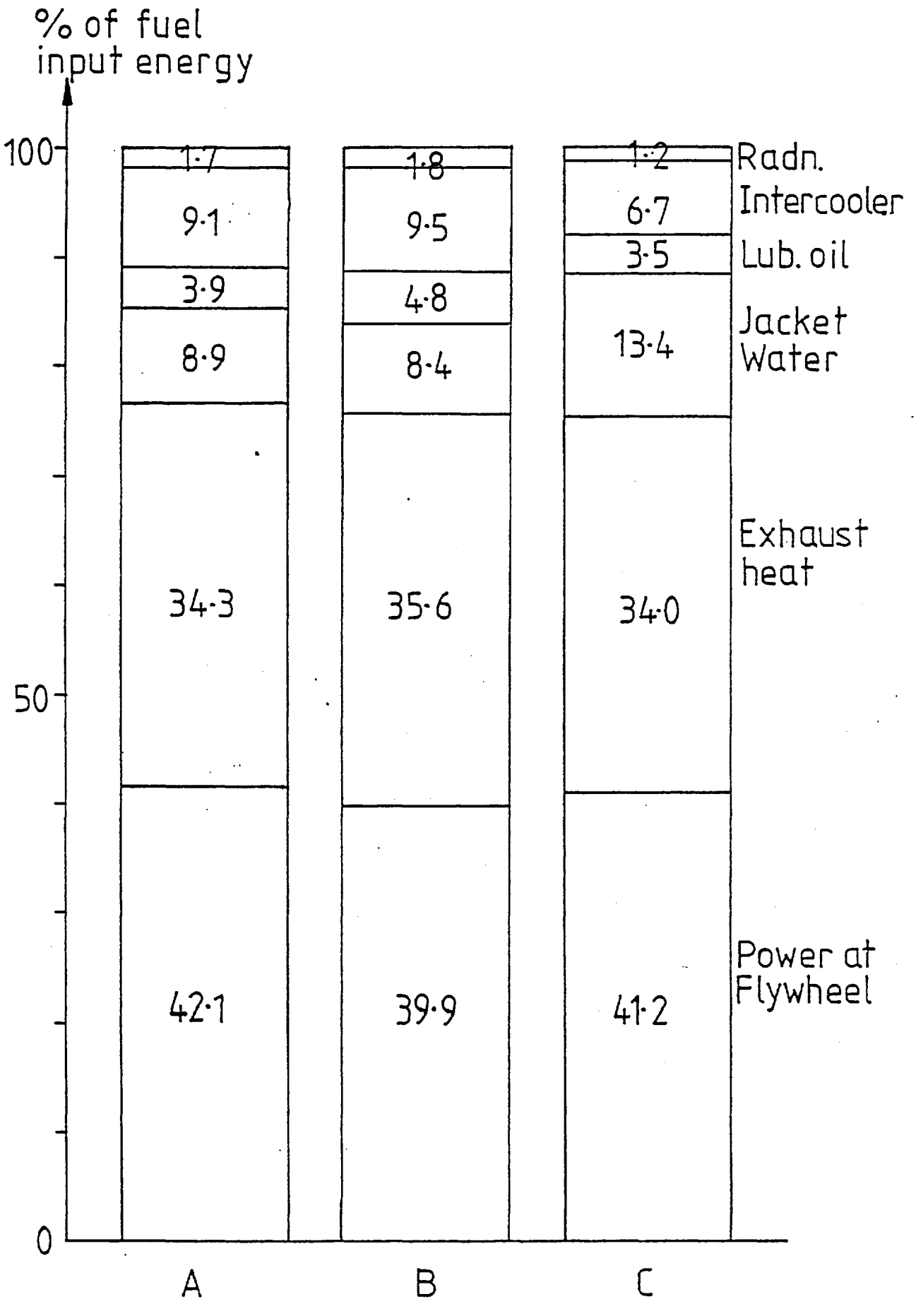

Fig. 3.1 Energy Balances for Modern 4-stroke Diesels

3.2 DESIGN CHANGES FOR CHP

The following possibilities for increasing the exhaust heat recovery will be considered:

1. The exhaust back pressure.
2. The exhaust valve opening.
3. The reduction of boost pressure.
4. The reduction of valve overlap.
5. Heat extraction before the turbine.
6. The gas temperature at the boiler exit.
7. Afterfiring.

They may be divided into those principally affecting engine operating conditions (1-5), and those affecting the waste heat boiler (6 and 7). The reasons for their choice are as follows:

1. The exhaust back pressure

Any back pressure imposed by the boiler on the engine, reduces the turbine power output. The boost pressure and trapped air-fuel ratio fall; the exhaust temperature rises. At present, diesel manufacturers seek to minimise the influence of the waste heat boiler on the engine, by imposing strict limits on the boiler pressure drop. The requirements for low pressure drop and high rates of heat transfer are in opposition, and hence boiler size and cost may be reduced by allowing higher pressure drops.

2. The exhaust valve opening

The exhaust valve typically opens 60° to 70° before the piston reaches the bottom of its stroke, thereby reducing the work expended by

the piston on the exhaust stroke. Changes to this timing may exchange small decrements in power for larger increments in available exhaust heat.

3. Reduction of boost pressure

Turbocharging has proved to be a successful way of reducing engine capital costs. Boost pressures at full load in the range 2.5-3 bar are common for modern engines: these give high trapped air-fuel ratios and hence reduced exhaust temperatures. By increasing the turbine effective area, the boost pressure is reduced and the available exhaust heat increased.

4. Reduction of valve overlap

Long valve overlaps, in the range 120-150 crank angle degrees, and hence high scavenge ratios of 1.3-1.4, are employed as another mechanism for reducing the thermal loading on engine components. A value for the scavenge ratio of 1.1 is generally sufficient to ensure adequate scavenge of combustion products.

5. Heat extraction before the turbine

Raised exhaust temperatures may lead to hot corrosion of turbine blades. By extraction of some heat before the turbine, the exhaust gas temperature at the turbine inlet can be reduced, and advantage taken of the higher rates of heat transfer from the hot gases.

6. The gas temperature at the boiler exit

The sulphur content of heavy fuel oils limits the boiler gas exit temperature to 175-200^{o}C, in order to keep tubing surfaces above the sulphuric acid dewpoint. Corrosion resistant or 'disposable' tubing offers a relatively simple and straightforward way of extracting more heat from the exhaust.

7. Afterfiring

Afterfiring into the engine exhaust at almost 100% efficiency, offers a way of meeting peaks in heat demand that is cheaper both in capital and running costs than conventional methods. It is included here although it is not strictly a way of increasing the fraction of engine exhaust heat that is recovered.

Two important parameters have been mentioned: the trapped air-fuel ratio (R_T) and the scavenge ratio (λ). The stoichiometric air-fuel ratio is 14.7 but engines always use quantities of air well in excess of this, resulting in lower exhaust temperatures and possible rates of heat recovery. These two parameters are measures of the excess air. Exhaust back pressure and boost pressure reduction principally affect the trapped air-fuel ratio, valve overlap reduction decreases the scavenge ratio. The consequences of reductions to both of these parameters will be discussed further in the section on thermal loading.

The low temperature heat is usually in three circuits, which are, in decreasing order of temperature, jacket water (approximately 10% of fuel input energy), lubricating oil coolant (5%), and intercooler (10%). The analysis will not go into the detailed methods of recovery of this heat, but will concentrate on the problems associated with any increase in temperature in these cooling circuits.

3.3 HEAT TRANSFER IN THE ENGINE

Engine design is limited by thermal and mechanical loading; it is important to consider what these limits are, and how the design

changes being considered may affect them. Increasing the heat recovery is likely to increase the thermal stress on the engine rather than the mechanical stress, and hence before considering the specific problems that may be encountered and some possible cures, the heat transfer processes in the engine will be discussed in some detail.

3.3.1 The Heat Transfer Process

The original source of thermal loading in the engine is the combusting gases in the cylinder. The dominant mode of heat transfer is turbulent forced convection, accounting for approximately 75% of the heat transferred to the cylinder boundaries. The remaining 25% is radiative transfer. Both gas and flame radiation contribute, but the latter is much more important.

There are many semi-empirical formulae for prediction of heat transfer. The range of engines for which each gives reasonable results is limited: the various formulae giving different results under the same conditions. As the dominant form of heat transfer is turbulent forced convection one would expect to use an equation of the form:

$$\dot{Q} = hA\,(T_g - T_w)$$

and that $Nu \propto Re^n$

where: $\dot{Q}$ = rate of heat flow to coolant.
h = overall heat transfer coeff.
A = area for heat transfer.
n = constant.

The actual form taken is usually somewhat more complicated: see for example ref.94 or ref.58 for a discussion of possibilities. Used in conjunction with experimental results it is suggested (ref.58) that an accuracy of ± 10% may be achieved for a limited range of operating conditions.

3.3.2 The Parametric Dependance of heat transfer

The rate of heat transfer will obviously vary spatially and through time. Fig. 3.2 taken from ref.94 shows the variation with time of the heat transfer rate for the components of a 4-stroke, 400 rpm engine at a bmep of 18 bar. The area under each curve being equal to the heat transferred per cycle to the cylinder head, liner, piston and exhaust valve/throat: these constituting the boundary of the cylinder. In table 3.1 (Ref.58) the percentage of fuel input energy transferred to the 4 components of a 16 cylinder RK3 engine at 1000 rpm are given. In figure 3.3 (Ref.58) the corresponding component temperatures are shown. It could be expected that the temperatures and relative loadings would be the same for the 6RKC engine used in the analysis of the next chapter.

The following features of the graphs and table are important:

1. A large portion of the heat is transferred before around 60° after top dead centre, the great majority during the closed cycle.

2. Although the exhaust valves are the hottest of the engine components only 10% of the heat transferred to coolant passes through the exhaust valves. Any change in the thermal loading of the exhaust valves will therefore have small effect on the overall percentage of heat lost to coolant.

3. The values of component temperatures shown are time-averaged. There will be a cyclic variation of $5\text{-}10^{\circ}C$ in the liner, head and piston surface temperatures and up to $25^{\circ}C$ in the exhaust valve.

At a given load, and for fixed injection timing, engine speed and coolant temperature, the gas temperature during the closed cycle will depend essentially just on the trapped excess air i.e. the trapped air-

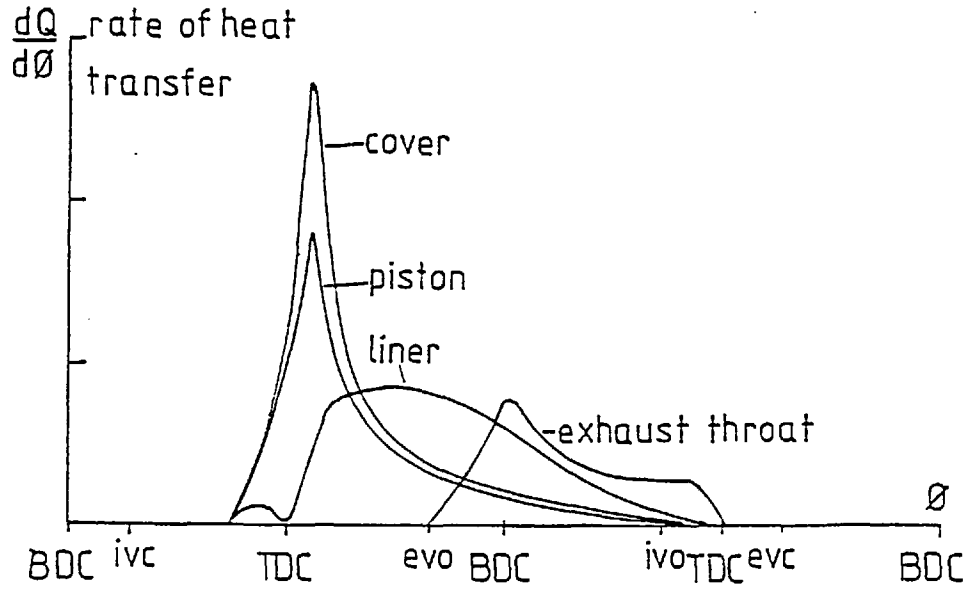

Fig. 3.2 Rate of Heat Transfer to Components (Ref. 94)

Fig. 3.3 RK3 Component Temperatures (Ref. 58)

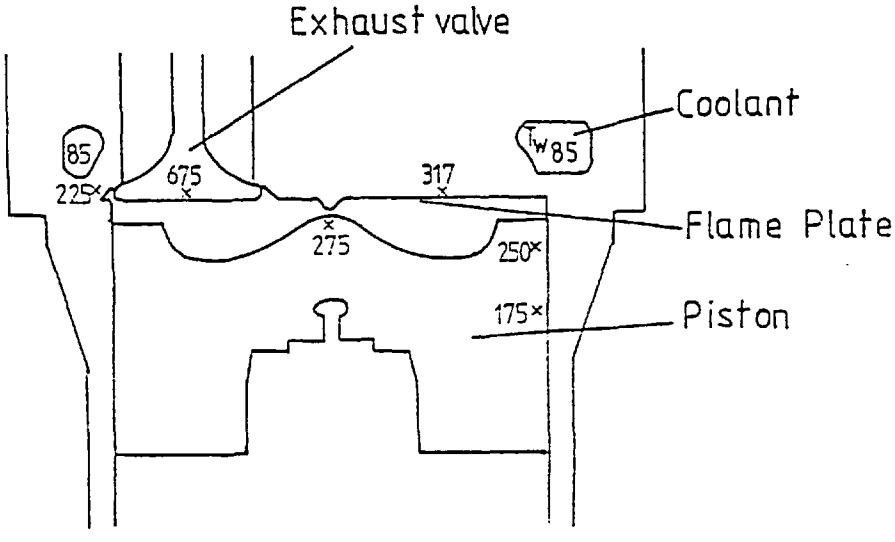

TABLE 3.1

Measured Results for Ruston 16RK3 Engine

Piston	3.1%	of fuel input energy
Liner	5.7%	
Exhaust Valves	1.0%	
Cylinder Head	2.5%	
Total	12.3%	

TABLE 3.2

Classification of Fuel Oils

Class	Viscosity SRI at 100°F	Water % vol max	Sediment % mass max	Conradson Carbon Residue % mass max	Sulphur % mass max	Ash % mass max
A2	41	0.05	0.01		1.0	0.01
B2	65	0.25	0.05	1.5	1.8	0.02
D	41	0.05	0.01	0.2	1.0	0.01
E	250	0.5	0.15		3.5	0.1
F	1000	0.75	0.25		4.0	0.15
G	3500	1.0	0.25		4.5	0.2
H	7000	1.0	0.25		5.0	0.2

fuel ratio. As nearly all the heat transfer to the piston, liner and cylinder head occurs during the closed cycle, the temperature of these components should depend almost exclusively on the trapped air-fuel ratio. The lower this ratio, the higher their temperatures. The effect of a reduced scavenge ratio will be negligeable as is indicated in Fig. 3.4 (ref.94), in which, amongst other things, the piston temperature and the scavenge ratio are plotted against the valve overlap.

The temperature of the exhaust valve will however be influenced not only by the trapped air-fuel ratio, but by both a reduction in valve overlap (and hence scavenge ratio), and by the timing of the exhaust valve opening. The loading of the exhaust valve is a critical design factor and merits a special section, but before that a quantitative example is given on the relationship between R_T and cylinder component temperature.

3.3.3 Component Temperatures

To a first approximation, for a given load, the closed cycle gas temperatures are a linear function of $(1/R_T)$. A simple order of magnitude calculation follows on the change in component temperatures, that might be expected from the changes envisaged to R_T.

$$\dot{Q} = hA\,(T_1 - T_2) \qquad \ldots\ldots \text{(i)}$$

$$\dot{Q}' = hA\,(T_1' - T_2) \qquad \ldots\ldots \text{(ii)}$$

where $\dot{Q}$ = rate of heat transfer.

A = area for heat transfer.

h = overall heat transfer coefficient.

T_1 = flame plate temperature.

T_2 = coolant temperature.

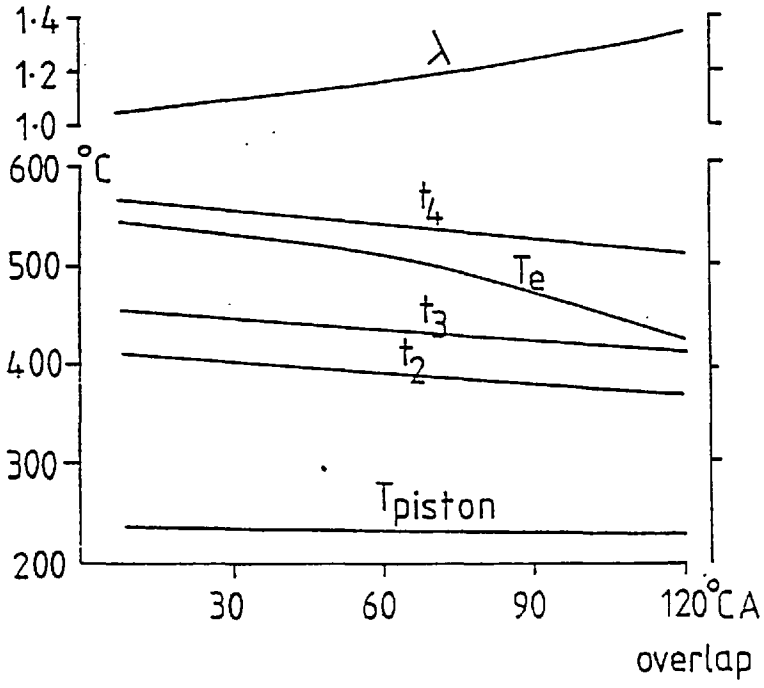

Fig. 3.4 Relation between Scavenge Ratio and Component Temperatures

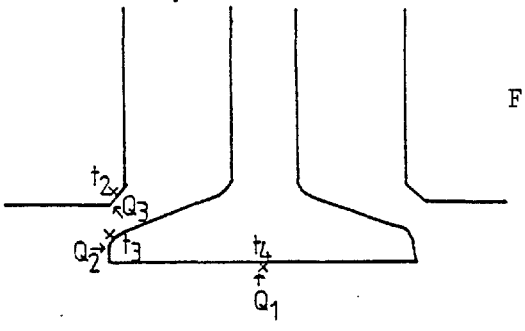

Fig. 3.5a Exhaust Valve

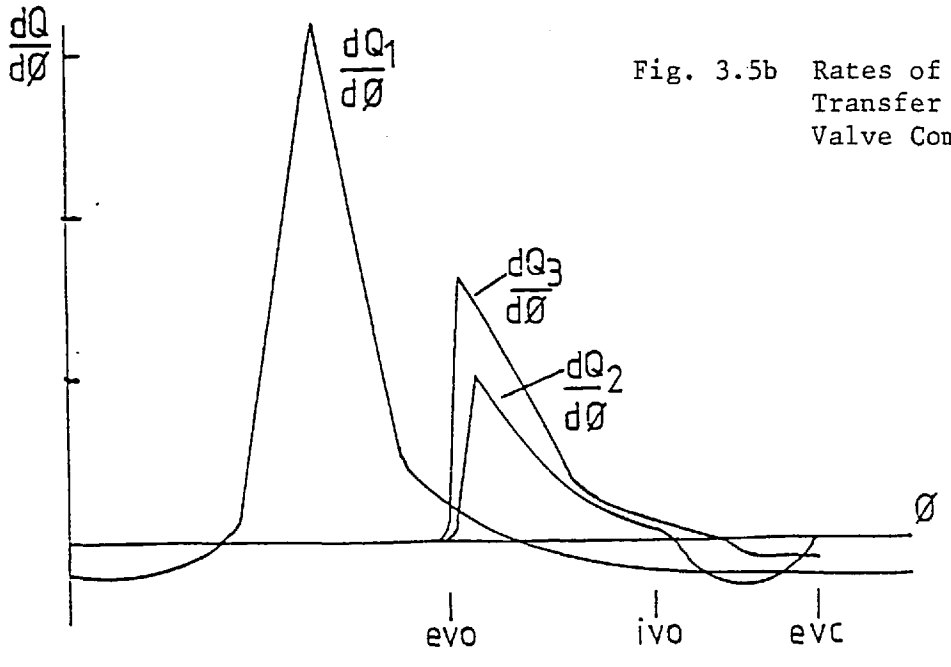

Fig. 3.5b Rates of Heat Transfer to Exhaust Valve Components

dashed superscript signifies after R_T reduction.

The heat transfer coefficient is assumed to remain constant with the changes in R_T. From (i) and (ii) $\frac{T_1'}{T_1} = \frac{\dot{Q}'}{\dot{Q}} + \frac{T_2}{T_1}\left(1 - \frac{\dot{Q}'}{\dot{Q}}\right)$

Considering the temperature gradient between the flame plate and cooling circuit of the cylinder cover shown in fig. 3.3 i.e. $\frac{T_2}{T_1} = \frac{85}{300}$, and for $\frac{\dot{Q}'}{\dot{Q}} = 1.12$ corresponding to a reduction in R_T from 28.6 to 24.4 (a result derived in the next chapter) then:

$$\frac{T_1'}{T_1} = 1.09 \quad \text{and} \quad \Delta T \text{ of the flame plate } \simeq 25^{\circ}C.$$

These increases in temperature will inevitably increase the thermal stress on the components. It may or may not be a problem depending on the 'reserve' of the engine. It must be emphasised that this calculation is only intended to give a rough estimate of the change in temperature; a more detailed step-by-step calculation would be needed to give more accurate predictions.

3.3.4 The Exhaust Valve Temperature

Figure 3.5a shows the heat flows and temperatures on an exhaust valve. For large engines most of the heat transferred to the valve plate is conducted through the valve seat rather than the stem. Hence:

seat on head temperature $\quad t_2 = t_1 + k_a (Q_1 + Q_2 + Q_3)$

seat on valve temperature $\quad t_3 = t_2 + k_b (Q_1 + Q_2)$

valve plate temperature $\quad t_4 = t_3 + k_c Q_1$

where k_a, k_b and k_c are the overall conductivities seat on head to coolant, seat on valve to seat on head, valve plate to seat respectively. The quantities of heat Q_1, Q_2 and Q_3 can be calculated step-by-step from turbulent heat transfer theory and summed over the cycle. This calculation has been performed in Ref. 94 and the resulting valve

temperatures are plotted in fig. 3.4, for a range of valve overlaps and hence scavenge ratios. It can be seen that the valve temperatures change much more slowly than the exhaust gas temperature: between 60° and 120°CA overlap the exhaust temperature falls by 100°C but the valve temperature by only 25°C.

It is worth considering in more detail the cyclic history of the heat transfer to the exhaust valve. Figure 3.6a shows the cyclic variation of cylinder temperatures calculated by 'Match 8' for the 6RKC engine for 3 cases:

1. $R_T = 28.6$, $\lambda = 1.26$: Normal design
2. $R_T = 28.1$, $\lambda = 1.06$: Reduced scavenge ratio
3. $R_T = 24.4$, $\lambda = 1.22$: Reduced trapped air-fuel ratio.

On the graph are marked the time averaged values of t_2, t_3 and t_4 taken from ref.58. Heat is transferred from gas to the valve rim and seat only during the time that the exhaust valve is open, Match 8 does not calculate rates of heat transfer to the valve components, but fig.3.5b shows them for a similar engine (Ref.94). It is evident that nearly all the heat transfer occurs between firing top dead centre and the inlet valve opening. When the temperature of the exhaust gas falls below t_2, t_3 or t_4 cooling of that component may occur. However fig.3.6b shows that the gas flow rates during overlap are not as great as those shortly after inlet valve opening, hence cooling of the valve by the gas will not be as vigorous as heating. This is supported by fig.3.5b.

To summarise, the thermal loading of the exhaust valves is basically determined in the period before inlet valve opening. If cylinder gas temperatures for this period remain the same then the exhaust valve temperature should not change greatly, hence the valve temperature is only weakly dependent on the scavenge ratio. If the cylinder temperature

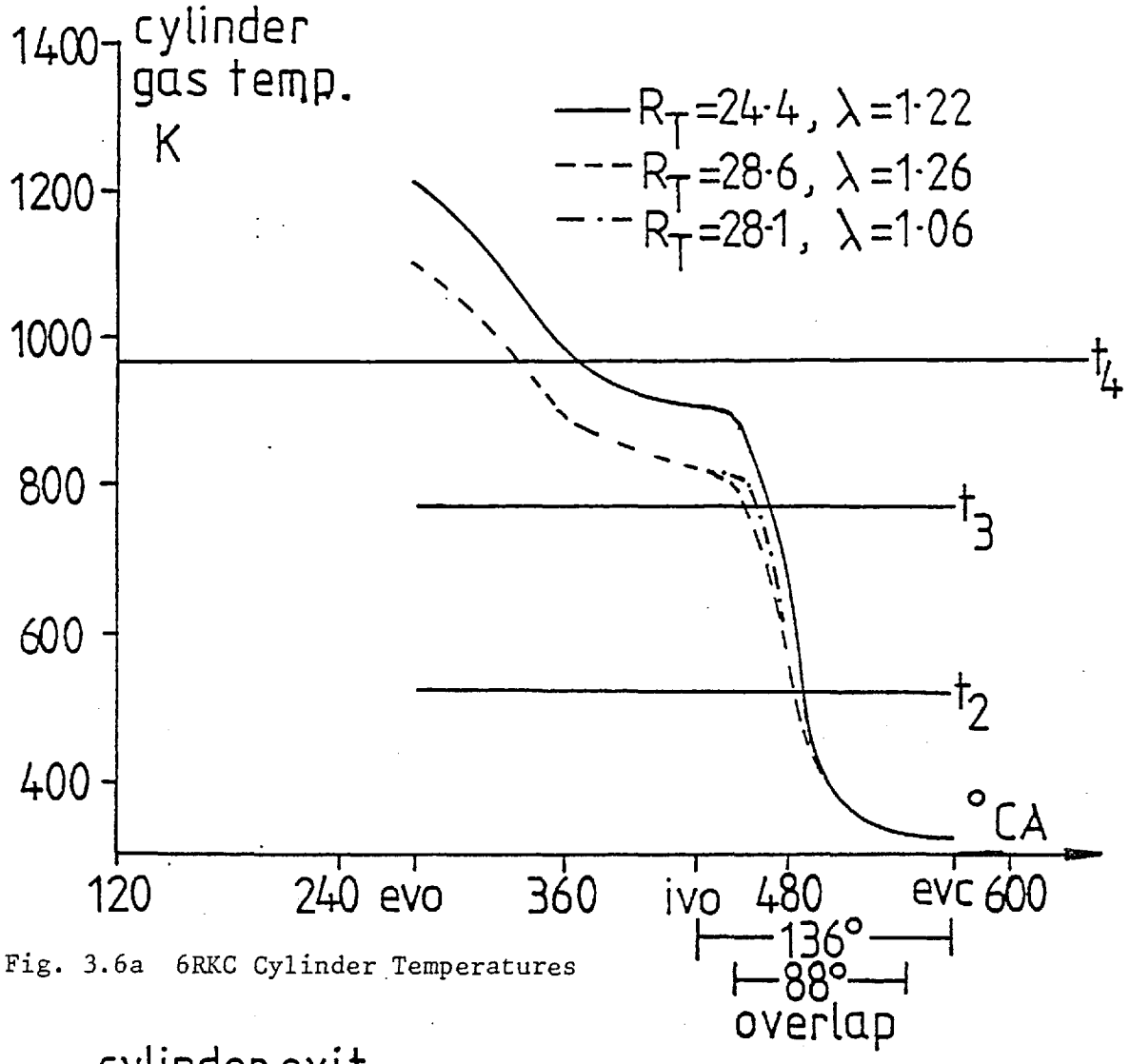

Fig. 3.6a 6RKC Cylinder Temperatures

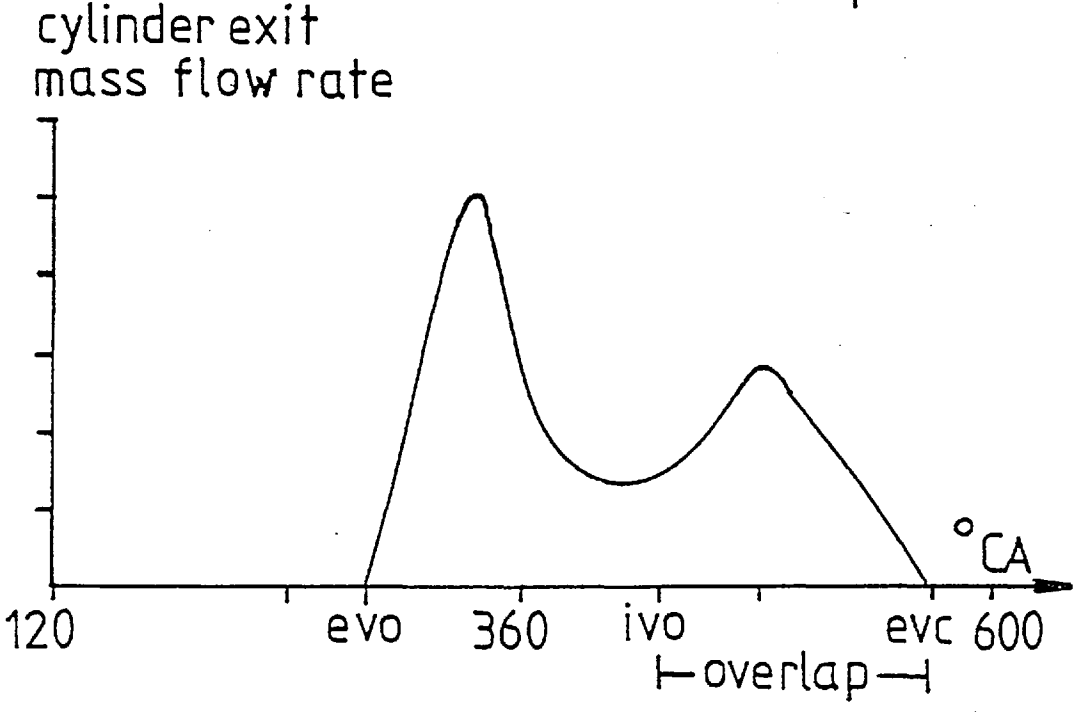

Fig. 3.6b 6RKC Cylinder Mass Flow Rates

before inlet valve opening increases, as with reduction in the trapped air-fuel ratio, then the loading will increase. That the exhaust valve temperature depends primarily on the trapped air-fuel ratio is supported in refs. 16 and 75.

3.4 THE PROBLEMS OF ELEVATED COMPONENT TEMPERATURES

The previous section has established the component temperature changes associated with the possible design modifications. The problems caused by elevated component temperatures will now be considered.

The fuel price differentials shown in fig. 3.7 mean in practice that the only likely economic fuels are the heavy fuel oils having high viscosities. Many of the problems of engine design are caused by the properties of heavy fuel oils.

3.4.1 Heavy Fuel Oil

Fuel oils are classified in table 3.2 (Page 58) taken from BS2869. The definition of heavy fuel oil is usually by its viscosity (eg. Mirrlees (Ref.64) choose a value of 150 SR1 at 100°F), but the more important properties are the others listed in Table 3.2. The critical contents are the Conradson Carbon Residue (causing fouling and smoke), the sulphur (low temperature corrosion), and the ash, particularly sodium and vanadium (high temperature corrosion). It can be seen that wide variations in these contents, may be expected within the classification 'heavy fuel oil'.

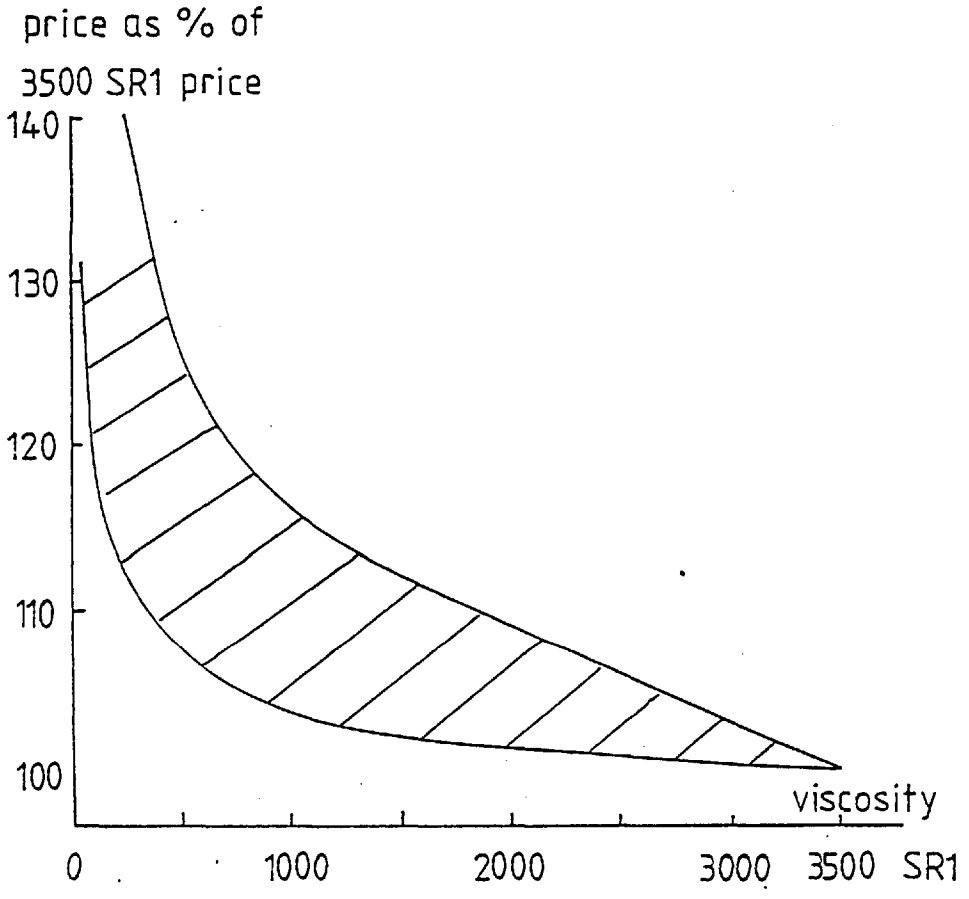

Fig. 3.7 Relation between Oil Price and Viscosity

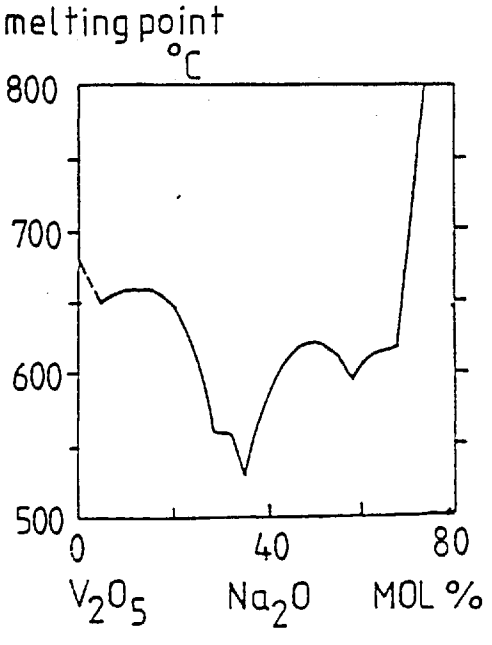

Fig. 3.8 Melting Points of Sodium-Vanadium Salts

At present most European refineries use atmospheric distillation (Ref. 25) leaving 40-50% residues, but there is a trend to adopt thermal cracking leaving 10% residue. High demands for the lighter fractions may therefore lead to deteriorating quality of the heavy fuel oils.

3.4.2 Some Limitations on Design

The following three factors limit permissible design modifications:

1. Hot Corrosion

Hot corrosion is caused by the deposition of molten sodium-vanadium eutectics on the metallic surfaces. Fig. 3.8 (Ref. 32) shows the melting points of the sodium-vanadium salts. The ratio of the sodium and vanadium contents is important, and the lowest melting point is 535°C for sodium vanadylvanadate (5.1.11). If metal temperatures can be kept substantially below this, they should be protected against hot corrosion.

2. Cold Corrosion

Sulphur present in the fuel can, during combustion, form sulphur dioxide and trioxide, which may combine with water vapour to form sulphuric and sulphurous acid. If the metal temperatures are allowed to fall below the dew point of the acid, the corrosive action may be severe.

3. Thermal and Mechanical Stress

Component load is made up of thermal and pressure stresses. The thermal stress only goes through a cycle with an engine loading cycle, whereas the pressure stress cycles with every engine cycle. It is the cycling of the thermal and pressure stresses which causes the problems, typically represented by fatigue cracks in components. Under unfavour-

able conditions the thermal and pressure stresses may reinforce each other.

3.4.3 Possible Remedies

Certain design and operational criteria may be adopted to counter the problems just mentioned:

1. Fuel Treatment

Centrifuging, filtering and heating must always be applied. Additives may be considered to counteract the sodium and vanadium salts (Ref. 78), but they will probably be expensive.

2. Lubrication

Wear of liners and piston rings due to the sulphur content of the fuel may be reduced by the use of an alkaline lubricating oil.

3. Cooling

More intensive cooling of hot surfaces may be applied to reduce the thermal stress and the possibility of hot corrosion.

4. Coatings/Materials

Harder materials or special coatings may be used to resist corrosion.

5. Maintenance

Proper maintenance is a prerequisite to reliable operation. For the prevention of excessive thermal loading it is important to include cleaning of turbochargers and intercoolers, and the prompt replacement of fuel nozzles.

3.4.4 The Design of Components

Each of the engine components has specific design problems associated with it. The various components will therefore be examined individually to more closely identify the problems resulting from the possible design modifications, and the measures that may be taken to prevent them.

1. Cylinder cover, liner and piston

The temperatures of the cover, liner and piston are not sufficiently high for hot corrosion, and the changes proposed to the trapped air-fuel ratio would not raise surface temperatures near the eutectic temperature. Low temperature corrosion may occur at the bottom of the liner if the surface temperature drops below 100-110^{o}C. A well designed engine should not suffer this problem, and any increase to gas temperatures should reduce it.

Carbonization of the lubricating oil is more of a problem and the liner at the top piston ring at tdc, and the top piston ring should be kept below 200^{o}C. The rate of carbonization doubling for each 10^{o}C above 200^{o}C (Ref. 79). The liner may be more intensively cooled by leading the coolant closer to the surface (see refs. 59, 32 for details). Methods of cooling the piston include oil injection through the connecting rod, cocktail shaker or cast in passages for oil cooling. A well designed cooling system can decrease the temperature at the top ring or crown by up to 50^{o}C over the uncooled piston (Ref. 79).

The thermal and mechanical stresses are greatest on the piston and cover. The part of the cover under the highest stress is the bridge between the valves where cracks may occur and which is the most difficult area to cool. In the piston, the crown is at the highest

temperature: the important consideration here being the decrease with raised temperatures of material strength. The same methods of more intensive cooling can be used to reduce thermal stress. The injector nozzle may also require cooling if higher gas temperatures are experienced.

2. Exhaust Valves

Exhaust valves operate under extremely unfavourable conditions of high thermal and mechanical stress and are susceptible to hot corrosion. As a result the extension of valve life presents the engine manufacturer with one of his most difficult problems.

The exhaust valve must seal properly. A scenario for how it may fail in this respect is as follows:

(i) Crushed ash or carbon deposits are trapped on the valve seat.

(ii) As a result the thermal conduction drops and a local 'hot spot' forms.

(iii) Local valve temperatures above 550^{o}C mean that hot corrosion can occur and a jet channel can develop.

Valve failure may also occur due to cracks which have originated at the valve plate centre where the yield is greatest (Ref. 58).

There are two approaches to deal with the problem:

(i) Keep the valve temperature as low as possible by intensive cooling, usually with valve cages (a problem here is distortion), occasionally with a seat in head design.

(ii) Use a harder, more expensive (eg. Nimonic) material for the valve.

Each method has its merits; there are also variations. For example, the valve itself may be cooled (Ref. 32).

As the loading on the valves increases, by going to poorer quality fuels or higher gas temperatures, both more intensive cooling and harder materials may be required. At present a valve life of 6000 hours with heavy fuel can be considered good practice but some manufacturers are considering 12000 hours (Ref. 59,32).

3. Turbine Blades

The first four design changes suggested in section 3.2 increase the exhaust temperature into the turbine. Two problems may result: deposition of, and hot corrosion by, the sodium-vanadium salts.

In order to be deposited or to cause corrosion the sodium-vanadium eutectics must still be molten when they reach the blades. It has therefore been commonly held that a limit on the average exhaust temperature of 550°C should be applied. However results of Ref.59 suggest that it is the sodium content of the fuel rather than the temperature which is the decisive factor. With pulse charging there is a temperature pulse during which gas temperatures may be considerably higher than the average; this has led one manufacturer to use constant pressure charging to avoid this (Ref. 83).

Water washing is usually effective in removing deposits (Ref. 68). To resist corrosion a coating can be applied to the blades. For example, a diffusion coating of Cr-Si alloy is resistant to Vanadium attack (Ref.78). Alternatively, in the case of CHP schemes, the exhaust temperature may be reduced below 550°C by the introduction of heat transfer surface before the turbine as already discussed. There is still the problem that the salts will then be deposited on the heat transfer surface. Provision must therefore be made for cleaning this.

Higher exhaust temperatures may also entail a more expensive material, eg. stainless steel, for the exhaust manifold, and perhaps

some attention to the expansion joints in the manifold.

To summarise this section on the design of components: modification to exhaust valve and turbine sufficient to resist the increases in thermal loading imposed by the changes considered, may be achieved relatively simply by replacing these components with ones having higher resistance to thermal stress. If modifications are required to piston, liner and cover then a more fundamental re-design of the engine may be needed. Changes to loading and hence components are less for a reduction of the scavenge air than the trapped air.

3.5 THE ECONOMIC CRITERIA FOR DESIGN MODIFICATION

The question arises as to what philosophy to adopt with regard to reliability and maintenance of the modified engine. Is a shortening of maintenance intervals acceptable, and what incremental capital investment is economic to restore maintenance intervals? What is the economic penalty of increased unreliability, ie. what are the costs of unplanned outages?

The net value of a design change is equal to:

(Saving in running cost) - (Increase in Maintenance Cost)

- (Increase in Capital Cost)

Hence for a worthwhile alteration:

$$(C_{HT}\ \Delta\eta_{HT} + C_{LT}\ \Delta\eta_{LT} + C_e\ \Delta\eta_b)w_f C_{al}.8760.L - w_f.8760.L.\ \Delta c_f - \Delta C - \Delta M_{lab.} - \Delta M_{comp.} > 0$$

where C_{HT} = value of exhaust heat

C_{LT} = value of low temperature heat

C_e = value of electricity

Δn_{HT} = increase in available exhaust heat

Δn_{LT} = increase in available low temperature heat

Δn_b = increase in engine brake efficiency

W_f = fuel flow

C_{al} = calorific value of fuel

L = annual load factor

ΔM_{lab} = change in annual maintenance cost - labour

ΔM_{comp} = change in annual maintenance cost - components

ΔC = change in annual charge on capital cost of engine

ΔC_f = change in fuel cost to engine.

In general, for any modification that gives a saving in running cost, the combination of values of ΔM_{lab}, ΔM_{comp}, ΔC and ΔC_f that maximises the net value of the alteration, should be chosen.

The expected cost of planned maintenance of the best modern engines is around 5% of the total costs per kwh (Ref. 32). To allow for unplanned maintenance this figure should be inflated by 50% as the most probable case, and 100% as the maximum (Ref. 90). This is notably lower than the 14-15% for older UK engines revealed in a survey of UK statistics (Ref. 23), which are therefore of limited value, as they are not representative of potential modern practice.

Table 3.3 shows that the majority of forced outages are caused by fuel injection equipment, cooling systems and valves. Many of the forced outages are therefore caused by items of equipment not exposed to gas flows, and will not be affected by the design modifications discussed in this work. It should be noted that the exhaust valves cause a significant proportion of the failures.

TABLE 3.3

Forced Outages of UK Diesel Plant (Ref. 23)

Cause	% of Total	Comments
1. Fuel Injection Equipment & Supply	34.96	of which 44% in high pressure pipes to injectors
2. Water Leakages & Cooling	21.56	
3. Valve Systems	19.60	of which 50% due to exhaust valve failures
4. Lubrication	5.23	
5. Turbochargers	3.96	2 out of 12 cases due to blade damage
6. Miscellaneous	14.69	
	100.00	

TABLE 3.4

Sutzer Z 40/48 Maintenance Schedule

	Overhaul Periods Hours	Expected Lifetime Hours	Dismantling and assembling times
Injection nozzle	2000-3000	6000-9000	30 minutes
valves	12000-18000	24000-36000	60 "
Piston ring	12000-18000	12000-18000	
Piston	24000-36000 (dismantling)	72000-108000	90 "
Piston ring groove		48000-72000 (reconditioning)	
Cylinder Liner	one every 12000-18000	72000-108000	60 "
Main bearing	25% every 12000-18000	36000-54000	90 "
Con. rod bearing	25% every 12000-18000	24000-36000	90 "
Cylinder cover			150 "

The objective of a maintenance schedule is to prevent costly forced outages. Table 3.4 shows a planned maintenance schedule for a Sulzer Z 40/48 medium speed 4-stroke engine run on 1500 SRI fuel; intervals may be somewhat shorter for 3500 SRI fuel (Ref. 60). It is indicative of the best in modern practice. An important feature of this table is that the overhaul periods are governed by the injector, valve and piston ring lives.

It is feasible that one might accept shortened maintenance schedules instead of making design changes to withstand higher thermal loading. However, planned maintenance costs will not rise linearly with the exhaust temperature. For example an exhaust valve life of 6000 hours may be reduced to several hundred hours if metal temperatures increase above the eutectic temperature, and a corrosion resistant material is not used. Reliability may also suffer, in which case the economic penalties of forced outages and secondary damage may be high. Therefore, unless the changes in maintenance intervals prove to be small, this will not generally be the best approach.

The modifications that may be necessary to withstand higher thermal loading may be divided into two types: those to equipment that will not be replaced eg. cooling circuit, and those to equipment with limited lives, eg. exhaust valves. The expense of the former may be largely research and development, but may involve more expensive production costs if a more sophisticated technology is required. As a result it is impossible at this stage to make any accurate estimate of the cost of this type of alteration. The second type of alteration will contribute to $\Delta M_{comp.}$ and is more easy to estimate eg. the introduction of nimonic values would entail an incremental expenditure of £90 per cylinder on the Ruston 6RKC engine (1978 costs), one of the engines used for the results of the next chapter.

The problems of corrosion might be solved by a shift to higher quality fuels. However, the fuel price differentials shown in Figure 3.7 militate against this in that for example a trebling of maintenance costs from 5 to 15% of the total running cost, only permits a small shift in fuel quality. There may be isolated cases where this is sufficient to avoid the problems.

3.6 SUMMARY AND CONCLUSIONS - CHAPTER 3

The optimisation studies may be divided into the high temperature heat of the exhaust, and the low temperature heat of the cooling circuits. Seven possibilities will be investigated for improvement to the high temperature heat recovery: five relating to the engine, and two to the exhaust heat recovery boiler. Two parameters, the trapped air-fuel ratio and the scavenge ratio measure the excess air and hence the recoverable fraction of exhaust heat. The increase in thermal loading is less for a reduction in the scavenge ratio than the trapped air-fuel ratio. Design changes to accept a reduction in scavenge ratio are therefore likely to be more straightforward than for a reduction in trapped air-fuel ratio; but both modifications should be within the scope of engine development.

CHAPTER 4

THE RESULTS OF DESIGN MODIFICATION FOR DIESEL COGENERATION

4.1 INTRODUCTION

The methods of analysis, the limitations on design and some possible modifications to the diesel cogeneration system have been given in the previous two chapters. Chapter 4 concludes the design modification work with the presentation of the simulation results for both the engine and exhaust heat boiler. The results on the enhancement of exhaust heat recovery are presented in section 4.2 for the engine simulation results, and in section 4.3 for the exhaust heat recovery boiler design. Discussion of the potential for upgrading the low temperature heat is then given in section 4.4, and finally the re-design options for the diesel cogeneration system are summarised in section 4.5.

4.2 EXHAUST HEAT RECOVERY - ENGINE SIMULATION RESULTS

The results of the computer simulations on the first five parameters mentioned in the previous chapter are first presented, (section 4.2.1). This section then goes on to look at combinations of effects (4.2.2), to present a comparison with published results (4.2.3) and the relationship between back pressure and boiler size (4.2.4), and finally to discuss the economics of the changes (4.2.5).

4.2.1 Parameters 1-5

Approaches were made to the UK engine manufacturers for the engine and turbocharger data required as input to the simulation program (see appendix 1). The most favourable response was received from Ruston Diesels Ltd., a subsidiary of the General Electric Company. Two of their engines were therefore chosen for the study. By studying specific engines the relative merits of, and potential problems associated with the possible design changes, may best be understood.

The first results presented are on the 9AT350, a medium speed, 4-stroke engine able to burn heavy fuels up to 3500 SRI viscosity. Information on the engine is given in table 4.1, and the simulated operating characteristics full load down to 50% load are shown in Fig. 4.1. This engine is still at the design stage and hence experimental results are not available, however the full load operating point (a nominal power of 3.3 MW) predicted by Rustons, is shown in Fig. 4.1 for comparison.

The second set of results are for the Ruston 6RKC engine, and are given for comparison purposes. This engine is available in 750

TABLE 4.1

The Ruston Engine 9AT350

Type:	Pulse turbocharged 4-stroke		
Turbocharger:	Napier 143-19.2 sp/JJ		
Speed:	600 rpm		
Cylinders:	9	Standard Valve Timings:	
Bore:	35.1 cm	evc	68° after tdc
Stroke:	37.1 cm	ivc	240° " "
Conrod Length:	0.784 m	evo	462° " "
Exhaust Manifolds:	3	ivo	620° " "
Compression Ratio:	12.4:1	Overlap	168°

full load output 3.3 MW

TABLE 4.2

The Ruston Engine 6RKC

Type:	Pulse turbocharged 4-stroke		
Turbocharger:	Napier SA085 132-509/381G		
Speed:	1000 rpm		
Cylinders:	6	Standard Valve Timings:	
Bore:	25.4 cm	evc	57° after tdc
Stroke:	30.5 cm	ivc	210° " "
Conrod Length:	0.61 m	evo	490° " "
Exhaust Manifolds:	2	ivo	641° " "
Compression Ratio:	12.5:1	Overlap	136°

full load output 1.3 MW

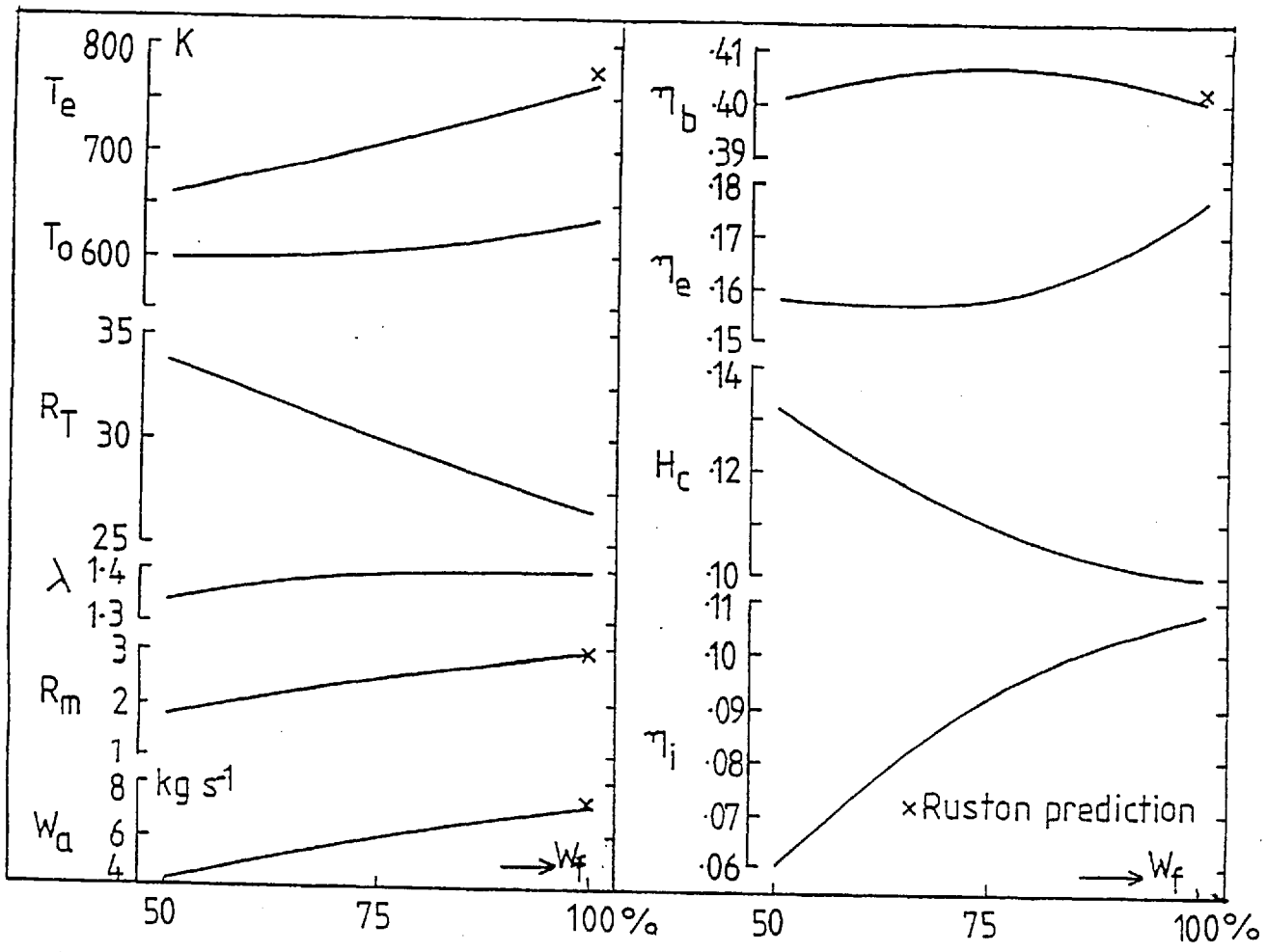

Fig. 4.1 9AT350 Predicted Characteristics

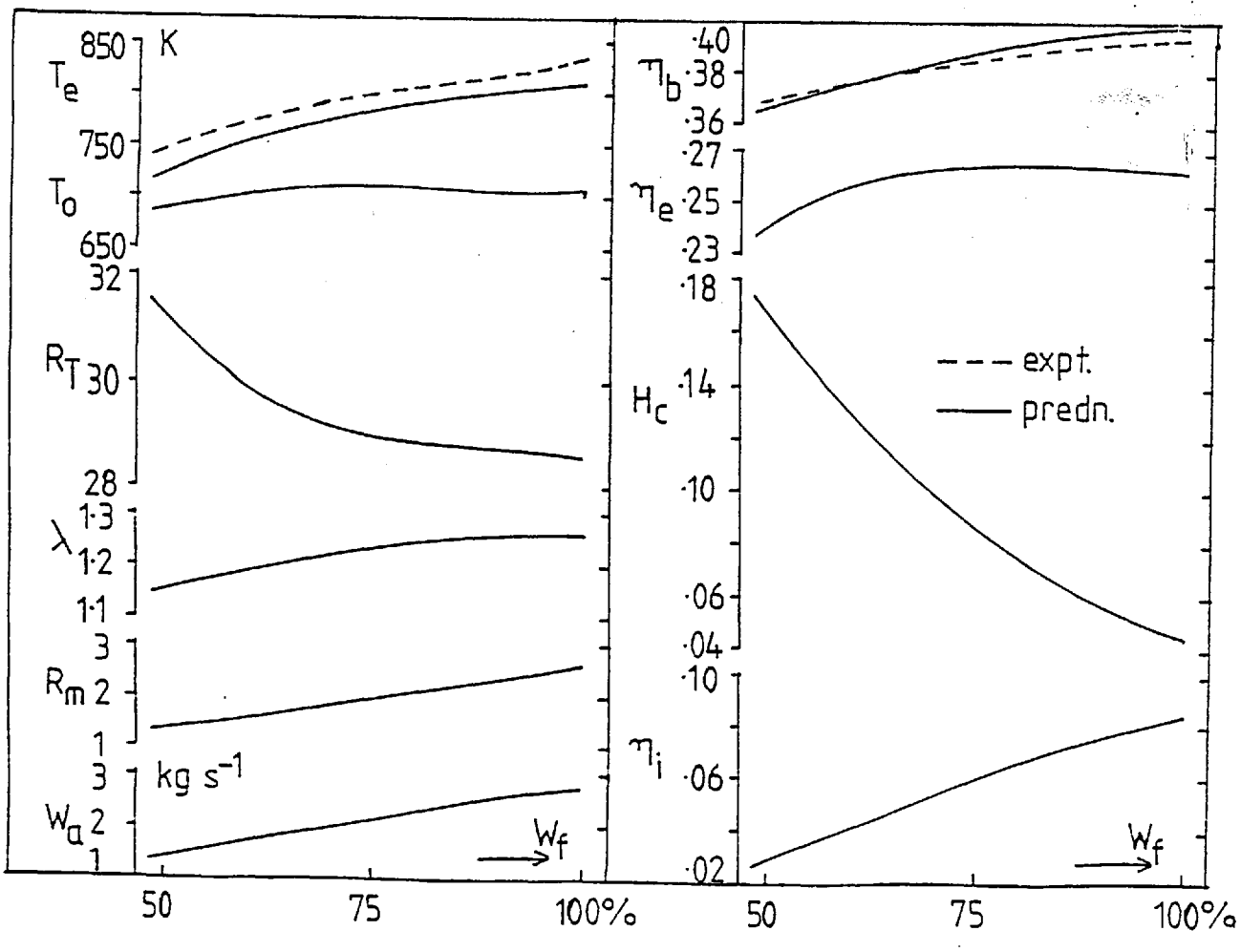

Fig. 4.2 6RKC Predicted Characteristics

and 1000 rpm forms: data was obtained for the 1000 rpm engine, and although at this speed it is not suitable to burn heavy fuel oil, the simulation results are included here for comparison. Engine details are given in table 4.2, and predicted and experimental operating characteristics in fig. 4.2.

The results will concentrate on the design point which is the full load operating condition. This is the general practice in the published literature: it is usually the case that an engine designed on the full load point, will operate satisfactorily at part loads. Some part load results are however included as a check. The results for the 9AT350 are presented first and in more detail, than the second set of results on the 6RKC.

9AT350

1. Back Pressure

The simulated engine response to back pressures up to 1.2×10^5 Nm^{-2}, well beyond those normally accepted for engine operation, are shown in figure 4.3. At this high back pressure the trapped air-fuel ratio is almost down to 24, a lower limit recommended by the manufacturer to ensure efficient combustion, and hence higher back pressures were not investigated.

Fig. 4.3 shows the parameters to respond approximately linearly to the increasing back pressure. There is a slight decrease in brake efficiency because more pumping work is expended against the higher exhaust manifold pressure on the exhaust stroke. The fraction of heat rejected to the engine coolant is slightly increased: the reduced trapped air-fuel ratio giving higher closed cycle temperatures (by 60-70^{o}C) and hence higher thermal loading. The changes in the fraction

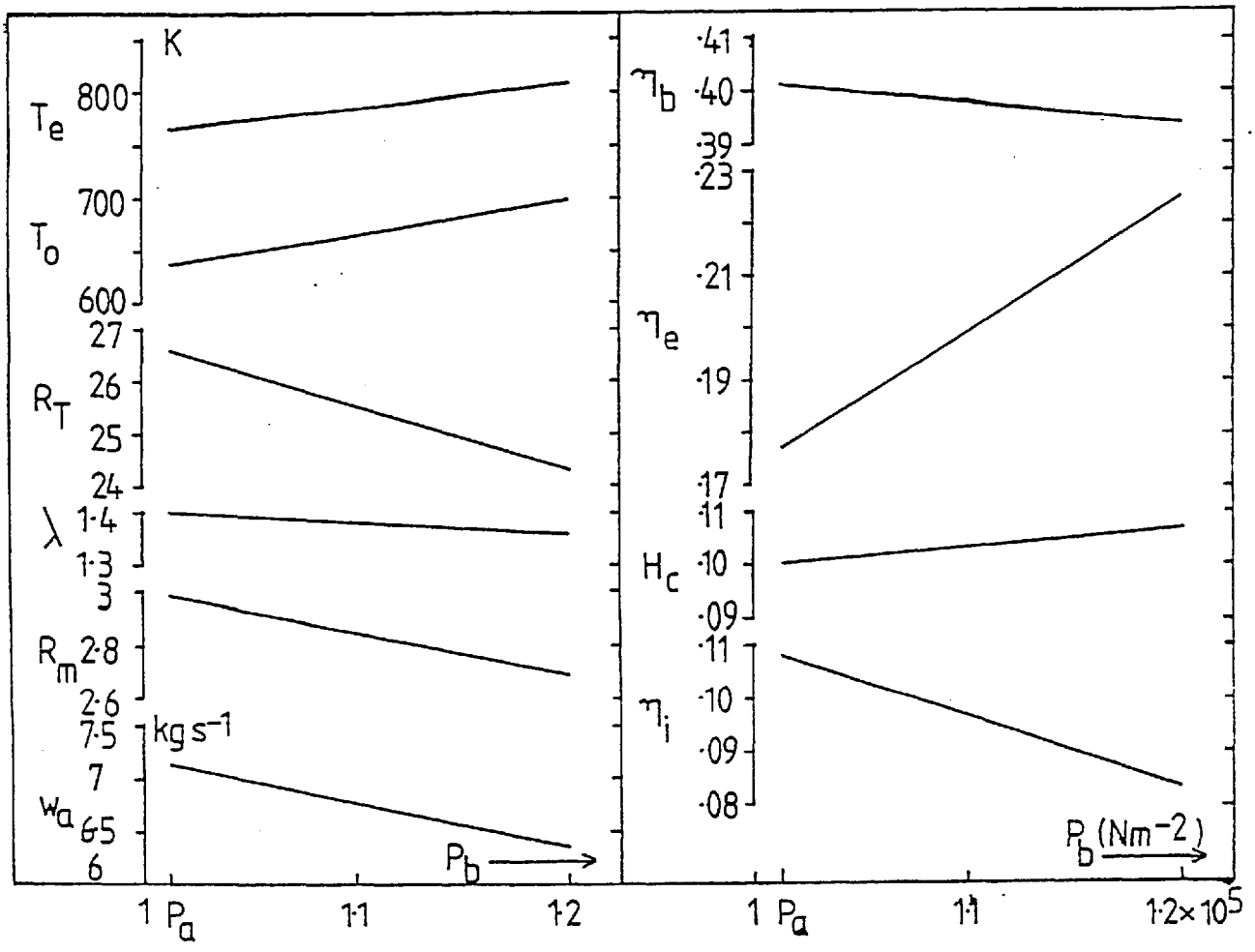

Fig. 4.3 9AT350 Exhaust Back Pressure

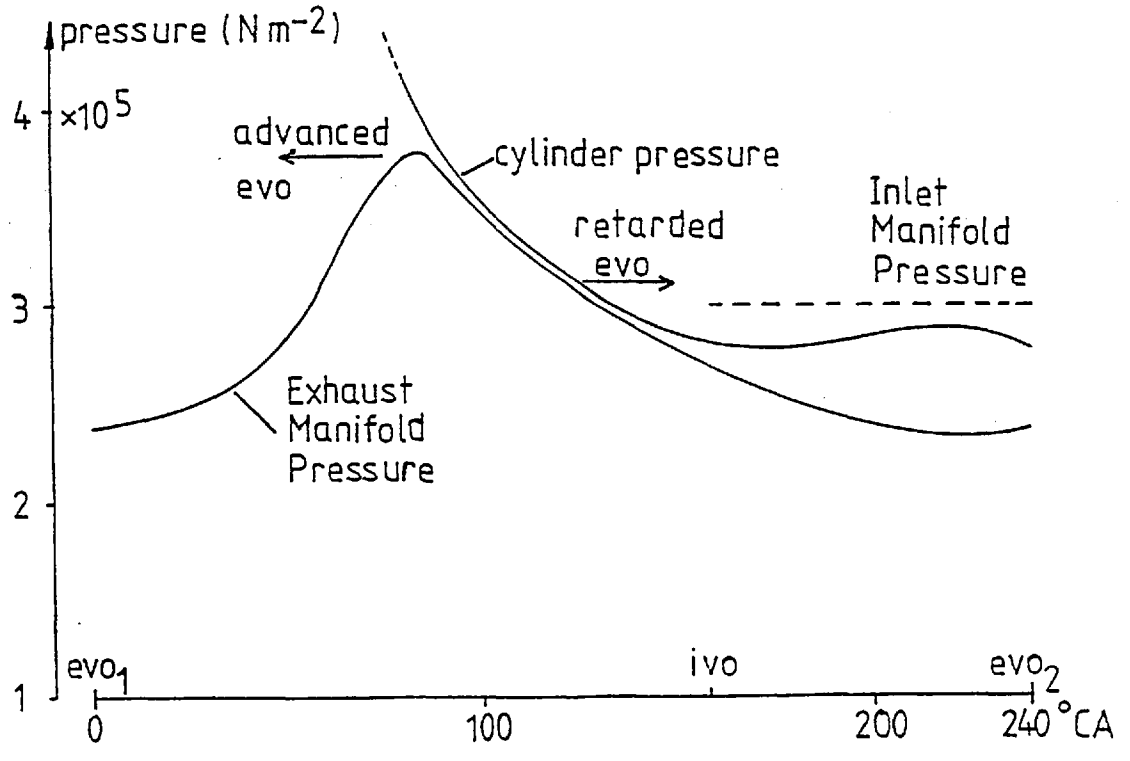

Fig. 4.4 9AT350 Predicted Control Volume Pressures during Open Period

of exhaust heat recoverable (η_e), based on a boiler exit temperature of 200°C to avoid corrosion, and the heat rejected to the intercooler are more marked. The increase in η_e, nearly 5% of fuel input energy at $P_b = 1.2 \times 10^5$ Nm^{-2}, results from the higher turbine outlet temperature, and hence the greater potential temperature drop across the boiler. The reduction in heat to intercooler, 2.5% of fuel input energy, is caused by the reduced airflow.

At a back pressure of 1.2×10^5 Nm^{-2} there is an increase in recoverable heat, including jacket water, intercooler and exhaust, of 3% of fuel input energy, and a decrease in brake power of 0.7% of fuel input energy. At a power to heat value ratio of around 3:1, the value added to the fuel is on balance increased. The advantage with higher back pressures of a smaller and hence cheaper exhaust heat recovery boiler will be quantified in section 4.2.4.

The heat rejected to the intercooler is at the lowest temperature of all the cooling circuits, and it may not be possible to find a use for it. The shift from η_i to η_e is therefore an advantageous shift from low to high temperature heat.

The step by step values of gas flows given by the program, reveal no problems with reversed flows at ivo within the range of back pressures investigated, but the possibility of pulse interference inherent in the long valve overlaps of this engine, is increased. The engine operating line does not move significantly nearer to the surge line of the compressor map, and hence there is no need to rematch the compressor.

2. Exhaust Valve Opening

The timing of the exhaust valve opening is severely restricted on the pulse turbocharged engine, by the interaction between the pressures in the exhaust manifold and cylinders. Early opening extends the period at the start of blowdown when two cylinders are open to the exhaust

manifold, and the blowdown pulse of one cylinder may interfere with the end of the scavenge period of the other (fig. 4.4). Delayed opening means that the cylinder pressure may still be high at ivo, and backflow from cylinder to inlet manifold may occur, with the concomitant problems of inlet valve contamination.

The standard timing for the exhaust valve opening on the 9AT350 is 102° after tdc: predicted operating conditions for evo up to 30° either side of this are shown in fig. 4.5. The period of exhaust valve opening is already long, and evo any earlier than standard results in pulse interference between cylinders, indicated by the rapidly decreasing airflow shown in fig. 4.5. For evo later than around 120° atdc, backflows cylinder to inlet manifold occur at ivo.

Within the very restricted range of acceptable values there is therefore no advantage for diesel CHP, of changing the timing of the exhaust valve opening.

3. Reduction of Boost Pressure

By increasing the turbine effective area the flow resistance is reduced, resulting in lower pressure drops across the turbine. Less energy is therefore extracted and the boost pressure falls. In accordance with the philosophy of making readily achievable modifications, turbine builds within the standard Napier range were used. These were simulated by applying correction factors for gas flow and efficiency to a standard map.

The results of the simulations are presented in figure 4.6. At a turbine effective area of 179 cm^2, corresponding to the build 570K, the trapped air-fuel ratio is down to 24:the lower limit suggested by the manufacturer.

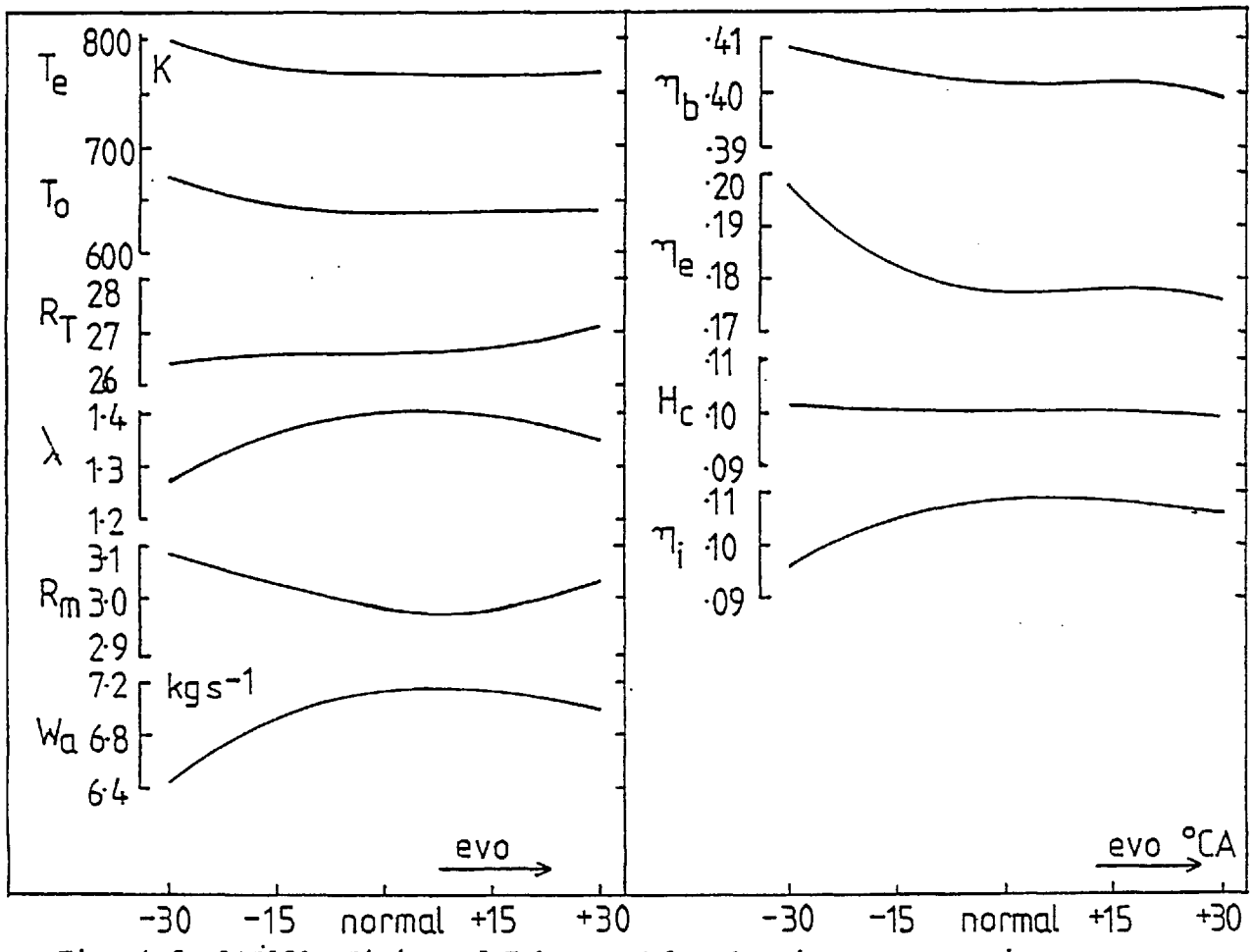

Fig. 4.5 9AT350 Timing of Exhaust Valve Opening

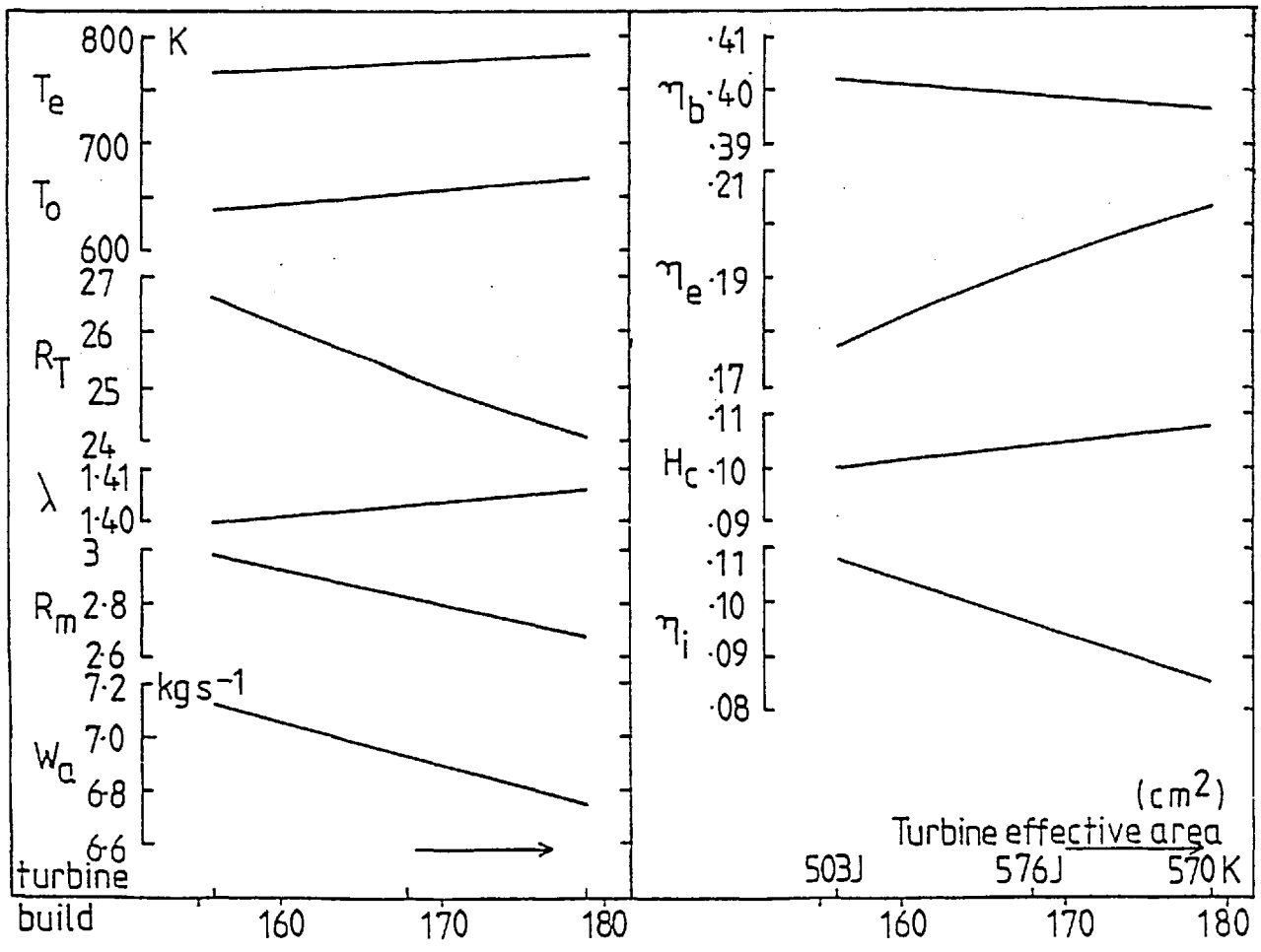

Fig. 4.6 9AT350 Reduction of Boost Pressure

The lower exhaust manifold pressure leads to an increase in λ, tending to oppose the exhaust temperature increases from reducing R_T. The turbine outlet temperature increases more rapidly than the turbine inlet temperature, because less energy is extracted from the exhaust gas. The result of these interacting influences is that at $R_T = 24$ the brake power is down by 0.4% of fuel input energy, heat to intercooler down by 2.3%, heat to jacket coolant up 0.8%, and to recoverable exhaust up 2.5%. The increase in heat to the exhaust is therefore almost balanced by the decrease in heat to intercooler: the advantage is the improvement of the grade of recoverable heat.

The operating line on the compressor map was found to move slightly away from the surge line, but not enough to justify a diffuser change. No problems with reversed flows were apparent. Closed cycle temperatures are increased by around 70°C; similar to the change for the increase in back pressure as might be expected.

4. Valve Overlap Reduction

At 168°CA the valve overlap on the 9AT350 is rather longer than most 4-stroke engines. This was reduced in steps of 10°CA to 98°CA, and the revised operating conditions calculated. The changes to ivo and evc were such as to maintain an approximately symmetrical straddle about tdc.

The design operating line on the compressor map must be chosen to maintain a margin of 10% of airflow from the surge line. It must also be clear of choking. The margin must be allowed in order to accept the gradual reduction in airflow due to compressor, turbine and intercooler fouling, and to be clear of surge under rapid load changes. Reduction of the valve overlap reduces the airflow at approximately constant boost pressure, and hence the compressor diffuser area must be reduced to maintain the margin from surge. Again the approach was

adopted of using diffusers from the standard Napier size range; these have been represented by compressor airflow correction factors of 0.91 for each diffuser size reduction applied to a standard map.

The results of the computer simulations are presented in figure 4.7. The discontinuities are caused by the diffuser changes. A lower limit on the scavenge ratio of 1.1 was recommended by the manufacturers, to ensure adequate scavenging of combustion products. At an overlap reduction of 70°CA λ is reduced to slightly less than this limit, and hence this was taken as the lowest acceptable valve overlap. The computed cylinder contents at evc indicate that scavenging is still adequate at an overlap of 98°CA.

The actual exhaust enthalpy decreases, but the increasing exhaust gas temperatures, 1.7°C/°CA overlap reduction, mean that the available exhaust heat increases. There is an increase in brake power fluctuating between 0.3 and 0.6% of fuel energy input, resulting from lower pumping work. The trapped air-fuel ratio stays fairly constant and hence so does the heat rejection to coolant. Lower gas flows result in a reduction of heat to the intercooler. At the lower limit on λ, η_e, H_c and η_b are increased by 7.2%, 0.2% and 0.3% of fuel input energy respectively, and η_i reduced by 2.9%. Thus there is an increase of 4.5% in available heat and it is of a higher quality, and unlike the case for boost reduction and back pressure increase, an increase in power output of 0.3%.

The possibility of pulse interference with the long valve overlap of the standard design, is eliminated with the shorter overlaps.

5. Heat Extraction before the Turbine

An example is given to illustrate the consequences of extracting heat from the exhaust gases before they reach the turbine. The full

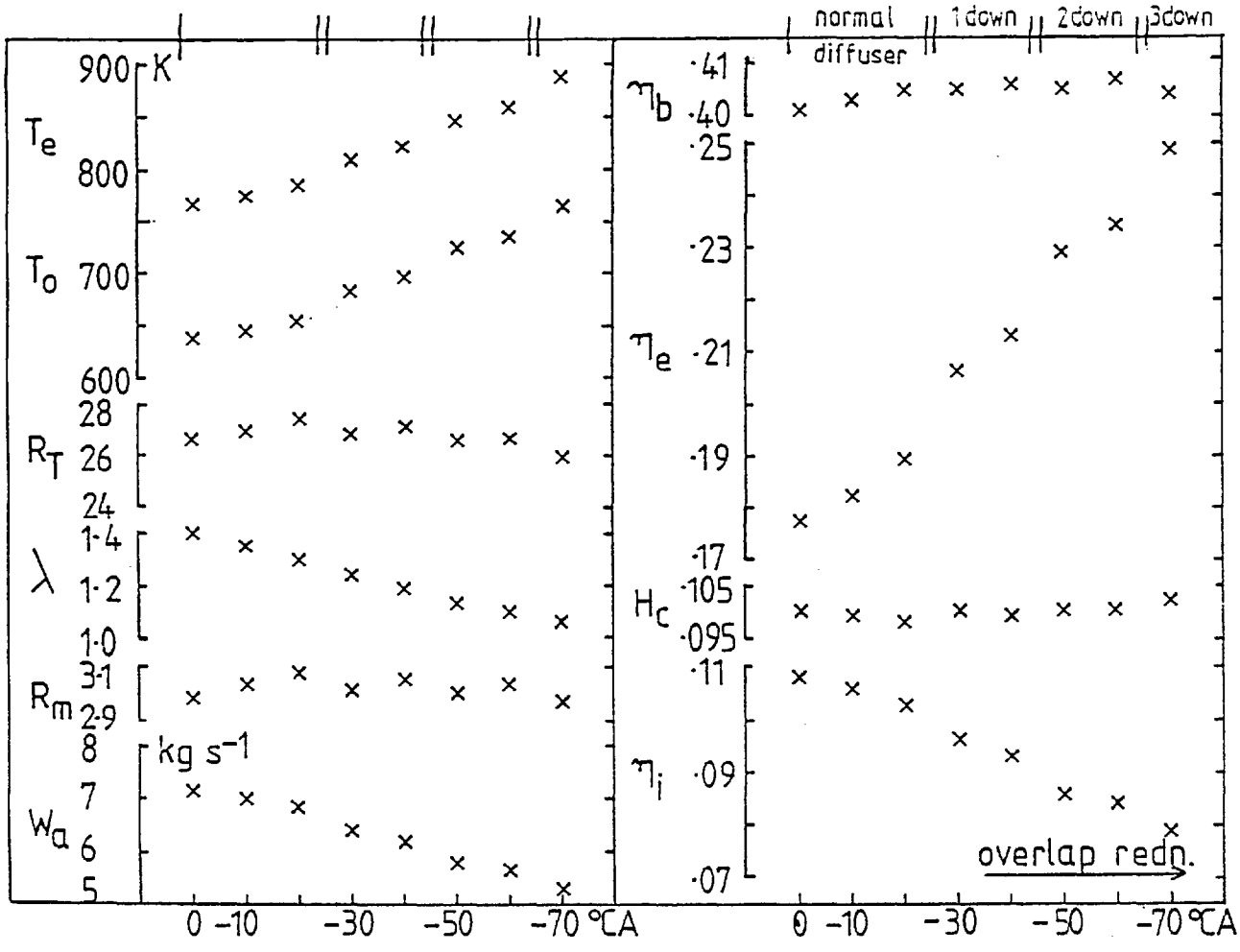

Fig. 4.7 9AT350 Overlap Reduction .

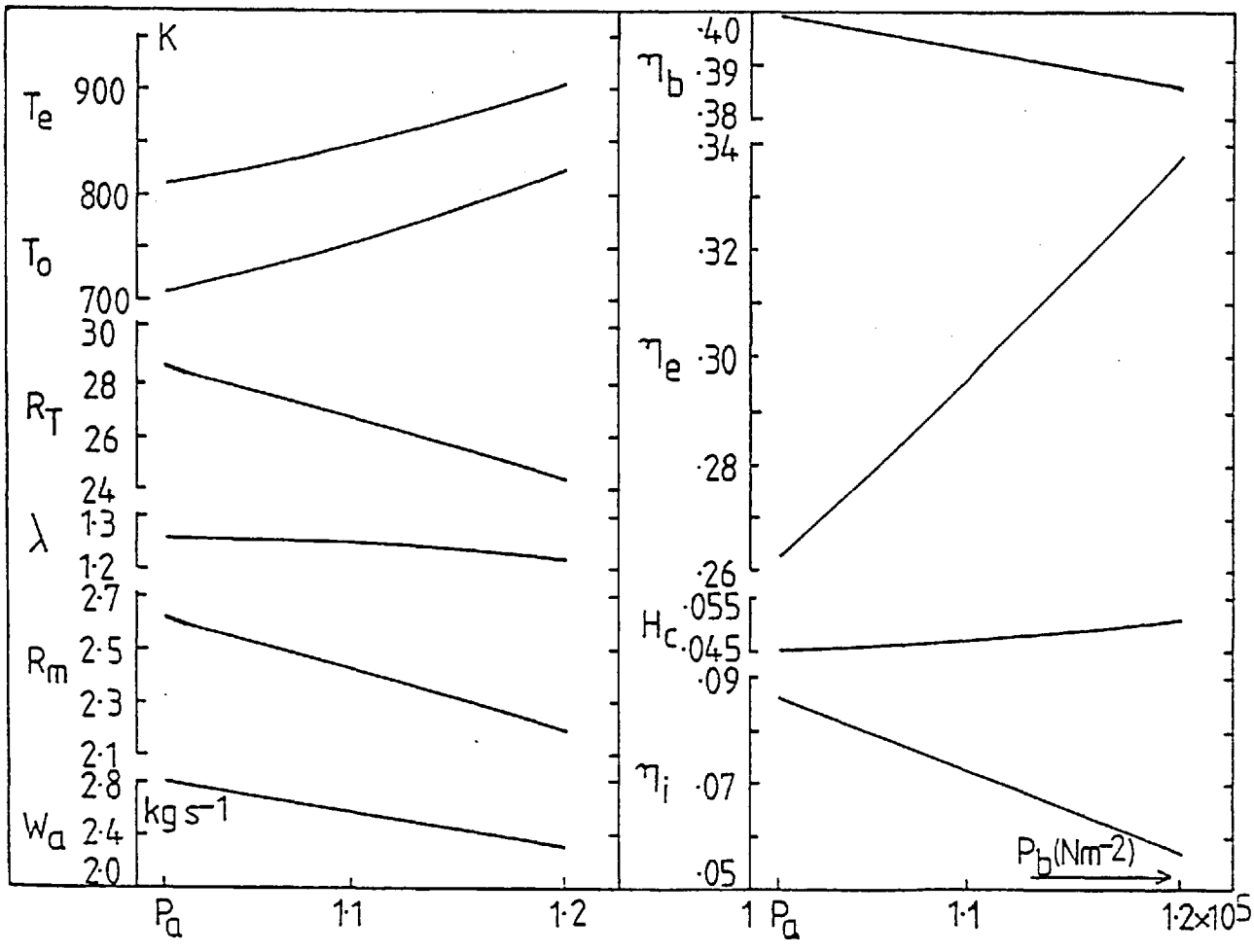

Fig. 4.8 6RKC Exhaust Back Pressure

load gas temperatures, at the turbine inlet when the overlap is reduced by 70°CA are close to 900K. An attempt was made to simulate the reduction of temperature below the sodium-vanadium eutectic temperature, thereby reducing the danger of sodium-vanadium contamination of the turbine.

Gas-in-tube or water-in-tube heat transfer arrangements might be used for the heat extraction. The physical characteristics of the latter would entail a change to constant pressure turbocharging, whereas pulse turbocharging could be retained with the former, although some ingenuity might be required in the exhaust manifold arrangement. In the example presented, the gas-in-tube heat transfer surface is used.

For turbulent gas flow in tubes: $Nu = 0.023\ Re^{0.8}\ Pr^{0.3}$ ... (i)

and $\dot{Q} = hA\ (T_{e_{av}} - T_w)$ ... (ii).

For 'tuned' pulses the exhaust manifold volume V_{em} must remain constant

hence $l = \frac{4V_{em}}{N\pi d^2}$ ... (iii)

where h = overall heat transfer coefficient from (i) (assuming gas side resistance dominates)

A = total heat transfer area.

$T_{e_{av}}$ = average of cylinder exit and turbine inlet gas temperatures

T_w = water temperature

N = number of tubes

d = diameter of tubes

l = length of tubes.

From these three equations therefore, one may determine the number and diameter of tubes for a required heat extraction before the turbine.

Numerical results of the simulations are shown in table 4.3. Column 2 shows that if heat transfer surface is introduced on its own, the turbine power falls, the boost pressure therefore falls and hence the thermal loading of all engine components increases. Moreover,

TABLE 4.3

Heat Transfer before Turbine on 9AT350

	1	2	3a	b	c	4
Overlap	98°	98°	98°	98°	98°	168°
Turbine build	503J	503J	441J	441J	441J	503J
" effective area (cm^2)	156	156	143	143	143	156
Heat Transfer	No	Yes	Yes	Yes	Yes	No
W_a (kgs^{-1})	5.27	4.92	5.37	5.21	5.04	7.12
R_m	2.97	2.74	3.05	2.94	2.83	2.98
R_T	25.9	24.2	26.5	25.7	24.8	26.6
λ	1.06	1.06	1.06	1.06	1.06	1.40
T_e (K)	885	858	852	839	825	766
T_o (K)	764	749	726	718	710	637
η_b	0.404	0.399	0.404	0.402	0.405	0.401
η_e before turbine		0.050	0.026	0.049	0.074	
after "	0.249	0.221	0.218	0.205	0.192	0.177
H_c	0.102	0.107	0.101	0.103	0.105	0.100
η_i	0.079	0.066	0.083	0.077	0.071	0.108

the turbine inlet temperature does not fall much because the airflow decreases. By reducing the turbine nozzle area by 8% the turbine power, and hence boost conditions, may be partially restored as columns 3a to c indicate. As can be seen, lower turbine inlet temperatures inevitably imply lower trapped air-fuel ratios and hence greater component loading, for the fixed turbine build. Only by going to a more efficient turbine, an option not available within the Napier range, would it be possible to both reduce the turbine inlet temperature below the sodium-vanadium eutectic temperature, and to restore the boost pressure and hence trapped air-fuel ratios to their normal values. Heat extraction before the turbine transfers loading problems from the turbine blades to engine components, and hence is of limited usefulness.

6RKC

1. Back Pressure

A back pressure of 1.2×10^5 Nm^{-2} was again found to correspond approximately to the lower limit of 24 on R_T. Results are therefore presented in fig. 4.8 for the range $P_a \leqslant P_b \leqslant 1.2 \times 10^5$ Nm^{-2}. The same trends are observed as for the 9AT350, the changes to η_e and η_i being larger than to η_b and H_c, although the trapped air fuel ratio falls more quickly and hence η_e rises further. At $P_b = 1.2 \times 10^5$ Nm^{-2} the available heat is increased by 5% of fuel input energy, the brake power is decreased by 1.3%.

2. Exhaust Valve Opening

Standard evo is 150° after tdc, and permissible values were found to be restricted to the range 135° to 175° after tdc, in order to avoid pulse interference effects. Again no significant improvement to CHP performance was found within the acceptable range.

3. Reduction of Boost Pressure

An increase in the turbine effective area by 18% was sufficient to reduce the trapped air-fuel ratio to 24 as fig. 4.9 shows. All trends are as for the 9AT350, but the exhaust heat recovery rises more quickly than the intercooler heat rejection falls. At $R_T = 24$, corresponding to a reduction in the full load boost pressure by 15%, the recoverable heat is increased by 2.2% of fuel input energy with a shift from low to high temperature, but this is counteracted by a reduction in brake efficiency of 0.8%.

4. Valve Overlap Reduction

The standard overlap on the 6RKC is shorter than that on the 9AT350: 136°CA as opposed to 88°CA. The normal scavenge ratio is 1.26 and hence the potential increases in available heat are smaller. The lower limit of 1.1 on λ is reached at an overlap of 88°CA, and corresponds to an increase in available heat of 3.4% and of power of 0.3%. The results are given in Fig. 4.10.

5. Heat Extraction before the Turbine

The results of the attempts to reduce the turbine inlet temperature for a valve overlap of 88°CA, followed a similar pattern to the example given for the 9AT350, and are shown in Table 4.4.

4.2.2 Further Improvements

So far each of the design modification options has been considered in isolation. However by the combination of changes further improvements may be achieved.

It was found for the 9AT350, that by reducing the turbine nozzle area to the next build down (441J), keeping the same turbine efficiency, that it was possible to increase the boost pressure ratio and hence the trapped air-fuel ratio, both for reduced overlap and increased

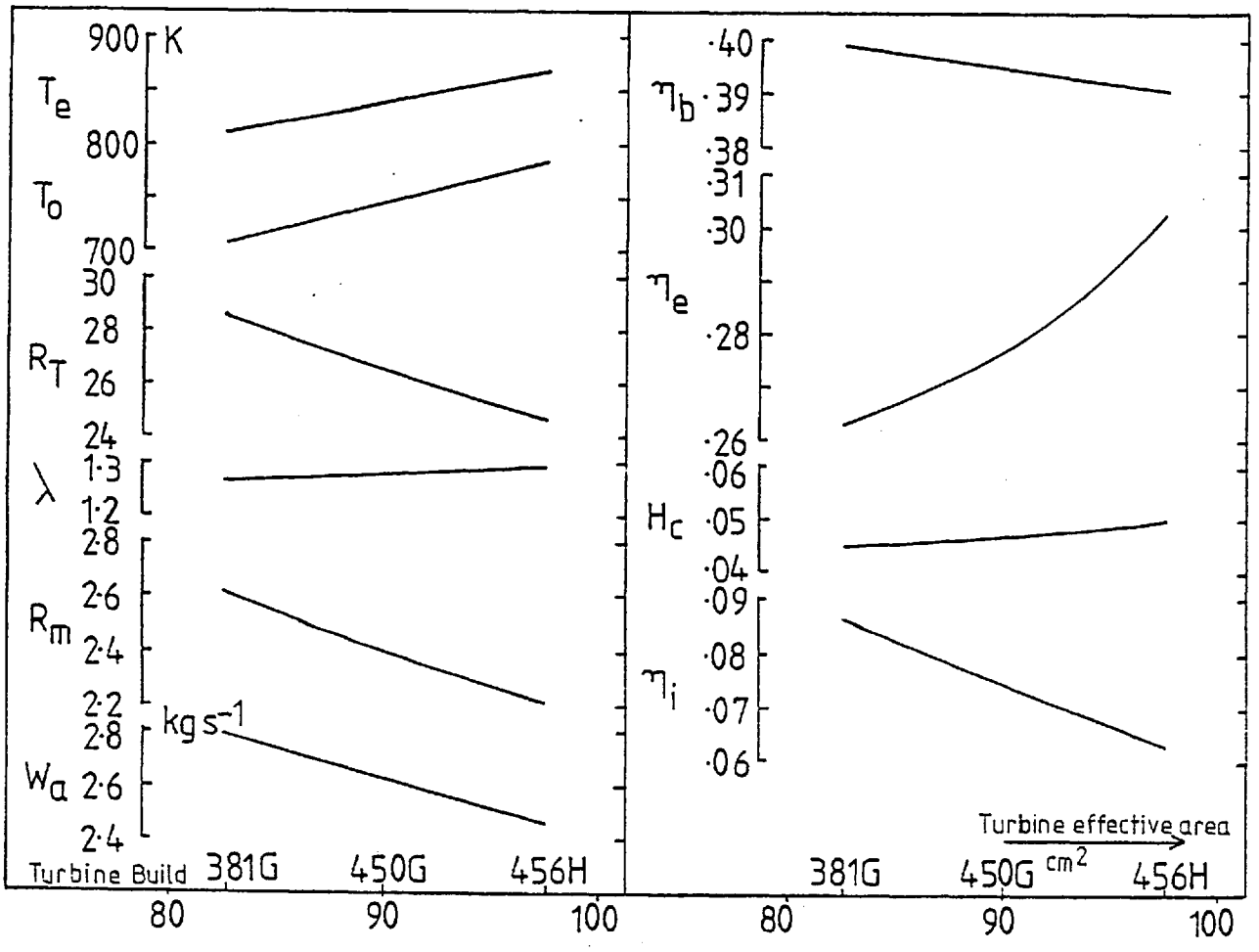

Fig. 4.9 6RKC Reduction of Boost Pressure

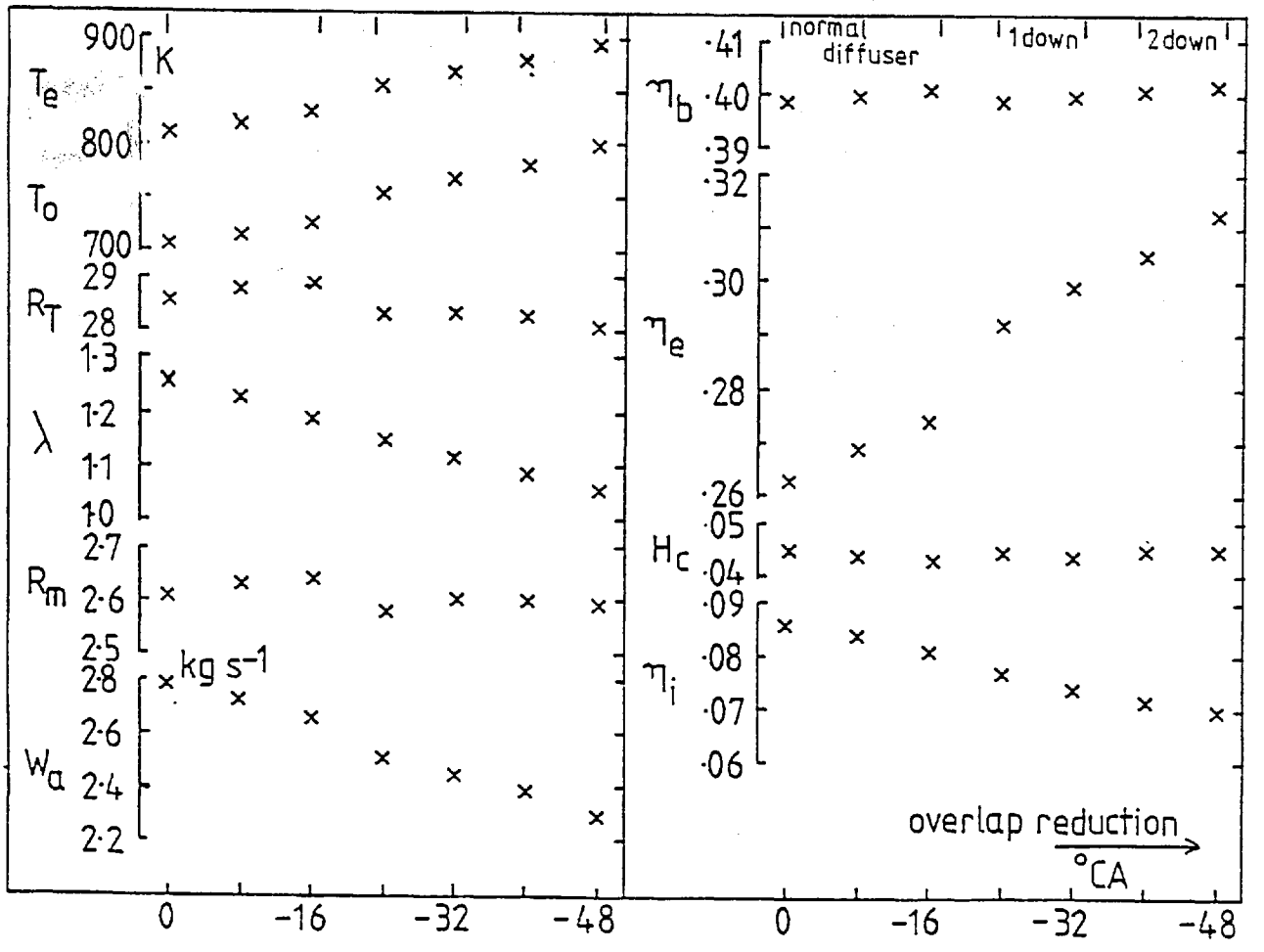

Fig. 4.10 6RKC Overlap Reduction

TABLE 4.4

Heat Transfer before Turbine on 6RKC

	1	2	3	4
Overlap	88^{o}	88^{o}	88^{o}	136^{o}
Turbine build	381G	381G	326G	381G
" effective area (cm^2)	82.6	82.6	75.2	82.6
Heat Transfer	No	Yes	Yes	No
R_T	28.1	24.8	27.0	28.6
T_e (K)	897	869	836	812
T_o (K)	798	787	741	707
η_b	0.402	0.392	0.397	0.399
η_e before Turbine		0.085	0.081	
η_e after "	0.313	0.261	0.237	0.263
H_c	0.045	0.050	0.047	0.045
η_i	0.070	0.062	0.067	0.086

back pressure conditions. Fig. 4.11 shows the full load operating point for the 9AT350 with 98°CA overlap and the 441J build turbine (an area reduction of 8% over the normal build). The trapped air-fuel ratio at full load is in fact higher than the normal design and hence thermal loading on all components except the turbine will be lower. There is still a gain of 5.4% of fuel input energy in η_e, 0.6% in η_b, a fall of 0.2% in H_c, 1.8% in η_i giving an overall improvement of 3.4% in heat, 0.6% in power.

With this overlap and turbine build the results of back pressure increase were simulated and are summarised in fig. 4.11 and table 4.5a. Table 4.5a shows the change in full load operating condition compared to the normal design. The increase in back pressure brings higher heat recoveries, lower brake power and an increase in thermal loading. However back pressure up to around 1.1×10^5 Nm^{-2} can be tolerated with only the same loading as the conventionally designed engine, but with higher heat recovery and the benefit of a cheaper boiler (quantified in the next section). At a back pressure of 1.2×10^5 Nm^{-2} R_T and λ are both down to their recommended lower limits: whichever ways are chosen to reach these limits the improvements to heat recovery, etc. will be similar.

A further option identified by the manufacturers was a newly available range of turbochargers having higher efficiencies than those considered so far. Results of introducing these were simulated by increasing the compressor efficiency by 6% and the turbine efficiency (503J build) by 7%. The results are shown in fig. 4.12 and table 4.5b for the 9AT350 at full load with 98°CA overlap and increasing back pressures, for comparison with the previous set of results. Although the improvement in heat recovery is somewhat less, power is increased and the thermal loading is reduced. The determinant of the optimum

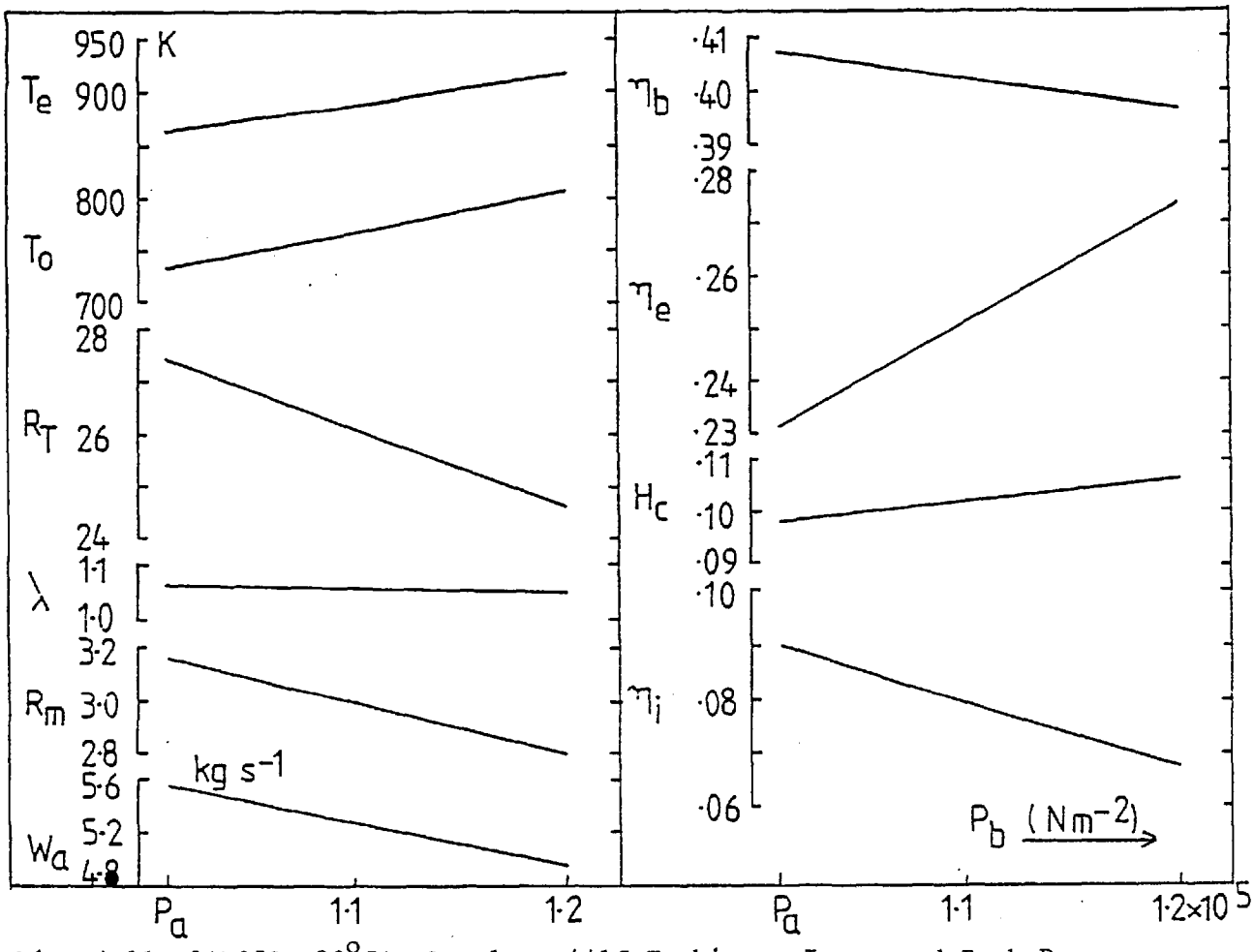

Fig. 4.11 9AT350 98°CA Overlap, 441J Turbine: Increased Back Pressure

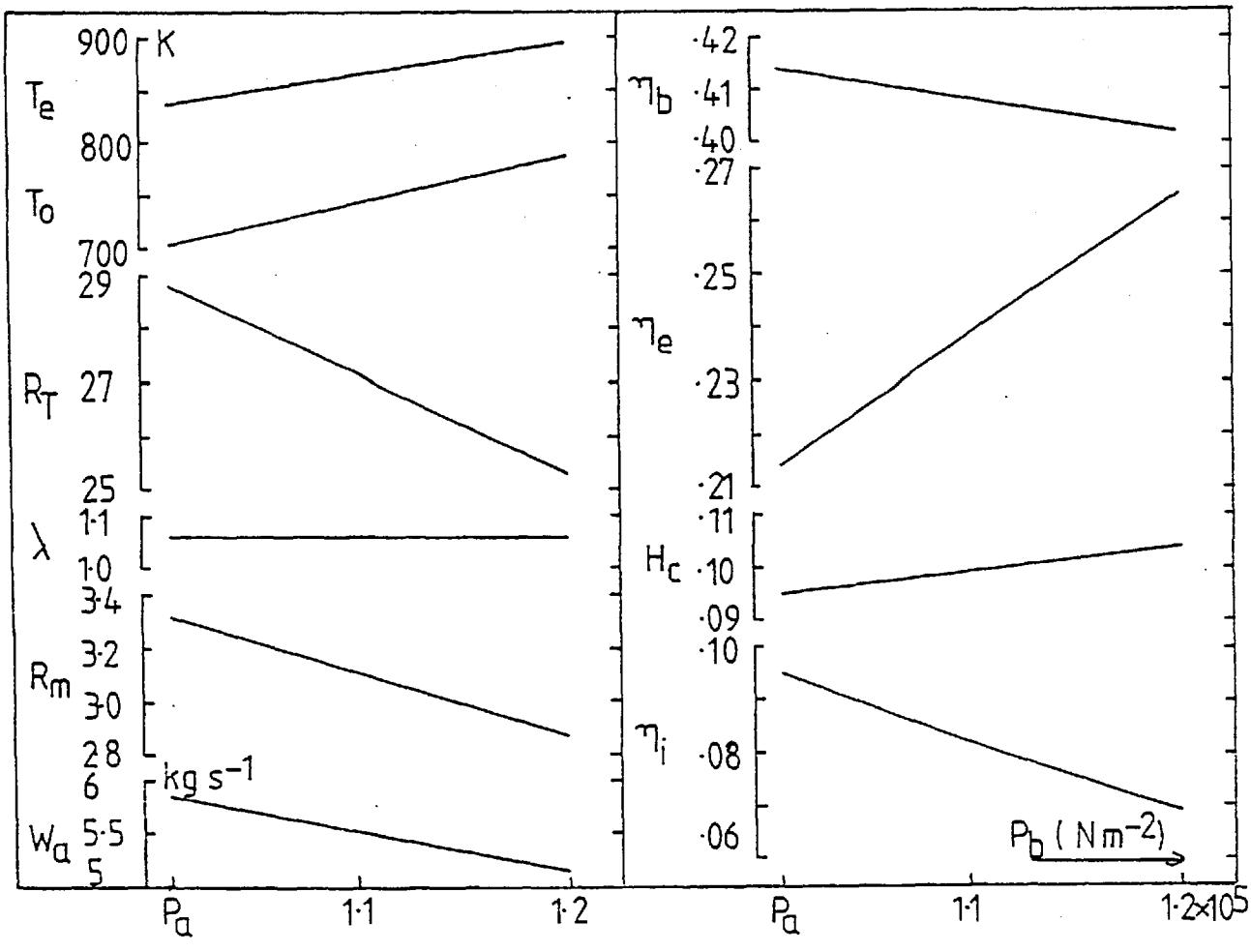

Fig. 4.12 9AT350 98°CA Overlap, Improved Turbocharger Efficiency

Energy Recovery and Back Pressure at Reduced Overlap: 9AT350

TABLE 4.5a

Turbine build 441J

Overlap 98^{o}

	P_b =	1.013×10^5	1.1×10^5	1.2×10^5 Nm^{-2}
change	$\Delta\eta_b$	+0.006	+0.001	-0.004
over	$\Delta\eta_e$	+0.054	+0.074	+0.097
normal	$\Delta\eta_i$	-0.018	-0.029	-0.040
design	H_c	-0.002	+0.002	+0.006
	heat	+0.034	+0.047	+0.063
	power	+0.006	+0.001	-0.004

TABLE 4.5b

Turbine build 503J Increase in compressor and turbine efficiencies

Overlap 98^{o} 6 and 7% respectively.

	P_b =	1.013×10^5	1.1×10^5	1.2×10^5 Nm^{-2}
change	$\Delta\eta_b$	+0.013	+0.007	+0.001
over	$\Delta\eta_e$	+0.037	+0.062	+0.088
normal	$\Delta\eta_i$	-0.013	-0.026	-0.039
design	H_c	-0.005	-0.001	+0.004
	heat	+0.019	+0.035	+0.043
	power	+0.013	+0.007	+0.001

will therefore be the relative values of heat, power and capital costs.

4.2.3 Comparison with Published Results

Although results presented by other authors relate to specific engines, and are to some extent determined by program techniques and assumptions made about other parameters, it is helpful to see if the same trends are observed elsewhere.

Very little systematic work has been published on the affect of back pressure on engine operating conditions. Results of Watson (Ref. 88) and Holler (Ref. 39) for turbocharged, 4-stroke engines show rates of increase of exhaust manifold temperature (T_e) with back pressure similar to those predicted for the Ruston engines.

The relationship between the boost pressure and the other operating parameters have been simulated by full step-by-step models by Woschni (Ref. 94), and Ryti (Ref.73). Both sets of results relate to modern 4-stroke engines: boost pressure ratios up to 2.5 are considered by Woschni, and beyond present technology to 4 by Ryti. Similar trends are observed: rising T_e and H_c, falling R_T and η_b with falling boost pressures, but with some variations in the rates of change.

The operating characteristics of valve overlaps in the range 0-120°CA are simulated in Ref.94, 80-135°CA in Ref.75, 20-120°CA in Ref.73. Between 80° and 120°CA overlap, the rate of increase of exhaust manifold temperature with overlap reduction, vary between 1°C/°CA for the constant pressure turbocharging engine of Ref.75, to 1.7°C/°CA for the pulse turbocharging of Ref.94. These may be compared to 1.7°C/°CA for the 9AT350 and 1.75°C/°CA for the 6RKC. Airflow reductions of 2.3%/°CA overlap reduction of Ref.75 to 3.6%/°CA of Ref.94, are comparable to the 2.6%/°CA for the 9AT350 and 3.6%/°CA for the 6RKC.

In response to receipt of the results from the Match 8 program, D. Sinha and K. Ball of Ruston diesel engines, reproduced some of the results for back pressure increase and overlap reduction for the 9AT350 with their own full step-by-step model. Overlap reduction to 110^{o}, and a back pressure of 1.1 bar at full load were simulated. Agreement between Match 8 and the Ruston model was good.

4.2.4 The Relationship between Back Pressure and Boiler Size

The capital cost of the exhaust heat recovery boiler depends strongly on the tubing area. To evaluate the saving in capital cost resulting from higher back pressures, the relationship between back pressure and tubing area must therefore be found. The wide variety of steam and feedwater conditions, boiler types and tubing types and arrangements make it difficult to generalise. A fairly 'typical' example will therefore be given, but specific calculations would be required if different steam conditions or boiler types were contemplated.

As stated in Chapter 2 water tube boilers are studied. Plain tubes are used, although some waste heat boiler manufacturers recommend finned tubes: the heat transfer and pressure drop formulations are similar. Table 4.6 from Ref.28 shows, for various in-line tube spacings, values of C_H and C_f used in the heat transfer formulation $Nu = 0.32\ C_H\ R_e^{0.6}$ and pressure drop $P = C_f\ Npv^2 \times 10^{-3}$ where:

p = gas pressure

v = gas velocity

N = number of longitudinal tubes.

For increases in spacing along the gas flow direction, C_f increases but C_H remains constant: it is best therefore to pack closely in the direction of gas flow. The ratio C_H/C_f increases with transverse spacing indicating the use of a wider transverse spacing. Studies using

TABLE 4.6

Heat transfer coefficients for cross-flow over plain tubes

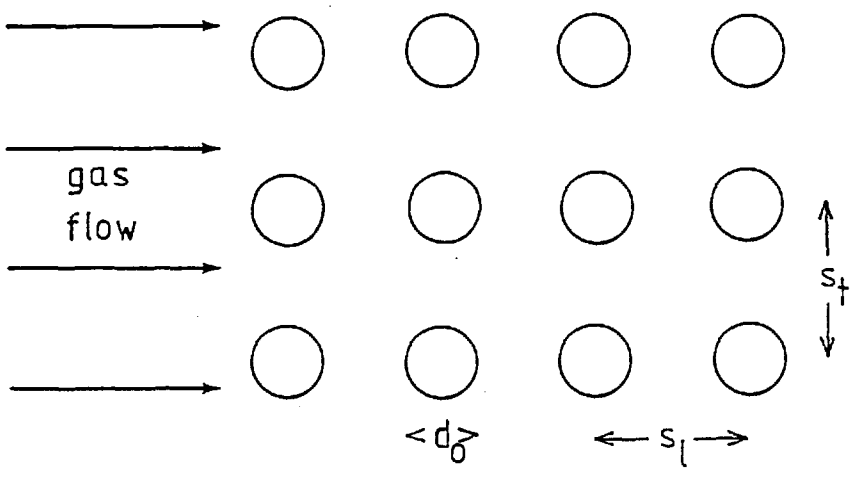

S_l =	$1.25d_o$			$1.5d_o$			$2.0d_o$			$3.0d_o$		
	C_H	C_f	C_H/C_f	C_H	C_f	C_H/C_f	C_H	C_f	C_H/C_f	C_H	C_f	C_H/C_f
S_t =												
$1.25d_o$	1.04	0.85	1.23	1.05	1.03	1.02	1.03	1.37	0.75	0.98	2.06	0.48
$1.5d_o$	0.96	0.65	1.48	0.96	0.78	1.24	1.01	1.04	0.97	1.01	1.56	0.64
$2.0d_o$	0.83	0.425	1.95	0.83	0.51	1.63	1.0	0.68	1.47	1.02	1.02	1.0
$3.0d_o$	0.81	0.23	3.52	0.81	0.28	2.89	1.02	0.42	2.43	1.02	0.56	1.82

the boiler simulation program supported these conclusions. No clear advantage is discernable from the use of staggered tube arrangements.

Tube spacings of S_l (longitudinal) = $1.25d_o$, s_t (transverse) = $2.0d_o$ (d_o = tube on boiler diameter) were taken for the example. Back pressure was varied by altering the number of transverse tubes and hence the minimum flow area (A_{min}). Then to a rough approximation heat transfer rate is proportional to $A_{min}^{0.6}$, pressure drop to A_{min}^{-2}. Feedwater temperature was 50°C; steam at 10 bar pressure with 20°C of superheat was produced. The boiler was designed to give a gas exit temperature of 200°C at full engine load.

The resulting relationship between tubing area and back pressure for the 9AT350 at full load is shown in Figure 4.13. The important feature is the rapid rate of decrease of tubing area for the first increments in back pressure, but diminishing reductions at higher back pressures. Considerable savings in tubing area may be achieved. It is to be expected that other tube arrangements and boiler types would show similar trends.

4.2.5 Economics of Engine Design Changes

The increments in value added to the fuel input for the 9AT350 engine, for changes to the heat and power recovery are shown in Figure 4.14. The values assumed for heat and power are heat from an oil fired boiler at 80% efficiency and the approximate marginal value of electricity, both in January 1978. A load factor of 0.75 and a project life of 25 years are used. Discount rates of 5 and 10% were chosen as representative of test discount rates used by the nationalised industries. The increments in net present values of recovered heat, for the reduced value overlap and raised back pressures, of between £100,000 and

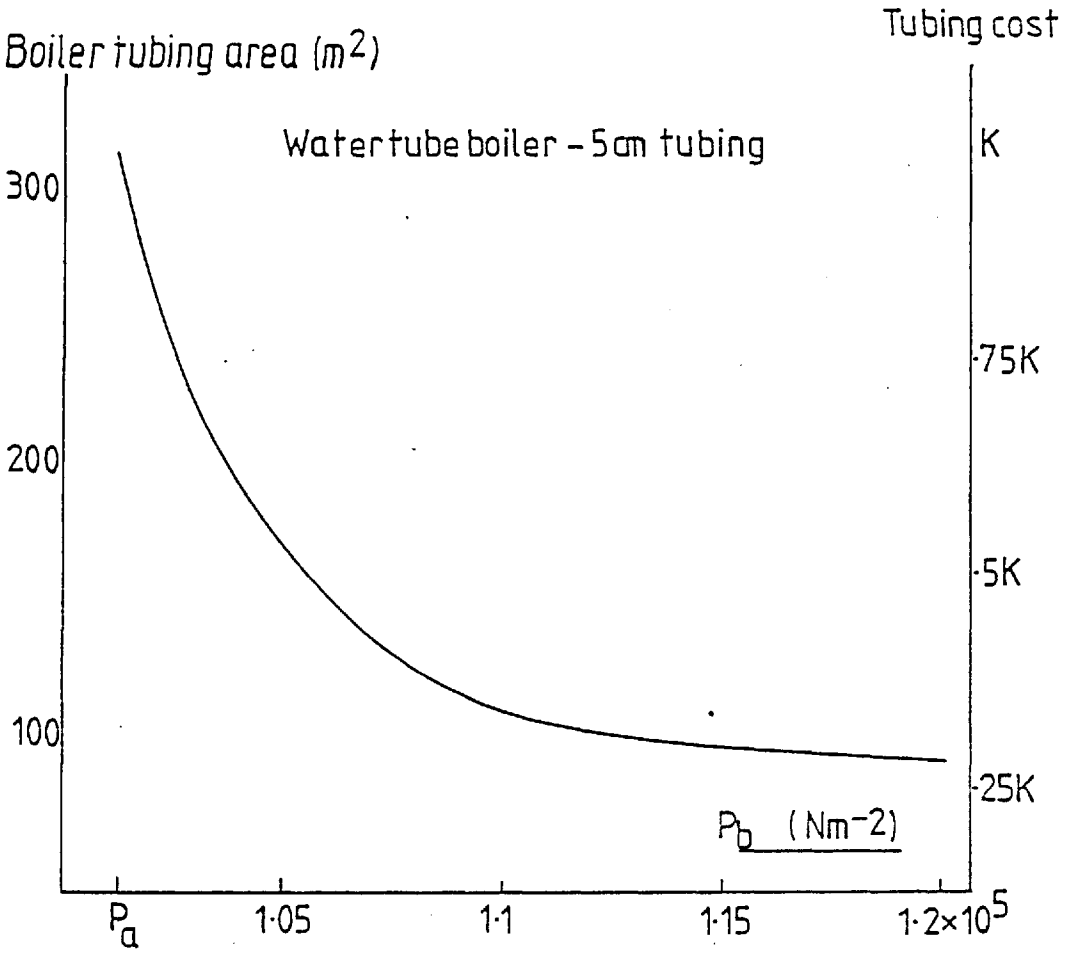

Fig. 4.13 9AT350 Waste Heat Boiler Sizing

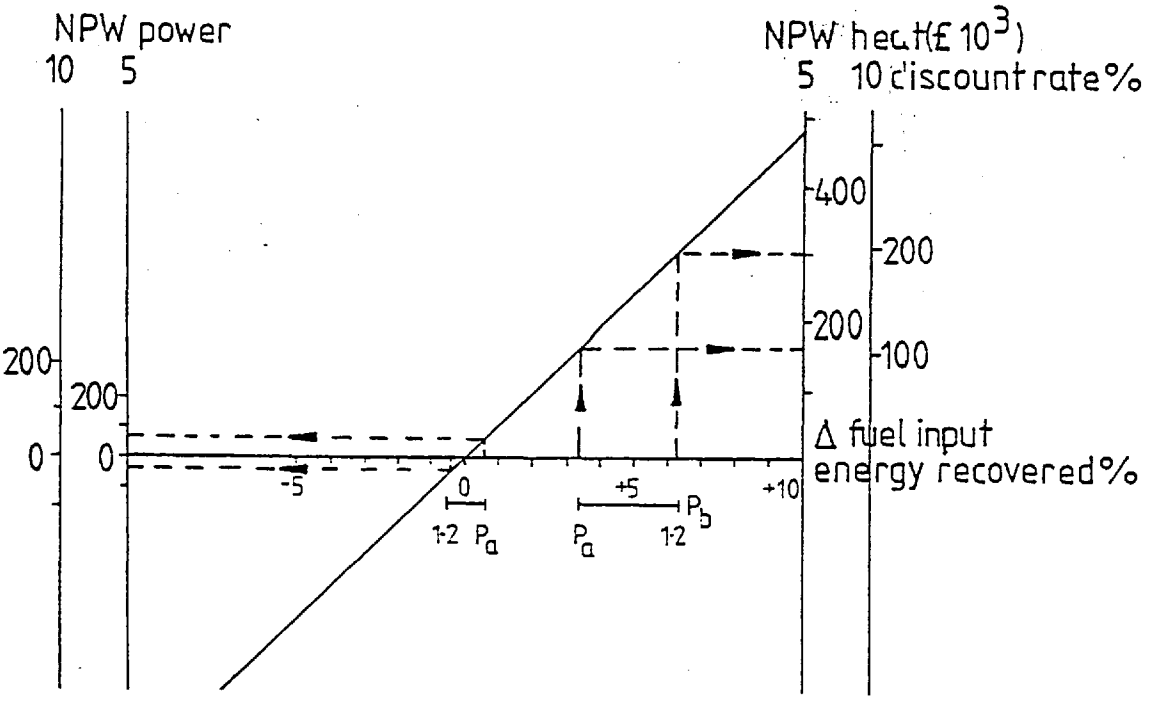

Fig. 4.14 9AT350 Value of Changes to Heat and Power Recovery

£300,000 may be compared to the £700,000 capital cost of a CHP scheme using the 9AT350 with a capital cost of £200/kW.

It is also interesting to compare the savings in boiler cost with higher back pressures, to the gains in value added to the fuel. A back pressure of 1.2×10^5 Nm^{-2} results in a reduction of boiler tubing area of 200 m^2 (Fig. 4.13), a saving of £12,000 at a tube cost of £10 m^{-1}. The increments in running value therefore dominate the saving in boiler capital cost.

The reduction of scavenge ratio imposes little additional thermal loading, and hence increases to engine capital cost should be small (possibly more expensive valves). The reduction of trapped air-fuel ratio however, imposes additional loading and increases in engine capital cost may be entailed. It is possible to evaluate what increases in engine capital cost are justified, and to find the optimal back pressure.

A good fit to the capital cost saving for the boiler (Fig. 4.13) was found from:

$$y \equiv A(1 - e^{-a\Delta P_b}) \quad \text{where A and a are constants.}$$

Making the very approximate assumption that the annual capital charge on the engine increases linearly with ΔP_b:

$$\text{Annual benefit of } \Delta P_b = A(1 - e^{-a\Delta P_b}) - (C_E + C_p - C_H)\Delta P_b$$

where C_E = rate of change of engine capital cost with P_b

C_p = rate of change of value of power output with P_b

C_H = rate of change of value of recovered heat output with P_b

This benefit may be maximised within the range $0 \leq \Delta P_b \leq 0.187 \times 10^5$ Nm^{-2}.

Differentiation reveals a maximum at $\Delta P_b = \frac{1}{a} \text{Log}_e \left(\frac{A\,a}{C_E + C_p - C_H}\right)$

In terms of F_c, the fractional increase in engine capital cost to operate with $P_b = 1.2 \times 10^5$ Nm^{-2} (ie. $R_T = 24.6$), and for the same

assumptions on operation and cost as mentioned in the previous paragraphs, (Discount rate = 10%), then if

$F_c > 14\%$ maintain $\Delta P_b \simeq 0$

$F_c < 2.4\%$ " $P_b = 1.2 \times 10^5 \ Nm^{-2}$

and for $14\% > F_c > 2.4\%$ the optimal back pressure lies between these limits.

4.3 EXHAUST HEAT RECOVERY - BOILER SIMULATION RESULTS

Consideration is given to the two possibilities, reduction of boiler exit temperature and afterfiring, mentioned in section 3.2. Modifications to the exhaust heat boiler may be made in conjunction with, or instead of, the engine design changes discussed in the previous section. They avoid the engine thermal loading problems associated with the engine modifications.

4.3.1 Boiler Gas Exit Temperature

It has so far been assumed that the gas exit temperature at the boiler exit is 200°C to avoid low temperature corrosion of the boiler. It is the purpose of this section to evaluate the benefits of, and to discuss the problems associated with, a reduction of boiler exit temperature below 200°C.

The fuel input energy recoverable as heat in the exhaust increases by 1% point/10°C reduction in boiler exit temperature. For heat valued at oil at £60/tonne (January 1978) burnt at 80% efficiency, and for a load factor of 75%, this 1% is worth £3,400 per year. The

capital cost of a low pressure drop water-tube boiler for the 9AT350 is around £20,000, and hence the high relative value of the heat may justify significant increases in boiler capital cost.

The limitation on the boiler exit temperature is the sulphuric acid content of the exhaust gas from the heavy fuel oil burning engine. Formed from sulphur trioxide and water vapour as the gas temperature drops below 550°C, it is not corrosive in the vapour form, but extremely so if metal surfaces are below the acid dew point and the acid condenses onto them. The dew point is between 113°C (1 ppm sulphur) and 152°C (100 ppm), and the maximum corrosion rate occurs at 20-30°C below this, Fig. 4.15 (from the boiler simulation program) shows that tube surface temperatures tend towards the water temperature, the gas side resistance dominates, and hence the lower the feedwater temperature the greater the potential dangers. Haneef (Ref.36) suggests stainless steel or 'corten' steel as being significantly more corrosion resistant than carbon steel. Glass and enamel coatings have also been suggested for economizer tubes.

An example of the economic returns possible from the reduction in boiler exit temperature are shown in Fig. 4.16 for a range of tubing lifetimes and costs, and for the reductions 200-175°C (Curve A), 175-150°C (B), 150-125°C (C). The heat recovery is from the 9AT350 at full load with an overlap of 98°CA and low pressure drops: the boiler tube spacing is chosen to minimise the interaction with the engine. Plain tubes are used, the boiler feedwater is at 50°C, 2 bar steam with 20°C superheat is produced.

The returns are very good, even if the tubes should cost several times the normal price of around £65 m^{-2}, as long as the tube life can be maintained above 2-3 years. It is implicitly assumed that the increments in the costs of boiler walls, cladding and headers are

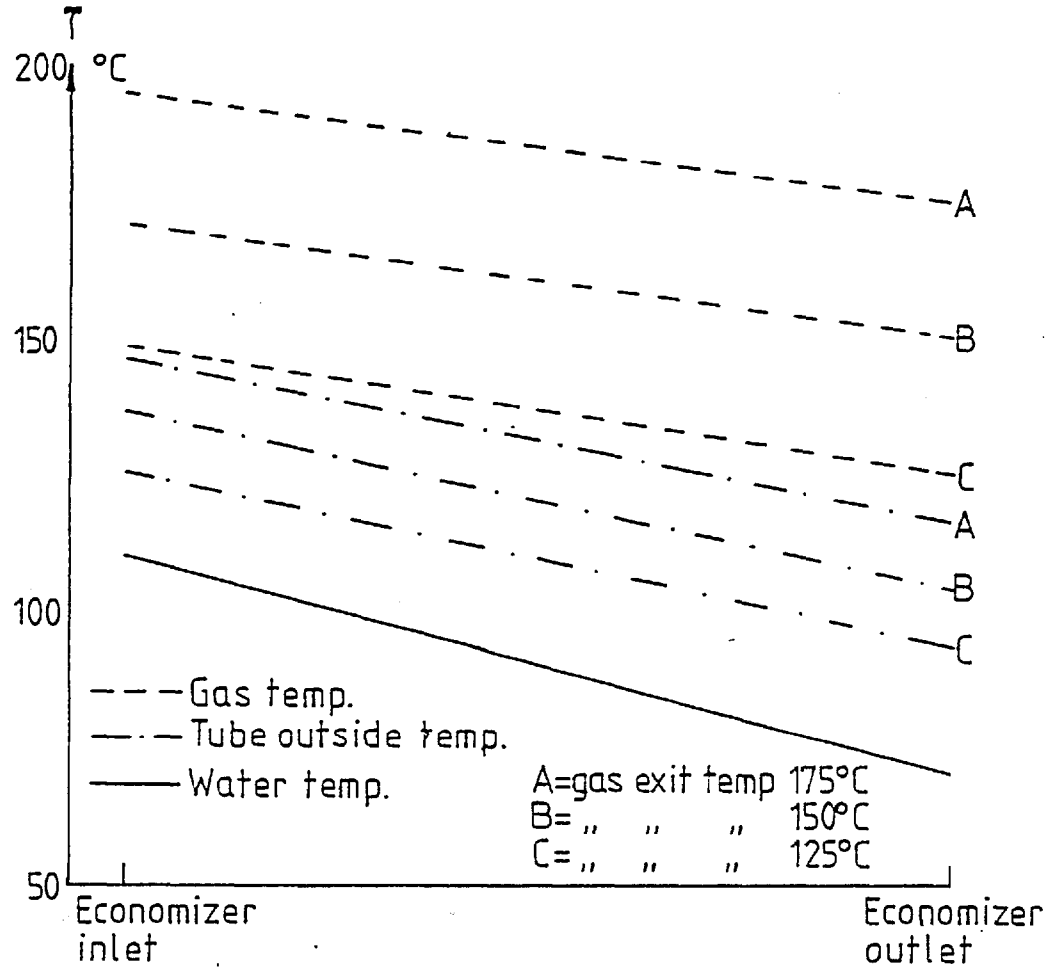

Fig. 4.15 Exhaust Heat Boiler: Tube Surface Temperatures

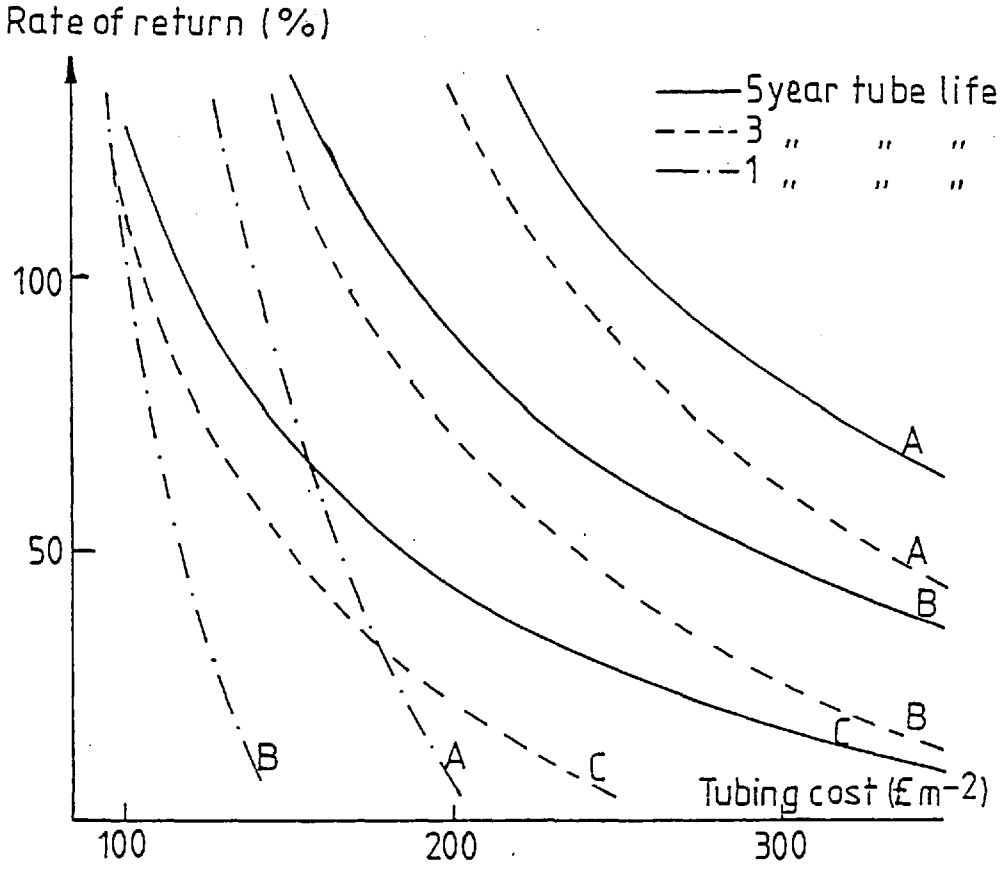

Fig. 4.16 Returns on Reduction in Boiler Gas Exit Temperature

included in the tube cost. A more expensive stack may be required in which case the returns would be somewhat reduced.

Some caution must be exercised in generalising from this example. Returns fall as the water inlet temperature is raised, because the water-gas temperature differential is reduced. Depending on the required steam conditions, it may not be possible to reach any desired boiler exit temperature: pinch point limitations may arise at the economizer-evaporator junction. A more precise estimation of the economic benefit of the reduction of boiler exit temperature, will therefore be specific to the particular water and steam conditions needed, and will also require experimental measurement of corrosion rates and corrosion resistant materials. However the analysis has indicated that the returns are probably high, and that expensive corrosion resistant or 'disposable' tubing are possible ways of achieving them.

4.3.2 Afterfiring

Afterfiring of heavy fuel oil into the engine exhaust after the turbine is an effective way of meeting further heat loads and imposes no additional load on the engine. The technology for afterfiring heavy fuel oil has been recently developed (Ref.49). Fuel, injected into the exhaust with pressurised air, is burnt at approximately 96% efficiency; the only losses being due to the slightly increased flow of dispersion air, and from radiation. Afterfiring down to 1.7% excess oxygen by volume has been achieved (Ref.49), but 3% is a reasonable limit to avoid smoking under rapid load changes.

The maximum heat flow available from afterfiring (H_{max}) is given by

$$H_{max} = \frac{\dot{m}_{f_{max}} \; C_{al} \; \eta_a}{\dot{m}_{f_{max}} + f + 1} \quad W_a \left\{ 1 + \frac{\dot{m}_{f_{max}}}{\dot{m}_{f_{max}} + f + 1} \right\}$$

where $\dot{m}_{f_{max}} = \frac{f - f_s - a(f+1)}{f_s + a}$, a = fraction of excess air in boiler exit gas. $\dot{m}_{f_{max}}$ = maximum fuel flow rate to afterfirer.

Thus the effective heat to power ratio ($^{Q}/_{P}$) of the engine can be varied. For example just considering exhaust heat recovery for the 9AT350 at full load, with 168°CA overlap and atmospheric back pressure $0.4 \leqslant {}^{Q}/_{P} \leqslant 3.1$, and at 98°CA overlap $0.6 \leqslant {}^{Q}/_{P} \leqslant 2.0$.

A CHP scheme may be required to produce a certain heat to power ratio, eg. a site where export of electricity is restricted and with high heat requirements. In this situation the modified engine, with increased available exhaust heat, may not be the best solution at high $^{Q}/_{P}$ as Fig. 4.17 indicates. Increasing available exhaust heat recovery entails reducing the excess air flow, and hence the potential for afterfiring.

The capital cost of control equipment for afterfiring is high, but particularly for large systems, it may, by displacing auxiliary boiler capacity, give overall capital savings. The saving in running cost means that afterfiring should constitute an effective way of meeting peaks in heat demand.

4.4 LOW TEMPERATURE HEAT RECOVERY

Around 25% of the fuel energy input appears as hot water or steam in the range 30-120°C. This heat is usually in three separate circuits:

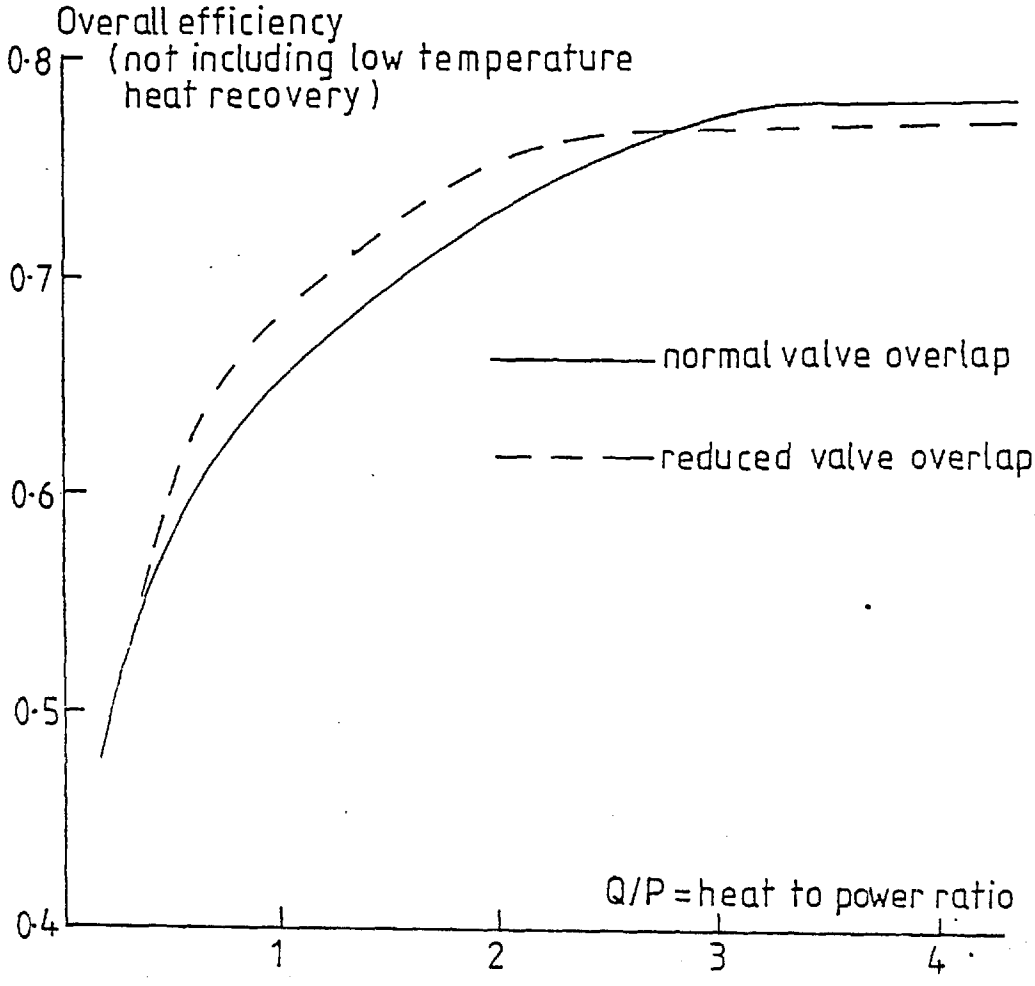

Fig. 4.17 9AT350 Overall Efficiencies with and without Overlap Reduction

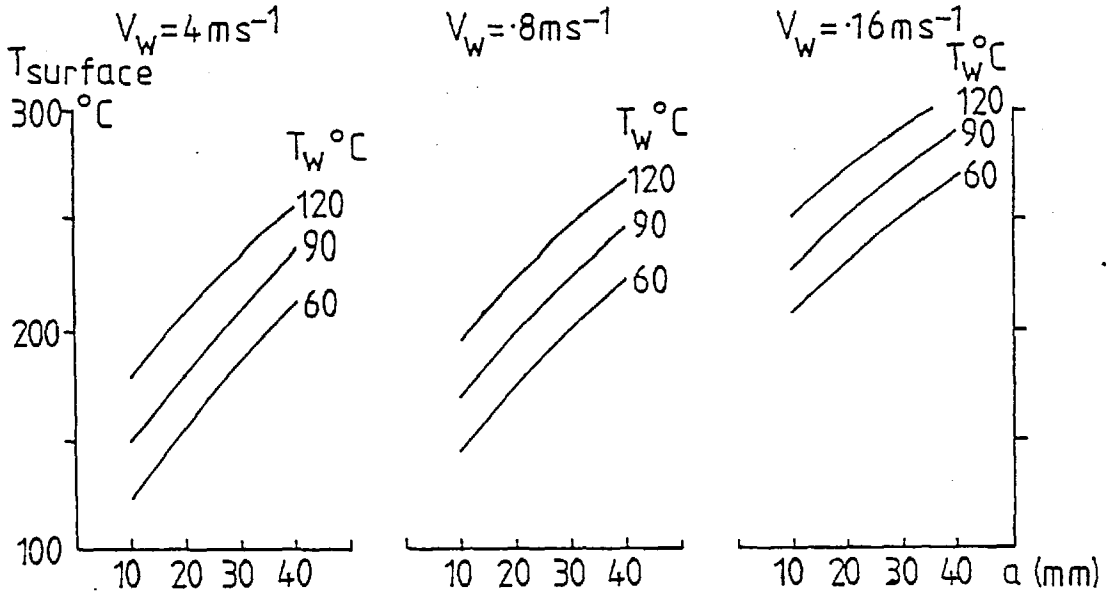

Fig. 4.18 Dependance of Metal Surface Temperature on Water Conditions (Ref. 93)

they are, in ascending order of temperature, the intercooler, the lubricating oil cooler, and the jacket water. Approximately 10% of the fuel input energy goes to jacket water, 10% to the intercooler and 5% to the lubricating oil. Further subdivisions may be used; for example separate circuits for the bore and head, and for valves and fuel injectors.

There is therefore a substantial rejection of heat at a low grade, whose use may be limited. If steam is needed then the requirement for heat below 100°C may be small, and restricted to feedwater heating. Some discussion is now given to ways in which the heat in these circuits may be upgraded, and of the economics of its recovery.

Jacket Water

Water temperatures at the jacket outlet are in the range 75-95°C in unpressurised circuits, and up to 120°C in pressurised circuits. Latent heat cooling may be used, in which case steam temperatures at the jacket outlet may reach 125°C.

For a given gas temperature the metal surface temperature is dependent on 3 variables, Fig. 4.18 (Ref.93):

(i) The water temperature (T_w)

(ii) The water velocity (V_w)

(iii) The distance from the water to the gas surface (a).

It would therefore appear possible, by varying the other 2 parameters, to increase the water temperature and leave the metal surface temperature unchanged. However:

(i) Increased water velocity implies increased pumping losses.

(ii) The reduction of the water-gas distance may involve major design changes.

(iii) In certain critical regions, e.g. the valve bridge, heat transfer is by nucleate boiling (Ref. 30), and hence the rate of heat removal is independent of the fluid velocity. It is in these same regions that it is most difficult to bring the water close to the gas.

On the whole then, any increase in water temperature will lead, at least locally, to higher metal temperatures.

Recently Sulzer have reported the successful operation of a medium speed engine with sensible heat cooling at 130°C (Ref.80). The increase of 50°C over the normal coolant temperature results in a decrease of 2% of fuel input energy to jacket water, a decrease of 1% to the lubricating oil, an increase of 1% to the exhaust, and no change to either brake power or intercooler heat rejection. There was a small increase (0.5%) in radiation loss. The expected expansions of block and cover were found to be small and acceptable. The temperature of the valves increased by only a few degrees, and stresses in the liner were in fact reduced.

This increase in coolant temperature significantly improves the utility of the jacket water, in that it can be used to raise low pressure steam.

Using sensible heat cooling avoids the vapour-lock problem encountered with latent heat cooling, that can cause severe local overheating, and which has made the practice unpopular. On this particular engine the increase in temperature has been achieved without thermal loading problems. However the considerations given above suggest that higher coolant temperatures must generally be adopted with some caution: the characteristics of individual engines will determine their ability to operate under the hotter conditions.

Lubricating Oil

The lubricating oil temperature at the engine outlet is in the range 60-100°C; that of the secondary water circuit, a few degrees lower. Oils are available, at a price, to operate at higher temperatures, (Ref.31), but this will significantly increase the cost of lubricating oil consumption, which is normally 5% of total engine running costs. The cooling effect of the oil will also be reduced.

Intercooler

Closed cycle temperatures rise rapidly with the water temperature of a single stage intercooler, and hence water temperatures in the range 25-45°C are normally employed. Any attempt to increase this temperature will significantly increase the engine loading.

Fig. 4.19 shows the results, simulated by Match 8, of raising the intercooler water temperature from 25°C to 100°C with constant intercooler effectiveness, for the 9AT350 at full load and normal design. The trapped air-fuel ratio falls, but the closed cycle gas temperatures (e.g. T_{max}) rise more rapidly than accounted for by this alone. At an intercooler water temperature of 100°C the closed cycle temperatures are up by around 150°C, resulting in significantly higher thermal loading and the possibility of pre-ignition due to the high temperatures on the compression stroke. Permissible increases to intercooler water temperature are therefore small, particularly if the engine design modifications of section 4.2 are contemplated.

A two-stage intercooler can however be used, in which case the water temperature of the first stage may be up to 100°C (Ref.61). Unfortunately the higher the temperature of the water of the first stage, the smaller is the fraction of the heat that may be recovered in it.

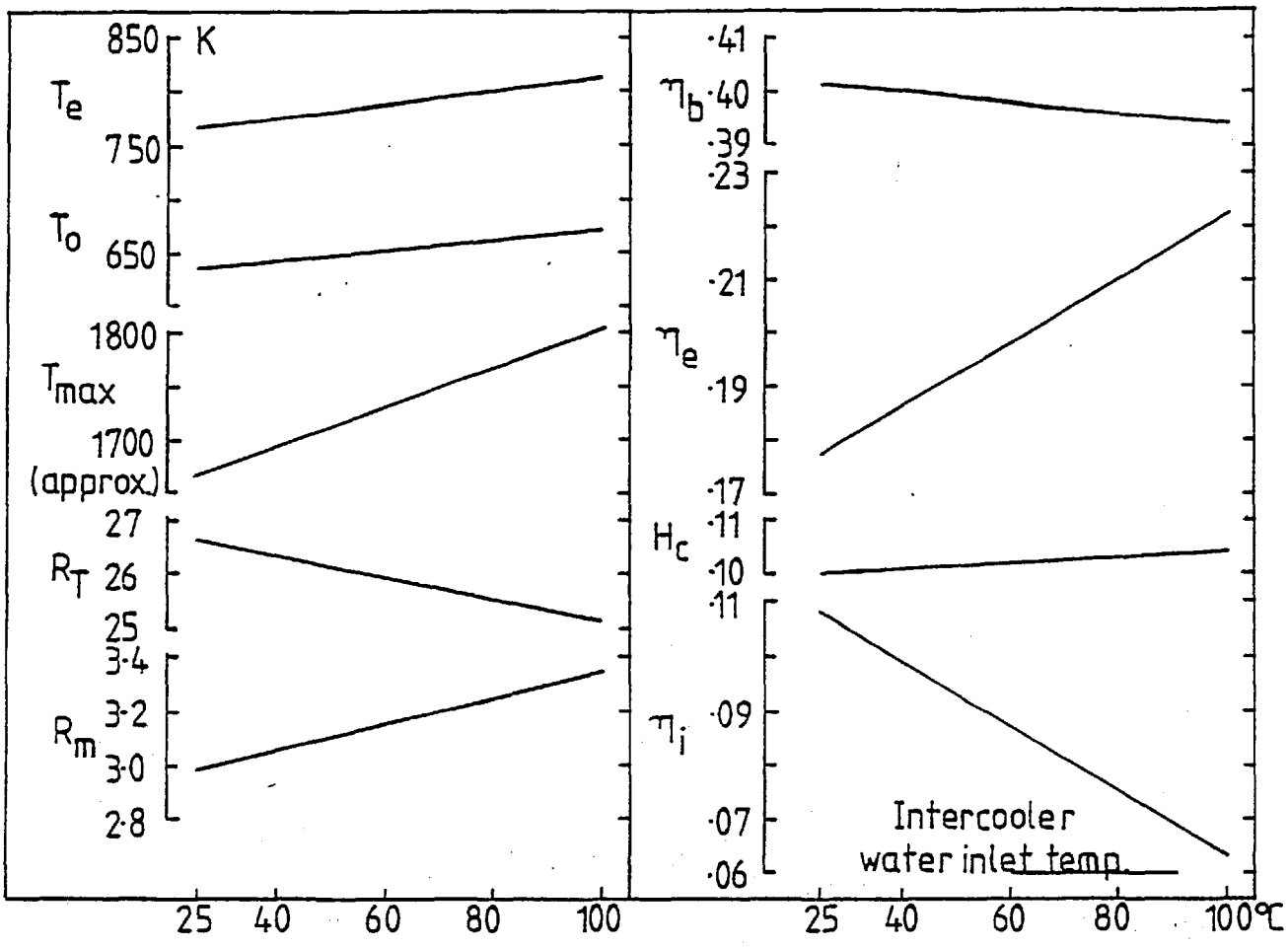

Fig. 4.19 9AT350 Rise in Intercooler Coolant Temperature.

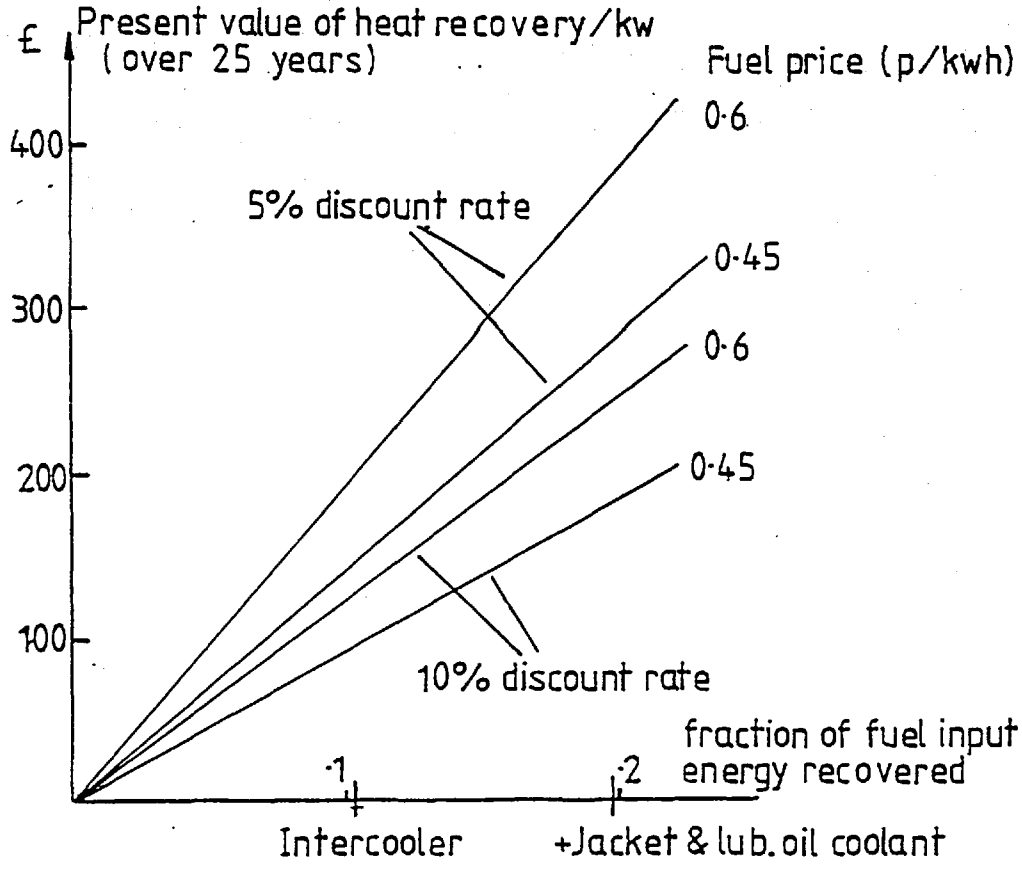

Fig. 4.20 9AT350 Present Values of Low Temperature Heat

The low temperature heat may be used to pre-heat boiler feedwater, depending upon the temperature and volume of condensate return, or for space heating. As will be demonstrated in Chapter 7, there are considerable requirements for hot water at temperatures below 80°C in industry. If the coolant temperatures are above 100°C, the ability to raise steam opens up yet wider markets. Provided that a use exists, considerable capital expenditure is justified for its recovery; the present values of the low temperature heat, at various discount rates and fuel prices, for one kW(e) of generation are shown in Fig. 4.20. Reduction of temperature differentials between primary and secondary cooling circuits, temperature increases of primary coolant where loading considerations permit, and the ingenious design of complete systems, particularly for flexibility at part load, may be considered.

4.5 SUMMARY ON DESIGN MODIFICATION OPTIONS

Of the engine design changes considered, that which gives the greatest improvement for cogeneration performance with the least thermal loading problems, is a reduction of the scavenge ratio by a reduction of valve overlap. With the normal turbine build, improvements of 4.5% of fuel input energy in heat recovery and 0.3% in power may be achieved on the 9AT350 at full load. A reduction of turbine effective area by 8% at the same time gives increases of 3.4% heat recovery, 0.6% power output, accompanied by an increase in trapped air-fuel ratio and hence easing of thermal loading problems. The scavenge ratio is abnormally high for this engine and hence the 3.4% improvement in heat recovery, 0.3% in power output for the 6RKC is perhaps more generally applicable.

Discussion with the manufacturers indicated that this modification should only require the adoption of the harder, 'nimonic' valves. The turbine should tolerate the higher temperatures. The modified engine would need some testing before its reliable performance could be guaranteed, but this is a near term design option.

The increase in back pressure and hence reduction of trapped air-fuel ratio is the second option that should be considered, and may be used in conjunction with a reduced scavenge ratio. Increased back pressure is a better option than a lower boost pressure for the reduction of trapped air-fuel ratio, as it has the added advantage of reduced capital costs for the boiler, whereas the latter has no such advantage.

With the overlap reduced to 98° on the 9AT350 and the reduced turbine effective area, increases of back pressure until the trapped air-fuel ratio is almost down to its lower limit of around 24, gives a further 2.9% of fuel input energy as recoverable heat, but at a penalty of a reduction of 1% in power output. Saving in boiler capital cost can be substantial, occurs for the first increments in back pressure, but is much smaller than the net present worth (using discount rates of around 10%) of the extra heat recoverable.

Increase of back pressure inevitably imposes added thermal loading, the optimal value will depend on the costs of making the engine withstand this. Reduction of trapped air-fuel ratio is therefore a longer term option, but one that should be achievable after a few years development.

Alteration to the exhaust valve opening timing was found to hold no advantages for cogeneration, but might be used for 'fine tuning' in conjunction with the previous two modifications. The effectiveness of

extraction of heat before the turbine to counter turbine loading problems is limited by the turbine efficiency. A more efficient turbine used in conjunction with the reduced scavenge ratio and/or reduced trapped air-fuel ratio, can lead to both improved heat and power recovery, and also reduced thermal loading.

The engines used for these studies are fairly typical of modern 4-strokes. Results for both were similar and it can fairly confidently be expected that other 4-stroke engines will show similar trends. The precise optimisation of parameters must be engine specific. Application to 2-stroke engines needs to be cautious due to the critical nature of the scavenge process, but some development along the lines outlined above may be possible.

A reduction of boiler gas exit temperature has been shown to be very attractive financially, but only general consideration has been given to how it may successfully be achieved. A reduction of boiler exit temperature by 75^{o}C adds between 5 to 7% of fuel input energy to exhaust heat recovery.

If raising the temperature of a low temperature circuit enables a use to be found for its heat that did not otherwise exist, the savings are substantial. The problems of thermal loading have been enumerated, but the example of Sulzer shows that temperatures may be raised in specific circumstances without problems.

Thus four basic opportunities have been identified: reduction of overlap and hence scavenge ratio, increase of back pressure for the engine, reduction of gas exit temperature for the boiler, and some possibilities for raising temperature in the low temperature circuits. All improvements should not be attempted simultaneously, but in principle with time for development, all modifications could be made. Figure 4.21 shows the resulting energy balances for the 9AT350 (at full load) of reducing

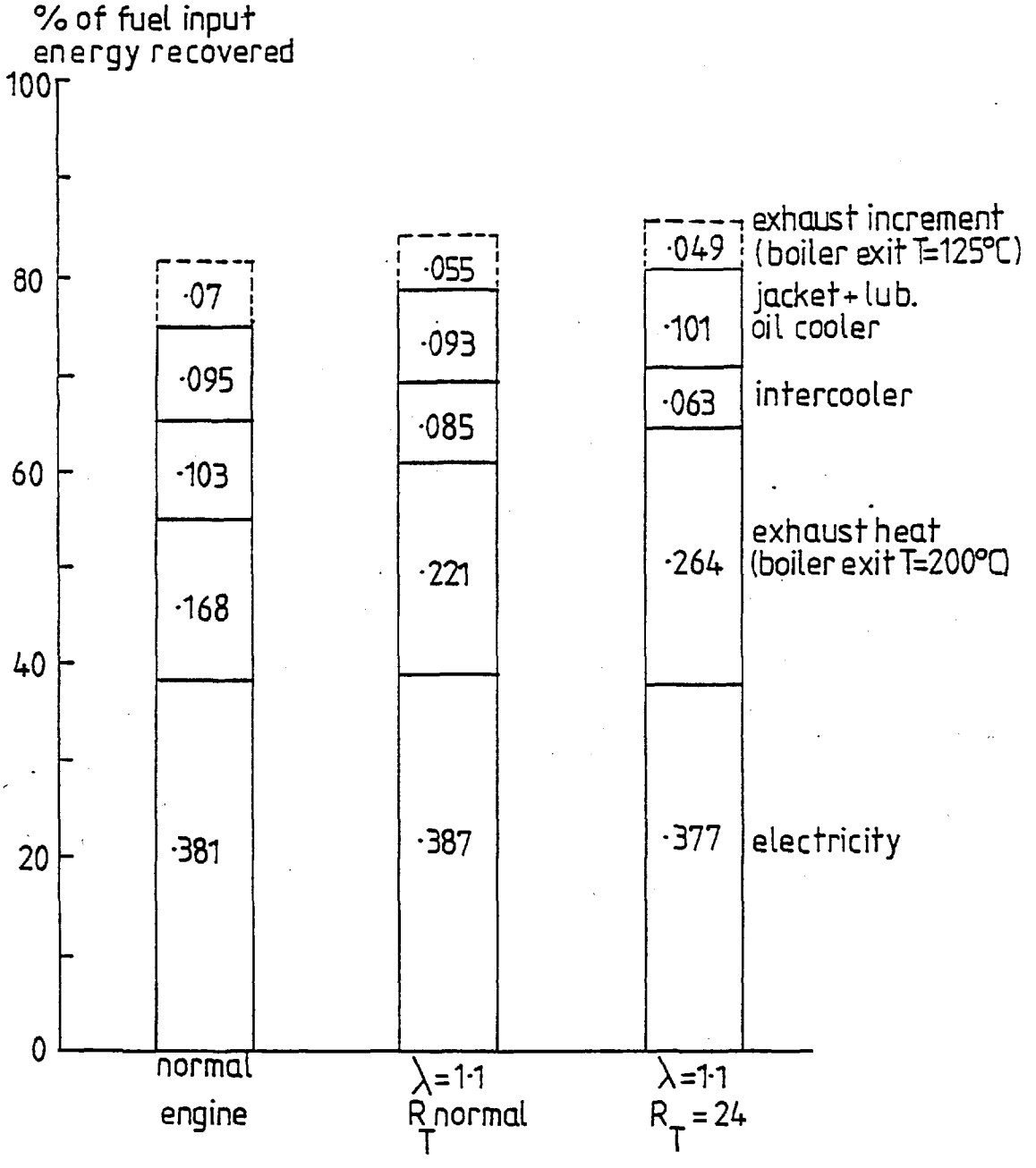

Fig. 4.21 Modified Energy Balances of 9AT350.

first the scavenge ratio (column 2) and then the trapped air-fuel ratio (column 3) to around their lower limits of around 1.1 and 24 respectively. Also shown are the increments in heat recovery by reducing the boiler exit temperature to 125°C. Losses of 2% of fuel input energy have been subtracted from electrical power output to allow for alternator efficiency of around 95%, and 2% for radiation (1% from η_e, 0.5% from H_c, 0.5% from η_i).

At the lower limits on trapped air-fuel ratio and scavenge ratio, and for a boiler exit temperature of 125°C, the recoverable exhaust heat is increased by approximately 15%, total recoverable heat by 10% of fuel input energy over the normally designed engine. There is a slight reduction in power output. Similarities in design of modern turbo-charged, 4-stroke engines, suggest that comparable improvements should be possible in other engines. The energy balances of columns 1 and 3 of fig. 4.21 have been used as the reference engine for the system integration work that follows in chapters 5 to 7.

No mention has been given to the effect of the alterations on engine emissions. Unfortunately time did not permit a detailed analysis to be made. The sulphur content of emissions is a consequence of fuel input rather than the engine operating conditions, hence the design modifications suggested would not alter it, although of course any heavy fuel oil burning CHP scheme might locally increase sulphur levels. The reduction of the boiler gas exit temperature would reduce plume buoyancy, and this could in unfavourable circumstances lead to unacceptably high local sulphur levels. NO_x formation occurs at high temperatures in the closed cycle: reduction of trapped air-fuel ratio may therefore increase NO_x emission but it was not possible to quantify the increase.

The process of diesel engine development is a continuous one, hence it has been implicitly assumed in this work that design change is by modification to existing engines rather than by any drastic return to first principles. It has been demonstrated that the recoverable heat may be increased by up to 10 percentage points by relatively minor design changes. At an electricity to heat value ratio of 2.5:1 this is equivalent to an increase in brake efficiency by 4 percentage points. Much research effort has been devoted to improving the engine brake efficiency from 36% to 40%.

It must be emphasised that this work is a demonstration of possibilities: much development work remains to be done on individual engines before they could be confidently expected to operate satisfactorily under these changed conditions. It is however a comprehensive attempt to quantify the improvements that might readily be made for cogeneration, to identify those most easily achieved and the problems that may be encountered. The magnitude of possible improvements suggest that the practical obstacles to the modifications may constitute worthwhile avenues of research for engine manufacturers to follow.

CHAPTER 5

THE OPTIMISATION OF THE OPERATION OF COGENERATION SCHEMES

5.1 INTRODUCTION

Chapters 2-4 have examined design improvements to diesel cogeneration schemes; chapters 5-7 will investigate how cogeneration schemes should best be operated to serve the Nation's interest. Chapters 5 and 6 examine the economics of the marginal cogeneration scheme, the comparison with competing technologies and the consequent potential are then discussed in chapter 7. This chapter concentrates on the theory of the operation of the marginal cogeneration scheme; chapter 6 gives examples and results.

The cost of electricity is composed of capital and operating costs. A cogeneration scheme therefore has 2 elements of value:

1. The operating costs that would otherwise have been incurred in producing the units of electricity generated by the CHP scheme.

2. The saving of construction of new Electricity Supply Industry capacity as a result of the introduction of the CHP scheme.

The sequence of calculations to derive the economic value of a CHP scheme and whereby the optimal operation may be determined is

shown schematically in Fig. 5.1. The calculation proceeds in essentially three stages. A value is first attached to units of electricity produced by the scheme (block 1). Knowledge of the value of units then allows the operation of the scheme to be simulated to minimise the running costs (block 2). Finally from the simulated CHP electricity output profile over the year, the capacity credit due to the scheme can be calculated. The displaced capacity is first calculated (block 3a), and then a value assigned to this capacity displacement (block 3b). The value of the scheme is the sum of the capacity and unit value elements, and the optimal installed capacity can then be determined. Sections 5.3, 5.4 and 5.5 correspond to the operations of blocks 1, 2 and 3 respectively.

Schemes may be owned and operated by the ESI or privately. If owned and operated by the ESI they should be automatically integrated with the investment and operational procedures as is other plant. If independently owned there is a choice of grid connection. Isolated schemes (sometimes referred to as 'Total Energy' schemes) must meet frequently unsynchronised and conflicting demands for both heat and power locally. This usually results in idle capacity, poor economic returns and little benefit to the Nation. It may therefore by surmised that benefit may be increased by grid connection allowing import and export of electricity, and thereby easing a local constraint by taking advantage of the National diversity in electricity demand.

This entails some trading arrangement between the site and the system: a linking tariff must therefore be established. The form of this tariff will be shown to be crucial to the benefit derived. The tariff will in general comprise a unit cost element (Fig. 5.1, block 1 and section 5.3), and a capacity element (Fig. 5.1, block 3 and section 5.5). Some important features of a tariff designed to maximise the

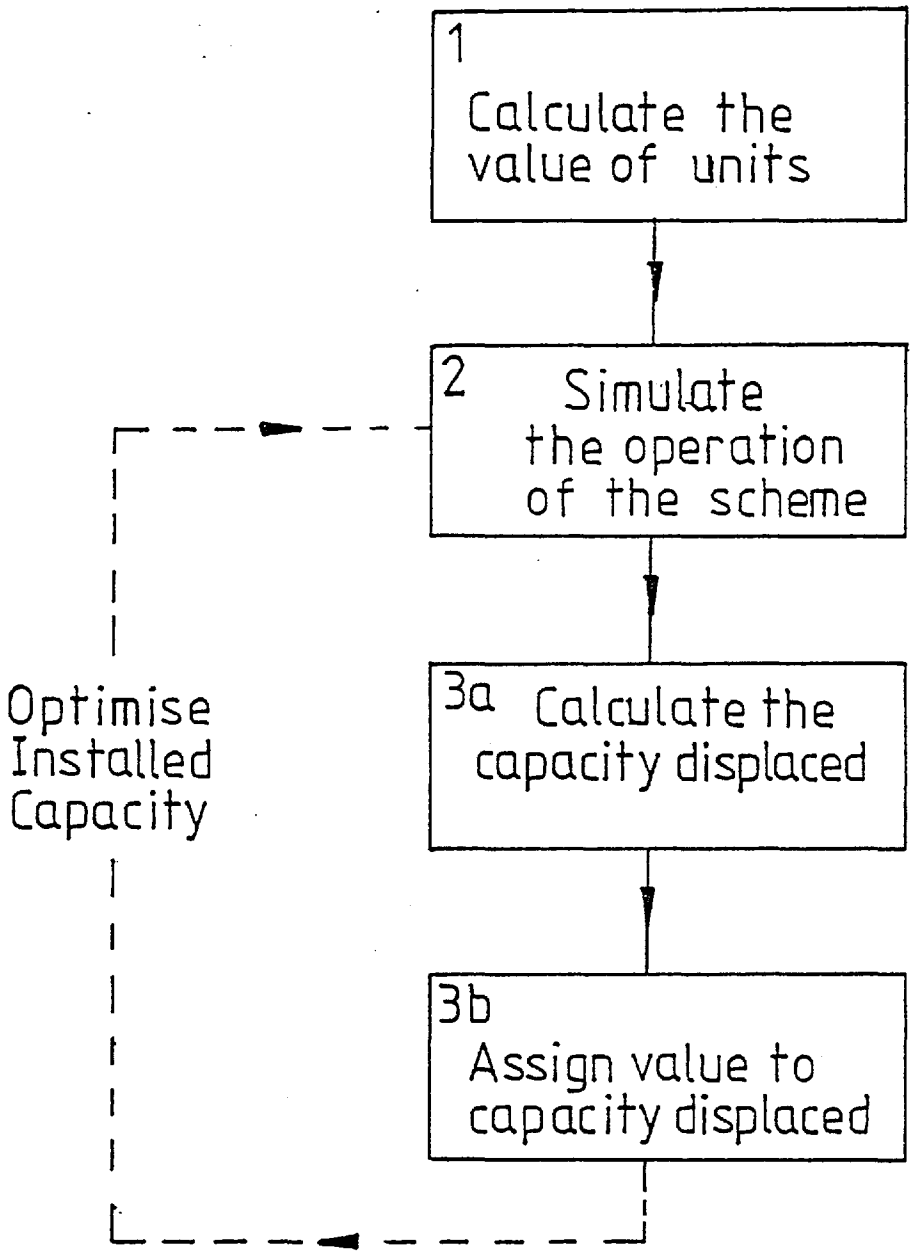

Fig. 5.1 Sequence of Calculations for Determination of Optimal Operation

National benefit from CHP will first be derived in the following section. The analysis is a modified version of one given in Ref.5.

5.2 OPERATION IN THE NATION'S INTEREST

Figure 5.2 shows schematically how the total annual electricity production from industrial CHP schemes depends on the price offered for electricity by the ESI. For any offer price above a minimum C_o there will be industrialists willing to export CHP electricity. The higher the price the more CHP electricity will be produced. Two curves, both monotonically increasing, of offer price C against CHP output E are shown in figure 5.2: the higher, $C = f_i(E)$, relates C and E if the owner of the plant assesses projects at industrial discount rates, and the lower, $C = f_N(E)$, relates C and E if the owner uses a test discount rate representative of the National Interest. Industrial discount rates are usually higher than the national one.

From figure 5.2, using industrial discount rates, if the offer price is C_1, E_1 units will be produced. The owners' net benefit is represented by area A_1, that of the ESI by A_2 (C_{marg} is the marginal cost of production of the ESI).

The three parties or 'interests' interacting in their attempts to maximise their own benefits, may be defined as the independent owner, the ESI and the Nation. If the owner uses an industrial discount rate and the Nation's Interest is incidental, then the ESI maximises its benefit: the area $A_2 = (C_{marg} - f_i(E_1))E_1$. This area is maximised when the offer price $C = f_i(E) = C_{marg} - E\, f_i'(E)$: f_i' is the derivative

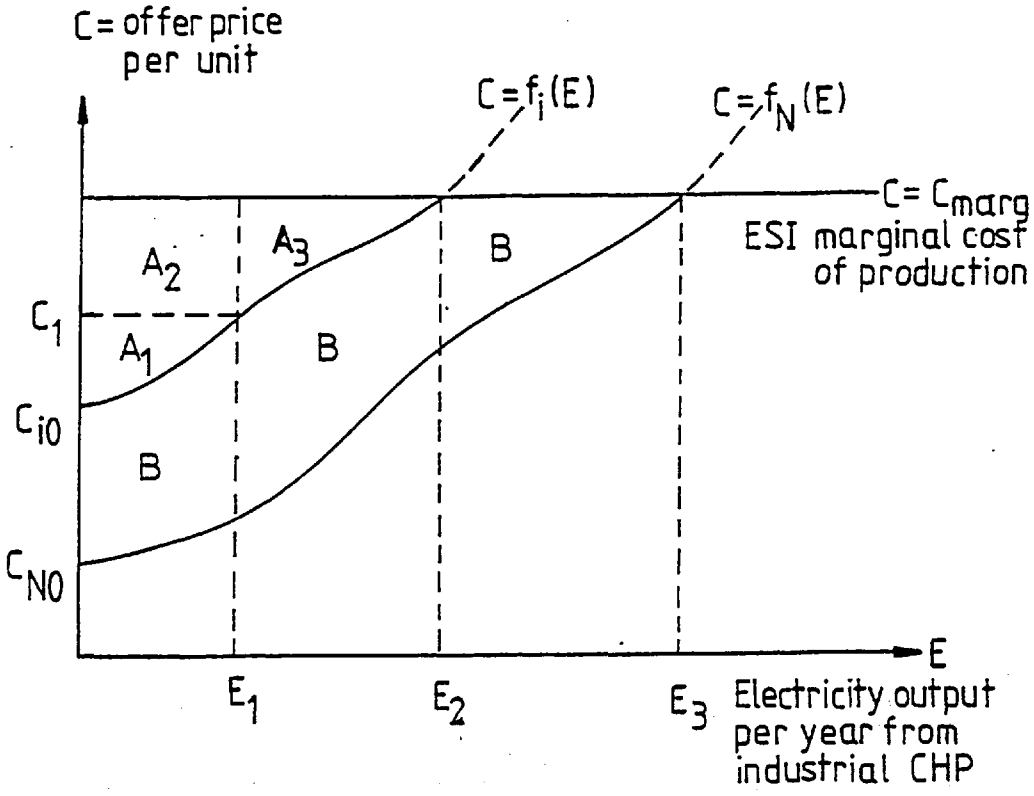

Fig. 5.2 Schematic Relationship Between ESI Offer Price and CHP Generation

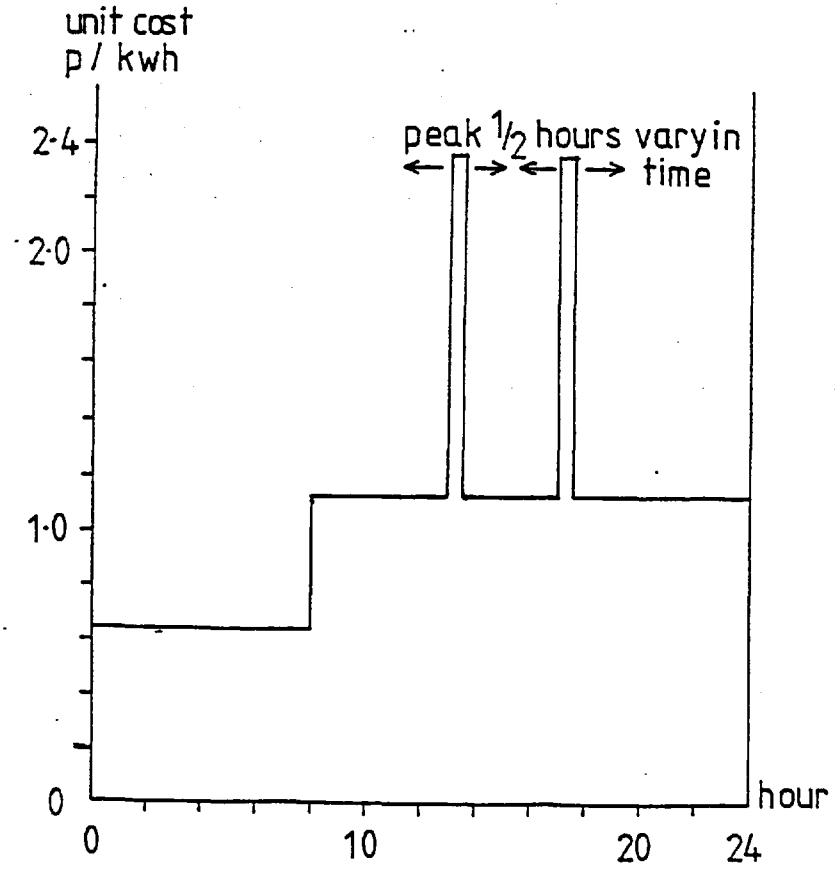

Fig. 5.3 BST Unit Costs 1977/78

of f_i and is always positive. It follows that it is in the interest of the ESI to offer a price below its marginal cost of production. The National benefit is the area $A_1 + A_2$ corresponding to the price $C_{marg} - E\, f_i'(E)$.

It is interesting to note that the present policy of the ESI towards the purchase of independently produced units of electricity, as outlined by Burchnall (Ref.8), corresponds fairly closely to the above conclusion. From paragraph 34, "As regards the kilowatt-hour price element, this will be between the producer's costs, and, as a maximum, the public supply marginal cost of production at the relevant times of day/year." The monopolistic ESI is therefore acting as a distributor of profits, to the dis-benefit (as will be demonstrated by the next example) of the Nation. This situation has been criticised elsewhere (Refs. 5 and 37).

The National benefit is the saving over the cost of ESI production, achieved from producing electricity by cogeneration (the costs for this being those perceived by the owner). If the owner uses an industrial discount rate and the ESI acts in accordance with the National Interest, then the National benefit is maximised by maximising the area = $E_1(C_{marg} - f_i(E_1)) + Ef_i(E_1) - \int_0^{E_1} f_i(e)de$. For a maximum $f_i(E) = C_{marg}$ i.e. the Nations benefit is maximised when the ESI offers a price equal to its marginal cost of production. The National benefit is then $A_1 + A_2 + A_3$. If the owner applies a National test discount rate the National benefit is further increased to $A_1 + A_2 + A_3 + B$*.

*Note: It has been implicitly assumed that C_{marg} remains constant with increments of CHP generating capacity. This is reasonable for increments small compared to total generating capacity; for large increments it will change. A slight modification is then required to the calculation, the principles however remain the same.

Not surprisingly therefore the Nation's economic interest is best served when all parties act in accordance with it. Conflicting interests of the parties lead to an economically sub-optimal solution. The value of CHP electricity from the marginal scheme is therefore the marginal cost of ESI production, and the Nation's benefit is maximised if electricity is traded at this price and a National test discount rate is used. This marginal value should be regarded as including both the capacity and running cost elements and is the long run marginal cost (LRMC) of electricity production.

An economic analysis based on electricity traded at long run marginal cost and projects assessed at national test discount rates, is essentially that which the ESI should perform. Therefore although the succeeding sections describe the methods for evaluating an independently owned scheme, the method is basically the same for ESI ownership. However there are some differences in value between independent and ESI schemes, resulting from operational and planning considerations. These differences will be pointed out during the following sections on methods of evaluation, and are discussed in more detail in section 5.6.

5.3 THE VALUE OF UNITS

The tariff acts as the link between the cogeneration site and the electricity supply system. Expectation of future tariffs is an essential factor in the investment decision on a cogeneration scheme. Knowledge of the present tariff enables the optimal operation of the scheme.

Section 5.2 has concluded that the tariff should represent the marginal generating cost of the ESI. It is theoretically possible to signal instantaneously the continually varying marginal production costs of the ESI, but this is not regarded as practical. The tariff therefore will be a compromise between accuracy and simplicity. In the following formulations it is assumed that the tariff is agreed in advance, for example at the start of each year, and thereafter, together with the site heat demand and fuel cost, determines the operation of the scheme. The unit cost element of the tariff therefore must represent the 'expected' marginal running costs of the ESI.

5.3.1 The Form of the Tariff

The marginal operating cost of the ESI varies through the day: it is low, during the night when the efficient base load units are at the margin, and high at times of peak demand when plant with high operating costs must be used. The capacity element will be determined by how much less capacity the ESI must install due to the presence of the CHP scheme. A tariff determined in advance must be based on consideration of the 'probable' or 'expectation' variations of cost over the day.

The Bulk Supply Tariff (BST) represents an approximation to the long run marginal costs of the ESI (Ref.10), and is the price paid by the Area Boards(responsible for selling electricity to the customers) to the Central Electricity Generating Board (CEGB) who generate the electricity and operate the long distance transmission network. It has therefore been suggested (Refs. 56,53) that the BST would represent a suitable valuation of units of CHP electricity and of the capacity installed.

Figure 5.3 shows the BST unit costs, characterised by sharp price differentials at the peaks. This is because as the system approaches the short duration peaks, it is not advisable to operate large units for a short period, even if they are available. Gas turbines are therefore used with consequent high running costs.

BST charges are calculated after the event, for example the timing of the peak charges is determined afterwards, and represent 'operational' rather than 'planning' marginal costs. As the aim is to define a tariff in advance, BST charges could neither be well defined nor accurately represent the value of independently generated electricity to the ESI.

The high value attached to electricity at the peak half-hours by the BST relates to the necessity for the ESI to have fast response generators under its own control, to meet short term increases in demand. The peak half-hours cannot be predicted one year in advance, and hence the signal provided by an advance tariff cannot in principle control an independent CHP site's contribution sufficiently well for its units to be valued at the full gas turbine displacement value.

Expected hourly marginal generating costs, taking account of random forced outages of system plants, can however be calculated from previous years' demand data. They are calculated for 'typical' days during the year, and reflect reasonably accurately the value to the ESI of CHP contributions at the margin. A 'Probabilistic Simulation Model' is used to calculate these values, and is described in section 5.3.3.

5.3.2 The Practical Application of a Tariff

An Area Board's costs are approximately 80% BST, the further 20%

being for local distribution, administration, consumer services, etc. (Ref.5). This additional cost must be passed on to customers, and hence if a site owner is able to import and export electricity at the marginal generating cost as calculated by the probabilistic simulation model, it would confer an unfair and unrealistic advantage to him over other industrial consumers. For the purpose of the economic analyses of chapter 6, this problem is side-stepped by considering the economics of the CHP scheme separately to those of the heat and power consuming site.

The site purchases electricity from the Area Board in the normal way (at the usual industrial tariff which includes a contribution to the Area Board's costs), and purchases heat from the CHP scheme (Fig. 5.4). CHP electricity is considered to be fed into the local grid. This is a realistic assessment of the economics of the scheme for 3rd party ownership, and also for the case where the owner of the site and scheme is the same to the extent that the Area Board's 20% is a fixed overhead. If part of the 20% is an Area Board unit cost, then the industrialist may rightly argue that his payment to the Area Board should be lower due to his local consumption of the electricity production. The site and system models developed are able to treat this case, but the economic analyses of chapter 6 do not.

5.3.3 The Evaluation of ESI Marginal Unit Generating Costs

A probabilistic simulation model was used to calculate expected electricity costs at the station gate. It was developed by A.P. Rockingham of Imperial College, originally for work on windmills, and adapted by Rockingham for this work on Cogeneration. It is based on a method originally proposed by Ringlee et al (Ref.74).

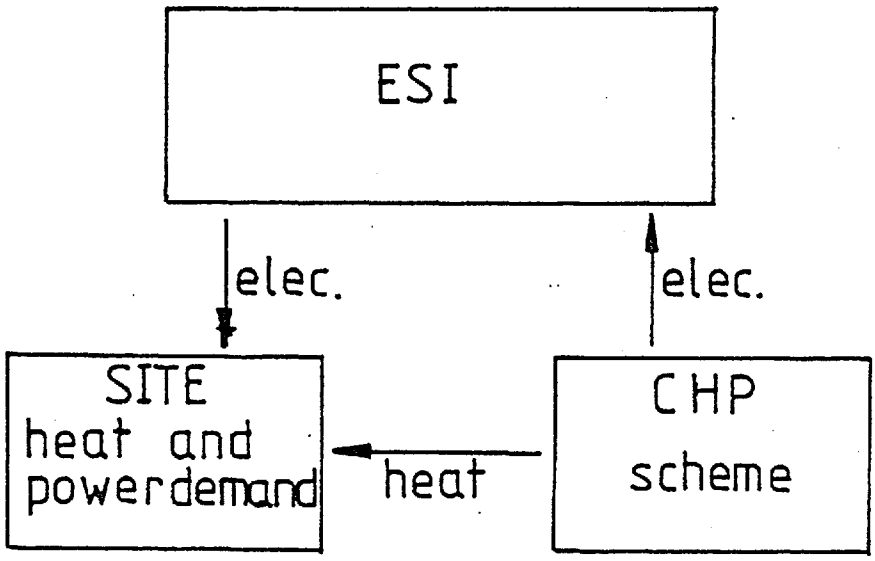

Fig. 5.4 Schematic Interchange of CHP Heat and Electricity

Forced outages of generating plant can significantly increase production costs. Many production cost programs ignore forced outages or include their effects by increasing the length of scheduled outages or reducing the plant maximum capability. Frequently it is found that peaking plant does not run in the simulations and hence marginal costs are underestimated. Attempts to force peaking units to run by requiring a minimum number of operating hours merely result in input and answers being equivalent.

The model is an expected cost computation. Expectation considers the scatter in production costs due to unscheduled outages and load deviations: it is simply an average of possible events. The method may very briefly be summarised as follows.

Plants are committed to load in a merit order, and hence may be labelled 1, 2, ..., j, ..., N. For any load (l), the probability (p_j^l) that plant j, with running cost c_j, will be called to meet this load can be calculated by a recursion relation (Ref.74). The expected marginal cost at load l, c(l), is then $\sum_{j=1}^{N} p_j^l \, c_j$. From demand data the probability of load l, q(l), may be calculated. The expected marginal cost $\bar{c}$ is then formed by convolution of the two probability functions ie. $\bar{c} = \int_0^\infty q(l)c(l)dl$.

Electricity production costs and the risk of system failure to meet demand, vary through the day and year. Hence hourly marginal costs were calculated for two typical days: one representing the days of the winter when peak system demand may occur, the other the rest.

The results of the expected cost computations are given in Chapter 6, section 6.4. It may be helpful at this stage to refer to Fig. 6.4, which shows the calculated values of expected marginal unit generating costs of the CEGB in 1977/78.

5.4 RESPONSE TO THE TARIFF: THE SITE MODEL

Knowledge of the tariff, fuel cost, the heat and possibly power demands enables the scheme to be operated. The optimisation of this operation is done by the site model. The results from the site model will permit the second element of CHP value, the capacity credit, to be calculated by the methods described in the next section. Then by comparing the economics of various possible prime movers for the scheme, the optimal investment decision may in principle be made.

In general the heat and power demands, and value of electricity will vary through time. The site model must determine the least cost operation of the plant for each moment in time, given information on the heat and power demands, and value of electricity. The approach adopted is to divide the day into time periods for which the electricity and heat demands and values may be considered constant. The model then operates the plant so as to minimise the cost function for each of these periods.

The general form of the cost function that must be minimised for each time period during which the parameters are considered constant is:

$$Z = \left[\begin{array}{l}\text{Cost of fuel and} \\ \text{maintenance to the prime mover}\end{array}\right] + \left[\begin{array}{l}\text{Cost of meeting} \\ \text{site's power demand}\end{array}\right] - \left[\begin{array}{l}\text{Value of} \\ \text{electricity} \\ \text{exported}\end{array}\right]$$

$$+ \left[\begin{array}{l}\text{Cost of producing the part of the site's} \\ \text{heat demand not recovered from the prime mover}\end{array}\right] - \left[\begin{array}{l}\text{Value of the site's} \\ \text{heat demand}\end{array}\right]$$

For the '3rd party' analysis (section 5.3.2) used in the next chapter, the second term is always zero, all electricity can be considered exported. If the model is to be used to evaluate the joint economics

of a site demand and CHP scheme, the final term is zero, the second and third terms depend on the site's power demand. In fact the second and last terms being constants in any one time period, the optimisation of prime mover power output is unaffected by whichever viewpoint is taken.

Various degrees of sophistication may be adopted for the form of the prime mover characteristics in the cost function equation. The simplest is the linear model in which prime mover brake efficiency and heat to power ratio are assumed not to vary with load. The prime mover is then characterised by its brake efficiency (η_b), recoverable heat to power ratio (r), and maximum power output (P_{max}). The optimisation process, essentially just evaluating at the slope discontinuities of the cost function, is described in Appendix 3. The simplicity of the linear model, although facilitating the rapid calculation of operating conditions, fails to provide sufficiently accurate answers in certain circumstances:

(i) Where the brake efficiency and recoverable heat to power ratio change significantly at part load; or to compare engines with similar full load, but different part load efficiencies.

(ii) In the case of a prime mover specifically designed to vary the recoverable heat to power ratio, for example the variable recuperation gas turbine.

(iii) The linear model may not give accurate information about the operating cycles of the engine. The actual engine characteristic may determine operating points far removed in power from those given by the linear model, but not necessarily so in value.

The first site model developed during this project was for some work in conjunction with the GEC Mechanical Engineering Laboratory on the variable recuperation gas turbine. A linear program was obviously inadequate, and hence a non-linear program was written for the gas turbine. It is described in Appendix 3, and is used in the next chapter to give some comparisons with the diesel engines.

In order to achieve more accuracy than that afforded by the linear model, in the simulation of the operation of a diesel cogeneration scheme, a non-linear model of this too was developed. The dependence of brake efficiency, recoverable heat and afterfiring capability on engine load are included, and several engines may be used. The model is described in Appendix 3. Its major simplification is to aggregate all heat recovery from the engine into one figure. It is possible that at part load, the low temperature heat circuits may not be in the required balance with the exhaust heat, and dumping may in fact occur that is not revealed by this aggregation. Future work might usefully develop a diverse heat grade simulation.

The question remains as to how the models are used. A requirement is certainly the heat, and possibly power demands, of the site over a period of time, preferably one year or perhaps more. The tariff gives an hourly variation of electricity price and hence hourly demands should if possible be obtained. With the additional knowledge of prime mover characteristics and the fuel cost, the optimal operation of the site over the year may be simulated.

The economic value of operation of the CHP scheme for that year is given as output. An investment decision requires knowledge of returns over the life of the project: assumptions on future prices and site demands will be needed. Finally the hourly power output data for the year for the scheme may be used to determine the

capacity displaced by the scheme, by the methods described in the next section. This capacity credit also forms an integral part of the investment decision data.

5.5 THE SAVING OF SYSTEM CAPACITY: THE CAPACITY CREDIT

The methods for evaluation of running cost savings from the cogeneration scheme have been described: the calculation of capacity saving remains. The ESI installs sufficient capacity to achieve a certain level of supply reliability. The choice of this reliability is complex and will not be discussed here. Additional capacity is installed to meet increments in system maximum demand and to replace obsolete plant. A Cogeneration scheme may only receive a capacity credit if construction of central plant is avoided.

In the case of ESI ownership the scheme can be integrated with normal planning procedures, and hence capacity credit calculated as for any other plant: there is no need to match local heat loads at system maximum demands. The only added uncertainty is the possibility of loss of heat load; a method for evaluating the consequences of this is given in section 5.5.2.

The analysis for independently owned schemes is not as straightforward and must again resort to probability theory. The calculation of capacity credit has two stages:

1. The calculation of capacity displaced: the 'MW/MW capacity credit' (Section 5.5.2).
2. The assignment of an economic value to this capacity displacement (Section 5.5.3).

Before doing this, it is essential to review the planning and construction procedures of the ESI.

5.5.1 Construction Times and Planning Horizons

The ESI annual planning horizon is determined by the construction time of new, large generating stations, and is presently 7 years (Ref.45). Estimates must be made of demand 7 years ahead, and plant margins must allow for the consequent uncertainty. Not all plants, notably gas turbines, require 7 years and they may be used as 'regulators' (Ref.4) in two ways:

1. Having determined an optimal construction mix 7 years in advance, the delayed construction of gas turbines enables the margin to be trimmed nearer the event.
2. Should construction programs fall short of demand, gas turbines may restore the balance before other plant.

Gas turbines also have the role, already mentioned, of peaking plant: they are fast response machines able to be brought on line at short notice.

To meet any increment in demand an optimal mix of high capital/low running cost plant and low capital/high running cost plant can in principle be found. The type of capacity that the CHP scheme can displace will have important bearing on the value to be assigned to the MW/MW capacity credit.

5.5.2 The Calculation of MW/MW Capacity Credit

From the hourly power output data obtained from the site model,

probabilistic density functions of the CHP electricity output are formed for each hour of the typical days. The mean and variance of these distributions is calculated. The effects of forced outage are included but those of the possibility of loss of heat load are not. In principle the effect of loss of heat load could be included by the convolution of a probability density function representing this loss of heat load with the density functions of site output from the site model. However lack of data and experience prevented quantification of these events.

Two methods of analysis were formulated to calculate the MW/MW capacity credit from this data. The more sophisticated, a probabilistic simulation model, uses the hourly probability density functions of site output. The second is a method using normal distributions, and just uses the mean and variance of site output.

The Probabilistic Simulation Model

The probabilistic simulation model is a system reliability model developed by A.P. Rockingham, originally for work on windmills (Refs. 71,72), and adapted by Rockingham for this work on Cogeneration. It is based on a method proposed by Booth (Ref.6). The model predicts the system reliability effects of system plant forced outage and uncertainty in output of independently operated CHP schemes. A description of the theory of the program is given in Appendix 4.

A year's system demand data is used to form hourly probability density functions of system demand for the two 'typical' days. In fact, depending on the planning horizon being considered, demand for a future year is required. Forecast uncertainty is included by convolving the demand probability density functions with a normal distribution having a mean equal to the increase in system maximum demand and a variance representative of the forecast uncertainty. The system

description and plant forced outage rates are given in chapter 6.

The Normal Distribution Approach

Two basic assumptions are made:

1. The probability density function for ESI demand 'at the peak' is a normal distribution $N(\mu_o, \sigma_o)$.
2. The probability density function for the CHP contribution 'at the peak' is a normal distribution $N(\mu_{CHP}, \sigma_{CHP})$.

The aim of the analysis is to find the required installed ESI capacity C, to meet a given system reliability criterion, before and after inclusion of CHP.* This system reliability criterion is the required loss of load probability (LOLP) (represented by the hatched area of Fig. 5.5) and is a function of k, f(k), where k is equal to the distance from the mean on N(0,1) corresponding to the required probability (see standard statistical tables) and hence $C = \mu + k\sigma$, $k = f^{-1}$ (LOLP) for any system.

The ESI plant (total capacity before CHP, C_o) is assumed to have a forecast mean availability at the peak a, and hence a $C_o = \mu_o + k\sigma_o$. Addition of CHP gives an effective load represented by $N(\mu_o - \mu_{CHP}, \sqrt{\sigma_o^2 + \sigma^2_{CHP}})$

$$\text{Hence } a\,(C_o - C_o') = \mu_{CHP} + k\,(\sigma_o - \sqrt{\sigma_o^2 + \sigma^2_{CHP}})$$

$$= \mu_{CHP} + k\,(\sigma_o - \sigma_o\,(1 + \frac{\sigma^2_{CHP}}{\sigma_o^2})^{1/2})$$

$$\sigma_{CHP} << \sigma_o \quad \Rightarrow \quad a(C_o - C_o') = \mu_{CHP} - \frac{k\sigma^2_{CHP}}{2\sigma_o}$$

(1) i.e. the effective load carrying capability (ELCC) of CHP =

* The analysis implicitly assumes that site output and ESI demand are stochastically independant. Some deterministic correlation may however occur if for example CHP output is strongly weather dependant.

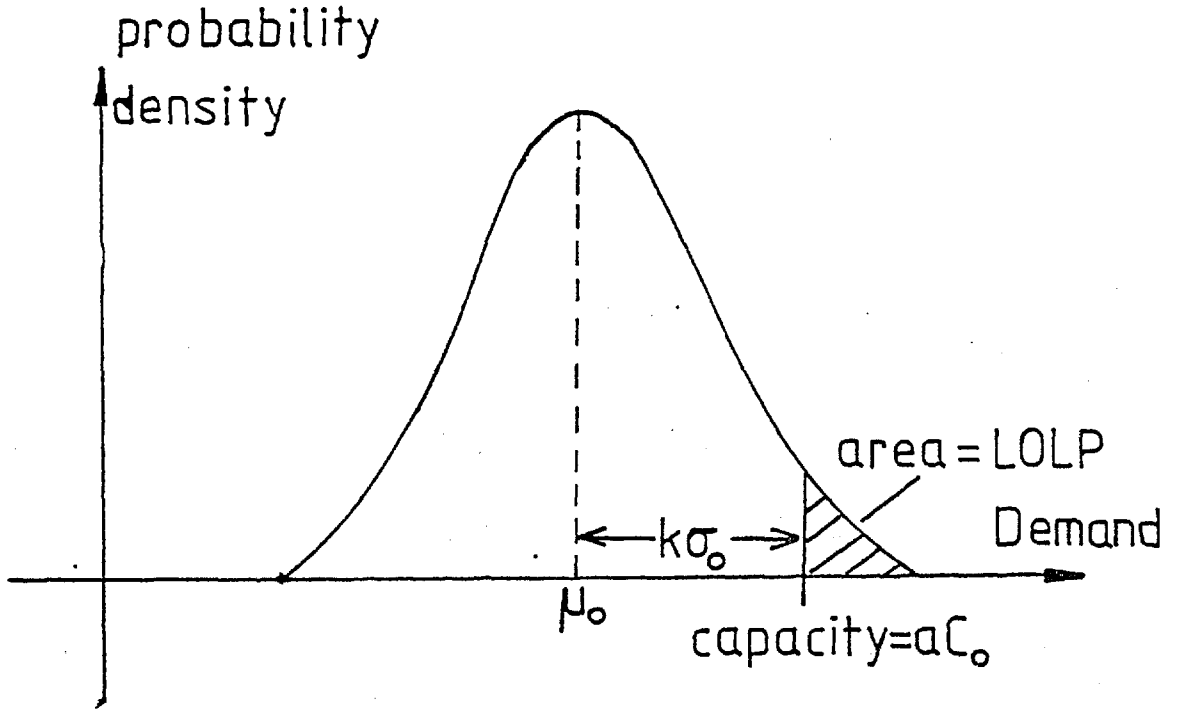

Fig. 5.5 Normal Distribution Approach to Capacity Credit

$$\frac{1}{a}\left(\mu_{CHP} - \frac{k\sigma^2_{CHP}}{2\sigma_o}\right)$$

The elements of the mean and variance for the system demand and CHP contribution, are now described. The methods by which the ESI estimate the mean value u_o of future system maximum demand, are described in refs. 45 and 4: basically being an aggregated econometric model, linking GDP to electricity demand with some allowance for price elasticity. The variance σ_o^2 comprises three elements:

(i) σ_f = standard deviation of peak demand due to forecast error

(ii) σ_w = " " " " " " " weather variation.

(iii) σ_a = " " " " " " " availability of plant.

Jenkin (Ref.45) gives values of σ_f = 9%, σ_w = 3.87%, σ_a = 3.75%, for the seven year forecast. σ_f will depend on the timescale of the forecast, σ_a and σ_w are independent of this. The mean availability of plant at the peak, a = 0.86.

The site model gives the mean and variance of the site output probability density functions. The forced outage of the CHP scheme must be subtracted. The mean value can be estimated from manufacturers' literature; the variance is not usually given however. Forced outage is represented by a normal distribution having mean μ_{FOR} and variance σ^2_{FOR}. An estimate of the standard deviation of the forced outage rate (FOR) was made: for 98% certainty that $0 \leq FOR \leq 2\,\mu_{FOR}$ then $\sigma_{FOR} \simeq \frac{\mu_{FOR}}{2}$.

Two further sources of uncertainty, not included in the analyses of chapter 6, but which might be considered, are those due to weather variations and loss of heat load. If p is the probability of loss of heat load in any year, then the mean availability of heat load in year n will be represented by a factor $\mu_n = (1-p)^n$, and a variance $\sigma^2_n = (1 - (1-p)^n)\,(1-p)^n$.

It has already been stated that σ_{CHP} is much smaller than σ_o. Some idea of the effect of the second term in equation (1) on the load carrying capability of the CHP scheme may be obtained from table 5.1. For a maximum system demand D, the system required loss of load probability is 0.03 at a demand 0.925 D (allowing for voltage reductions before load shedding) (Ref.45). For a 77/78 system maximum demand of around 43 GW, installed capacity 56 GW, this gives a value of $k = 1.88$ and $\sigma_o = 2.37$ GW without forecast uncertainty, $\sigma_o = 4.28$ GW with 7 year forecast uncertainty. Table 5.1 then tabulates the values of standard deviation of CHP output to give certain percentage reductions in ELCC of the CHP scheme for various sizes of scheme. Results of the next chapter will show that the second term of equation (1) will generally be negligeable compared to the first.

Comparison of the Methods

The probabilistic simulation model is the more sophisticated of the two methods described. It therefore places heavy demands on computing resources, whereas the normal distribution approach requires none. Some uncertainties in the assignment of a value to the MW/MW capacity credit will be described in the next section, and hence it may be unreasonable to strive for very accurate values to the MW/MW capacity credit. The normal distribution approach can however fail under certain circumstances, in which case the probabilistic simulation model would be required:

1. The variance of CHP output has been shown to generally have negligeable impact on capacity credit. However if the output variance is not negligeable then the assumption that site output is normally distributed becomes important. Site output is in fact not normally distributed, and hence the method may fail if variance is significant.

TABLE 5.1

Variance on CHP output

$\sigma_f = 0$ (No forcast error)

μ CHP MW	1%	5%	10% ← % reduction in ELCC CHP due to CHP variance
	σ_{CHP}		
1	4.9 MW	10.9	15.4
10	15.5	34.5	48.7
100	49	109	154
1000	155	345	487

$\sigma_f = 0.09$ (7 year forcast error)

μ CHP MW	1%	5%	10%
	σ_{CHP}		
1	6.7	15.1	21.3
10	21.3	47.7	67
100	67	151	213
1000	213	477	670

2. The mean and variance of site output is obtained for each hour of the typical days. The system maximum demand which defines the installed capacity requirement, is most likely to occur around 1700-1800 hours on a winter working day, but may occur at any time of those days. If the mean of site output varies from hour to hour, then further methods, for example the probabilistic simulation model, are required to give the relevant weightings to the various hours.

5.5.3 The Assignment of Value to the MW/MW Capacity Credit

The final stage in the calculation of the economic benefit of a cogeneration scheme is to assign a value to the MW/MW capacity credit. A method proposed by Berry (Ref.4), and illustrated in figure 5.6, is used to determine the effect of the introduction of a unit of plant, and to determine optimal system plant mix.

The net annual cost of the introduction of a unit of plant is the annual charge ($\emptyset$) on the plant, minus the saving in generating costs on the units displaced. Thus for a base load nuclear plant going in at the top of the merit order it is equal to:

$$\emptyset_N + (\gamma_N - \gamma_{ma})\tau$$

where γ_{ma} = average marginal price of units (p/kWh)

τ = hours of operation

γ_N = nuclear running cost (p/kWh)

$\emptyset_N$ = annual charge on Nuclear Plant.

For a gas turbine at the bottom of the merit order, the net annual cost is just equal to $\emptyset_G$.

For a system containing the optimal mix of plant, determined by the construction illustrated in figure 5.6, the net annual costs of all plant are equal. The value of a unit of capacity to the system

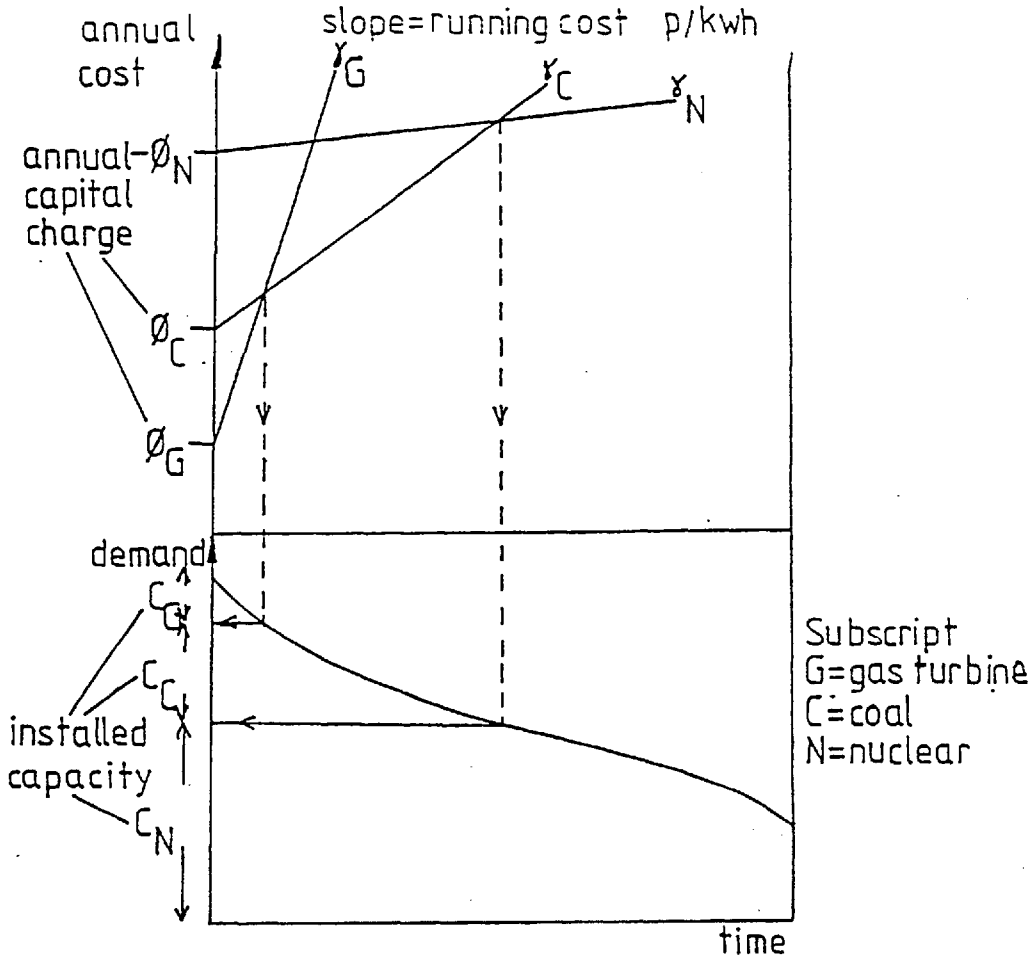

Fig. 5.6 Determination of Optimal System Mix (Ref. 4)

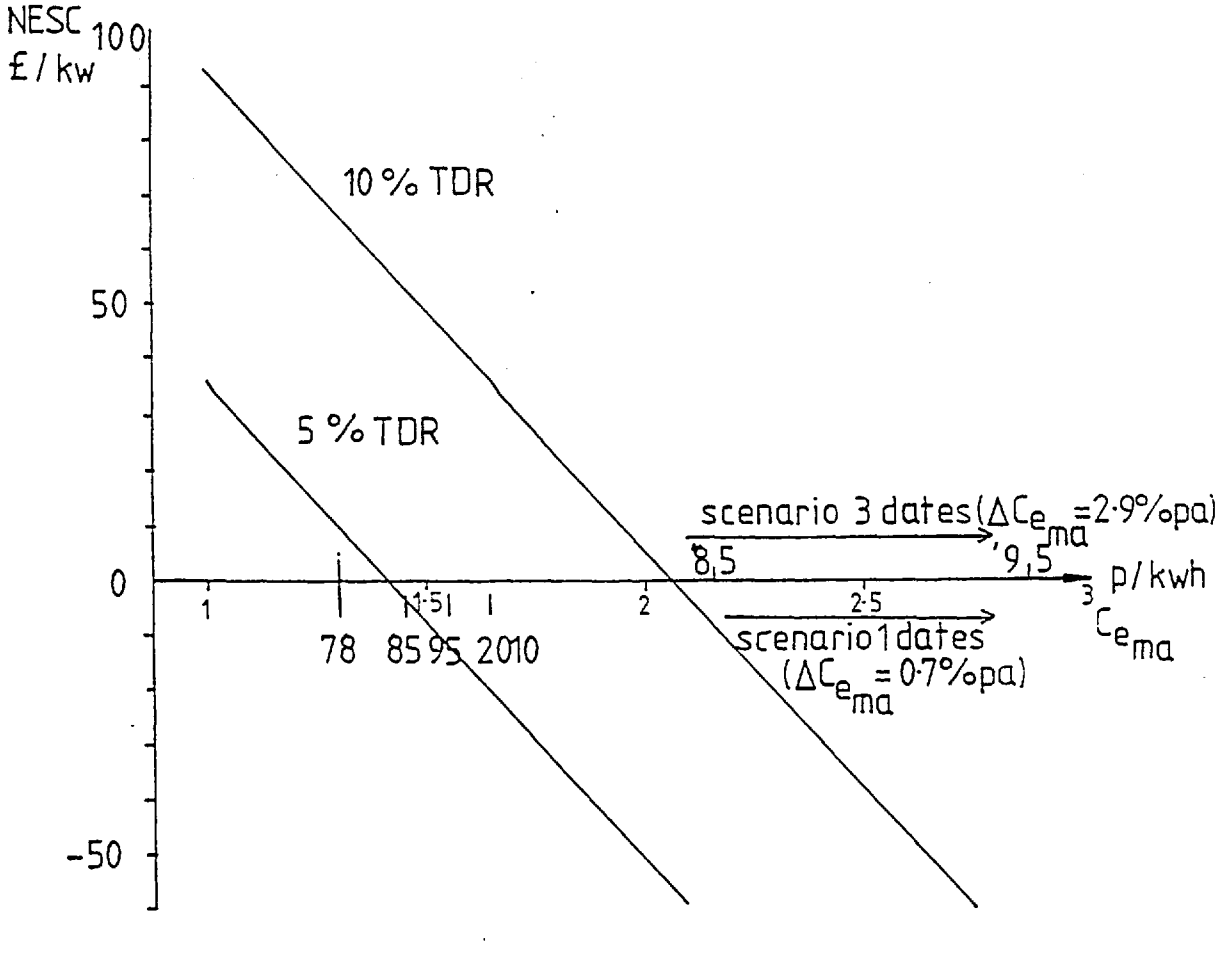

Fig. 5.7 NESC of Base Load AGR Capacity

is just the annual charge on a unit of gas turbine capacity.

In a sub-optimal mix, the plant with the lowest value of (capital charge - operating savings) would be chosen to meet increments in maximum demand. This quantity, (capital charge - operating savings), is called the 'Net Effective System Cost' (NESC), and is a measure of the value of capacity. The NESC of a unit of plant may be negative in which case it would be installed regardless of an increase in maximum demand.

The above analysis has been simplified in order not to obscure the principles; further sophistication may be adopted:

1. The availability and effective load carrying capability have not been specifically mentioned. They may be included as follows:

$$\text{NESC/kW firm capacity} = \frac{\emptyset}{\text{ELCC}} + \frac{1}{\text{ELCC}} \sum_{i=1}^{8760} \frac{P_i}{P_{max}} (\gamma - \gamma_{i_{marg}})$$

where P_i = power generated by plant in hour i

$\gamma_{i_{marg}}$ = marginal electricity unit cost in hour i

P_{max} = plant maximum capacity.

In this way the results from the probabilistic simulation models or normal distribution method, assigning values to ELCC and $\gamma_{i_{marg}}$, may be integrated with the Berry approach, giving more accuracy.

2. For constant electricity demand and price, and fuel prices the net effective system cost(NESC) and net present worth (NPW) criteria are equivalent, being related by the formula

$$\text{NESC} = \frac{-\, i \times \text{NPW}}{\left(1 - \frac{1}{(1+i)^N}\right)}$$

where i = discount rate

N = plant life.

However if electricity or fuel prices rise then the NPW criterion would be preferentially used.

The evaluation of independently owned CHP schemes has been divided into capital and running cost elements. The value to the ESI of units is always the marginal running cost. Although the ESI may have the option of investment in plant with NESC<0, the value of independent capacity is:

$$\text{Maximum } (0, ELCC_{CHP}.NESC_{min})$$

where $ELCC_{CHP}$ = effective load carrying capability of CHP scheme

$NESC_{min}$ = lowest alternative NESC plant investment option for ESI.

The CHP scheme does not in any sense pre-empt the ESI's installation of plant with NESC<0, and hence they would not wish to charge for the privalege of installing capacity.

The situation may therefore arise where an independent scheme may go ahead that would not be acceptable to the ESI. The reason may for example be a local requirement for a more secure electricity supply, but if due to restricted independent investment opportunities it could lead to a mis-allocation of resources in the national sense. There may then be an argument that to maximise the Nation's interest, the capacity element should be $ELCC_{CHP}.NESC_{min}$, whatever the value of $NESC_{min}$.

Does the ESI have plant available with NESC<0? Perhaps the most likely contender, in an era of rising fossil fuel prices, is nuclear plant, and so figure 5.7 presents the results of NESC calculations for base-loaded AGR capacity. Calculations are based on a 7 year construction period, 70% availability, and capital and running costs taken from Ref.20. Marginal running costs are calculated by the probabilistic simulation model for a time base of January 1978, and are assumed to continue to be dominated by fossil prices (justified in the next chapter). Low and high fossil fuel price growth rates are investigated by incrementing marginal electricity prices by 0.7% and 2.9% per annum

respectively (Ref.20). Discount rates of 5% and 10% are used.

The net effective system cost of the AGR is sensitive to both the discount rate and the rate at which fossil fuel prices rise, but on the whole has, or will tend towards, a negative value as fossil fuel prices rise. It is therefore quite possible that if units are valued at the marginal electricity price, then, using this analysis, capacity per se has little value to the ESI.

The above analysis has made one important simplification in that not all plant have the same construction times, and some may have special features required for the operation of the system. It has already been mentioned that gas turbines are used as 'regulators' and to meet the peaks in demand, and therefore gas turbine capacity is usually included in plant expansion programs. The extent to which cogeneration schemes can substitute for gas turbines will have an important influence on the value assigned to their MW/MW capacity credit:

1. CHP schemes have similar construction times, around two to three years, as gas turbines, and hence may be used as regulators of system capacity in the same way.

2. Diesel and gas turbine CHP schemes would have the fast response properties necessary to meet system peaks. However during the winter little spare capacity will generally be available, and it has therefore been suggested (Ref.62) that, if ESI operated, when the peak is anticipated the CHP plant would be off-loaded to less flexible steam plant, and would pick up load when the peak occurs. The extent to which independently operated CHP schemes could reduce gas turbine capacity at the peak, would depend on the success of the pricing signal; but during the winter the scheme will usually be base loaded during working hours and hence unable to load follow at the peaks.

CHP capacity will therefore have two elements of possible value to the ESI:

1. At any stage in the CHP scheme's life there is a finite probability that the ESI construction programme will not have proved sufficient to match demand. The short construction time plant options open to the ESI will then determine the value assigned to the MW/MW capacity credit.

2. The CHP scheme can be included in the ESI 7 year plan, in the year that a firm commitment is made to construction. The value of CHP capacity would then be determined by the NESC of competing plant. If gas turbine capacity is included in the construction programme, the value assigned to the capacity displaced may, bearing in mind the previous comments, be the cost of gas turbines.

The uncertainties in $NESC_{min}$ and the ability of CHP capacity to substitute for gas turbines, has made the discussion of value to MW/MW capacity credit somewhat inconclusive. If ESI owned CHP schemes can fulfill the role of gas turbines, they will arguably determine the value of capacity displaced by independent CHP schemes. The highest value that can be assigned is probably that of gas turbines, the lowest zero or even negative values.

5.6 A DISCUSSION ON OWNERSHIP

This chapter has identified the mode of operation of CHP schemes to maximise the national interest, and has described the methods by which scheme operation may be analysed. Little has been said about

the relative merits of ownership, and hence the chapter ends with some discussion of this subject. CHP schemes will be broadly classified into ESI and independently owned and operated schemes.

The ESI in the UK is basically divided into two parts: the CEGB and the Area Boards. If owned by the CEGB the scheme would be fully integrated with its planning and operational procedures. Units would have 'operational' values, somewhat higher than expectation values, because the scheme can displace peaking plant. The capacity credit could be calculated as for any other CEGB plant. Because the CEGB uses a National test discount rate, the Nation's benefit from CHP could be expected to be maximised.

The Area Boards can also install generating capacity, and the Hereford scheme (Ref.76) is a well publicised recent example of an Area Board owned CHP scheme. The Area Board would value electrical capacity and units at Bulk Supply Tariff rates. This is a reasonable approximation to long run marginal costs, but suffers the disadvantages, in terms of the overall optimisation of CHP electricity, of:

1. Not automatically, accurately reflecting the value of capacity in the short term (the construction period of central plant).
2. It does not distinguish between the value at the peak of units from base loaded and of peak-lopping plant.

CHP schemes are an optional investment for an Area Board and hence a higher test discount rate than that recommended for the Nationalised Industries will tend to be used, resulting possibly in a misallocation of National resources in the various options for generation investment. Area Boards do however have the advantage of being in contact with industry, and are in the best position to make the necessary local commercial arrangements. If a large contribution from CHP is con-

templated, a decentralisation of responsibility for electricity generation to an Area Board structure might be advantageous.

Independently produced units and capacity will be lower in value than from ESI schemes due to the imperfection of the tariff as a signal. Industrialist's test discount rates are higher than National test discount rates, especially for non-production investment (Ref.84), and hence generation opportunities of greater value than those installed by the CEGB are lost. This imbalance in investment criteria could however be removed by grants or tax allowances from Government. With a co-operative ESI offering the marginal value for exported electricity, the investment criteria for industrial CHP could be brought in line with that necessary for the maximisation of the National benefit.

However the industrialist is not in business to produce electricity, and hence may generally not be interested or qualified to do so. Despite all the right economic signs, industry therefore might still not wish to install CHP schemes. A National Heat Board might therefore be considered (various forms have in fact been proposed, eg. Ref.17), whose job would be to install and operate CHP schemes and act at the interface between industry and the ESI. They would have the necessary expertise and enthusiasm to promote CHP, and being a Nationalised Industry could apply the National test discount rate. A disadvantage is the introduction of another bureaucracy. A 'competitor' to the ESI might have beneficial results.

The aim of national policy should be to set up a system whereby the Nation's benefit is maximised, and hence where contributions from all sources are fairly valued in respect of this consideration. A mix of private and ESI cogeneration could be expected. The difference between the values of ESI and Independent cogeneration electricity

should be small. The results of the next chapter although derived from expected values, and hence being directly applicable to the valuation of independent schemes, will be a close valuation of industrial cogeneration from ESI schemes.

5.7 SUMMARY AND CONCLUSIONS - CHAPTER 5

The following important conclusions have been reached in this chapter:

1. The National benefit is maximised when independently generated electricity is traded at marginal value and a National test discount rate is used to assess schemes. Similarly the ESI should assess cogeneration schemes with the same criteria as other plant options.

2. A CHP scheme has two elements of value: that of the units generated and of its contribution to capacity.

3. The trading arrangement is determined by a tariff which is a compromise between accuracy and convenience: expectation values of ESI marginal generating costs are calculated by a probabilistic simulation model for 2 'typical' days of the year.

4. The response to the tariff is simulated by the site model: non-linear site models have been developed for both diesel engine and gas turbine CHP schemes.

5. The capacity credit is calculated in two stages: firstly the MW/MW capacity credit and secondly the assignment of a value to this.

6. Two methods have been formulated to calculate the MW/MW capacity credit: the more sophisticated is a probabilistic simulation model, the other a method using normal distributions.

7. The value assigned to the MW/MW capacity credit depends largely on the ability of CHP schemes to displace peaking plant, and on cost estimates for nuclear power.

8. Although operational advantages will confer a higher value to ESI cogenerated electricity, the differential over independently generated electricity should be small.

CHAPTER 6

CASE STUDIES ON THE MARGINAL COGENERATION SCHEME

6.1 INTRODUCTION

Chapter 6 presents case studies for two industrial sites to illustrate the use of the methods described in the previous chapter.

Descriptions of the heat and power demand characteristics of the two sites, the plant of the CEGB system, and the prime movers used for the CHP studies, are first presented in section 6.2. This is followed by details on plant capital costs, and on scenarios for fuel and electricity prices (6.3). The chapter then follows a similar pattern to sections 5.3-5.5 of chapter 5, by presenting results of the marginal generating cost calculation (6.4), operation of the site models (6.5), and calculation of capacity credit (6.6). The resulting economics for CHP schemes using diesel engines at the two sites for the fuel price scenarios are then given in section 6.7. Finally some further applications of the models are described including, gas turbine schemes, engine modifications, afterfiring, tariffs and energy conservation.

The results presented are for the marginal CHP scheme. All costs have been reduced to January 1978 values in real terms.

6.2 THE SITE AND SYSTEM DESCRIPTIONS

6.2.1 The Industrial Sites

Detailed heat and power demand data for two sites were obtained. They are as follows:

Site 1: Engineering Firm - Midlands

The heat load is mainly a space heating load with some demand for hot water. The electrical load is for the industrial process. The heat load is therefore seasonal; the electrical load fairly constant. Heat and power load duration curves are shown in figure 6.1. Heat is distributed in the form of pressurised hot water at 150°C.

Site 2: Batch Chemical Firm - North West

The heat load is for process steam and has a higher annual load factor than the space heating load of site 1, as can be seen from the heat load duration curve of figure 6.2. Process steam is required at 10 bar and 180°C. Approximately 50% is spoiled in the process, and hence condensate make-up is 50%. The condensate is returned at approximately 150°C.

The problem of matching the heat available from the engine to that required, is immediately obvious. To heat 1 kg of water by 100°C requires 420 kJ, whereas the isothermal conversion to steam at a temperature $\geq$100°C requires approximately 2280 kJ. The Ruston AT350 engine at normal design has around 18% of fuel input energy as available exhaust heat (at a temperature sufficiently high to convert water to steam), and around 22% as heat at $<$100°C. Thus even if all the water converted to steam by the engine is feedwater make-up, heated to 100°C

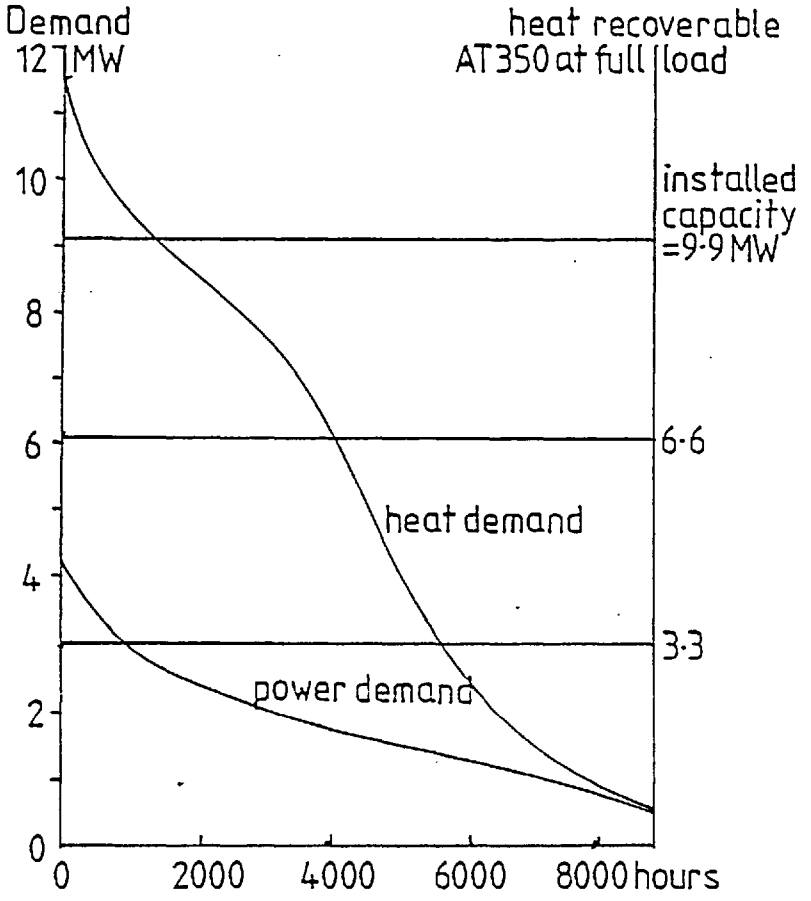

Fig. 6.1 Site 1 Heat and Power Load Duration Curves

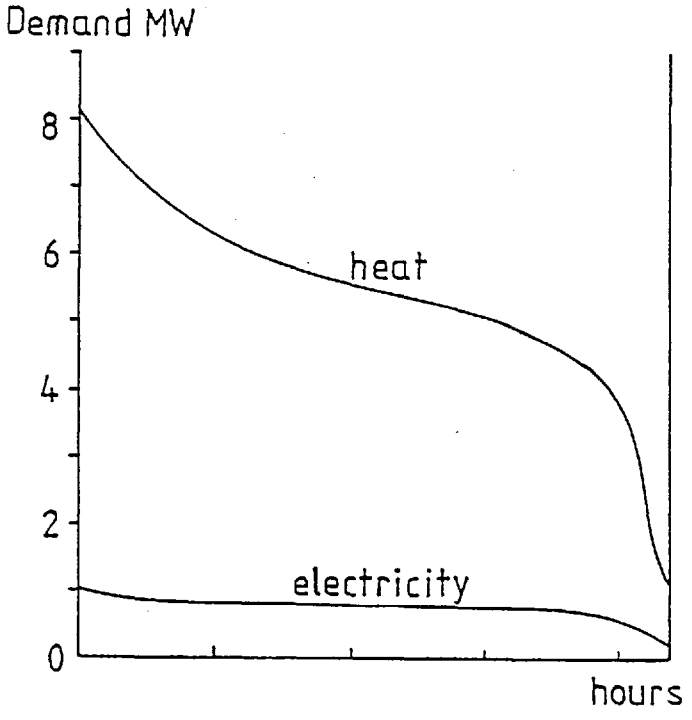

Fig. 6.2 Site 2 Heat and Power Load Duration Curves

by the cooling circuits of the engine, only a small fraction of the available low temperature heat can be utilised. Alternatively the contribution of cogeneration is severely limited if the use of all the low temperature heat for feed heating determines the size of the scheme. To improve the fraction of low temperature heat recovered, either its temperature must be raised (section 4.4), or a separate use found for low temperature heat $<100^{o}C$.

It may be possible, or the economics may favour even with replacement of distribution mains etc., to lower the temperature of the distributed heat. The design philosophy of one centralised boiler house, plus minimisation of capital cost of the distribution network, favours a one high grade of heat system. The best design approach in a diesel powered CHP scheme may be to have perhaps several, lower grade heating circuits, requiring higher capital cost but inducing considerable savings in running costs. The cogeneration scheme must not be considered in isolation, but viewed as an integral part of an energy conservation and supply investment decision.

It will generally be easier to reduce the temperature of heat demand for space heating applications than for process, where expensive re-design of process methods may be necessary. It has therefore been assumed in the case studies that for site 1, all the low temperature engine heat is usable (possibly entailing some changes in heat delivery methods), but that for site 2 none can be used. In this way the two extremes of heat recovery possibilities for the engine will be illustrated.

6.2.2 The CEGB System

The model of the CEGB system used in the probabilistic simulation

models, is based on data taken from references 9, 11, 18 & 20, and is outlined in Table 6.1. The plant and costing breakdown is a result of the contradictory requirements of realism and limitations on computing resources. The following comments are needed:

1. The system was modelled in the years 77/78 and 84/85; the installed capacity in the latter case being based on scheduled construction completion (Ref.9) and of planned decommissioning.

2. Unit generating costs shown are at the station gate, and have all been adjusted to January 1978 money values.

3. A 20% outage for maintenance was assumed during the 'off-peak' season.

6.2.3 The Prime Movers

In order to maintain continuity and to show the economic benefits of the design changes postulated in chapters 3 and 4, the Ruston AT350 engine is used, as the model engine. It is in any case fairly typical of modern 4-stroke design. This engine will be available in sizes ranging from 3 cylinders at 1.1 MW up to 18 cylinders at 6.6 MW. The gas turbine used is a GEC EM-27 variable recuperation turbine, having a maximum power output of 1.9 MW, and described more fully in Ref.52.

The characteristics of the 9AT350 engine have been given in chapter 4, and are taken to be similar for the other sizes of this engine. Lubricating oil costs and maintenance costs are for convenience taken to be proportional to the cost of fuel used in the engine. For fuel oil priced at 0.45 p/kwh, lubricating oil is taken as 5% and maintenance at 10% of fuel cost. These figures are deduced from Ref.15 and relate to an engine of 125 kW/cylinder. Engines of higher output per cylinder may have lower maintenance costs; alternatively costs for older or

TABLE 6.1

CEGB System

Type	Unit Size	FOR		Generating Cost/kWh Jan. 78 Price Level	Installed Capacity MW	
	MW	1977	1984	1977	1977	1984
N	620	-	0.20	-	-	3720
N	460	0.15	0.15	0.54	3688	3688
F	620	-	0.20	-	-	8060
F	430	0.15	0.15	1.136	24080	24080
F	200	0.10	0.10	1.254	6400	6400
F	160	0.10	0.10	1.361	3680	3680
F	100	0.10	0.10	1.291	5000	5000
F	90	0.10	0.10	1.490	5040	5040
F	65	0.10	0.10	1.758	2535	2535
F	60	0.10	-	1.900	2280	-
F	60	0.10	-	2.000	1200	-
GT	80	0.05	0.05	3.50	2240	3520
					56,043	65,723

N = Nuclear

F = Coal or Oil fired

GT = Gas Turbine

TABLE 6.2

Scenarios for future coal prices

p/kWh of coal	Profile 1	Profile 2	Profile 3	Profile 4
1985	0.52	0.47	0.38	0.33
1995	0.69	0.61	0.45	0.35
2010	1.37	0.92	0.60	0.40

poorly maintained engines could be significantly higher. The engine is assumed to be on forced outage 5% of the time and planned outage 10% of the time. Design efficiencies of modern industrial fossil fuel fired boilers are around 80%, and this figure is used as the auxiliary boiler efficiency in the site models. Afterfiring efficiency is taken as 96%.

6.3 SOME BACKGROUND ON PRICES

6.3.1 Scenarios for Fossil Fuel and Marginal Electricity Prices

The differentials between the prices of fossil fuels, nuclear power and marginal electricity will be central in determining the economics of cogeneration schemes. Ideally probability distributions would be estimated for future fuel prices, and CHP planning decisions made with expectation values of return which included fossil fuel and electricity price uncertainty. However the effort required for this was beyond the scope of this research project, and instead scenarios were used covering a range of possible futures regarded by the Dept. of Energy (Ref.20) as including extreme possibilities.

Table 6.2 shows various possible profiles of future coal costs as proposed in Ref.20. The extreme low and high cases respectively represent costs held down by successful NCB investment, and coal prices close to central estimates for oil. Between 1985 and 1995 they correspond to price rise rates of 0.7% and 2.9% per annum. Although it should be noted that the Profile 1 figure of Ref.20 of 0.52/kwh for

coal in 1985 corresponds to a very high 7.6% per annum increase in the real price of coal between 1978 and 1985.

An important question is how marginal electricity prices will be related to fossil fuel prices over the next 25 years, and in particular whether nuclear power can influence this marginal cost.

The Department of Energy 1978 Green Paper (Ref.21) gives high and low growth rates for simultaneous maximum demand (SMD) of 3% and 2% respectively. These equate to SMD in the year 2000 between 66 and 82 GW. The CEGB load duration curve shown in figure 6.3 (Ref.41), gives a base load of 14 GW in 1982. The load duration curves for 2000 represented approximately by the straight full and dashed lines are for 2 assumptions about load shape development. The full line corresponding to a base load multiplied by the factor $\frac{SMD_{2000}}{SMD_{1982}}$, and the dashed line being an increase in base load by $SMD_{2000} - SMD_{1982}$. The four lines therefore approximately cover the extremes expected by the Department of Energy in the year 2000.

The required new plant construction by 2000 to give a 20% margin, is 27 GW for 2% growth and 61 GW for 3% growth. The maximum possible new nuclear capacity on line by 2000 is stated as 35 GW (Ref.21). The effective nuclear capacities in 2000, allowing for an availability of 0.7, in the 2% growth case (27 GW of construction) and 3% growth case (35 GW of construction), are marked in Fig. 6.3.

It is then apparent that within the range of 'conventional' energy futures, apart from a small influence by nuclear electricity during the summer night, the expected marginal cost will be determined by fossil fuel prices. This is most useful as it allows the conclusion that the shape of the diurnal marginal electricity cost will remain reasonably constant, and prices can, to a first approximation, just be

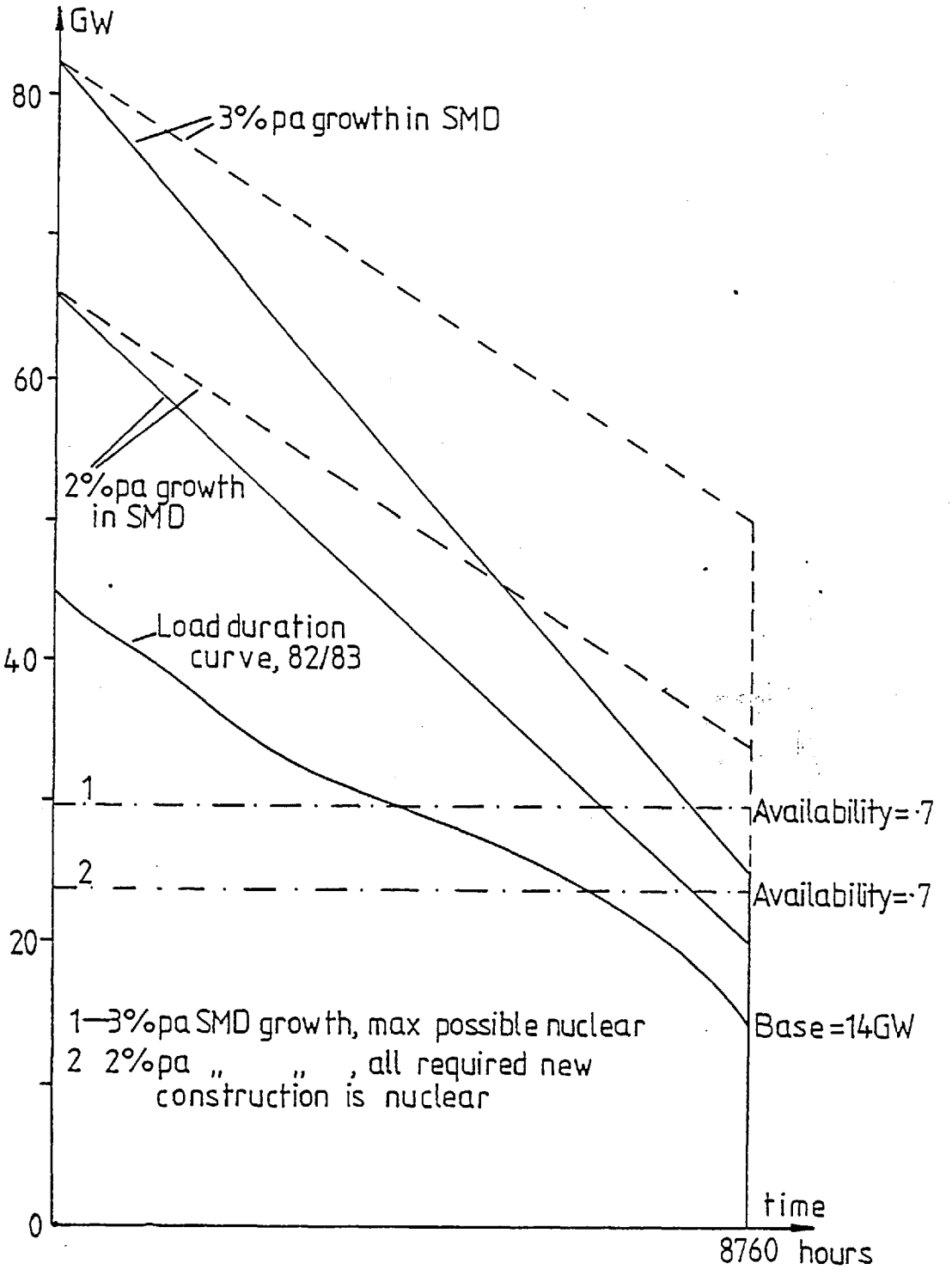

Fig. 6.3 CEGB Load Duration Curves: 1982 and 2000

inflated by the rise in fossil fuel prices. Gradual small improvements due to the displacement of more efficient fossil plant may be expected, but these have been neglected in the following analyses. It is of course possible that the future will lie outside those presented here: some modification would then be required to the results and conclusions that follow.

Marginal electricity generation is dominated by coal burn; it is therefore assumed in the scenarios used that marginal electricity prices rise at the same rate as coal prices. It is therefore implicitly assumed that gas and oil burn is substituted by coal (as far as possible), if coal becomes significantly cheaper than oil and gas, or that gas, oil and coal rise at similar rates. It is unlikely that oil or gas prices would rise more slowly than the coal price.

In order to cover a full range of possibilities the following 3 scenarios were investigated:

Scenario 1: Annual rate of rise of the marginal electricity price $\Delta C_{marg} = 0.7\%$ and of the price of fuel to the scheme $\Delta C_f = 0.7\%$ per annum. ie. coal and oil prices follow a low price growth rate path corresponding, for coal, to the rate of increase between 1985 and 1995 of profile 4 (Table 6.2).

Scenario 2: $\Delta C_{marg} = 0.7\%$, $\Delta C_f = 3.5\%$ per annum. ie. coal prices are kept reasonably low as in scenario 1, but oil prices double in 20 years.

Scenario 3: $\Delta C_{marg} = 2.9\%$, $\Delta C_f = 2.9\%$ per annum. ie. both coal and oil rise at the higher rate, profile 1 (1985-1995) of Table 6.2: a doubling time of 25 years. In each case the starting point for annual increments is the January 1978 actual value: thus actual values are less in the high growth case than actual profile 1 values.

Thus the influence of the relative values of capital and fuel, and a high relative rise of oil with respect to electricity (a most disfavourable case for diesel cogeneration) are covered. The case of electricity prices rising more quickly than oil is considered unlikely.

6.3.2 Plant Capital Costs

It is the incremental cost of the CHP scheme that must be used for the capital cost in assessing the economics of the scheme. Hence the capital cost will rarely include the cost of auxiliary boilers; the afterfiring rig is only included if there are existing, serviceable boilers; the distribution network only if it needs replacing or extending.

Table 6.3 shows three sources of information on diesel CHP capital costs:

Source 1: (Ref.62) Installation date is 1980, and costs include interest during construction, but no information is given on dating of capital costs. If January 1980 costs then deflation to January 1978 gives £205/kW_e.

Source 2: (Ref.35) December 1976 prices if inflated to January 1978 give £230/kW_e.

Source 3: The total cost is £330/kW_e but the cost of the auxiliary boilers would not normally be included in the incremental cost. Distribution costs are higher than would be met on a single site, which leaves £210/kW_e for a project installed in 1980.

A January 1978 capital cost for diesel CHP of £200/kW_e is there-

TABLE 6.3

Diesel Capital Costs

McLellan (Ref. 62) - Source 1

Installed capacity	24 MW_e		
Plant Cost	£5.75 m	≡ £240/kW	Comments
Building & foundations	0.45 m	£ 19/kW	(i) includes interest during construction
Waste heat boiler	0.35 m	£ 14/kW	
Total	6.55 m	£273/kW	(ii) installation date 1980

Gurney (Ref. 35) - Source 2

Installed Capacity	15.36 MW		
Generators	£1.84 m	≡ £120/kW	
Major Plant	0.85 m	£ 55/kW	(i) 6 small engines
Ancilliary Plant	0.29 m	£ 19/kW	
External Works	0.09 m	£ 6/kW	
Total	3.07 m	£200/kW at Dec. 76	≡ £230/kW at Jan. 78 prices

Price (Hereford Scheme) - Source 3

Engines	£133/kW_e	≡ £210/kW_e completion date December 1979
Buildings	£ 67/kW_e	
Waste Heat Boilers	£ 10/kW_e	
Auxiliary boilers	£ 40/kW_e	≡ £16/kW_{th}
Distribution	£ 83/kW_e	= £33/kW_{th}
	£333/kW_e	

fore felt to be reasonable. This is perhaps optimistic and sensitivities to £250 and £300/kW_e are investigated.

6.4 TARIFF RESULTS

A two season year was chosen: the 'winter' season comprising weekdays, November to February inclusive, and the summer season, the rest. This choice was decided by the desire to highlight the differences in daily marginal price variation winter to summer, and to facilitate the accurate determination of capacity contribution at times of potential system maximum demand. Annual system maximum demand falls on working weekdays between December and February (Ref.45): the response of CHP schemes to well defined expected marginal costs is therefore procurred by this winter season. The inclusion of November and holidays should not significantly distort results. Summer season cost values are perhaps a little distorted by the inclusion of winter weekends, but this is done for simplicity in tariff structure. The maintenance schedule tends to equalise the marginal cost and the risk of loss of load, between summer and winter.

The expected marginal costs were calculated by the probabilistic simulation model described in section 5.3.3, using the system plant described in table 6.1, and a year's hourly CEGB demand data for 1977/78 (April to April). Costs calculated are station gate costs, and make no allowance for transmission losses.

Results for 1977/78 are shown in fig. 6.4. The marginal cost has features that could be expected: a winter peak at around 5-6 pm, a night valley and fairly constant values during working hours. The summer

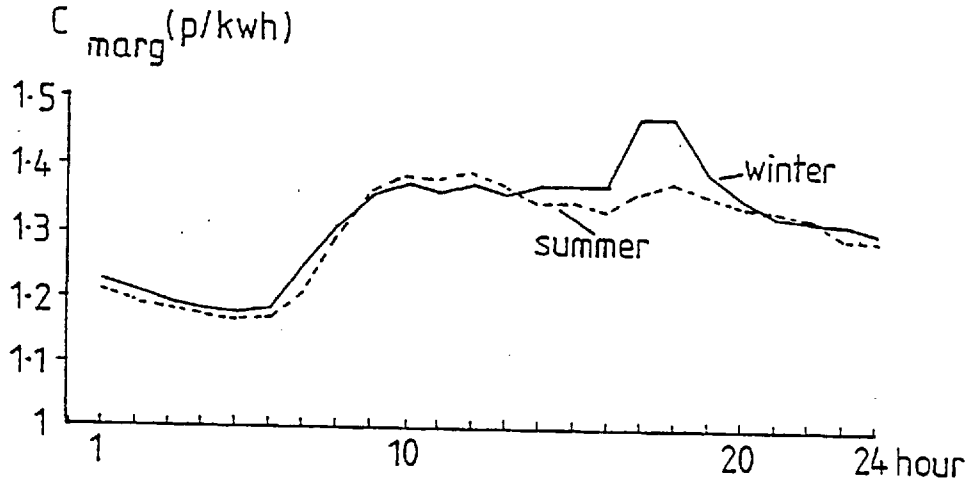

Fig. 6.4 Predicted CEGB Expected Marginal Generating Costs 1977/78

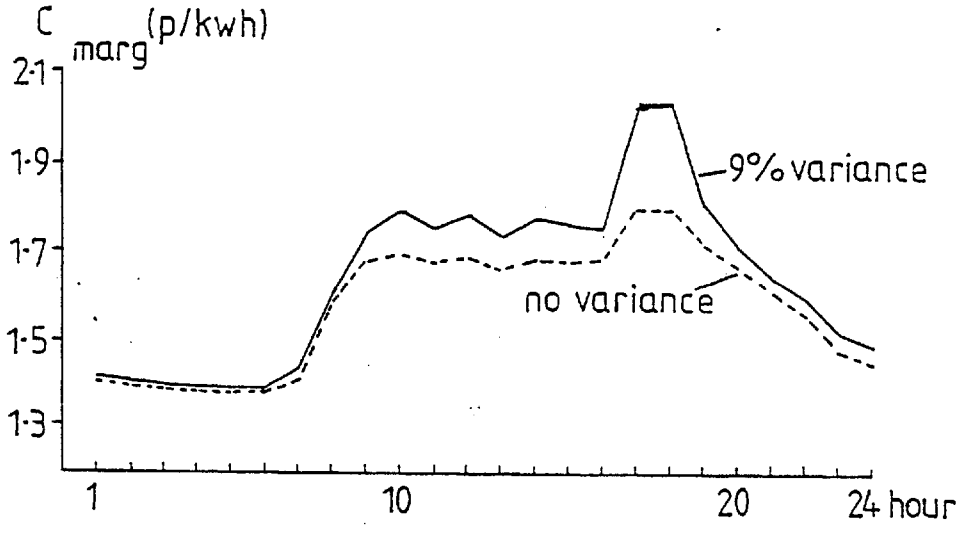

Fig. 6.5 CEGB Expected Marginal Generating Costs 1984/85 - Winter Season

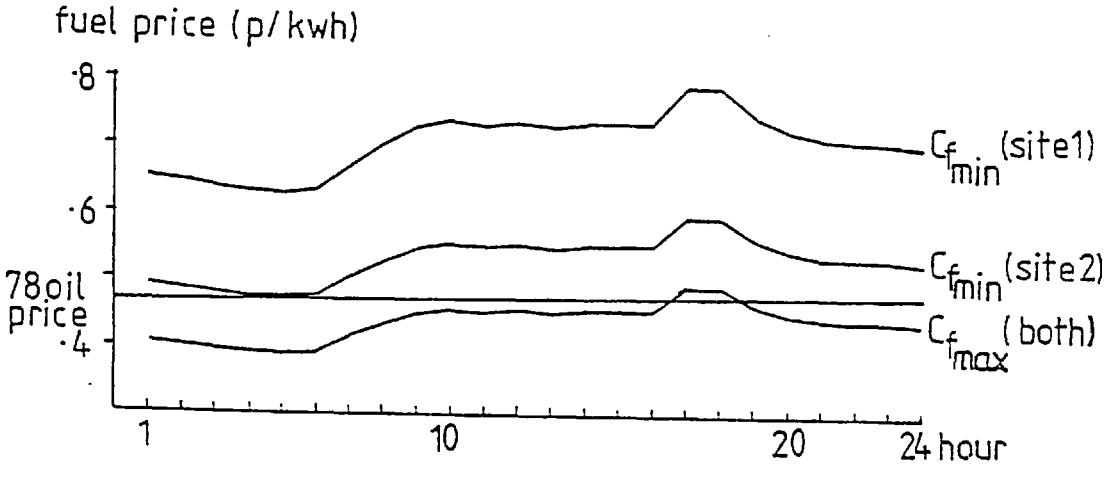

Fig. 6.6 Break-even Fuel Costs 1977/78

curve lacks the sharp afternoon peak, but has a broader peak in the late morning. Fossil fuel costs dominate the marginal costs throughout. The average of the marginal costs ($C_{e_{ma}}$) is approximately equal to the Bulk Supply Tariff energy charges for that year (with fuel cost adjustment), being 1.297 p/kwh on average, compared to 1.231 for the Bulk Supply Tariff. A difference of 5%, easily accounted for by the inaccuracies of both pricing methods, and the imperfection in allocation of capital costs.

Marginal costs were also calculated for 1984/85 (approximately the last date for which the system is presently determined), using postulated electricity demand for both scenarios 1 and 3, with and without a 7 year forecast variance of 9% (Ref.45). Demand in 1984/85 is calculated from 1977/78 hourly demand figures by multiplying by the factor of 1.2 = $\frac{SMD_{1984}}{SMD_{1977}}$, where SMD_{1984} is a CEGB estimate (Ref.9). Results for the scenario 3 calculations are shown in Fig. 6.5. The system in 84/85 has less reserve capacity than in 77/78 which means that the hourly marginal cost variation over the day is larger: less efficient plant are 'expected' to cover daytime peaks. Inclusion of forecast variance increases expectation values because generating costs increase more rapidly as one moves down the merit order.

Beyond 1984/85 uncertainty in fossil fuel price, electricity demand and the plant in the system are all factors in the calculation of marginal prices. Installation date in the case studies presented is assumed to be January 1978; project life is 25 years. To make an investment decision and in order to calculate capacity displacement in future years, estimates of fossil price, electricity demand and system plant could be made, a tariff calculated, and the site model used to simulate CHP operation, for each year over the lifetime of the plant. This would be very time consuming and hence a simplified approach was adopted.

Using the 1977/78 tariff the site models were run for a wide range of fuel costs (0.35-0.75 p/kWh). The method for each of the scenarios was then:

Scenario 1: The ratio $\frac{C_f}{C_{marg}}$ remains constant and hence the optimal operation of the CHP scheme will be unaltered by fuel price changes. The scheme's operating profit is just increased by 0.7% per annum.

Scenario 2: The ratio $\frac{C_f}{C_{marg}}$ is calculated for each year n over the project lifetime. Then assuming constant C_{marg} the fuel cost is determined for year n, and the profit for each year extrapolated from the table of operating values. Each year's profit is then multiplied by $(1.007)^n$.

Scenario 3: As for 1 but with the profit being increased by 2.9% per annum.

Although this approach ignores the affects of the changing margins between system demand and installed capacity, it is felt to be a reasonable approximation. It is implicitly assumed that the price of heavy fuel oil continues to determine the value of industrial heat. This may be questionable if the oil price rises significantly faster than other fuels, although inertia and the operational advantages of oil will ensure that it will still be widely used over the lifetime of any plant installed at present.

6.5 APPLICATION OF THE SITE MODELS

Hourly demand data for each of the sites for one year were used. Each diesel engine was assumed to be out of operation for five weeks

in the summer for maintenance. In addition they were assumed to be subject to a forced outage rate of 5%. Operation was simulated by the site models for fuel prices between 0.35 and 0.75 p/kwh, and for a range of installed capacities. Before discussing capacity credits in the next section, and the overall economics of the schemes in section 6.7, some preliminary comments are made on sensitivities of site operation.

Some approximate information is readily available about the sensitivity of CHP output to the ratio $\frac{C_f}{C_{marg}}$. Electricity from the engine is at a minimum price when the heat demand, $H > Q_{emax}$ then the maximum permissible fuel price for breakeven with the central supply $C_{f_{min}} = \frac{C_{marg}}{\frac{k_m}{\eta_e} - \frac{r}{\eta_{aux}}}$. CHP electricity price is a maximum when $H = 0$, then the maximum permissible fuel price for breakeven with the central supply $C_{f_{max}} = \frac{\eta_e}{k_m} C_{e_{marg}}$, $Q_{e_{max}}$ = maximum heat recoverable from the engine.

The other symbols are explained in Appendix 3. This is approximate as it ignores benefits from afterfiring which will favour CHP electricity production.

$C_{f_{min}}$ and $C_{f_{max}}$ have been plotted in fig. 6.6 for each hour of the winter day for both sites using the 77/78 tariff. Also drawn is the January 1978 heavy fuel oil price to industry (Ref.18) of 0.47 p/kwh. If C_f is below $C_{f_{min}}$ the scheme will generate when $H \geq Q_{e_{max}}$, and if C_f is below $C_{f_{max}}$ then production of electricity alone is cheaper on site. Fig. 6.6 therefore shows that site 2 will be much more sensitive to fuel price rises than site 1, and that both sites will generate without any heat load at the afternoon peak.

Fig. 6.7 shows weekly heat outputs from a 6.6 MW engine on site 1,

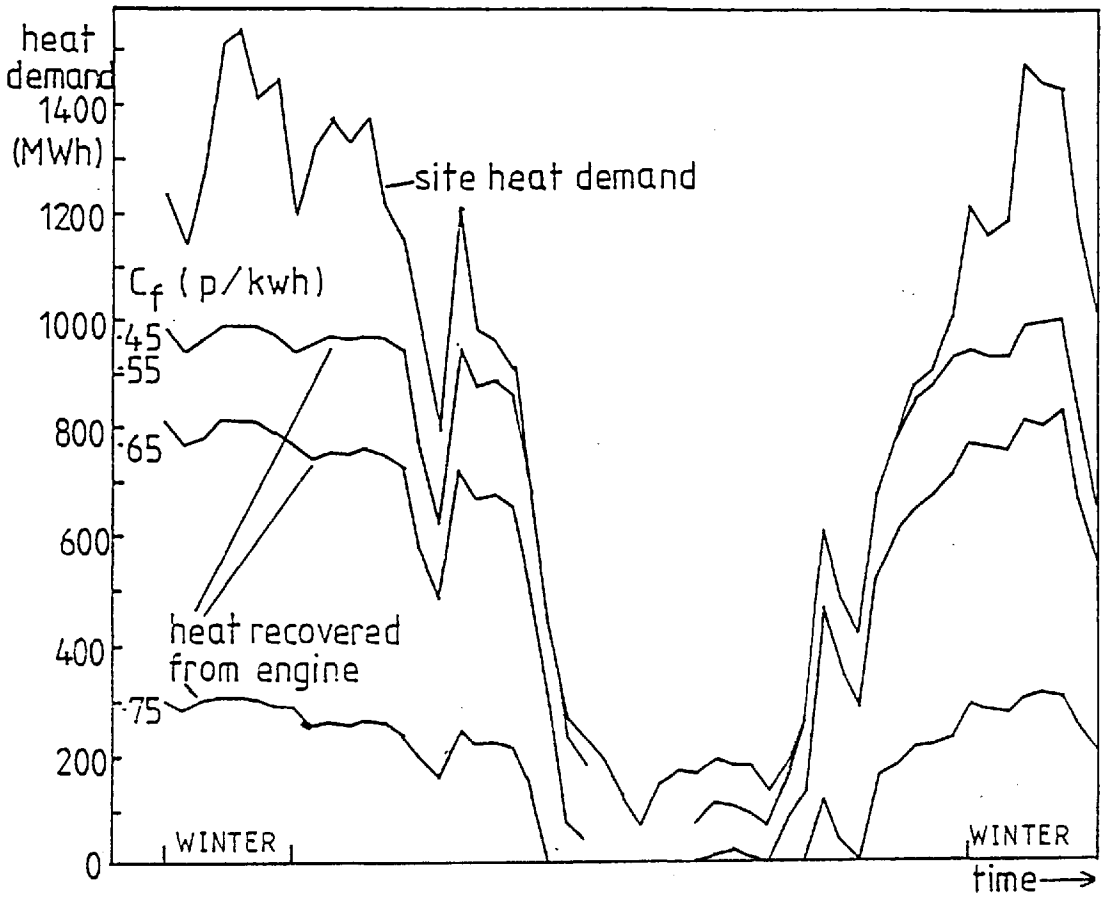

Fig. 6.7 Heat Recovery From 6.6 MW Engine, Site 1

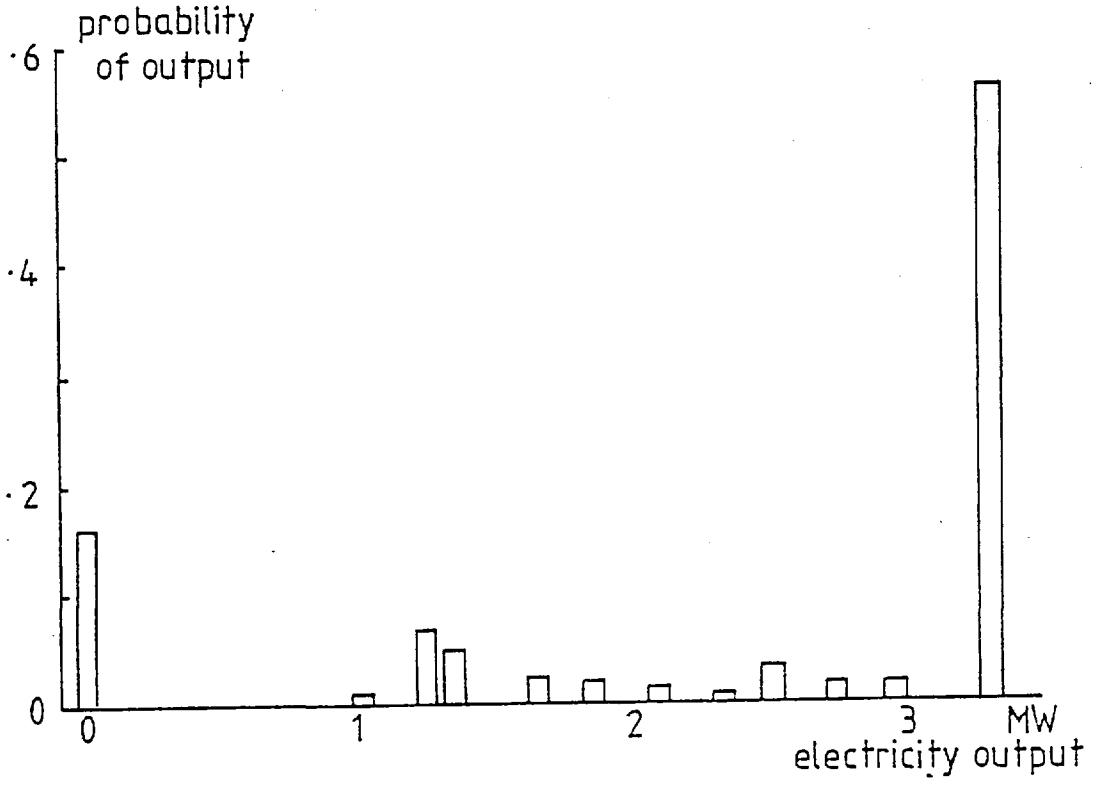

Fig. 6.8 Example of Probability Distribution of Output

for a range of fuel prices. Two important features are discernable:

1. Winter output for each fuel price is fairly stable because installed capacity is such that engine heat recovery is less that the site average heat demand. In this way the scheme is less sensitive to fluctuations in heat demand in future years. Installing capacity giving engine heat recovery less than the site maximum heat demand and topping up preferably with after-firing, alternatively with auxiliary boilers, also improves load factors on the expensive components of the schemes.

2. The drops in output between C_f = 0.55-0.65 p/kwh and 0.65-0.75 p/kwh, might have been deduced from fig. 6.6.

Some more discussion is given to the sensitivity of capacity displacement to fuel price and installed capacity in the next section.

Data is also available, if required, from the site model on hourly CHP operation, which enables plant cycling conditions to be examined. Information is also given on the contributions of after-firing and auxiliary boilers, on heat dumped, import and export of electricity and site thermal efficiencies.

6.6 RESULTS ON MW/MW CAPACITY CREDIT

The system simultaneous maximum demand occurs during the 'winter' season, hence it is the winter probability density functions that are of interest in the calculation of the MW/MW capacity credit. The hourly probability density functions of site output for 'winter' and 'summer' are not in fact normal distributions, as the example of fig. 6.8 indicates.

Problems were encountered with the probabilistic simulation system reliability model when examing a CHP scheme of 5-10 MW in a system of 50 GW. Computer storage and running time requirements are strongly dependent on the size of the steps used to represent the system. For example a step size of 200 MW gives running times of around 120 central processing seconds on a CDC 6600 computer: times rapidly increase for smaller steps. The generally small relative size of CHP schemes results in rounding errors being important, and they were in fact found to swamp the details being sought. To artificially increase CHP scheme size would be to give output variance an importance not there in reality.

Within the confines of available computing resources and the time available for program redevelopment, it was not possible to obtain useful results from this probabilistic simulation model. However in principle this method can work, and in practice might be made to do so with more careful attention to the avoidance of rounding errors. Another line of development would be to modify the marginal cost model, thereby avoiding the rounding errors introduced by deconvolution.

The site model also gives the hourly mean and variance of the site output probability density functions: figures 6.9 a-c and table 6.4 show some examples of the results for the two sites. Figs. 6.9 a-c just show the mean of site output given by the model, and hence do not include the effects of forced outage or loss of heat load. The important features of the results are itemised as follows:

1. As the ratio $\frac{C_f}{C_{marg}}$ increases, the mean value of site output (μ_{CHP}) decreases. For site 1 output is stable up to $C_f \simeq 0.65$ p/kwh and μ_{CHP} changes only slightly. Output from site 2 however is very sensitive to any increases in fuel price. From $(\mu, \sigma)_{CHP}$ the capacity displacement can be calculated at any particular fuel

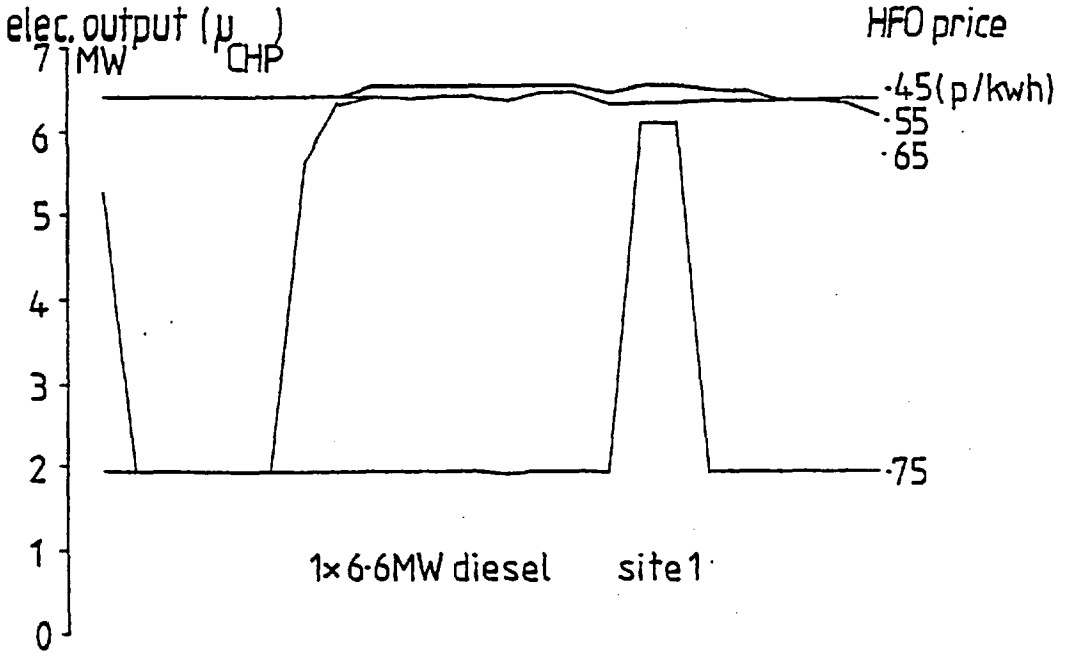

Fig. 6.9a

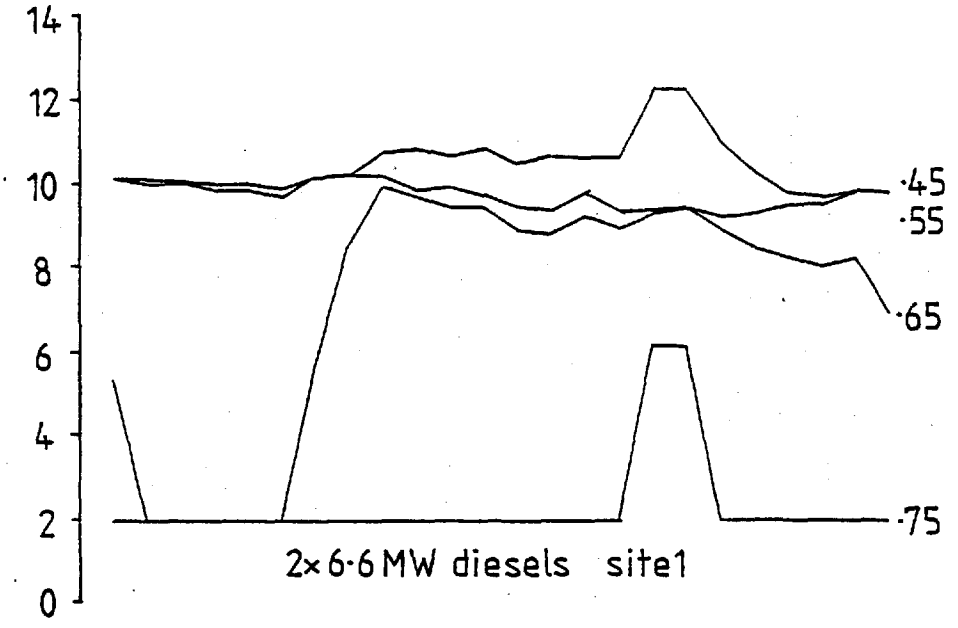

Fig. 6.9b

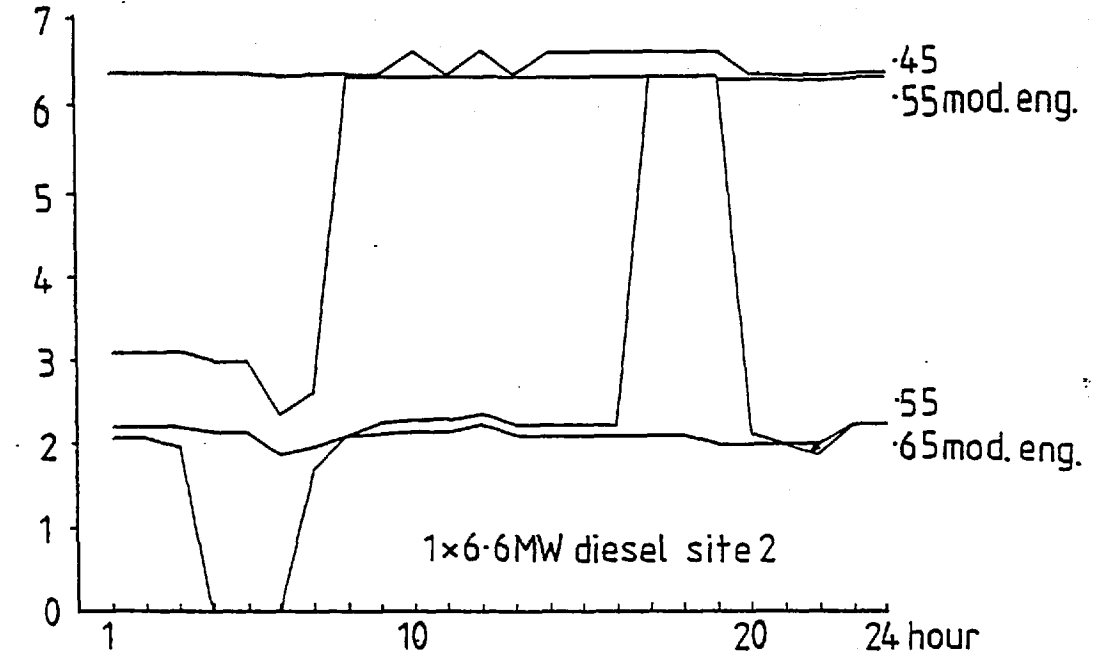

Fig. 6.9c

Mean Values of Winter Season Outputs

TABLE 6.4

Variance of Site Output

Installed Capacity	C_f(p/kwh)	Site 1 μ_1	Site 2 μ_2	Site 3 σ_1	Site 4 σ_2	(σ_o = 4.28 GW) Reduction in MW/MW capacity Credit due to variance (%)	
						1	2
	0.45	3.1	3.1	0.38	0.26	0.001	0.0005
3.3 MW	0.55	3.1	2.1	0.59	0.51	0.002	0.003
	0.65	2.8	1.7	0.54	0.61	0.002	0.005
	0.45	6.2	6.1	0.79	0.99	0.002	0.004
6.6 MW	0.55	6.1	2.5	1.17	0.63	0.005	0.004
	0.65	5.1	1.7	0.98	0.65	0.004	0.006
	0.45	8.7	9.1	1.34	1.72	0.005	0.008
9.9 MW	0.55	8.6	2.9	1.84	0.85	0.009	0.006
	0.65	6.7	1.7	1.52	0.60	0.008	0.005
	0.45	9.9	12.0	1.38	2.47	0.004	0.01
13.2 MW	0.55	9.2	3.2	2.20	1.12	0.012	0.009
	0.65	6.8	1.7	1.87	0.65	0.012	0.006

price. A probability distribution can in priciple be formulated for the future fuel price (eg. a 7 year horizon), and from that directly the probability distribution for capacity displacement.

2. For $C_f < C_{f_{min}}$ output is fairly stable over the day if $Q_{e_{max}}$ is less than the winter average site heat demand, but less so if greater capacities are installed.

3. Table 6.4, shows $(\mu, \sigma)_{CHP}$ given by the site model for the 2 sites for various fuel prices. The $(\mu, \sigma)_{CHP}$ shown include the effects of forced outage. Also shown is the percentage reduction in the MW/MW capacity credit due to the output variance on a 7 year forecast (σ_o (system load standard deviation) = 4.28 GW). In all cases the reduction because of variance can be seen to be negligeable. The MW/MW capacity credit is therefore just the mean of CHP output divided by ESI plant availability at the peak. For the values of $(\frac{\sigma}{\mu})_{CHP}$ shown in table 6.4, the variance would only lead to significant reductions of capacity credit for schemes larger than around 1 GW.

4. In the cases where μ_{CHP} is reasonably constant over the hours other than 0-8, the capacity displacement is well defined. However if μ_{CHP} varies some method of weighting the contribution over the day is needed: it is here that the probabilistic simulation model or some similar method is required. It may be noted that a substantial contribution at the afternoon peak is frequently expected, even when output through the rest of the day is small.

5. The one further contribution to the CHP output probability density function is likely to be the probability of loss of heat load. The variance of a probability distribution assigned to this is unlikely to make the overall variance significant.

6.7 THE ECONOMIC RETURNS ON DIESEL ENGINE CHP SCHEMES AT THE TWO SITES

Tables 6.5a,b show the returns on installed capacities of diesel engines between 3.3 and 13.2 MW, for the two sites under the 3 fuel price scenarios. Returns are shown with no capacity credit and for capacity credits received from year 1 of the project. This capacity credit has been calculated by the Normal Distribution method of section 5.5.2, using the site model results of section 6.6. The maximum value of gas turbine displacement has been assigned to this MW/MW capacity credit (5.5.3); which for a £200/kW gas turbine gives £14.2/kW/annum for a 5% discount rate, and £22/kW/annum at a 10% discount rate. The load factor (L) shown is the ratio of the sum of site heat demands $\leq Q_{e_{max}}$ to the total heat recoverable from the engine if availability is 100%.

Both Internal Rate of Return (IRR), and Net Present Worth (NPW) at 5 and 10% discount rates, are shown. IRR although being a simple, fairly clear indication of economic value, says nothing about the amount of capital that should be invested. NPW is therefore shown which, if a 'cost of capital' has been decided, can indicate how much capital to invest. A 5% discount rate has been used for capacity credits in the IRR calculations.

Much information is given in tables 6.5a and b: the following comments are made on their contents:

1. A capital cost of £200/kW has been used: higher costs will give diminished returns and smaller optimal installed capacities. An increase of £50/kW will decrease NPW by £0.05 million/MW

TABLE 6.5a

Returns on Diesel CHP Site 1

IRR (%) (5% discount rate on displaced gas turbine)		no capacity credit Scenario			capacity credit year 1 Scenario		
L	Installed Capacity (MW)	1	2	3	1	2	3
0.82	3.3	17%	10	20	24	19	26
0.68	6.6	12	2	15	19	13	21
0.56	9.9	10	<0	12	16	10	18
0.43	13.2	8	<0	10	13	7	15

		No Capacity Credit						Capacity Credit Year 1					
NPW (£m)		5% TDR			10% TDR			5% TDR			10% TDR		
L	Installed Capacity (MW)	Scenario 1	2	3	Scenario 1	2	3	1	2	3	1	2	3
0.82	3.3	1.1	0.2	1.6	0.4	0.0	0.7	1.7	0.8	2.3	1.0	0.6	1.3
0.68	6.6	1.2	-0.2	2.0	0.2	-0.5	0.6	2.4	0.8	3.2	1.5	0.6	1.9
0.56	9.9	1.1	-0.7	2.1	-0.1	-1.0	0.4	2.8	0.8	3.8	1.7	0.6	2.2
0.43	13.2	0.8	-1.3	1.9	-0.5	-1.6	0.0	2.7	0.4	3.9	1.5	0.2	2.0

TABLE 6.5b

Returns on Diesel CHP Site 2

		No Capacity Credit			Capacity Credit Year 1		
L	Installed Capacity (MW)	Scenario 1	2	3	Scenario 1	2	3
1	3.3	10	<0	13	17	0	19
0.98	6.6	6	<0	8	13	0	15
0.96	9.9	5	<0	7	12	0	14
0.88	13.2	3	<0	5	11	0	12

		No Capacity Credit						Capacity Credit Year 1					
NPW (£m)		5% TDR			10% TDR			5% TDR			10% TDR		
L	Installed Capacity (MW)	Scenario 1	2	3	Scenario 1	2	3	Scenario 1	2	3	Scenario 1	2	3
1	3.3	0.4	-ve	0.7	0.0	-ve	0.2	1.0	-ve	1.4	0.6	-ve	0.8
0.98	6.6	0.1		0.6	-0.4		-0.2	1.4		1.8	0.8		1.0
0.96	9.9	-0.1		0.6	-0.8		-0.5	1.8		2.4	1.0		1.3
0.88	13.2	-0.5	↓	0.3	-1.3	↓	-0.9	1.9	↓	2.6	1.1	↓	1.5

installed. This is sufficient to eliminate benefits under scenario 2 with no capacity credits for site 1, and virtually so if no capacity credits under all scenarios for site 2. Internal rates of return are reduced by around 3-5 percentage points for a capital cost of £250/kW, but reductions are smaller for further increments in the capital cost.

2. Approximately half the value of the capacity credit is lost if the start of credits is delayed by the first 5 years of the project. Returns are less sensitive to the timing of credits thereafter.

3. Comparison of returns under the three scenarios shows scenario 3 to give an IRR 2-3 percentage points better than scenario 1, representing the higher value of fuel with respect to capital. Returns under scenario 2 are significantly less, despite the higher values attached to heat in this scenario, and become rapidly worse if the start of the project is delayed.

4. If the minimum rate of return acceptable to an industrialist is around 20-25%, then it may be seen that full heat recovery, a high load factor, capacity credits, and a fuel price rising not much more rapidly than the marginal electricity price, are required.

5. The National test discount rate in recent years has been 5-10%, in which case a much wider range of projects match the investment criterion. Although it must be noted that even if CHP schemes meet the test discount rate, other electricity investment options may give better returns.

6. That schemes give acceptable returns without capacity credits imply that they are justifiable on energy savings alone: their net effective system cost is negative. Similarly as diesel CHP and central gas turbines have similar capital costs, it is possible, particularly if ESI operated, that schemes may be acceptable on

capacity credits alone.

7. Curves of NPW against installed capacity may be drawn for each scenario, in order to find the capacity giving the maximum NPW. Maxima are found to be fairly broad implying that the precise capacity is not critical for any particular scenario. Maxima are sensitive to discount rate, fuel price scenario and capacity credits.

The results of Table 6.5 cover a reasonable range of possibilities. Comparisons will be made in the next chapter with other electricity supply investment options. Table 6.5 is only a summary of some of the results calculated and available: results obtained from the site models do in fact allow a much wider range of fuel price scenarios, discount rates and capacity credits to be investigated.

6.8 SOME FURTHER INVESTIGATIONS OF CHP SCHEMES

Some more examples of the application of the site and system models are given in the next 5 sections.

6.8.1 The Values of Afterfiring and of Engine Design Modifications

Afterfiring

It has been assumed in the studies of sections 6.6 and 6.7, that afterfiring of heavy fuel oil in the engine exhaust is utilised. In order to evaluate the afterfiring rig, 3.3 MW and 6.6 MW engines were simulated at site 1 with and without afterfiring. Using a fuel oil

price of 0.45 p/kwh and 77/78 marginal electricity prices, savings of £22,400 and £14,400 per annum, for afterfiring capacities of approximately 9 MW_{th} and 6 MW_{th}, were achieved for the 3.3 and 6.6 MW engines respectively. The efficiency of on site fuel utilisation is increased by 5-6 percentage points at site 1.

Engine Design Modifications

In order to investigate operational changes resulting from engine design modification a 6.6 MW AT350 engine was simulated on the 2 sites, having $R_T = 24$, $\lambda = 1.1$ and a boiler exit temperature of 125°C. Energy balances for this 'extreme' proposal are given in fig. 4.21, column C. Changes to some key parameters over those of the 'normal' engine for the 2 sites, are shown in Table 6.6 for a fuel price of 0.45 p/kwh and 77/78 marginal electricity prices, both constant over the life of the project. Definitions of η_{site} (efficiency of CHP fuel utilisation) and E_s (energy saved by the CHP scheme) are given in section 6.8.4.

The increases in economic value are in both cases fairly substantial. Savings are higher for site 2 reflecting not only a larger percentage increase in heat recoverable, but also the shift from low temperature to high temperature recoverable heat. CHP capital costs could increase by 16% and 45% for sites 1 and 2 respectively, to equalise IRR with and without engine alterations. Engine design modification is therefore especially valuable in the situation where only exhaust heat may be recovered.

The change in energy saved by the CHP scheme (E_s) may be negative, as shown for Site 1 and a central generating efficiency of 28%. Increases in recoverable heat imply that a given heat load may be met with less electricity generated: the sign of the change in E_s will depend on the relative values of central and CHP electrical generating efficiencies.

TABLE 6.6

Value of Design Modification

		Site 1	Site 2
Assumes Constant Capital Cost	Change in NPW at 5% discount rate	+£0.37 m	+£0.69 m
	" " 10% " "	+£0.23 m	+£0.45 m
	" " IRR	+2% points	+5.5% points
	" " η_{site}	+10% points	+5.3% points
	" " E_s at 28% central generating efficiency	-2 GWh/annum	+10.3 GWh/annum
	" 33% " "	+2.7 " "	+10.9 " "

6.8.2 Tariff Comparisons

Section 5.1 established that a marginal cost tariff was required to maximise the National benefit derived from CHP, and this tariff has been used exclusively so far. A comparison is made in this section with two alternative tariffs:

1. Nothing offered for exported units: a situation sometimes encountered and for which many CHP schemes have in the past been designed.

2. A price half-way between the producer's marginal cost and the ESI's marginal cost as suggested by Burchnall (Ref.8). The producer's marginal cost actually depends on the tariff but for this study was defined as the unit cost of CHP electricity allowing a full heat recovery credit.

It is instructive to compare the returns and optimal installed capacities in each case.

Figure 6.10 shows the NPW at 5 and 10% discount rates of investment in a range of engine capacities at site 1 under the 3 tariffs. A January 1978 fuel oil cost of 0.47 p/kwh and 77/78 marginal electricity prices, both constant over the life of the project have been used. Capital costs are £200/kW; no capacity credits have been given.

The results of figure 6.10 show small increases in returns and optimal installed capacities between 'zero export' and 'half-way pricing' tariffs, but significant increases for marginal pricing. The introduction of capacity credits would further magnify the differences. For 'half-way pricing' the ESI acquires some saving in operating cost for no significant capital expenditure. If CHP annual profit is defined as the saving in the site owners cost of

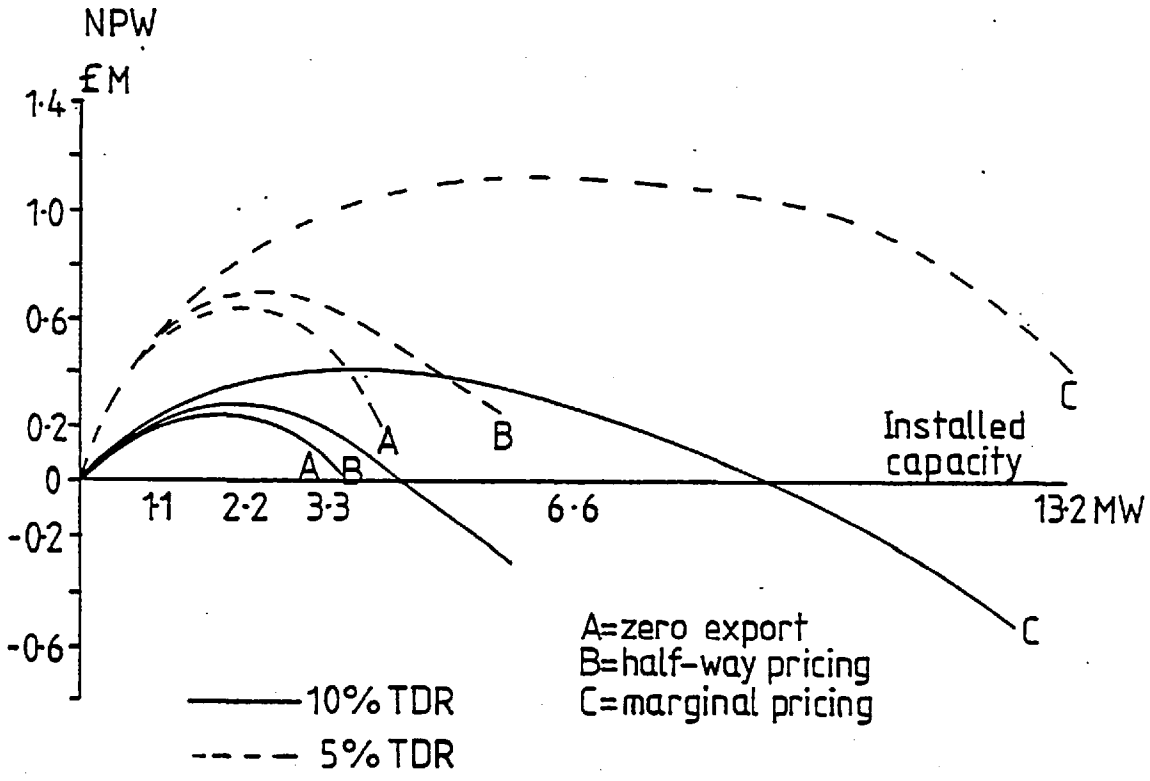

Fig. 6.10 Effect of ESI Offer Price on Installed Capacity

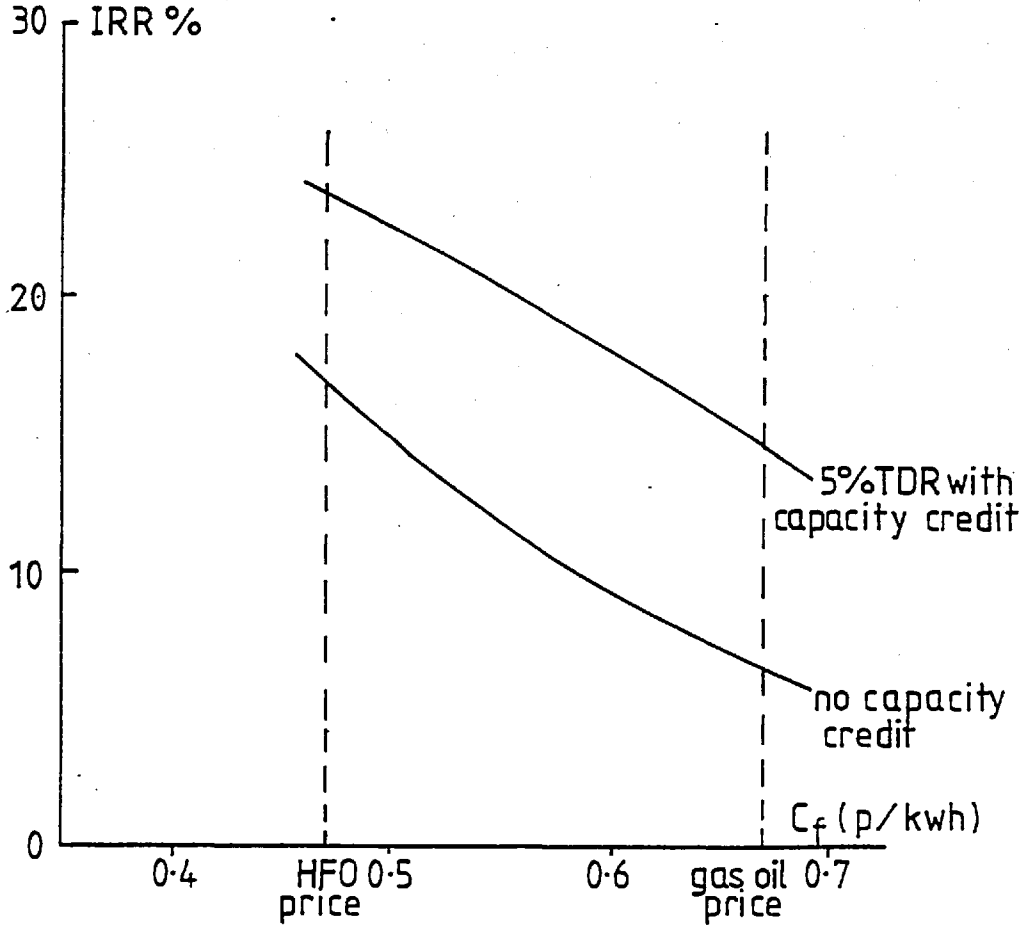

Fig. 6.11 Returns on Gas Turbine at Site 1

meeting his heat and power demands on installation of the CHP scheme, then the ESI's operating saving as a percentage of the site owner's CHP profit is 1.3%, 11.7%, 26.2% and 74% for 1.1, 2.2, 3.3 and 6.6 MW engine schemes. A 6.6 MW scheme therefore gives an ESI annual saving of £71,400; the cost of transmission reinforcement would in many cases be negligeable.

6.8.3 Gas Turbines at Site 1

The gas turbine was simulated for site 1 in order to provide a comparison of performance with the diesel engine. The variable recuperation turbine was simulated, this having been described in more detail in reference 52. Characteristics of the turbine are shown in fig. A3.4. The 1.9 MW gas turbine was found to be a reasonable size for the site and returns are plotted in fig. 6.11 for a variety of fuel prices, with and without capacity credits. All prices are as at January 1978. The following comments are made:

1. Fig. 6.11 shows that if gas is sold at the heavy fuel oil price, then the gas turbine can almost match the rate of return given by a 3.3 MW diesel. Less maintenance costs (assumed rather optimistically zero for the gas turbine analysis), less outage and slightly lower capital costs (taken as £175/kW), almost make up for the smaller value added in the fuel conversion.

2. The energy saved by the scheme is significantly less than for a diesel scheme: approximately 20 GWh per annum as against 50 GWh/annum for a 3.3 MW diesel. The full potential energy savings to the Nation of the industrial heat load are therefore not realised.

3. The variable recuperator on the 1.9 MW gas turbine costs approximately £40,000 and was found to give a simple payback period of

around 3 years, even with grid connection. The variable recuperator therefore provides a useful flexibility for meeting complex site heat demands as at site 1.

4. In the industrial contract market (>100,000 therms/annum) that is under consideration here, British Gas follows a policy of pricing at the alternative fuel price in any particular application. The aim is to fit their high quality fuel into 'premium' uses. Gas for boilers has therefore, until recently, been available on an interruptible basis, at heavy fuel oil prices; whereas to a gas turbine the gas is at gas oil prices whether the supply be needed firm or interruptible.

Figure 6.11 illustrates that the economics of gas turbine CHP are severely impaired by this pricing policy. While ever gas was being sold for boilers at heavy fuel oil prices this policy could be condemned as leading to a sub-optimal utilisation of the Nation's fuel resources. Gas turbine CHP schemes having the same overall efficiency as boilers, but converting a portion of the fuel to a high quality energy source, are discouraged to the benefit of boilers. However the Gas Board are not now making contracts for gas supplies at heavy fuel oil prices, and hence the gas turbine CHP schemes being at present unable to burn heavy fuel oil, must be evaluated at gas oil related prices.

6.8.4 Energy Conservation

CHP is frequently proposed as an energy conserving technology. It is therefore important to quantify the efficiency of energy utilisation and energy conservation by the CHP scheme. Two parameters are defined:

$\eta_{site} = \frac{H+P}{F}$: is the efficiency of fuel conversion by the scheme.

$E_s = \frac{H}{\eta_{aux}} + \frac{P}{\eta_{grid}} - F$: is the energy saved by the fuel conversion of the CHP scheme.

H = heat consumed on site.

P = Power produced by the CHP scheme.

F = Fuel converted by the scheme.

η_{aux} = Auxiliary boiler efficiency.

η_{grid} = Efficiency of ESI electricity conversion.

η_{site} and E_s may be likened to IRR and NPW: η_{site} is a simple indication of the thermal efficiency (as against economic efficiency), but E_s is required to find how much energy can be saved.

Values of η_{site} and E_s are given in table 6.7 for a range of installed engine capacities and fuel prices on site 1. Results on E_s are based on an average ESI generating efficiency of 28%. Although when considering the displacement of marginal units a lower ESI generating efficiency might be justifiable.

η_{site} increases with fuel price, but E_s does not necessarily increase also. As fuel prices rise less electricity is produced by the scheme: instead the engines run at low loads and afterfire to meet the valuable heat load. A small installed capacity is more efficient but saves less energy.

6.8.5 Maintenance Scheduling

In order to plan its summer maintenance the CEGB must have information on the expected output from CHP schemes during these months. This is particularly important if CHP schemes form a significant part of the Nation's electricity supply, whether ESI or independently owned. If a significant CHP programme is envisaged, particularly one based on space

TABLE 6.7

Energy Conservation Site 1

		→ Installed Capacity (MW)			
		3.3	6.6	9.9	13.2 MW
Fuel price p/kwh	η_{site}				
0.35		0.75	0.66	0.45	0.41
0.45		0.78	0.71	0.55	0.55
0.55		0.80	0.74	0.59	0.65
0.65		0.81	0.76	0.64	0.70
0.75		0.85	0.82	0.83	0.82
		3.3	6.6	9.9	13.2 MW
Fuel price p/kwh	E_s (GWh /yr)				
0.35		54.6	93.9	60.5	64.2
0.45		52.4	87.2	76.5	96.4
0.55		51.1	79.9	71.5	87.8
0.65		44.1	63.2	56.4	66.3
0.75		26.9	26.3	25.3	26.2

heating loads, then the problem of having sufficient time for maintenance may become acute.

The timing of maintenance is important, particularly at the shoulders of the annual demand, when the plant margin may be at a minimum (fig. 6.12 from Ref.10). A comprehensive treatment of maintenance scheduling is not attempted here, but fig. 6.13 illustrates the useful information available from the modelling techniques developed. The case in point is a 6.6 MW engine installed on the space heating load of site 1 in 77/78 with a fuel price of 0.55 p/kwh. The expected CHP contributions for months 5, 6, 9 and 10 are shown; months 7 and 8 being influenced by the engine's own annual maintenance.

The hourly expected mean outputs shown can be utilised in simple techniques, based on some expectation of the time of occurence of summertime peaks, or the hourly probability density functions of site output could be used with a suitable probabilistic simulation model.

6.9 SUMMARY AND CONCLUSIONS - CHAPTER 6

The methods of analysis of the marginal CHP scheme have been tested on two rather different CHP sites. The models and methods have, with the exception of the system reliability program , been found to work well. Development of the system reliability program should be possible, to complete a set of convenient and useful models for CHP analysis.

A range of economic values to the Nation of CHP schemes on the 2 sites have resulted: the returns being strongly dependent on fuel price scenario, discount rate, rate of heat recovery and timing and size of capacity credit. Results of chapter 7 will facilitate comparison

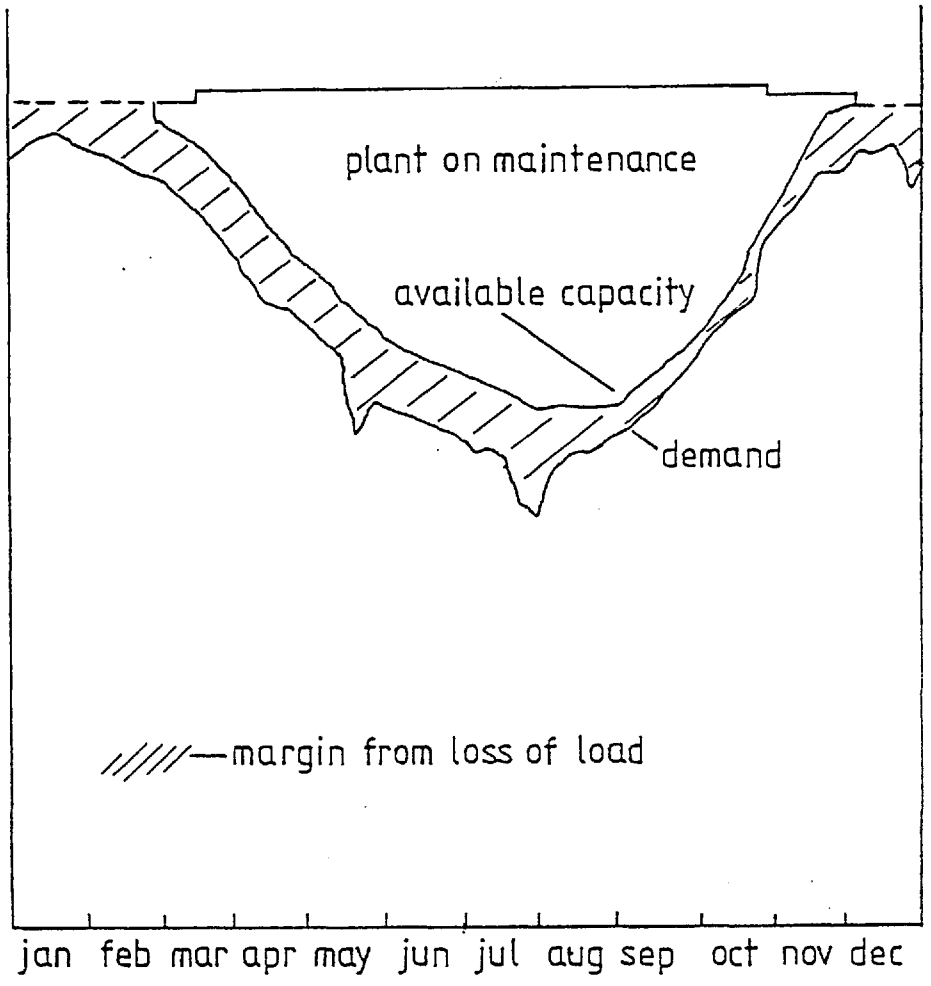

Fig. 6.12 CEGB Annual Maintenance Margins (Ref. 10)

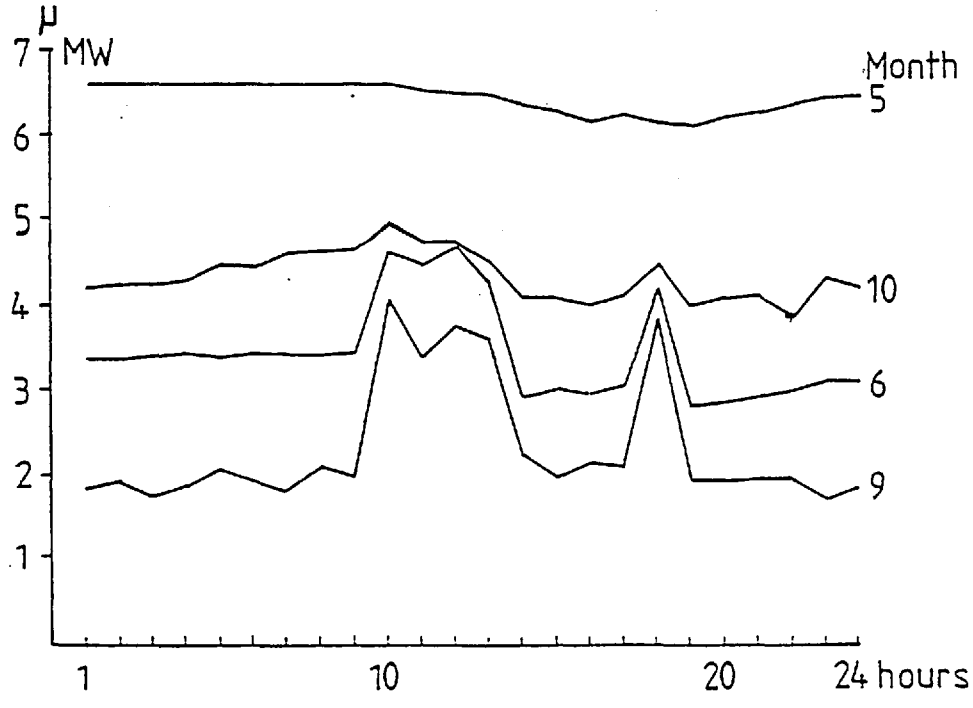

Fig. 6.13 Information for Maintenance Scheduling

of diesel CHP returns with other electricity supply options.

CHAPTER 7

THE POTENTIAL OF DIESEL COGENERATION IN UK ELECTRICITY SUPPLY

7.1 INTRODUCTION

Chapter 7 puts the work of the previous chapters in perspective by assessing the potential role of diesel cogeneration in electricity supply. Further meaning will be given to the returns on diesel cogeneration calculated in chapter 6, by comparing them with other electricity supply options.

The three important factors in this assessment are presented in sections 7.2, 7.3 and 7.4. Firstly some details of the UK industrial heat load are given, secondly a comparison is made of the returns on CHP and central supply options, and in section 7.4 the methods for determining optimal plant mix are described. Finally the strands of evidence are drawn together in section 7.5 to make an assessment of the potential of diesel CHP in the UK: the emphasis being on determining the principle constraints, rather than attempting to make accurate predictions of amounts.

7.2 SOME DETAILS OF THE UK INDUSTRIAL HEAT LOAD

As explained in chapter 1 industrial cogeneration schemes are studied in this thesis because of their generally denser loads and higher load factors than domestic space heating loads. Among the determinants of industrial cogeneration potential are therefore the size and characteristics of the industrial heat load. This section is essentially just a survey and discussion of the information available on this heat load.

7.2.1 The Size of the Industrial Heat Load for CHP

The most comprehensive survey in the UK of industrial fuel usage is Reference 27, compiled for the Energy Technology Support Unit (ETSU) by the National Industrial Fuel Efficiency Service (NIFES). This gives a breakdown of the 1976 industrial heat load into process and space heating applications and gives the temperatures of the water, steam and direct heat required. It does not give any information on the timing of heat usage or load factors, nor are the sub-divisions of required heat quality as detailed as would be desired for a comprehensive CHP study. Neither of the other two surveys that were considered, by the Science Policy Research Unit (SPRU) of Sussex University (Ref.13), and the Confederation of British Industry (CBI) (Ref.14), are as comprehensive, although the work at SPRU is still in progress and may eventually give more detailed information.

Figure 7.1 shows the industrial heat usage in 1976 at temperature levels feasible for CHP (Ref.27): consumption is broken down into 8

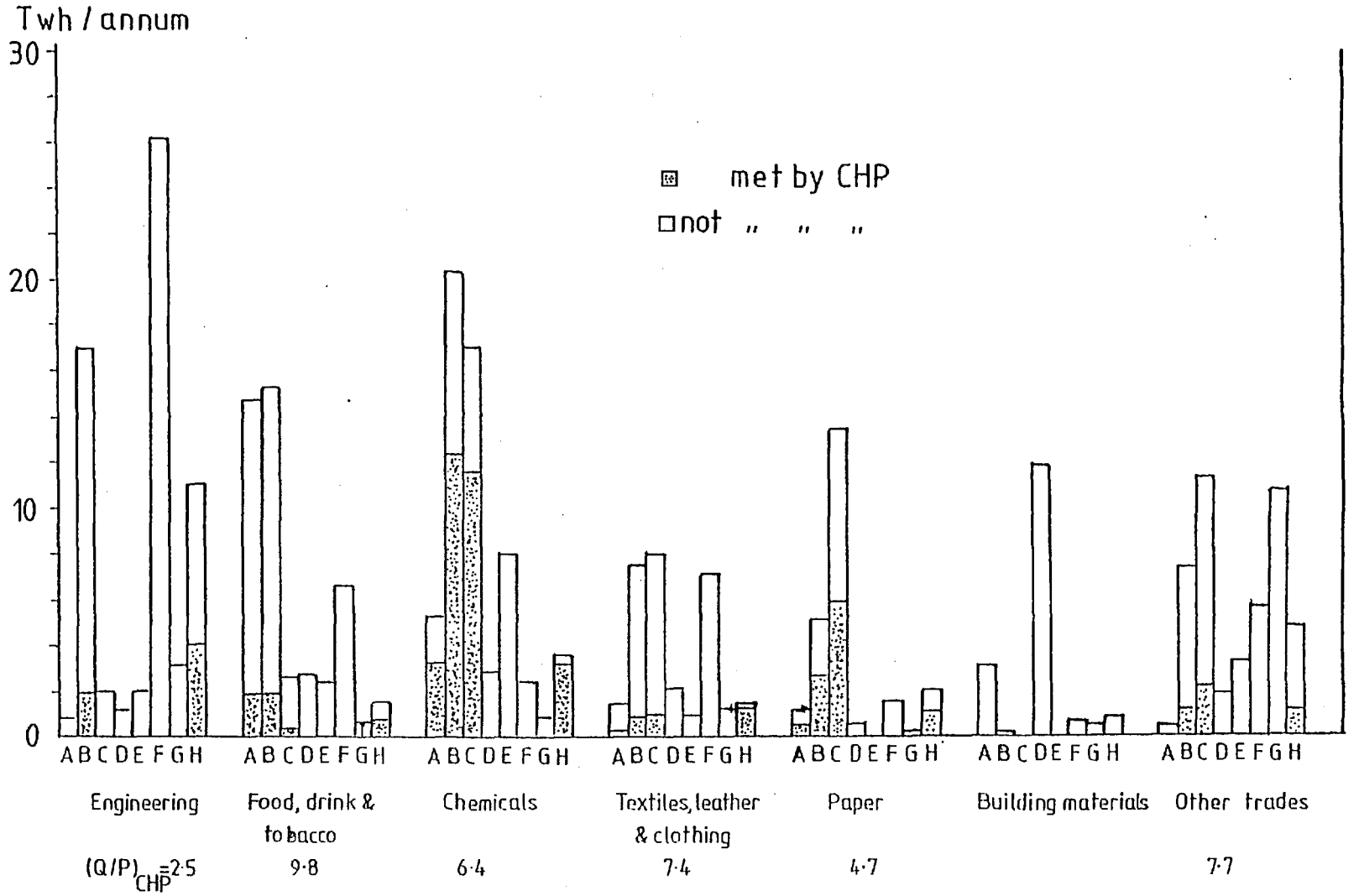

Fig. 7.1 UK Industrial Heat Consumption 1976 (Ref. 27)

Key to Figure

	Purpose	Medium	Temp.
A	Process	Water	<80°C
B	"	Steam/Water	80-120°C
C	"	" "	>120°C
D	"	Direct Fire	<200°C
E	"	" "	200-400°C
F	Space/Water heating	Central Steam/water	
G	" " "	Local boiler	
H	" " "	Direct Acting	

TABLE 7.1

Total Industrial Heat Base for CHP in 1976

(Excluding Chemical Feedstocks and the Iron and Steel Industries)

	TWh	% of Total
A	26.8	9
B	73.5	26
C	53.8	19
D	23.2	13
E	17.5	
	194.8	
F	50.1	33
G	17.2	
H	26.2	
	93.5	
	288.3	≡ 33 GW_h at L = 1

end-use qualities and 7 industrial sectors (the iron and steel and petrochemical industries are not included). All steam and hot water loads and direct fired processes <400°C are considered to be, in principle, potentially able to be met by CHP schemes. Table 7.1 gives industrial totals by end use quality.

The heat load represents 60% of gross energy supplied to these industries in 1976, or 45% of their primary fuel consumption. It is 12% of total national fuel consumption. At a load factor of 1 it corresponds to 33 GW_{th}, comparable to the 32 GW_{th} of peak district heating load at a density >20 MW/km^2, considered to be potentially economic for district heating/CHP by the Marshall Report (Ref.17). This district heating load is however at a much lower load factor (<40%) and hence total district heat requirements at densities greater than 20 MW/km^2 are less. The district heating figure includes 3 GW for industrial space heating and hence there may be some overlap in the 2 loads.

Figure 7.1 also shows the portion of the heat loads already met by CHP schemes, and the ratios of heat recovered to electricity generated in these sectors. These industries generate 10.5 TWh of electricity, of which 70% is estimated to be from CHP schemes (Ref.17), in association with 57 TWh of heat; giving an overall CHP heat to power ratio of 7.7:1. Most of the CHP is in the chemical and paper industries which have a history of cogeneration. The figures show substantial areas as yet not met by CHP: of particular interest are the space heating loads in the engineering and other trades sectors, and the process loads in the food and textile sectors.

7.2.2 Heat Load Quality

The required grade of heat is an important factor in the viability of CHP schemes, particularly for diesel engines where large quantities of heat are available at a low temperature.

Table 7.1 gives a breakdown of heat loads by grade. Further sub-divisions of the water/steam process load at temperatures $>80^{o}C$, into water and steam requirements, would be of great use, but is unfortunately not available. A survey of 10 factories producing a wide range of products shows the steam/water division to be 46%/54% (Ref.1), indicating that as much as a half of the water/steam process load $>80^{o}C$, may be hot water.

The space heating load (total 33%) is made up of 17% central steam/water, 6% local boiler and 10% direct-acting. Thus for over half the space heating load, distribution networks must already exist. Hot water ($<100^{o}C$ for local distribution) is the ideal medium for heat distribution because of its low ratio of volume to heat content.

This analysis says nothing of the association of process and space heating loads, which may substantially increase the fraction of recoverable heat for diesel engines.

7.2.3 Load Factors

No comprehensive survey of the timing of industrial heat loads or of heat load duration curves has been performed. The diversity of industrial activity makes it difficult to generalise from case studies, for example sites 1 and 2 of chapter 6, presented in the literature. An attempt is made in this section to gather together some further available information, but a much more thorough survey is needed.

Heat loads may be divided into those for space heating and for process.

The report of McLellan and Partners (Ref.62) purports to have established generalised methods of formulating space heating loads from averaged air temperatures and the degree day concept. Master curves of space heat requirements are constructed showing an 8 month heating season and a noticeable dip between 1400 and 2200 hours. These are two important and unfavourable features: the first reduces load factors, the second would reduce the winter CHP contribution at the afternoon electrical demand peak. 10% accuracy was claimed in applying these methods to specific sites, but in fact only one space heating load was actually measured (factory A), which did not show the two features mentioned above as strongly as predicted.

Curves of the percentage of total annual heat demand against load factor (defined as the ratio of average to peak heat demand), are shown in Fig. 7.2 for the 3 cases given in Ref.62 and for site 1 of chapter 6. Load factors for both the site heat demands actually measured are higher than those theoretically predicted. Thermal inertia of the building, imperfection of the space heating controls, and variance from standard weather conditions may be sources of some of the differences. Some useful redistribution of heat load could be achieved by short term thermal storage. In addition to a space heating load most industries will have some requirement for hot water and possibly a small process load. These can make quite significant improvements to load factors as illustrated in Fig. 7.2 for site 1.

The wide range of industrial processes makes it even more difficult to generalise than for space heating, but load factors will frequently be higher. Fig. 7.3 shows a histogram of load factors quoted by Merz and McLellan (Ref.63), as a result of a survey of potential CHP sites. The histogram covers both space and process loads, but is of limited

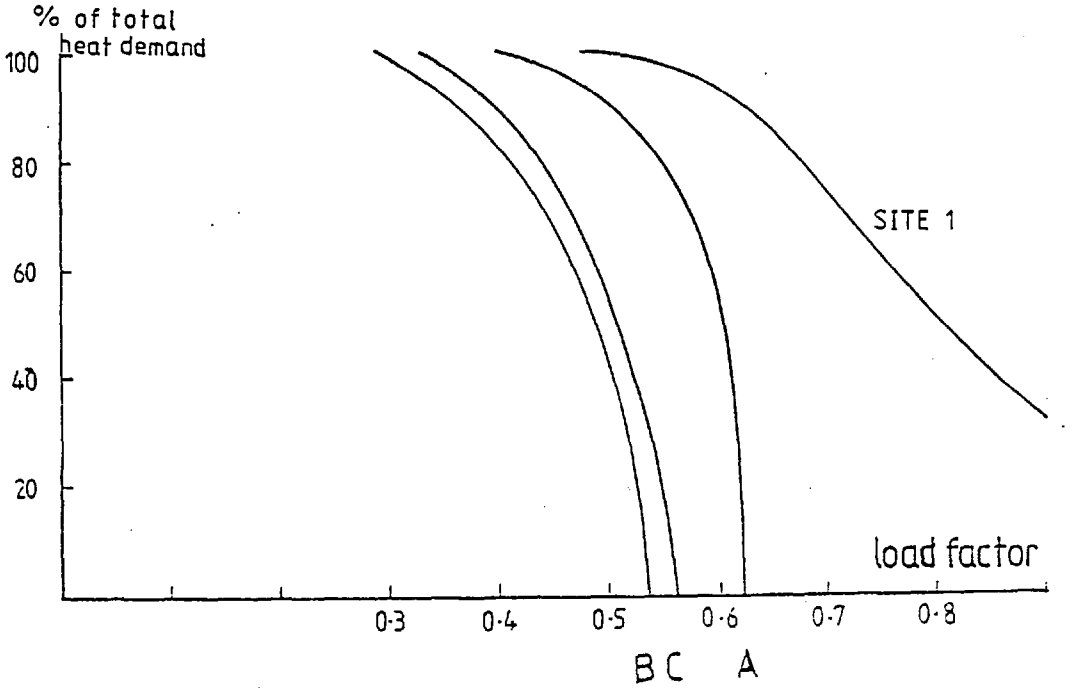

Fig. 7.2 Percentage of Site Heat Demand against Load Factor - Examples

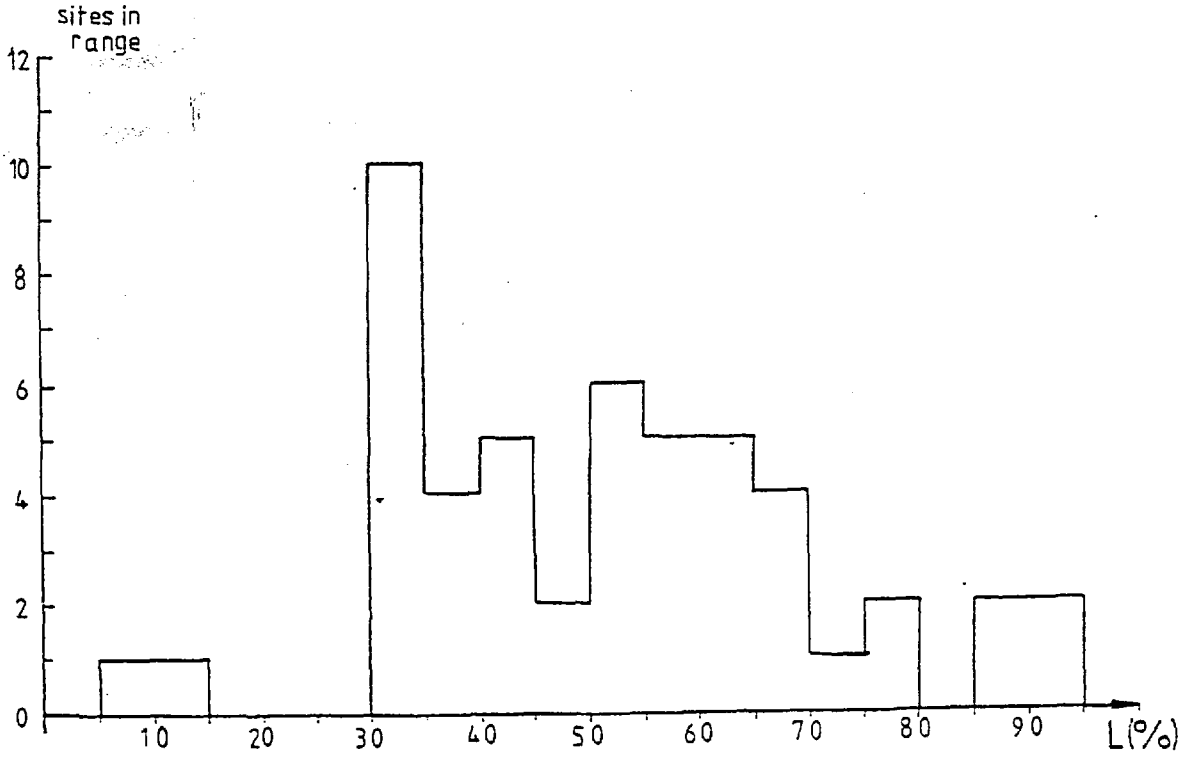

Fig. 7.3 Histogram of Site Load Factors (Ref. 63)

value as it gives no information on the more important heat load duration curve, whereby the relation between the percentage of heat load met and the CHP load factor may be determined. Load factors for 10 diverse sites given in Ref.1 show rather higher values, between 0.7 and 0.8.

The winter-summer variation will tend to be smaller for process than space heat, although the heat load of site 2 shows that some variation does occur. The diurnal variation of heat load will depend on the pattern of working, but many processes are run continuously.

A broad spectrum of heat load duration curves is to be expected both for space heating and process loads. The association of the two is also likely to be important, as is the linking of neighbouring sites. More thorough studies of industrial heat loads will be needed for more accurate appraisals of industrial cogeneration potential.

7.2.4 Size Distribution of Industrial Heat Loads

The size distribution of industrial heat loads is a useful parameter: grid connection may be uneconomic for small sites, and economics of scale may influence the choice of plant for large sites. Fig. 7.4 shows the results of a survey of heat use in Merseyside (Ref.57). Some reservations must be made about the generality and accuracy of these results: the survey area contains a large number of chemical industries and hence is not representative of the country as a whole, and the response from the smaller sites was not high, therefore possibly underestimating the number of loads less than say 2-3 MW_{th}.

Nevertheless Fig.7.4 gives interesting information on, mainly process, industrial heat loads. The size distribution of space heating

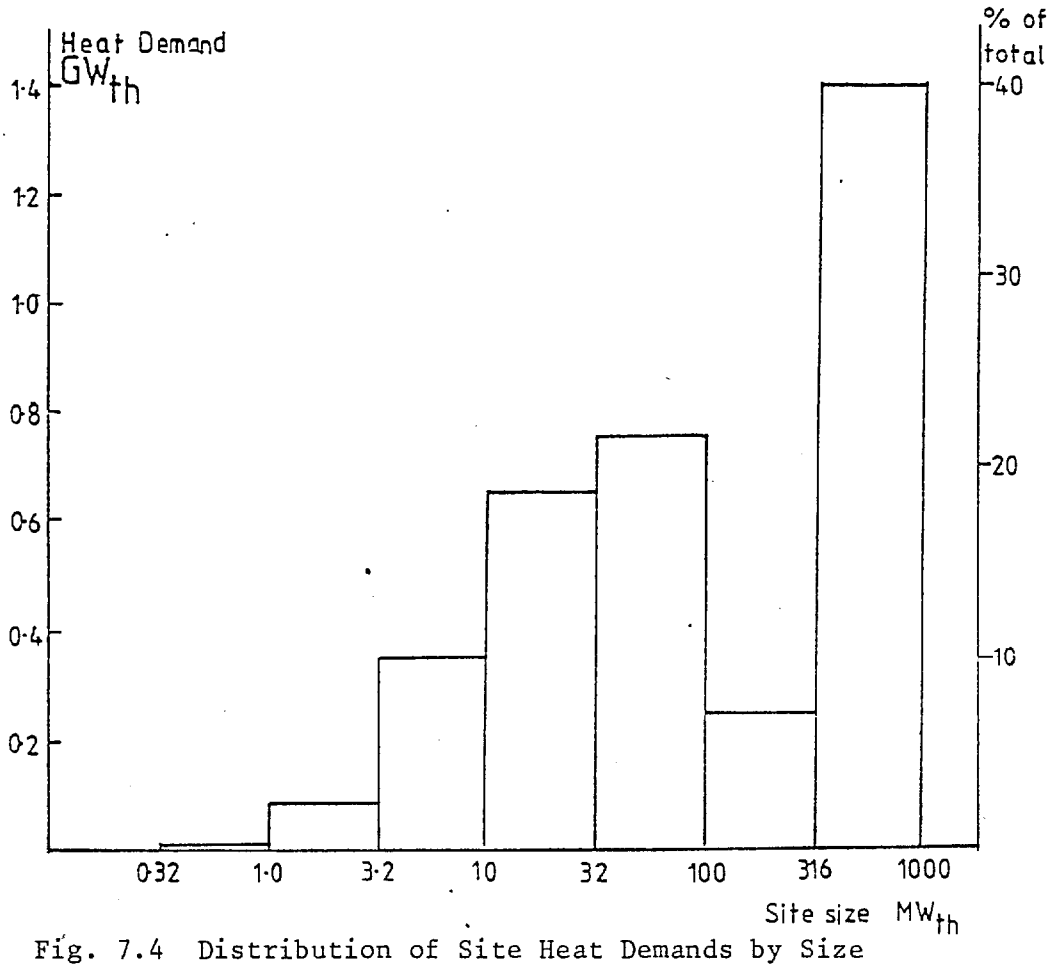

Fig. 7.4 Distribution of Site Heat Demands by Size on Merseyside

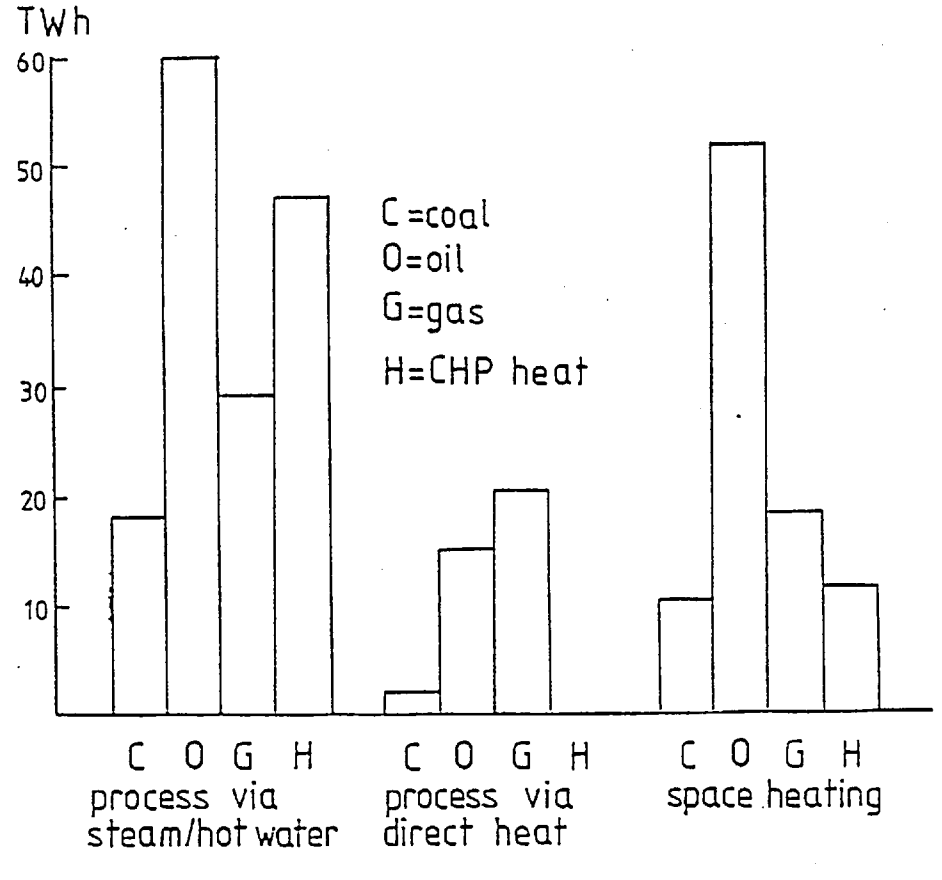

Fig. 7.5 Heat Load Distribution by Fuel Usage

loads should closely parallel the size distribution of firms, as perhaps measured by the number of employees. More than 50% of the heat load occurs in the range 1-100 MW_{th}: potentially suitable for diesel engine applications. Outside this range the considerations mentioned in the first sentence may be important.

7.2.5 Fuel Usage for Industrial Heat

Fig. 7.5 compiled from Reference 27 shows the distribution of fuel usage for the industrial heat load of fig. 7.1 and table 7.1. The heat load is divided into 3 types: process via steam/water, process via direct heat and space heating. Four sources of heat are considered: coal, oil, gas and CHP heat.

It is immediately apparent that a CHP scheme would mainly displace oil and gas usage in industry; the percentage share of coal in the industrial market having fallen from 63% in 1960 to 14% in 1977. Oil accounts for 45% of the heat load shown. The fuel displaced on the ESI system will mainly be coal.

7.3 AN ECONOMIC COMPARISON OF ELECTRICITY SUPPLY TECHNOLOGIES

As mentioned in the last chapter, it is not the economics of diesel CHP in themselves which is important, but diesel CHP returns in comparison with those on other CHP and central, electricity only technologies. In order to make the comparison some generalisation is necessary and some of the accuracy of detail of the methods of chapters 5 and 6 will be lost.

It is impossible to cover all possible CHP values in one figure: Fig. 7.6 maps the IRR on diesel CHP for scenario 1 in terms of the two parameters, load factor (L) and r, the ratio of recoverable heat to power output. The time average of the January 1978 expected marginal electricity costs of Fig. 6.4, being $C_{e_{ma}}$ = 1.3p/kwh, has been used; all other parameters are as used in chapter 6, eg. capital cost = £200/kW, η_b = 0.38, etc. Values of r for full heat recovery (0.92), no intercooler heat recovery (0.705), and no low temperature heat recovery (0.44) for the AT350 engine are marked.

The benefits from afterfiring, assuming no incremental capital costs are incurred, are also indicated: the full line includes no benefit from afterfiring, the dashed line has assumed that afterfiring meets 50% of the heat load. Factors may be used to adjust the values in Fig. 7.6 for other values of the parameters, eg. increased capital costs or alternative fuel price scenarios, but inaccuracies will increase as values move away from the central case. It will therefore generally be advisable to revert to a time averaged expression for annual CHP value:

$$\text{Annual Value/kW}_e \text{ installed} = (1\text{-FOR})\, L \left\{ C_{e_{ma}} + \frac{C_f\, r}{\eta_{aux}} - \frac{k_m C_f}{\eta_b} \right\} \cdot \tau$$

$$+ C_f \left\{ \frac{1}{\eta_{aux}} - \frac{1}{\eta_a} \right\} \frac{u}{1-u}\, r\, L\, (1\text{-FOR})\, \tau \;+\; C_c$$

where τ = time period (1 year)

u = fraction of the total heat load not met by auxiliary boilers that is met by afterfiring

C_c = capacity credit/kW.

From this the IRR or NPW may be calculated (eg. Fig. 7.6). This method of averages, while providing approximate answers sufficient for the comparisons of this section, in no sense displaces the need for

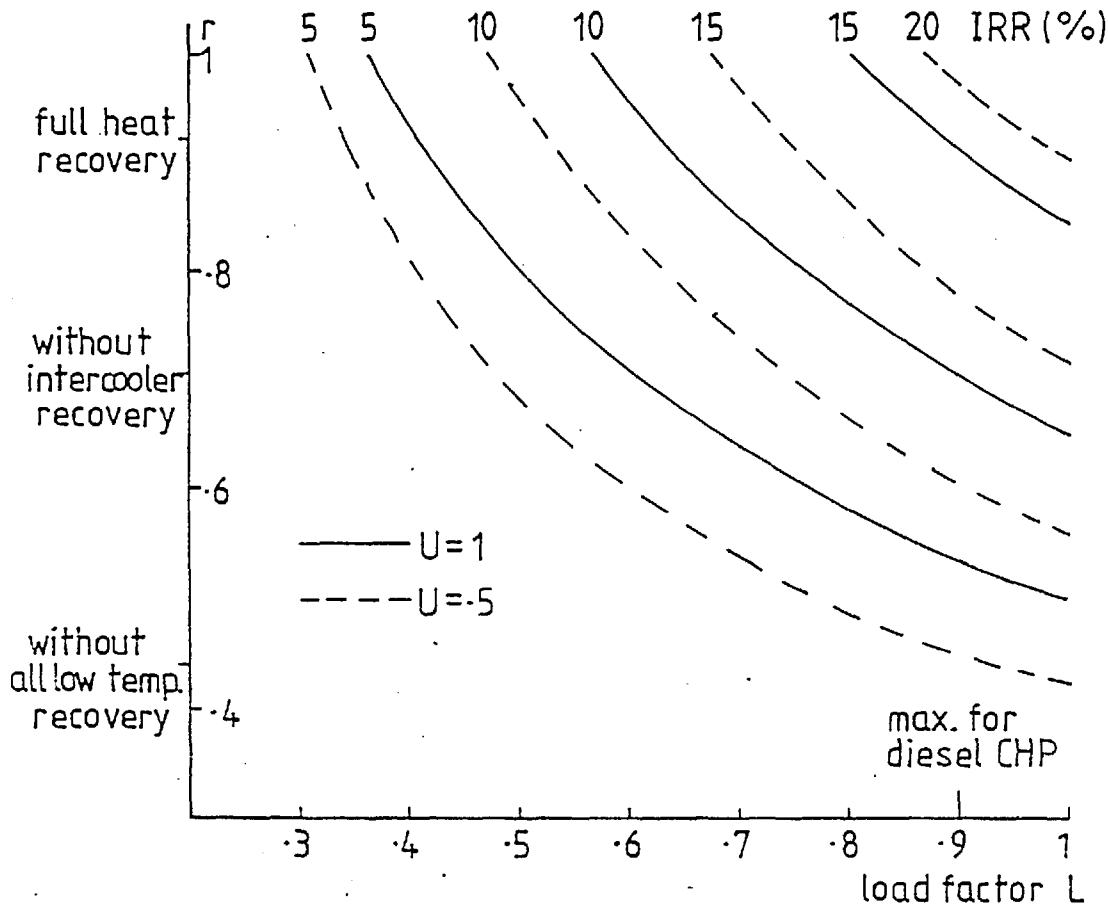

Fig. 7.6 IRR on Diesel CHP

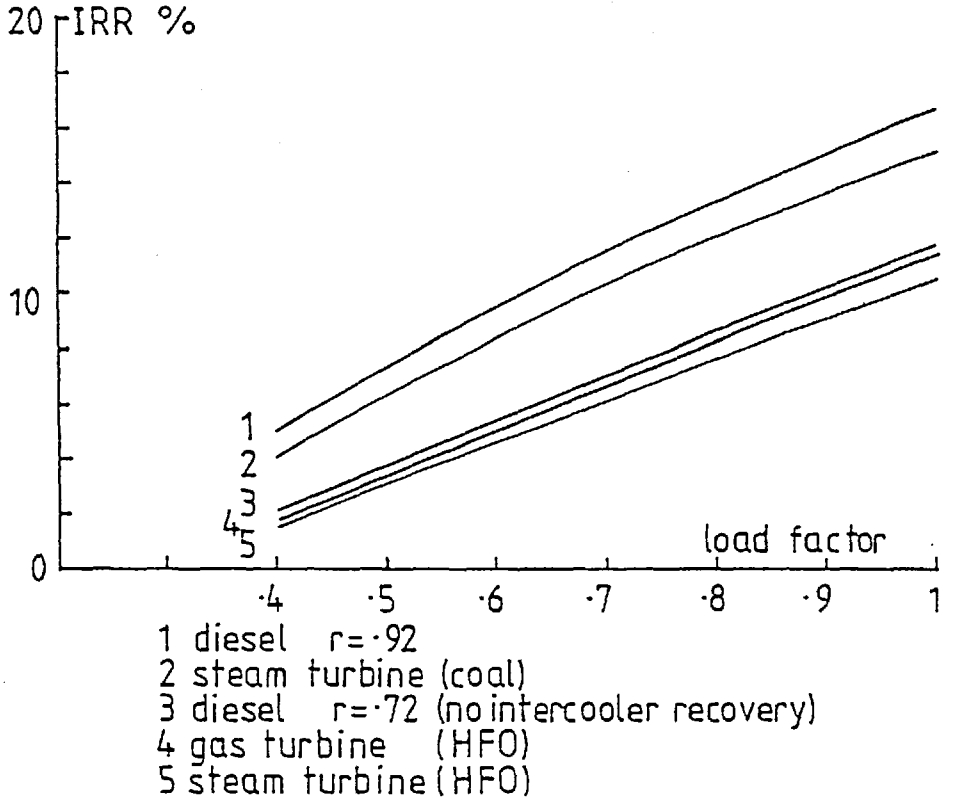

Fig. 7.7 Returns on Diesel and Other Prime Mover CHP

the more detailed studies of chapter 6 for investment decisions. The method also becomes inaccurate when the cost of CHP electricity is comparable to C_{marg}.

Returns on diesel CHP are also presented in fig. 7.7, alongside returns on two other established cogeneration technologies: the steam and gas turbines. Again time averaged values have been used. Results are for scenario 1 fuel prices (Section 6.3.1) and schemes commencing electricity production in January 1978. As far as possible costs and characteristics of gas and steam turbines are from Ref.17 and are shown in Table 7.2; the incremental capital cost of a coal burning steam turbine is a fairly rough estimate for a large ($\geq$30 MW) turbine from Ref. 92. No capacity credits are included, nor are the benefits of afterfiring.

Gas turbines are seen to give a reasonable IRR on heavy fuel oil, but give very low returns if burning gas oil. It should be noted that the overall gas turbine efficiency ($(1+r)\eta_b$) = 0.66 for this turbine, is rather less than frequently quoted, and some turbines may improve on these figures. Gas turbines must therefore be developed for operation on heavy fuel oils to be serious contenders for CHP schemes; in which case they could possibly displace diesel schemes where full heat recovery cannot be achieved.

Steam turbines burning coal closely match the performance of diesel schemes with full heat recovery in this scenario, but using oil can only better the diesel if only a very small proportion of the low temperature diesel heat may be used. Lower fuel costs for the coal burning steam turbine and the low maintenance costs, almost make up for the lower value added to the fuel. If the oil price should rise with respect to that of coal, then depending on the rate of rise and the date of scheme implementation, the steam turbine may beat the best

TABLE 7.2

Costs and Characteristics of CHP Prime Movers

	η_b	Γ	$(1+\Gamma)\eta_b$	£/kw Incremental Capital Cost	(p/kwh) Jan. 78 Fuel Cost	FOR	k_m
1. Heavy fuel oil Steam Turbine	0.096	7	0.77	330	0.47	0.05	1.014
2. Coal " "	0.096	7	0.77	400	0.3	0.05	1.014
3. Gas Turbine	0.24	1.73	0.66	190	0.47 HFO	0	1.05
					0.67 Gas Oil		
4. Diesel	0.38	0.44-0.92	0.55-0.73	200	0.47	0.05	1.15

diesel scheme. However the energy saved by the low power to heat ratio steam turbine will be much less than for the diesel.

These very approximate comparisons have only considered conventional CHP technologies. The diesel engine has the important feature of a high brake efficiency (η_b), but its economics for CHP are impaired by the prospects for future oil prices. A high brake efficiency coal burning technology is needed, which, depending on its capital cost, may match the returns on diesel CHP, and be insensitive to future oil price rises.

The established, normal practice in electricity supply is large, central coal or nuclear plants. Diesel CHP as an electricity supply option must therefore be compared to these, in order that the best mix of plant may be determined.

The CEGB sell electricity at long run marginal costs (LRMC), which includes both capacity and running cost elements. The following returns on investment in plant are based on gas turbines as marginal capacity and the expected marginal costs as calculated by the probabilistic simulation model. The returns are calculated on the capital cost of the plant, for their electricity production sold at LRMC and short run marginal cost (SRMC), (ie. not including a capacity element).

IRR on plant for scenario 1 fuel prices are shown in fig. 7.8; they have again been calculated for an averaged marginal electricity cost in January 1978 of $C_{e_{ma}}$ = 1.3 p/kWh. Capital costs for modern coal, and for Advanced Gas Reactor (AGR) stations are given as £290/kW and £470/kW respectively at January 1977 prices in Ref.20. These have been inflated by 10% to give January 1978 costs; and including interest at 10% during construction (capital expenditures assumed evenly distributed over 7 years), they give £475/kW for coal and £770/kW

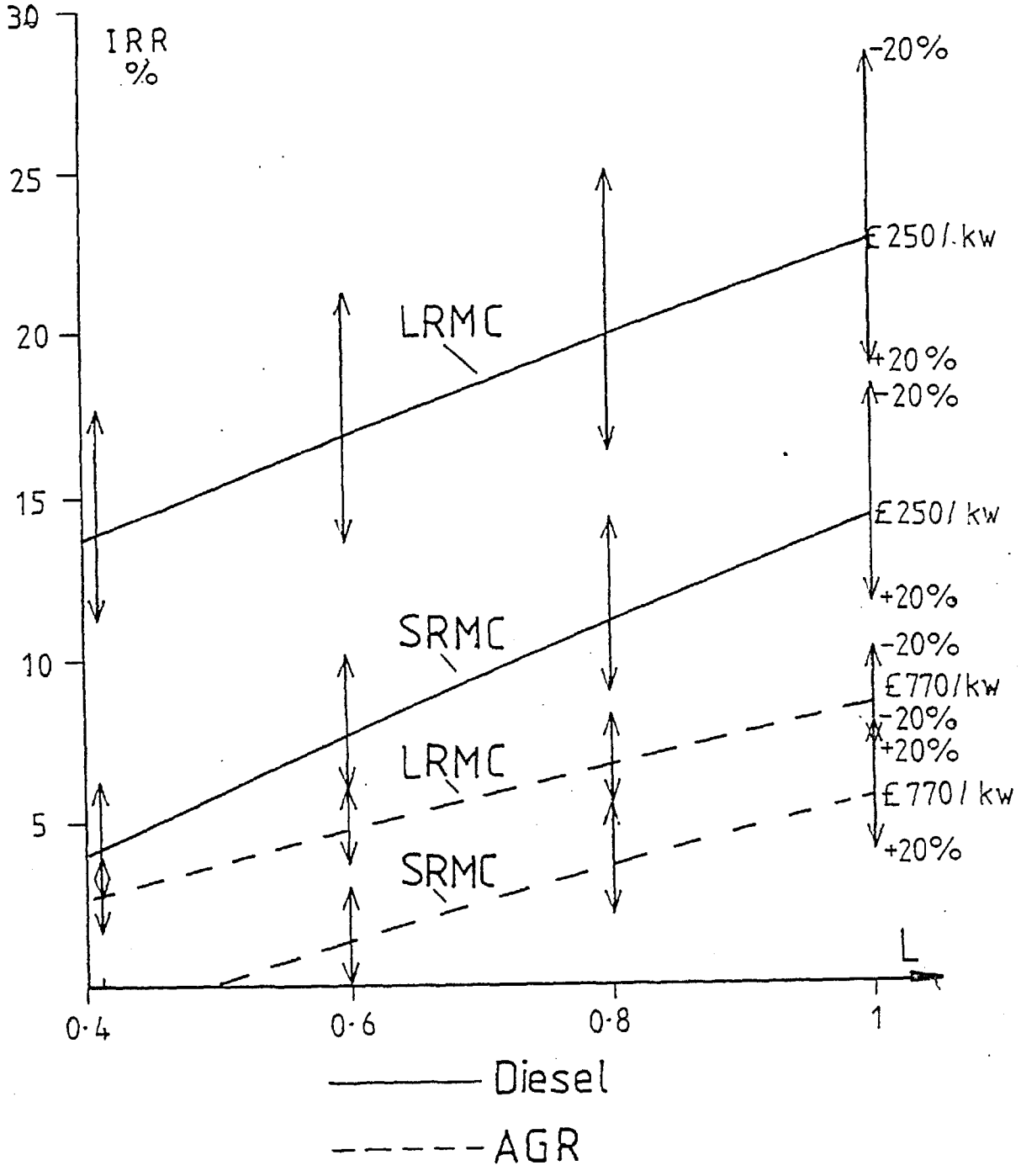

Fig. 7.8 IRR on Diesel CHP and AGR Capacity for Scenario 1 Fuel prices

for AGR stations. Sensitivity of returns to ± 20% on capital cost are also shown. Section 6.3.2 deduced a capital cost for diesel CHP of £200/kW, but it may in some circumstances be higher, hence £250/kW has been taken as central, -20% giving the £200/kW figure, +20% gives £300/kW.

Running costs are taken from table 6.1 as 1.136 p/kWh for coal stations, 0.54 p/kWh for AGR stations, and are consistent with $C_{e_{ma}}$ = 1.3 p/kWh. Gas turbine capacity has been amortised at 10% which gives an annual charge of £22/kW. Forced outage rates are 0.2 for nuclear, 0.15 for coal and 0.05 for diesel. Full heat recovery (i.e. r = 0.92) is assumed for the diesel scheme.

Diesel CHP for scenario 1 gives much higher returns in this analysis than AGR stations, and returns are more greatly increased by the inclusion of a capacity element in the IRR calculation. Returns on coal plant were found to be very poor, less than nuclear, and hence are not shown. Scenario 3 fuel prices increase the IRR on diesel CHP by around 2 percentage points, and on nuclear by 4 percentage points. Scenario 2 results show nuclear returns unchanged, but diesel CHP return on SRMC to be at best 4-5%, but still around 14-15% at high load factors with a capacity element (LRMC).

If heavy fuel oil and coal prices rise at approximately the same rate, then diesel CHP in this economic analysis, gives better returns than AGR stations for most rates of diesel heat recovery. This is due to the high capital cost of nuclear power. Alternatively, if oil prices rise quickly with respect to coal, then diesel CHP returns are greatly reduced and project life is curtailed. UK and World oil reserves are much less than reserves of coal and hence oil prices will tend to rise faster than those of coal: the rate of relative price rise is a critical determinant of the possible contribution of diesel

CHP. Fig. 7.9 has therefore been drawn to illustrate how diesel CHP life and economics will be affected. Diesel CHP generating cost is calculated as $C_f \left(\frac{k_m}{\eta_b} - \frac{r}{\eta_{aux}}\right)$; the coal price and hence $C_{e_{ma}}$ rises at 0.7% per annum. The intersect of CHP generating cost and $C_{e_{ma}}$ approximately determines the termination of project operation; the area (eg. A) between $C_{e_{ma}}$ and CHP generating cost is a rough measure of benefit from CHP.

Fig. 7.9 illustrates the sensitivity of the benefit area and project life to the rate of rise of oil price. The AGR generating cost of 0.54 p/kWh gives a much larger benefit area, but of course requires much larger investments. The development of high brake efficiency coal CHP technologies, with say $\eta_b \sim 0.4$, r=1 would give January 1978 generating costs around 0.4 p/kWh; its IRR would then depend on capital cost.

7.4 THE DETERMINATION OF OPTIMAL PLANT MIX

Before section 7.5 which pulls together the information and ideas of sections 7.2 to 7.3 to make an assessment of diesel CHP potential, the existing methods that might be considered to determine optimal plant mix in an electricity supply system are reviewed. The methods of chapter 5 for evaluation of the marginal cogeneration scheme, are not sufficient for this purpose.

The simplest problem is that of determining the optimal mix for a new load duration curve, when there are no existing plant. The method proposed by Berry (Ref.4) is suitable for this. However no account is taken of existing plant in the system. A method proposed

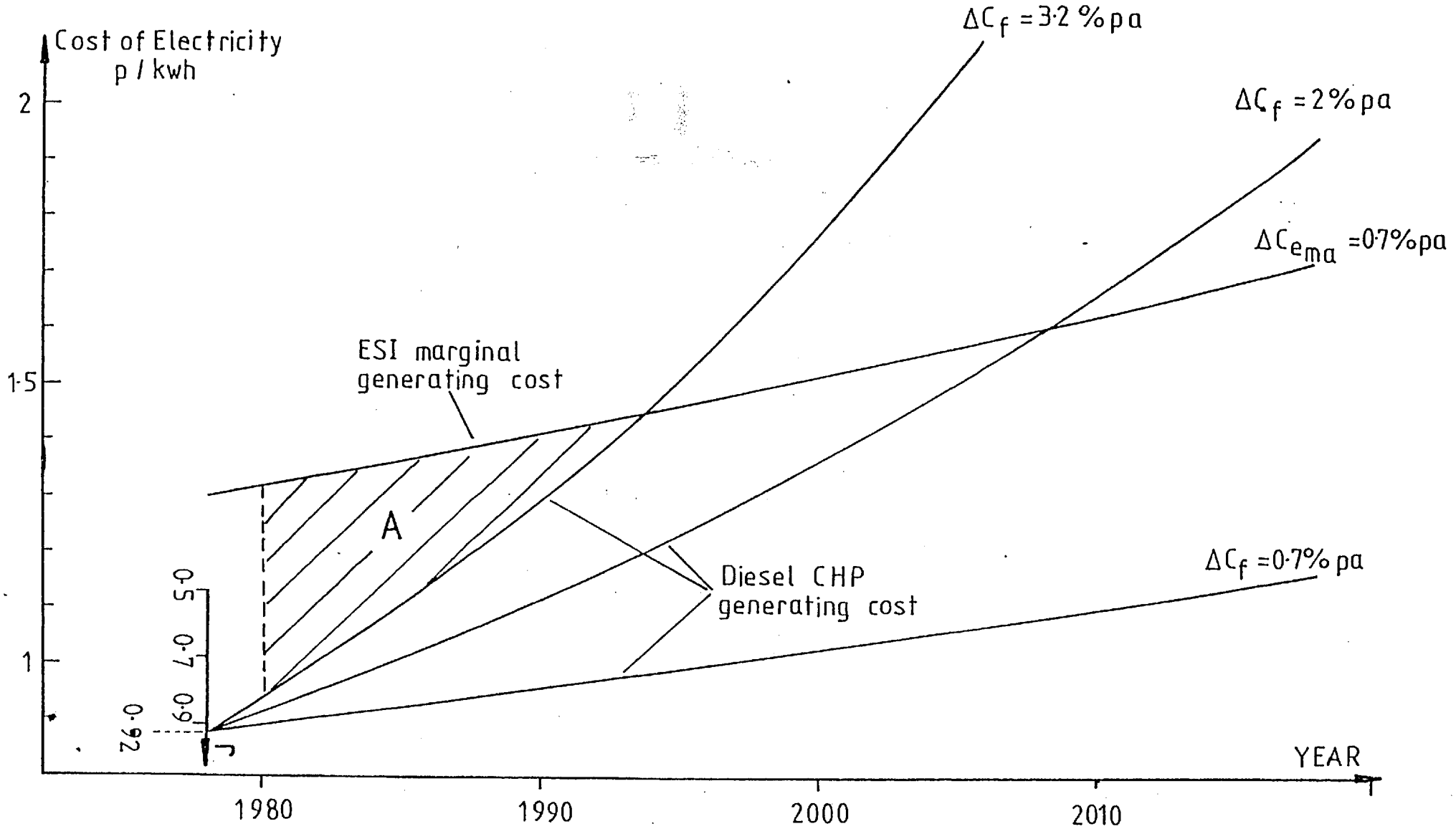

Fig. 7.9 Benefit Area on Diesel CHP

by Lucas (Ref.53) makes allowance for existing plant, but does not consider future changes in the relative running costs of plant. Phillips et al (Ref.67) describe an approach, used in planning studies by the CEGB, to optimise the plant investment programme over a number of years, and which considers these changes in future costs. One further method should be mentioned: that proposed by Parmantier (Ref.66). It purports to optimise the amount, timing and operation of an electricity supply system incorporating CHP. Some reservations must however be expressed about the ability of a global optimisation to optimise across a large number of widely varying CHP sites and to also include the ESI system.

The method of Lucas was developed specifically for the assessment of CHP potential, and deals with the transition from an existing load duration curve and capacity, to a future load duration curve. It gives the optimal type and quantity of new capacity to meet the increment in demand, and to replace out-moded capacity, for a given set of economic assumptions. Fig. 7.10 illustrates the method. Cost lines for proposed new plant (eg. 1 and 2) are constructed, as is the locus of the end point of the cost polygon for existing plant (l_p). The point of intersection determines via the construction shown, the new and existing capacities required. If CHP sites of only limited load factor are available, then further sophistication can be introduced.

This method, although being accurate within its assumptions, has the following faults:

1. All costs are assumed constant through the life of the plant.
2. No account is taken of the correlation between CHP output and ESI demand, which becomes important when the scheme is not a baseload plant. It is implicitly assumed that a site load

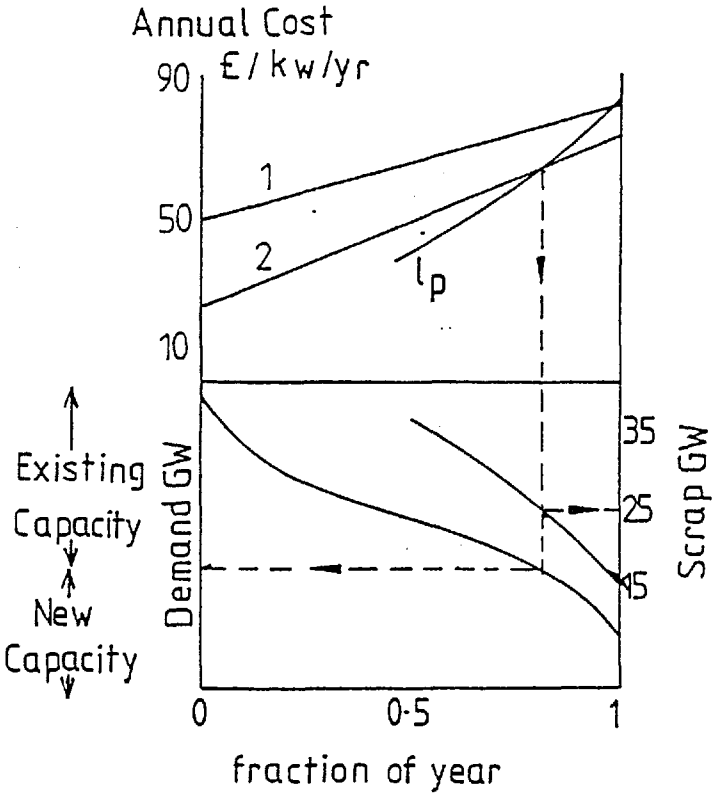

Fig. 7.10 Assessment of CHP Contribution (Ref. 53)

factor and a system load factor correspond.

3. The system reliability effects of the inclusion of CHP are not considered.

A plausible line of research would therefore have been to develop a system plant mix model incorporating these considerations. However the very significant influence of uncertain future oil prices on CHP economics has already been shown, and there is also the likelihood that any large diesel CHP contribution would be pre-empted by rapidly dwindling oil supplies. On balance, in the context of this thesis, it was decided that a less rigorous appraisal of diesel CHP potential might be adopted. The development of the more sophisticated system model, could be of benefit to future CHP studies.

7.5 THE POTENTIAL OF DIESEL CHP IN THE UK

In this section the considerations of the previous three sections are drawn together in a discussion of diesel CHP potential. The approach is to make approximate estimates and to examine the constraints determining them, rather than to attempt accurate predictions.

Before discussing in detail the system and heat load constraints on diesel CHP, two further impacts of a substantial CHP contribution are mentioned:

1. The variance of the output of the marginal CHP scheme has been shown to be generally negligeable for capacity planning considerations. If there are n CHP schemes each having probability of output at the

peak described by the normal distribution $N(\mu_{CHP}, \sigma_{CHP})$, then the summed CHP output is described by $N(n\mu_{CHP}, \sqrt{n}\ \sigma_{CHP})$. Hence the total adjustment to capacity displacement due to CHP output variance is $\frac{kn\sigma^2_{CHP}}{2\sigma_o}$ (see expression (1) in section 5.5.2). The variance adjustment to capacity credit to each scheme is, to a first approximation, unaffected by the presence of the others.

ESI operational demand variance (σ^2_p) is defined here as the variance on expected demand on a time horizon required for operation of plant, and is smaller than the capacity planning variance σ^2_o. The 'operational variance' adjustment on expected CHP output is then $\frac{kn\sigma^2_{CHP}}{2\sigma_p}$. If this is taken as representative of the uncertainty, on the system operating time horizon, in independently owned CHP output, then some additional operational flexibility may be required of the marginal ESI plant. If the CHP capacity is ESI owned then the problem does not exist.

2. Long construction times impose long capacity planning horizons. A commitment to CHP for system expansions would reduce the planning horizon to 2 to 3 years, and hence the less uncertain demand prediction would require a smaller margin of excess capacity to meet given system reliability criteria.

7.5.1 System Constraints

CHP capacity might be considered to meet load growth, or, if its net effective system cost (NESC) is deemed to be negative, to replace existing capacity for its running cost savings. In general the optimal amount and type of new plant to meet an increment in demand and to replace existing plant, will depend on both the form

of the increment in demand and the cost advantages of new plant. For the present purposes it is convenient and sufficiently accurate to consider load growth and displacement of existing capacity separately.

A 2% per annum rate of growth of simultaneous maximum demand (SMD) would require around 10 GW of new capacity in 10 years, although present UK over-capacity, could reduce this depending on the level of electricity supply reliability required. If just meeting increments in SMD then to a first approximation, assuming a sufficiency of suitable sites, diesel CHP economics change with time only to the extent that the oil price rises with respect to coal. Capacity credits are perhaps justifiable depending on the NESC of alternative plant. Installation rate is constrained by the rate of rise of SMD, which for oil based CHP may determine the final total contribution.

If displacing existing capacity the IRR on increments of CHP capacity decreases because C_{marg} decreases. The rate of decrease of C_{marg} will be an important factor in determining the optimal amount of capacity to displace existing plant. C_{marg} at all loads was calculated by the probabilistic simulation model (described in section 5.3.3) and is displayed in Fig. 7.11 alongside the 1977/78 CEGB load duration curve. It can be seen that over a wide range of loads C_{marg} changes only slowly. C_{ema} is reduced from 1.3 to 1.2 p/kWh when a constant load of 10 GW is displaced. This in itself will not substantially reduce the IRR on diesel CHP.

7.5.2 Heat Load Constraints

Diesel CHP may also be constrained by the industrial heat load. Sites giving high load factors (L) and rates of recoverable heat (r)

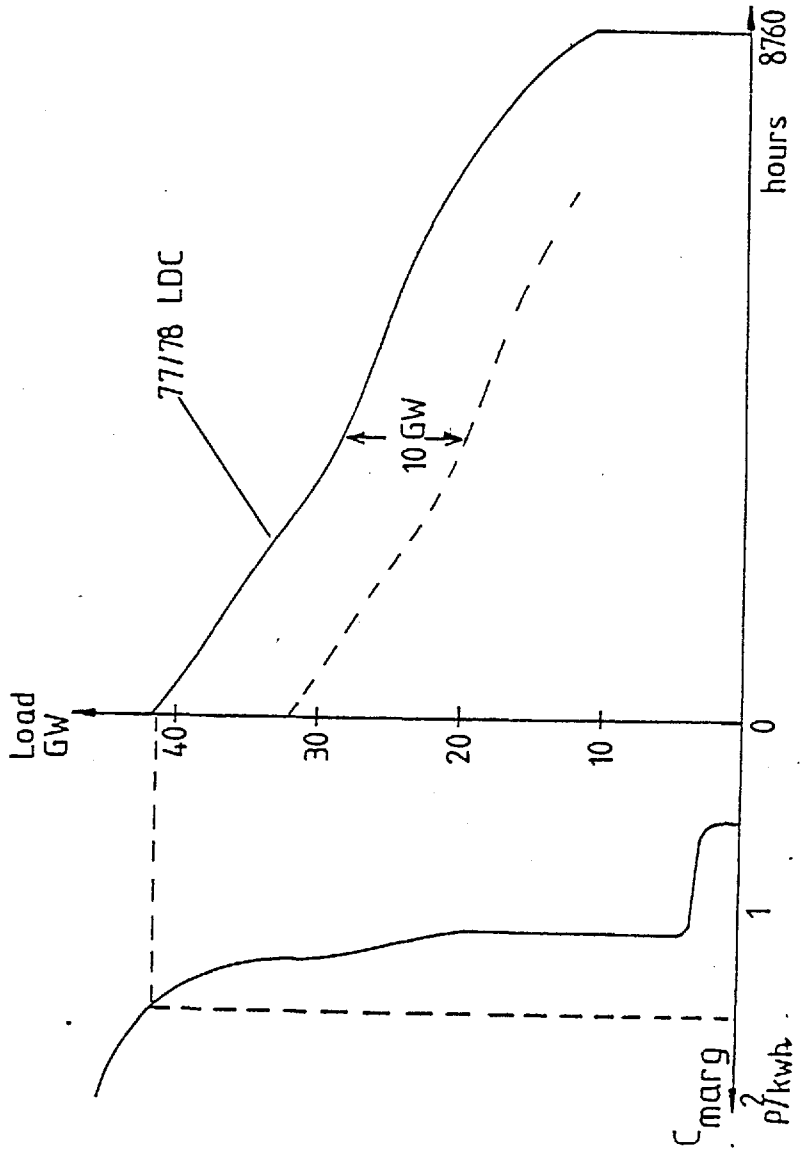

Fig. 7.11 CEGB Expected Marginal Generating Cost at all Loads

are most suitable: returns diminish more quickly with lower r than L. Unless design modification allows jacket coolant temperatures greater than 100°C (section 4.4), high values of r will only be achieved if there is a substantial requirement for hot water alongside a steam demand. 'Complimentary' loads are therefore sought.

Heat load factors are less important, as by installing diesel capacity such that the maximum recoverable engine heat is some fraction of the peak heat load, the load on the expensive generating plant can be increased. Process load factors are generally higher than those for space heat, but the association of a small process or hot water demand with the latter may improve load factors as fig. 7.2 indicates.

A brief breakdown is now given of the heat loads in the industrial sectors of Fig. 7.1, to help identify those sectors with the greatest potential:

1. Engineering.

A substantial space heating load (around 40 TWh/annum) exists coupled with a somewhat lower requirement (18 TWh) for low temperature process heat ($\leq$120°C). Little CHP so far installed; site 1 may be typical.

2. Food, drink and tobacco.

A substantial low temperature process requirement (30 TWh) coupled with a smaller space heating load (8 TWh). Little CHP so far installed.

3. Chemicals.

Large process load (40 TWh) but small space heat load. Most already met with high heat to power ratio CHP schemes.

4. Textiles.

Process (15 TWh) and space heat (8 TWh) in ratio 2:1. High load

factors likely and little CHP.

5. Paper.

Mainly process and little space heat. Around 50% of process heat already produced in CHP schemes.

6. Building Materials.

12 TWh of direct process at $<200^{\circ}C$ and 3 TWh of low temperature hot water ($<80^{\circ}C$) for process. No CHP.

7. Other Trades.

Fairly large space heating and some low temperature process heat, but may be unsuitable for CHP as this sector is largely construction.

As indicated in section 7.2.1, the information is not as detailed as would be required for an accurate assessment of the suitable industrial heat load. However a very approximate estimate is made as follows. The three sectors appearing to offer the greatest potential are Engineering (20 TWh process - 40 TWh space heat), Food and Drink (30 TWh process - 10 TWh space heat), and Textiles (15 TWh process - 10 TWh space heat). Giving totals of 65 GWh process associated with 60 GWh space heat. The on-site association of the two types of load should enable high rates of heat recovery, say $r \geq 0.7$, and if site 1 is taken as typical, around 50% of heat demand may be met at $L \geq 80\%$. This then corresponds to a contribution of 8 GW peak at 80% load factor.

7.5.3 Summary on Cogeneration Potential

The previous considerations have indicated that around 10 GW of diesel CHP might at present meet government investment criteria if the marginal cost trading conditions described in section 5.2 exist; but

that a time limit on the installation of economic projects is imposed by the probable future rises in oil prices relative to other fuels. The final diesel CHP contribution would then be determined by the physical constraint of the possible rate of installation of schemes. The time limit for coal based CHP is not as critical, and hence a thorough study of coal CHP should be made using the economic appraisals outlined in chapter 5, as the indications are that its potential may be considerable.

Conventional coal based CHP technology employs steam turbines which have high heat to power ratios, and hence do not maximise the savings, of money or energy, possible from the industrial heat load. Development of high brake efficiency (η_b) coal CHP is mainly focussed on pressurised fluidised bed combustion in combined cycles (Ref.38). Coal gasification in combined cycles offers the potential of yet higher values of η_b. Further ahead the burning of coal dust in diesel engines has been attempted in the past (Ref.82), and is again attracting development attention (Ref.69).

The new coal burning technologies envisaged for central electricity generation are those using pressurised fluidised bed combustion or gasification in combined cycles. These will give improvements in electricity generating efficiency of only 1 or 2 percentage points over the best conventional steam cycles, and hence similar technologies used in CHP schemes, having similar capital costs, and low electricity production costs, will be at an advantage. The high unit cost of small steam turbines may however impose a lower limit on the size of economic combined cycle CHP schemes. In the longer term then, when oil and gas are largely depleted, an electricity supply comprising of a mix of nuclear, high brake efficiency coal CHP, and renewables, is feasible. In the intervening period diesel cogeneration could

act as an intermediary facilitating the necessary changes in electricity supply infrastructure for substantial decentralised inputs, and allowing institutional and operational problems to be resolved.

Diesel cogeneration, while displacing oil in industry (Fig. 7.5), would mainly displace coal for electricity generation. Any decisions on diesel CHP would therefore be influenced by Governmental policy regarding future oil use in the UK. Policy will be shaped by estimates of the price and availability of, and national security considerations resulting from reliance on, imported oil towards the end of the century. However the ESI rightly argues for a diversity in fuel mix for electricity generation, and an oil based component could be ideally met by diesel CHP: running costs are sufficiently less than the new central oil stations for them to be replaced.

Summing the heat and power requirements of the industrial sectors shown in Fig. 7.1, reveals an overall heat to power ratio for industry of 3.7:1. High brake efficiency CHP will therefore generally entail substantial export of electricity from the industrial sites, and hence the institutional barriers presently restricting cogeneration must be resolved. Unless the economic conditions necessary for maximisation of national benefit from CHP are imposed, there is a danger of 'locking up' cogeneration potential. This may be done both by the installation of low pressure coal burning boilers in industry as the shift occurs from oil to coal for heat supply over the next 25 years, and by the installation of new central coal and nuclear capacity by the ESI.

CHAPTER 8

CONCLUSIONS

The thesis has covered a wide range of topics, some perhaps not in the depth of detail that could be achieved if they alone were the subject of study. However the aim of the work leading to this thesis was to analyse how the maximum benefit might be derived from diesel CHP, and hence facets of both design and operation must be examined. Returns on the overall optimisation are likely to be greater than those on the optimisation of any one particular aspect.

The design optimisation work considered several possible modifications to engine and heat recovery equipment. The effects of each modification considered could have been predicted by the models and experience of the manufacturers, although the continuation of past development paths would make it unlikely for them to do so in the context of CHP. The value of this work is therefore not so much in the prediction of individual effects, as in its comprehensive and systematic analysis of the relative merits of the possible design modifications for CHP.

The models of engine and exhaust heat recovery boiler developed for the design work, are at a level of sophistication tailored to component optimisation within larger systems. They should therefore be of use in similar studies of diesel engines in novel configurations

with other plant, for example if heat pumps were introduced into a diesel cogeneration system.

The development of the methods for the optimisation of the operation of diesel cogeneration schemes permitted the calculation of economic returns on example sites, and the more general electricity supply option comparisons of chapter 7. The sensitivity of these results to the future oil/coal price ratio has already been emphasised, and it is the models and methods of analysis themselves, and the identification of the principle determinants of value which are the more important.

Some details of CHP operation such as the balancing of the supply and requirements of the various heat grades, have been glossed over, in order to concentrate on the 'overview' of optimal CHP operation. Once the basic principles of CHP operation have been established, further more detailed studies of the practical difficulties of specific scheme operation may be undertaken. In deriving the evaluation of optimal operation, it has been assumed that with ingenuity the practical difficulties will in most cases be soluble.

Many of the conclusions have already been noted within the text and little more needs to be added at this stage. Substantial improvements to the rate of heat recovery of diesel cogeneration schemes may be made by reducing the excess air used in the cycle, achieved more easily by a reduction of scavenge airflow than trapped airflow; or by lowering the exhaust heat boiler exit temperature. Raising the temperature of the engine cooling circuits would significantly increase the number of applications in which high rates of heat recovery could be achieved. Development of engines for CHP should give more rapid returns than a continuation of past development trends.

For the Nation to derive maximum benefit from CHP, independently cogenerated electricity should be traded at the electricity supply industry's marginal cost and schemes assessed at the test discount rate used by the ESI. The ESI should include CHP with their other plant options and apply the same financial criteria. The marginal value of units may be calculated by the probabilistic simulation model described, the variance on site output will generally have little influence on capacity displacement, but the assignment of value to this capacity displacement will depend on the ability of CHP to displace peaking plant. A substantial heat load exists in industry and hence the potential contribution is large for CHP schemes having a high electrical generating efficiency and using a fuel whose price does not rise quickly relative to the ESI's marginal fuel. The reasons for this rather more optimistic conclusion of the potential for industrial cogeneration than those of Refs. 5, 17, 47 are inherent in regarding CHP as an integral part of the Nation's electricity supply system.

Because of the broad scope of the thesis it has not been possible to cover some topics in the depth that might be desired. Many avenues of further research may be identified.

It has already been mentioned in the conclusions to chapter 4, but is worth reiterating here, that the design modification study presented here is just a first stage, and that further more detailed modelling and experimental testing is required. Also a subject for practical research and testing by the manufacturers is the raising of engine coolant temperatures. Another approach to the same problem of upgrading the low temperature heat may be to incorporate a heat pump into the system: a heat pump is needed that can operate reliably at around $100^{\circ}C$.

This study has been concerned with design modification to the diesel engine. Similar studies might usefully be undertaken of other CHP technologies, and in particular for advanced coal burning schemes where optimal CHP design may influence component development at an early stage.

Cogeneration schemes should not be studied in isolation from the heat and power demands that they must meet. Modifications to these demands may be beneficial to CHP operation and should be considered in conjunction with the design of the CHP scheme.

With the decline of supplies of cheap oil and gas over the next 20 years, industry will be forced to invest in new heat supply equipment, notably for a wide scale conversion to coal. At the same time the ESI will be considering the design and installation of advanced fossil fired plant to meet increments in electricity demand. It is therefore an opportune time for a study optimising across the boundaries of heat and power supply to investigate how these two important sectors of energy demand may best be met. The indications are that coal based, high electrical generating efficiency cogeneration may be the most suitable. Such a study would have to include the system operating characteristics when there is a large industrial CHP contribution, not considered in depth in this thesis, and also a more comprehensive survey of industrial heat loads.

The future holds the prospect of higher energy demand expectations and diminishing supplies of convenient high energy density fossil fuels. Energy conversion of the remaining fossil fuels will therefore become less efficient as the sources of the prime fuels are exhausted, unless energy conversion and end use are more closely tailored to maximise the rates of energy recovery. CHP may be regarded as one example of this conservative philosophy. At the same time investment criteria

for supply and conservation must be made at least equivalent, if not biased in favour of conservation. Unless these approaches are adopted, it may be difficult in the UK to continue to derive our present level of end use benefit from energy consumption.

APPENDIX 1

MATCH 8: A DIESEL SIMULATION PROGRAM

The Match 8 program simulates the steady state performance of a 4-stroke, turbocharged diesel engine running at constant speed. A steady state requires that both the mass flows, and the compressor power input and turbine power output be balanced. Two nested iterative loops are therefore used: the inner achieves the mass-flow balance, and the outer the turbocharger power balance.

The logical structure of the program is shown in the flow diagram, fig. A1.1. It is written in FORTAN IV, is divided into 12 sub-routines, and typically takes 10-15 seconds central processing time on the Imperial College CDC 6600 computer for each stable operating point.

Theory

The engine cycle may be divided into two parts: the closed cycle where the cylinder is isolated from exhaust and inlet manifolds, and the open cycle where one or both of the inlet and exhaust manifolds can exchange gases with the cylinder. The approaches to each part will be described separately.

Closed Cycle

The analysis of the closed cycle is a modification of a method used by Wallace and Way of Bath University (Refs. 87,29). This is itself

Flow diagram

Fig. A1.1

Match 8 Flow Diagram

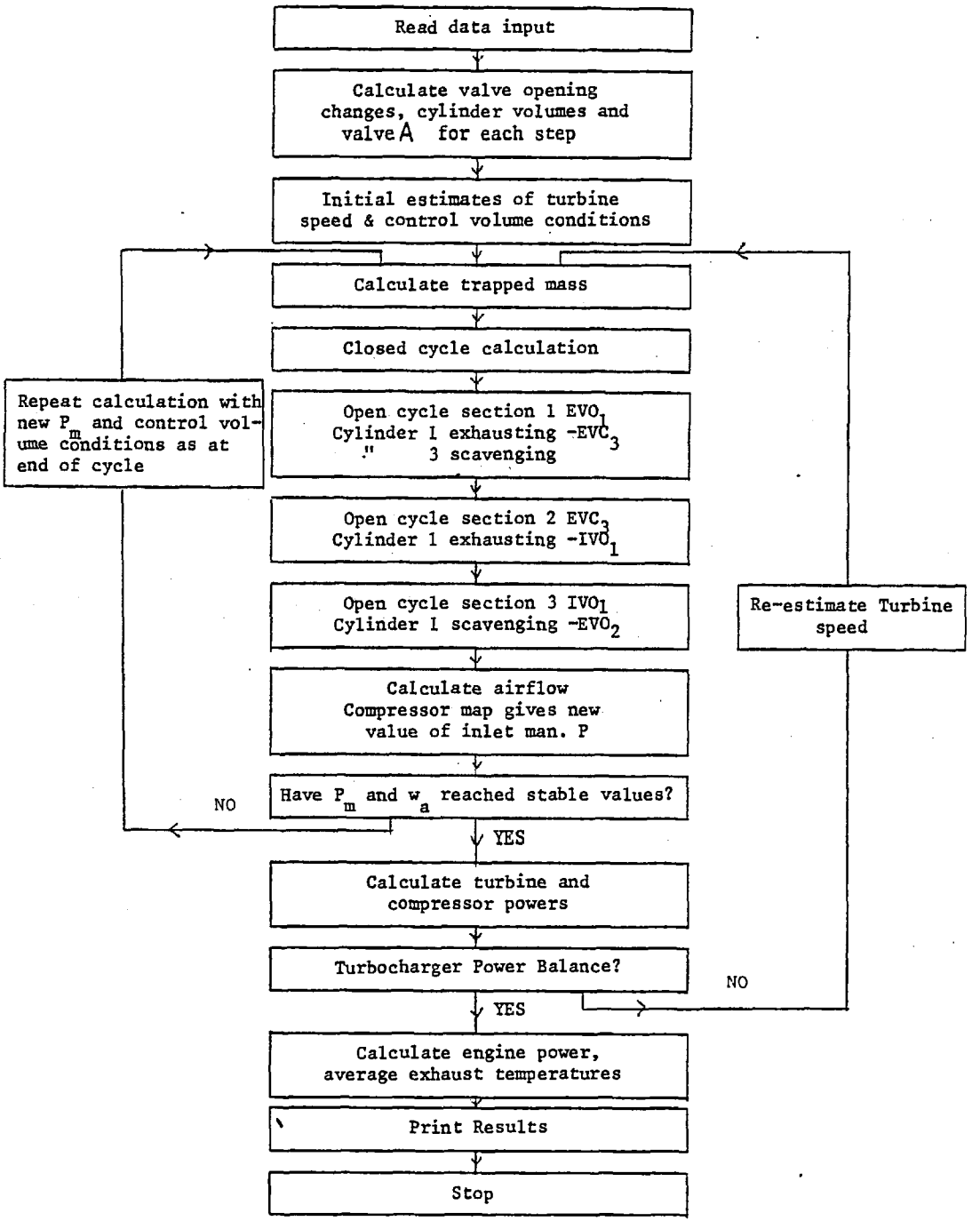

a more sophisticated version of the simple limited-pressure, or dual cycle.

The closed cycle is essentially divided into 5 sections as shown in figure A1.2:

1. $1 \longrightarrow 2$ is an adiabatic compression. Over a compression ratio of around 10:1 the pressure and temperature change significantly and hence the compression is split into 10 steps, due allowance being made for the variation of C_p and γ with temperature.

2. $2 \longrightarrow 3$ is an essentially constant volume combustion starting at 5° btdc and ending 5° atdc. The fraction of the fuel input burnt at this stage is determined as follows:

From the fuel preparation rate equation due to Way (Ref. 87):

$$dm_f = k_f (m_{finj} - m_f)d\theta$$ (a key to the symbols is given at the end of this appendix.)

α is the fraction of fuel burnt at constant volume and

$$\alpha = \frac{365 - X_{inj}}{D_{inj}} - \frac{(1-e^{-k_f(365-X_{inj})})}{k_f.D_{inj}} \text{ for } 365-X_{inj} < D_{inj}$$

or $$\alpha = 1 - \left\{ \frac{1 - e^{-k_f.D_{inj}}}{k_f.D_{inj}} \right\} e^{-k_f(365-(X_{inj} + D_{inj}))} \text{ for } 365 - X_{inj} \geq D_{inj}$$

this leaves a fraction $\beta = 1-\alpha$ split equally between the constant pressure and constant slope combustion sections described next.

Some of the heat released will however be lost to the coolant. Wallace uses a simple, experimentally determined relationship between H_c, the fraction of heat lost to coolant, and $^{w_f}/_{N_s}$, the general form of which is shown in fig. A1.3.

A modification was introduced to this because the fraction of heat rejected to coolant will depend significantly on R_T. To a first approximation closed cycle temperatures and heat loss will, for constant

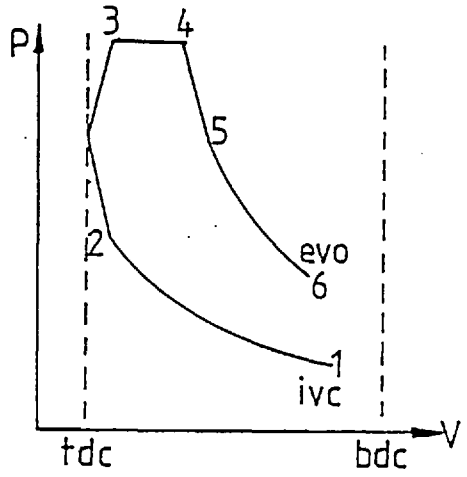

Fig. A1.2 Closed Cycle Model

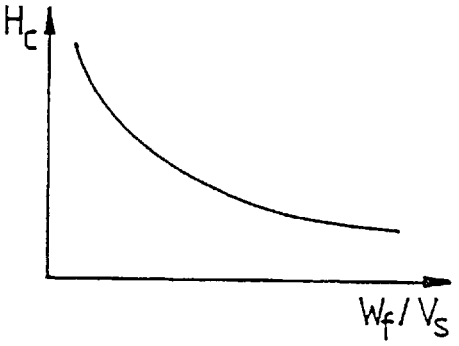

Fig. A1.3 Heat to Coolant Curve

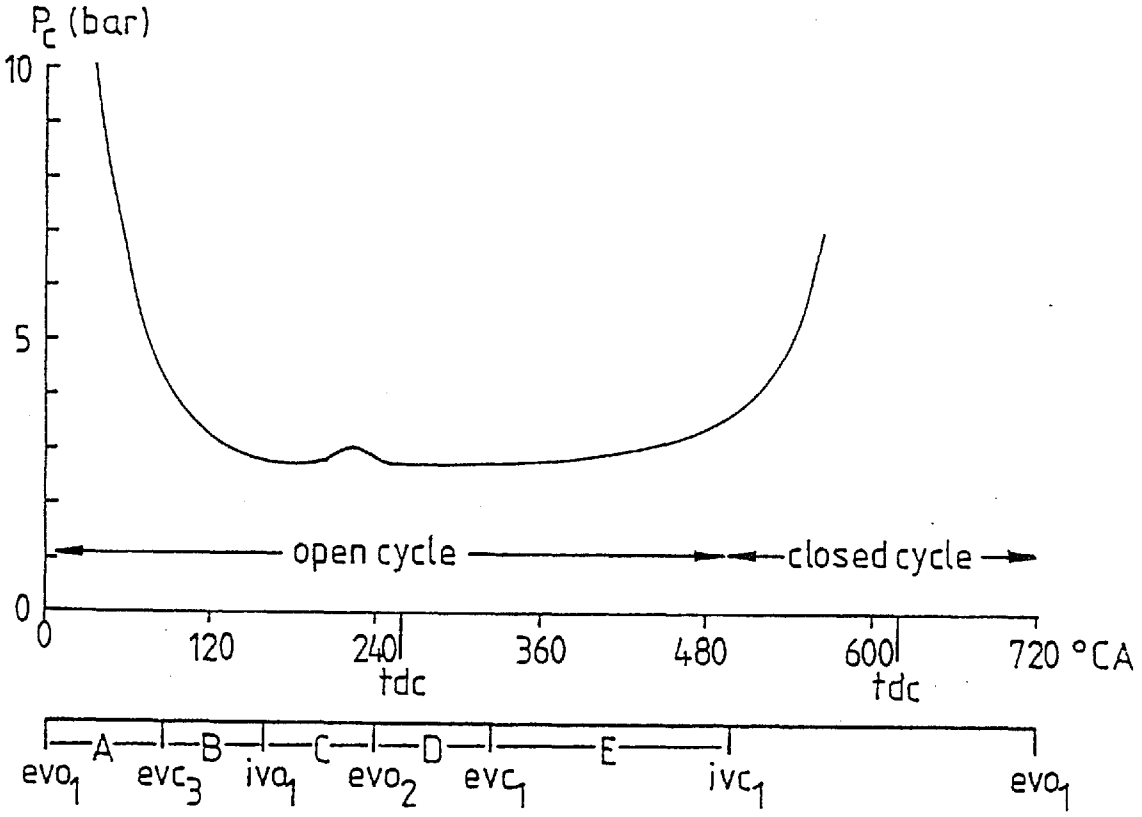

A = cyl.1 exhaust, cyl. 3 scavenge
B = cyl.1 exhaust
C = cyl.1 scavenge
D = cyl.1 scavenge, cyl. 2 exhaust
E = cyl.1 induction

Fig. A1.4 Sequence of Cylinders to Exhaust (3 Cylinders to 1 Exhaust Manifold)

values of other parameters, be linearly related to $(^{1}/_{R_T})$.

Hence an equation of the form:

$H_c = C_1 \left\{\frac{w_f}{v_s}\right\}^2 + C_2 \left\{\frac{w_f}{v_s}\right\} + C_3 + {}^{C_4}/_{R_T}$ was used, where the coefficients C_1, C_2, C_3 and C_4 are determined from experimental results if they are available, or from simple consideration of heat transfer theory if they are not.

H_c is subtracted first from β and then from α giving effective fractions of heat released as follows:

$$\left.\begin{aligned}\beta' &= 1-\alpha-H_c \\ \alpha' &= \alpha\end{aligned}\right\} \beta \geq H_c$$

$$\left.\begin{aligned}\beta' &= 0 \\ \alpha' &= 1-H_c\end{aligned}\right\} \beta < H_c$$

From these $T_3 = \dfrac{m_{t1}C_{v2}T_2 + m_{f1}\,\alpha' C_{a1} - 0.75(P_3-P_2)(V_2-V_c)}{(m_{t1} + \alpha m_{f1})C_{v3}}$

3. $3 \longrightarrow 4$ is a constant pressure release of the fraction $\frac{\beta'}{2}$ of heat input.

$$\therefore \quad T_4 = \frac{(m_{t1} + \alpha m_{f1})C_{p3}T_3 + m_{f1}\frac{\beta'}{2}C_{a1}}{(m_{t1} + (\alpha + \frac{\beta}{2})m_{f1})C_{p4}}$$

$$\text{and} \quad V_4 = \frac{(m_{t1} + (\alpha + \frac{\beta}{2})m_{f1})RT_4}{P_4}$$

4. $4 \longrightarrow 5$ is a constant slope release of the fraction $\frac{\beta'}{2}$ of heat input. The point 5 being chosen so that the slope of $4 \longrightarrow 5$ merges smoothly with the slope of the section $5 \longrightarrow 6$ which is an adiabatic expansion.

Calculation reveals that $P_5 = \dfrac{-a_3 + \sqrt{a_3^2 - 4a_2a_4}}{2a_2}$

where $a_2 = V_4(\tfrac{1}{2} - \dfrac{C_{v5}\gamma_5}{R})$

$$a_3 = (m_{fl}\beta' C_{al}/_2 + (m_{tl} + m_{fl}(\alpha + \frac{\beta}{2}))C_{v4}T_4)(1 + \gamma_5)$$

$$a_4 = -P_4(m_{fl}\beta' C_{al}/_2 + (m_{tl} + m_{fl}(\alpha + \frac{\beta}{2}))C_{v4}T_4) - \tfrac{1}{2}P_4{}^2V_4$$

and $$V_5 = \frac{\gamma_5 V_4 P_5}{P_5(1+\gamma_5) - P_4}$$

5. 5 ⟶ 6 is an adiabatic expansion, split into 10 steps with varying C_p and γ as for the compression.

The work done per cylinder during the closed cycle is then found by summing the $P\Delta V$ terms over the steps.

Open Cycle

The engine is divided into control volumes. The analysis of the open cycle can be performed using just 4 volumes: the inlet and exhaust manifolds, and two cylinders (labelled X and Y). The arrangement is shown in figure A1.5.

The pressures, temperatures and compositions of cylinders X and Y and of the exhaust manifold vary continuously throughout the cycle. Inlet manifold pressure and temperature are assumed constant. The volumes of X and Y also vary. Boundary conditions are imposed by the turbine and the compressor. All changes are assumed to be quasi-steady.

The open cycle is treated in three sections:

1. One cylinder scavenging and one cylinder exhausting (for 3 or 4 cylinders connected to one exhaust manifold), or no cylinders connected to the exhaust (for 1 or 2 cylinders connected to one exhaust manifold).
2. One cylinder exhausting only.
3. One cylinder scavenging only.

The sequence of events is illustrated in figure A1.4, for three cylinders connected to one exhaust manifold, 240° firing interval.

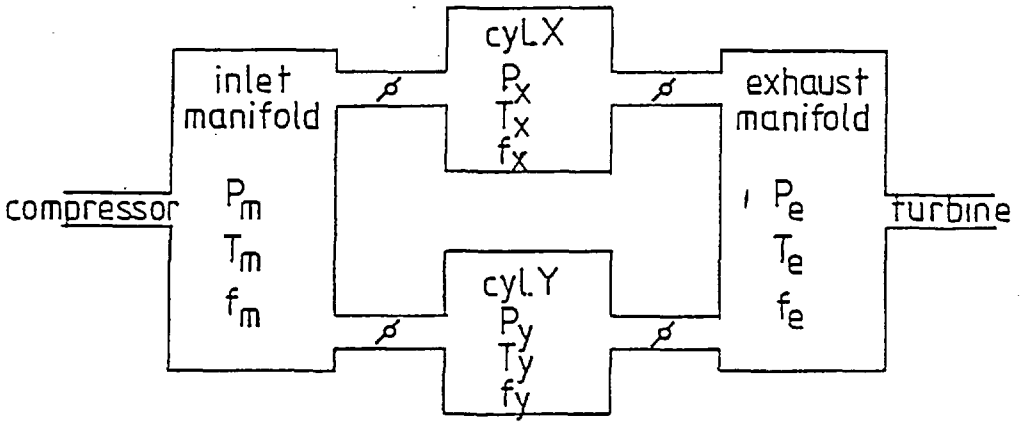

Fig. A1.5 Control Volumes for Open Cycle Calculation

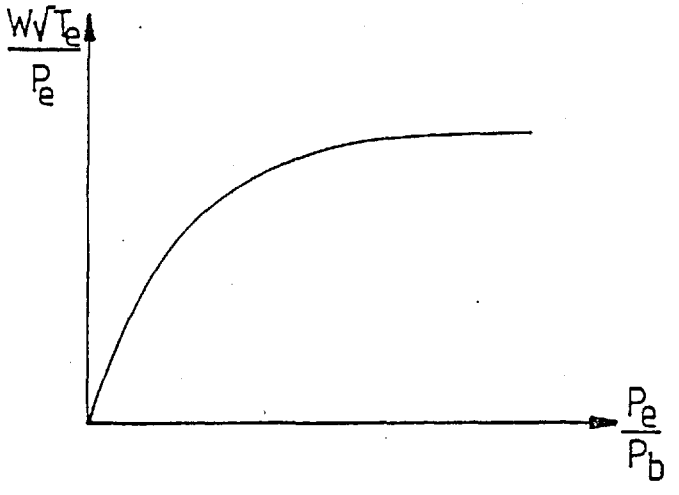

Fig. A1.6 Turbine Flow Characteristic

Each section is split into steps, each of 4-5° CA duration, the general energy balance equation across each step for any control volume being:

$$m_{i+1}u_{i+1} - m_i u_i = \Sigma\Delta m_{in} h_{in} - \Sigma\Delta m_{out} h_{out} - P_i\Delta V - \Delta Q$$

$$\text{giving } T_{i+1} = \frac{m_i C_{vi} T_i + \Sigma\Delta m_{in} C_{Pin} T_{in} - \Sigma\Delta m_{out} C_{Pout} T_{out} - P_i\Delta V - \Delta Q}{m_{i+1} C_{vi+1}}$$

$$\text{also } m_{i+1} = m_i + \Sigma\Delta m_{in} - \Sigma\Delta m_{out}$$

$$P_{i+1} = \frac{m_{i+1} R T_{i+1}}{V_{i+1}}$$

$$f_{i+1} = \frac{m_{fi} + \Delta m_{fin} - \Delta m_{fout}}{m_{ai} + (\Delta m_{ain} - \Delta m_{aout})}$$

The following assumptions have been made:

1. Fluid properties are uniform throughout the control volume.
2. Ideal mixing of gases.
3. Flow is inviscid and wall friction is neglected.
4. The gas obeys the perfect gas equation: C_p, C_v and γ vary with the temperature and the fuel-air ratio.

The mass flows between and out of control volumes are calculated for each step using the values of temperature and pressure at the start of the step:

1. The flow through the turbine is calculated from the turbine flow characteristic (fig. A1.6) and is a function of T_e, P_e and P_b.

2. Flow from cylinder to exhaust manifold from evo to ivo is calculated from the compressible flow equations:

$$\Delta m_{cx} = A_e \frac{P_x}{\sqrt{T_x}} \sqrt{\frac{2\gamma_x}{(\gamma_x - 1)R}\left[\left\{\frac{P_e}{P_x}\right\}^{2/\gamma_x} - \left\{\frac{P_e}{P_x}\right\}^{\frac{\gamma_x+1}{\gamma_x}}\right]} \quad \text{for } \frac{P_e}{P_x} > \left\{\frac{2}{\gamma_x+1}\right\}^{\frac{\gamma_x}{\gamma_x-1}}$$

$$\text{or } \Delta m_{cx} = A_e \frac{P_x}{\sqrt{T_x}} \sqrt{\frac{\gamma_x}{R}\left[\frac{2}{\gamma_x+1}\right]^{\frac{\gamma_x+1}{\gamma_x-1}}} \quad \text{for } \frac{P_e}{P_x} \leq \left[\frac{2}{\gamma_x+1}\right]^{\frac{\gamma_x}{\gamma_x-1}}.$$

A_e being the effective exhaust valve area for the step.

3. During the scavenge period, compressible flow inlet manifold to cylinder, and cylinder to exhaust manifold cannot be used with step size of the order of 4^oCA. The scavenge flows into and out of the cylinder for this step length are comparable to the mass of the cylinder contents, and hence instabilities due to rapidly oscillating cylinder pressures and temperatures may occur. In order to eliminate these oscillations the step size must be reduced to around 0.5 - 1^oCA, giving unacceptably long running times. A different approach based on the dominant physical processes during overlap was therefore adopted.

As the inlet valve is opening, the upwards movement of the piston is displacing gas out of the exhaust valve, the inlet valve is controlling the flow of cooler, denser scavenge air into the cylinder. The incoming air will occupy a volume dependent on P_m and T_m and hence displace a similar volume of cylinder contents through the exhaust valve. Around tdc, piston displacement reduces and flow through the valves is dominated by scavenge airflow. After tdc the descending piston induces fresh air into the cylinder, and the exhaust valve controls the scavenge flow. The following model was therefore used:

1. Straightforward scavenge $P_m > P_c > P_e$

Before tdc Δm_m calculated from the compressible flow equation P_m to $\frac{P_m + P_e}{2}$ using the minimum of A_e and A_i, and a discharge coefficient for fine tuning,

$$\Delta m_c = \frac{P_c}{P_m}\frac{T_m}{T_c}\Delta m_m + \frac{P_c \Delta V_{cyl}}{RT_c}$$

after tdc Δm_m comprises two parts: a scavenge part calculated as

before tdc + $\frac{P_m \Delta V_{cyl}}{RT_m} \eta_{vol}$ (an induction component)

and $\Delta m_c = \Delta m_m - \frac{P_m \Delta V_{cyl}}{RT_m} \eta_{vol}$

2. Blowback from the exhaust manifold $P_e > P_m$

Δm_c (into the cylinder) calculated from compressible flow P_e to $\frac{P_m + P_e}{2}$ using min (A_e, A_i) and a discharge coefficient,

$$\Delta m_m = \frac{\Delta V_{cyl} \eta_{vol} P_m}{RT_m} - \frac{P_c}{T_c} \Delta m_c \frac{T_e}{P_e}$$

3. Cylinder pressure greater than inlet manifold pressure: $P_m < P_c > P_e$

$\Delta m_m = 0$

Δm_c from compressible flow equation P_c to P_e

The model gives a cylinder pressure diagram during the overlap period of a form similar to that found in experiments (fig. A1.7).

Input/Output data

The following information is required as input data:

1. Turbine and compressor maps as two dimensional arrays and illustrated in figures A1.6, A1.8 and A1.9.

2. Gas specific heats at constant pressure and volume, and their ratio as two dimensional arrays.

3. Valve timing and valve effective areas.

4. The timing of the start of fuel injection and its duration; fuel rate and fuel calorific value.

5. The heat to coolant curve.

6. The number of exhaust manifolds, their volume and area.

7. Cylinder bore, stroke, compression ratio, con-rod length and engine speed.

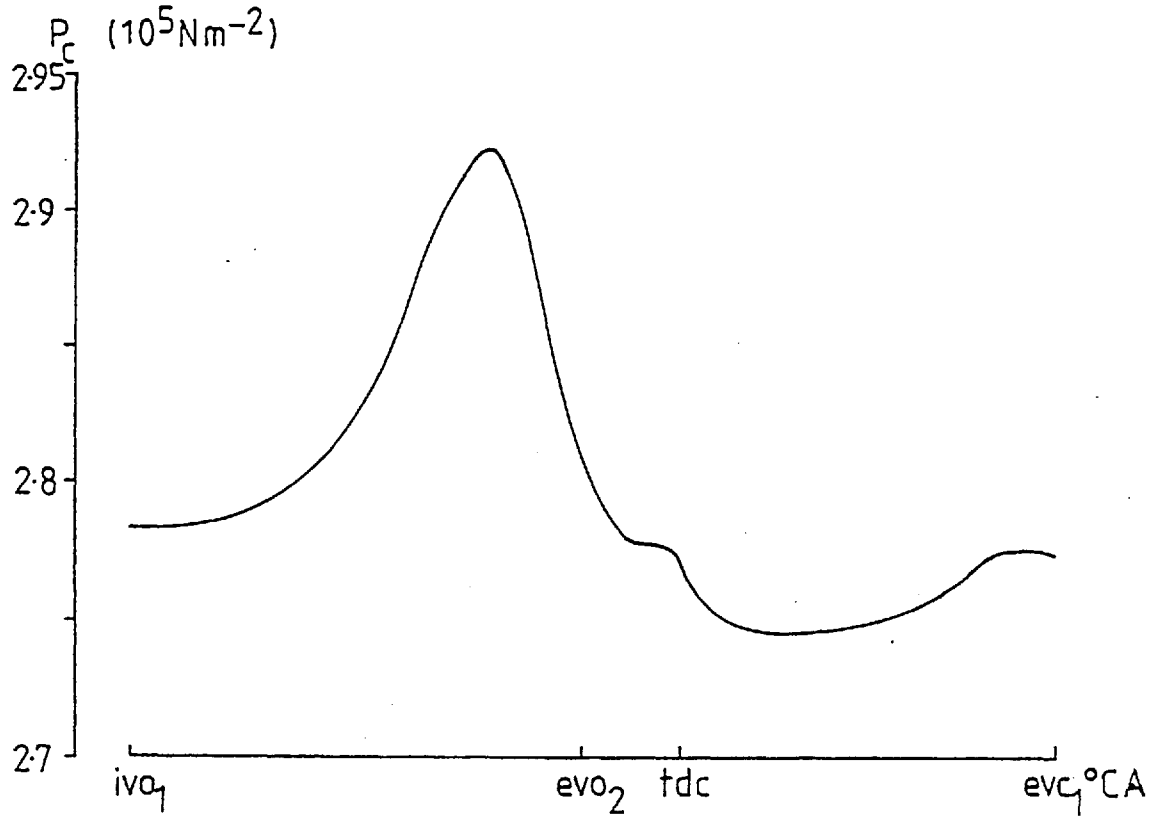

Fig. A1.7 Predicted Cylinder Pressure Diagram during Overlap

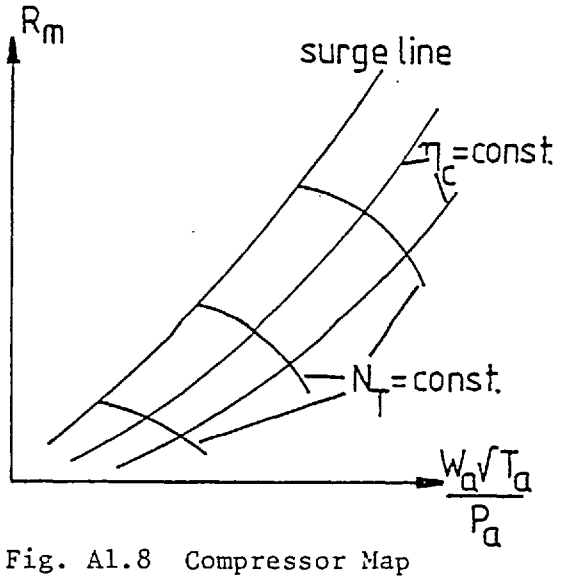

Fig. A1.8 Compressor Map

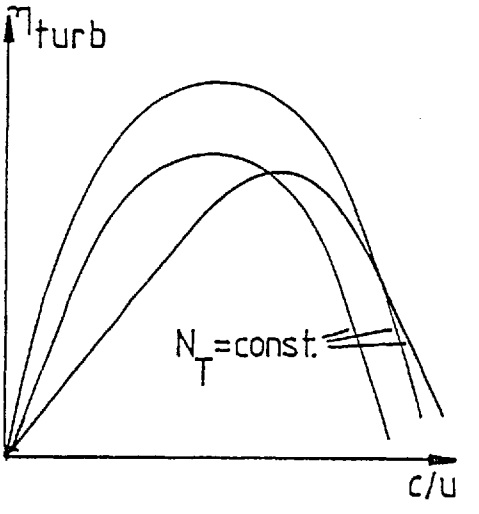

Fig. A1.9 Turbine Efficiency Characteristic

8. Friction data.
9. Ambient temperature and pressure.
10. Discharge coefficients and volumetric efficiency.
11. The number of steps and the required accuracy of iterations.
12. Initial estimates of the inlet manifold pressure, the cylinder pressure and temperature and the turbine speed, in order to commence the iterations. Less accuracy is required for these initial estimates than is typically the case for the full step-by-step models.

Output data consists of:

1. The power output and heat to the exhaust, engine coolant and the intercooler.
2. The average exhaust temperature.
3. The engine airflow, the trapped cylinder mass at inlet valve closing, and the inlet manifold pressure ratio.
4. The turbocharger power.
5. The step-by-step, open cycle values of the exhaust manifold pressure and temperature, and the cylinder pressure, temperature and fuel-air ratio.

Symbols Local to Appendix 1

A_e = Exhaust Valve Effective Area.

A_i = Inlet Valve Effective Area.

C_{al} = Calorific Value of Fuel.

$C_{1,2,3,4}$ = Constants in Heat to Coolant Curve.

C_p = Specific heat at constant pressure.

C_v = Specific heat at constant volume.

D_{inj} = Duration of fuel injection.

dm_f = Fuel prepared in crank angle $d\theta$.

$d\theta$ = Increment in crank angle.

f = Fuel/air ratio.

h = Specific Enthalpy.

H_c = Fraction of fuel input energy to coolant.

k_f = Constant in fuel preparation equation.

m_c = Mass flow through exhaust valve: cylinder to exhaust manifold.

m_f = Mass of fuel already prepared.

m_{finj} = Mass of fuel injected.

m_{fl} = Mass of fuel per cylinder per cycle.

m_m = Mass flow through inlet valve: inlet manifold to cylinder.

m_{tl} = Trapped mass of air per cylinder per cycle.

P = Pressure.

P_b = Back Pressure.

Q = Heat Energy.

R = Gas constant.

R_T = Trapped Air fuel ratio.

T = Temperature.

u = Specific Internal Energy.

V = Volume

V_c = Clearance volume.

V_{cyl} = Cylinder Volume.

V_s = Swept Volume.

$\dot{w}_f$ = Rate of Mass Flow of Fuel to Engine.

X_{inj} = Start of Injection.

α = Fraction of Fuel Burnt at Constant Volume.

β = Fraction of Fuel Burnt at Constant Pressure and Slope.

α' = Modified Fraction of Fuel Burnt at Constant Volume.

β' = Modified Fraction of Fuel Burnt at Constant Pressure and Slope.

Δx = Change in x.

η_{vol} = Volumetric Efficiency.

γ = Ratio of Gas Specific Heats.

Subscripts: a = air

c = cylinder

e = exhaust manifold

m = inlet manifold

x = cylinder X

y = cylinder Y

2,3,4,5 = Points in Closed Cycle (Fig. A1.2)

in = flow into control volume

out = flow out of control volume

i and i+1 = start and finish of step i.

APPENDIX 2

THE BOILER SIMULATION PROGRAM

The program predicts the performance of a watertube exhaust gas boiler comprising economizer, evaporator and superheater sections, illustrated schematically in fig. A2.1. The directional arrows on the water flow paths may be reversed to represent parallel or counter-flow arrangements. Each section is treated separately and is divided into increments of tubing area. The analytical procedure to find a stable operating point, or to size the boiler to produce desired water/steam conditions, consists of three iterative loops: two sequential inner loops and one outer loop. The logical structure of the program is shown in the flow diagram (fig. A2.2). It is written in FORTRAN IV and is divided into ten subroutines.

Theory

The gas pressure and temperature, and the water temperature are calculated at the beginning and end of each increment of tubing area. The derivations of the equations used follow:

Economizer/Superheater

For step j:

$$\dot{m}_g \left(C_{pgj}\, T_{gj} - C_{pgj+1}\, T_{gj+1}\right) = \dot{m}_s \left(C_{pwj}\, T_{wj} - C_{pwj+1}\, T_{wj+1}\right)$$

$$= U_j\, \Delta A_j \left(\frac{T_{gj+1} + T_{gj}}{2} - \frac{T_{wj+1} + T_{wj}}{2} \right)$$

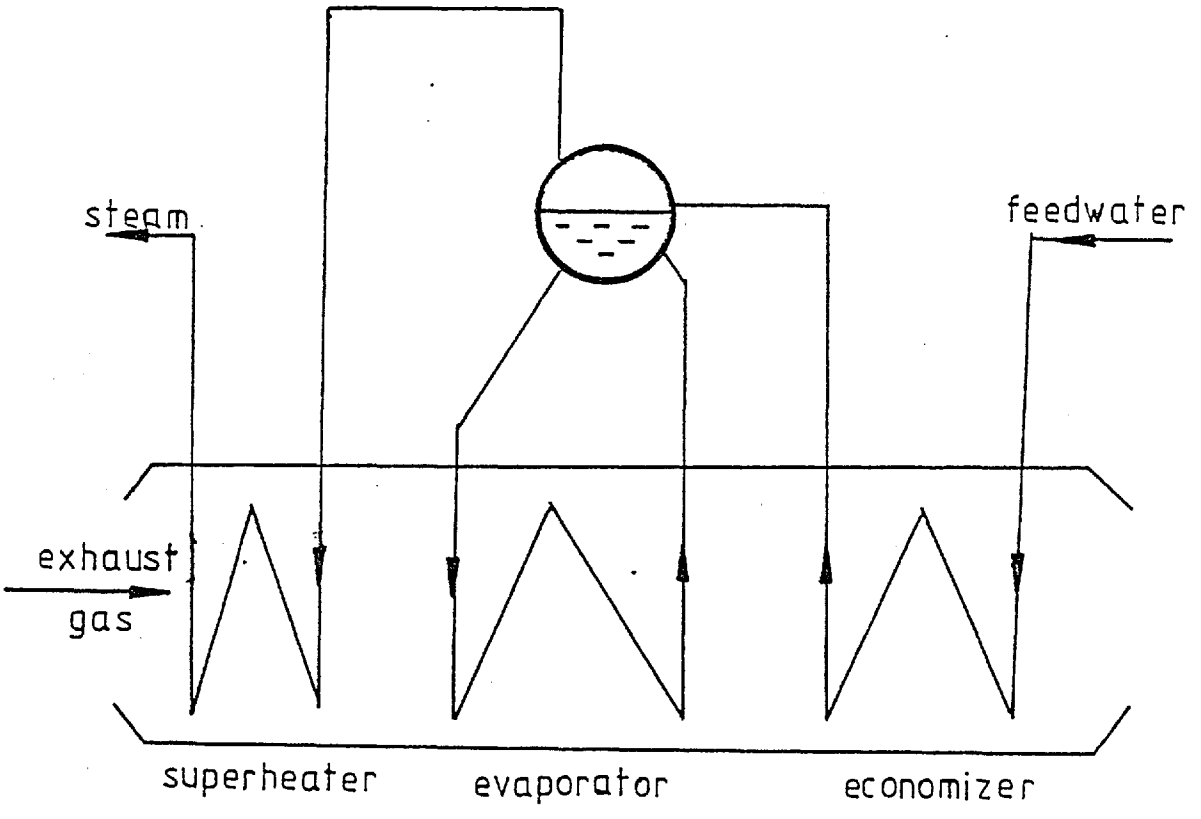

Fig. A2.1 Schematic Diagram of Watertube Exhaust Gas Boiler

Fig. A2.2

Boiler Simulation Program Flow Diagram

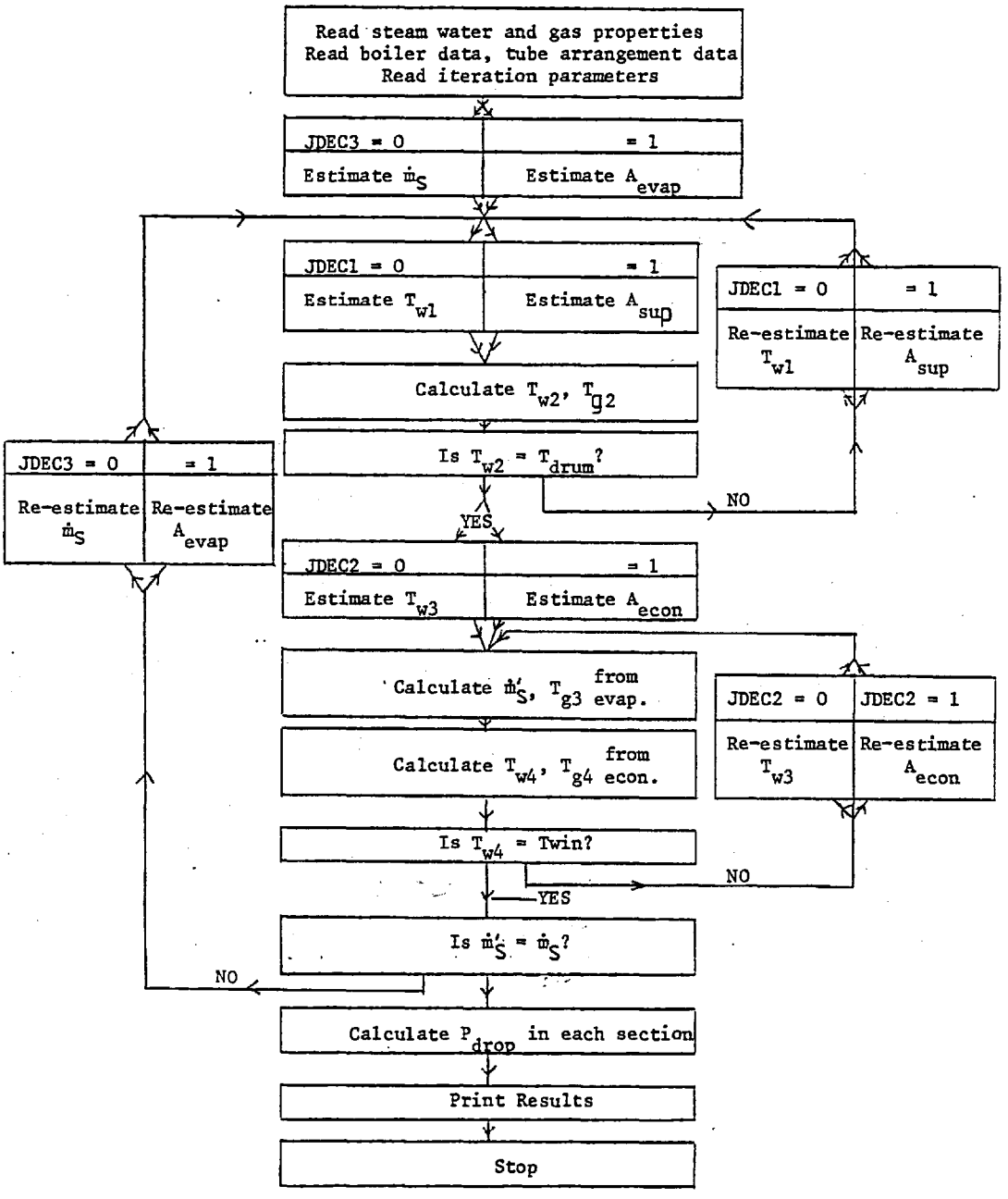

This being a simple First Law energy balance across the step (it is assumed that no heat is lost from the boiler). A counterflow arrangement is assumed for positive values of $\dot{m}_g$ and $\dot{m}_s$.

From these simultaneous equations the water and gas temperatures may be calculated at the end of the step as follows:-

$$T_{wj+1} = \frac{(\dot{m}_s C_{pwj} + \dot{m}_g C_{pgj+1} K_1) T_{wj} + \dot{m}_g (C_{pgj+1} K_2 - C_{pgj}) T_{gj}}{\dot{m}_s C_{pwj+1} - \dot{m}_g C_{pgj+1} K_1}$$

and $T_{gj+1} = K_2 T_{gj} + K_1 (T_{wj} + T_{wj+1})$

where $K_1 = \frac{U_j \Delta A_j}{U_j \Delta A_j + 2 \dot{m}_g C_{pgj+1}}$ and $K_2 = \frac{2 \dot{m}_g C_{pgj} - U_j \Delta A_j}{U_j \Delta A_j + 2 \dot{m}_g C_{pgj+1}}$

The overall heat transfer coefficient U_j is calculated from

$$U_j = \frac{1}{\frac{d_o}{d_i}\frac{1}{h_i} + \frac{A_o \mathrm{Log}(d_o/d_i)}{2\pi k l} + \frac{1}{h_o}}$$ (See for instance Ref. 40)

where:

(i) h_o is calculated from $Nu = C Re^n Pr^{1/3}$; the values of C and n depend on the tube arrangement, and for plain tubes were taken from ref. 34.

(ii) Re is based on the maximum velocity of gas in the tube bank.

(iii) The gas flow is assumed turbulent.

(iv) Gas properties are evaluated at the average film temperature

$$T_f = 0.25(T_{gj} + T_{gj+1} + T_{wj} + T_{wj+1})$$

(v) h_i for fully developed turbulent flow from $Nu = 0.023 Re^{0.8} Pr^{0.4}$ (Ref. 24), and for laminar flow $Nu = 1.86 Re^{1/3} Pr^{1/3} (d_i/l)^{1/3}$, a slight simplification of a formula in Ref. 77. Transition normally occurs in the range $2000 < R_e \leq 4000$ (Ref.40), in the program transition at 2000 is assumed.

(vi) Fluid properties are evaluated at the average fluid bulk temperature for the step.

Evaporator

The increment in steam generation $\Delta\dot{m}_{sj}$ for each evaporator step is determined by:

$$\dot{m}_g(C_{pgj}T_{gj} - C_{pgj+1}T_{gj+1}) = \Delta\dot{m}_{sj}(C_{pw2}T_{w2} - C_{pw3}T_{w3}) = U_j\ \Delta A_j\left(\frac{T_{gj+1} + T_{gj}}{2} - T_{w2}\right)$$

whence $\dot{m}_s = \text{evaporator} \sum\Delta\dot{m}_{sj}$

$$T_{gj+1} = \frac{T_{gj}\left(\dot{m}_g C_{pgj} - \frac{U_j\ \Delta A_j}{2}\right) + U_j\ \Delta A_j\ T_{w2}}{\frac{U_j\ \Delta A_j}{2} + \dot{m}_g C_{pgj+1}}$$

and $$\Delta\dot{m}_{sj} = \frac{\dot{m}_g(C_{pgj}T_{gj} - C_{pgj+1}T_{gj+1})}{C_{pw2}T_{w2} - C_{pw3}T_{w3}}$$

U_j is calculated as for the economizer and superheater sections except that the water side thermal resistance for nucleate boiling heat transfer is assumed zero.

Pressure Drop

For step j $$\Delta P_j = \frac{2F\ G_{max}^2\ N_j}{\rho}\left\{\frac{\mu_{gw}}{\mu_{gb}}\right\}^{0.14}$$ (Ref.43)

For plain tubes:

$$F = \left\{0.044 + \frac{\frac{0.08S_1}{d_o}}{\left\{\frac{S_t - d_o}{d_o}\right\}^{0.43 + 1.13d_o/s_1}}\right\} Re^{-0.15}$$ inline tubes

$$F = \left\{0.25 + \frac{0.118}{\left\{\frac{s_t - d_o}{d_o}\right\}^{1.08}}\right\} Re^{-0.16}$$ staggered tubes

and $N_j = \frac{N}{n_{div}}$ for inline or staggered arrangements with the minimum flow area in the transverse direction.

$N_j = \frac{N-1}{n_{div}}$ for staggered arrangements with the minimum flow area in the diagonal direction.

Input/Output data

1. Fluid property data common to all runs are:

   (a) Steam conductivity, prandtl number and enthalpy, and water enthalpy are dependent on both temperature and pressure, and are represented by two dimensional arrays.

   (b) Water conductivity, prandtl number and viscosity, steam viscosity, gas conductivity and viscosity are essentially dependent only on temperature and are represented by polynomials.

2. Tube type, spacing, diameter and length for each section are input data.

3. The gas and water conditions at the boiler inlets, and the steam conditions in the separator drum are required.

4. The program may either calculate fluid outlet conditions for given tubing areas, or the tubing area required to give stated fluid outlet conditions. The choice is determined for each section by values assigned to the decision parameters JDEC.

5. The output also includes the gas and water temperatures at, and pressure drops across, each step through the boiler.

Summary

The program is versatile in being able to handle a wide variety of input and output data, any of the boiler sections may be omitted if necessary. Extension to firetube boilers was not attempted, but would be relatively straightforward. Running times are short: around 2 seconds CPU time on a CDC 6600.

Symbols Local to Appendix 2

A_o = Tube outside area per unit length.

C_{pg} = Specific heat at constant pressure of gas.

C_{pw} = Specific heat at constant pressure of water.

d_i = Tube internal diameter.

d_o = Tube outside diameter.

F = Friction factor.

G_{max} = Maximum mass flow per unit area.

h_i = Internal heat transfer coefficient.

h_o = External heat transfer coefficient.

k = Thermal conductivity of tube.

l = Tube length.

$\dot{m}_g$ = Mass flow of gas through boiler

$\dot{m}_s$ = Steam/water flow rate.

N = Tube number.

Nu = Nusselt Number.

n_{div} = Number of divisions.

P = Pressure.

Pr = Prandtl

Re = Reynolds Number.

s_l = Tube longitudinal spacing.

s_t = Tube transverse spacing.

T_f = Film temperature.

T_g = Gas temperature.

T_w = Water temperature.

U = Heat transfer coefficient.

ΔA = Increment of tubing area.

μ_g = Gas viscosity.

ρ = Density

Subscript w = wall.

b = bulk.

APPENDIX 3

THE SITE MODELS

The theory of the site models is described in this appendix. The linear model is first given: this was not in fact programmed for the computer, but the theory is given for comparison with the 2 site models actually used. These are the variable recuperation gas turbine, and diesel engine CHP site models. The optimisation of the operation and the characteristic representation is first given for one variable recuperation gas turbine, followed by a proof of the operating mode for several identical prime movers. Finally the model of the diesel engine CHP site is described.

The Linear Model

The characteristics of the prime mover are assumed not to vary with load. It can therefore be represented by:

η_b, its brake efficiency

r, the ratio of recoverable heat to power produced

P_{max}, its maximum power output.

For the most straightforward system comprising just prime mover with waste heat recovery, plus auxiliary boiler, the cost function has 4 forms depending on whether P is greater or less than K, and rP is greater or less than H, where:

P = power produced by the prime mover

H = site heat demand

K = site power demand.

The values of the cost function are as follows (the cost function shown is that of the site owner operating the scheme i.e. the cost of meeting the site's power demand is included):

Case 1. $P \geq K$ and $rP \geq H$ gives $z' = \frac{C_{e2}.K}{C_f} + P\left\{\frac{1}{\eta_b} - \frac{C_{e2}}{C_f}\right\}$

where $z' = {}^{z}/_{C_f}$

and C_{el} = electricity import price

C_{e2} = electricity export price

C_f = cost of fuel to site

The slope of z' with respect to P, $s_1 = \frac{1}{\eta_b} - \frac{C_{e2}}{C_f}$

2. $P \geq K$ and $rP < H$ gives $z' = \frac{C_{e2}.K}{C_f} + \frac{H}{\eta_{aux}} + P\left\{\frac{1}{\eta_b} - \frac{C_{e2}}{f} - \frac{r}{\eta_{aux}}\right\}$

slope $s_2 = \frac{\eta_{aux} - r\eta_b}{\eta_{aux}\eta_b} - \frac{C_{e2}}{C_f}$ where η_{aux} = auxiliary boiler efficiency.

3. $P < K$ and $rP \geq H$ gives $z' = \frac{C_{el}.K}{C_f} + P\left\{\frac{1}{\eta_b} - \frac{C_{el}}{C_f}\right\}$

slope $s_3 = \frac{1}{\eta_b} - \frac{C_{el}}{C_f}$

4. $P < K$ and $rP < K$ gives $z' = \frac{C_{el}.K}{C_f} + \frac{H}{\eta_{aux}} + P\left\{\frac{1}{\eta_b} - \frac{C_{el}}{C_f} - \frac{r}{\eta_{aux}}\right\}$

slope $s_4 = \frac{\eta_{aux} - r\eta_b}{\eta_{aux}\eta_b} - \frac{C_{el}}{C_f}$

Two relations between the slopes are evident:

$$s_1 = s_2 + \frac{r}{\eta_{aux}} \qquad s_3 = s_4 + \frac{r}{\eta_{aux}}$$

At the optimum the prime mover will operate at one of the slope discontinuities P=0, ${}^{H}/_{r}$, K or P_{max}, illustrated in figure A3.1. Five

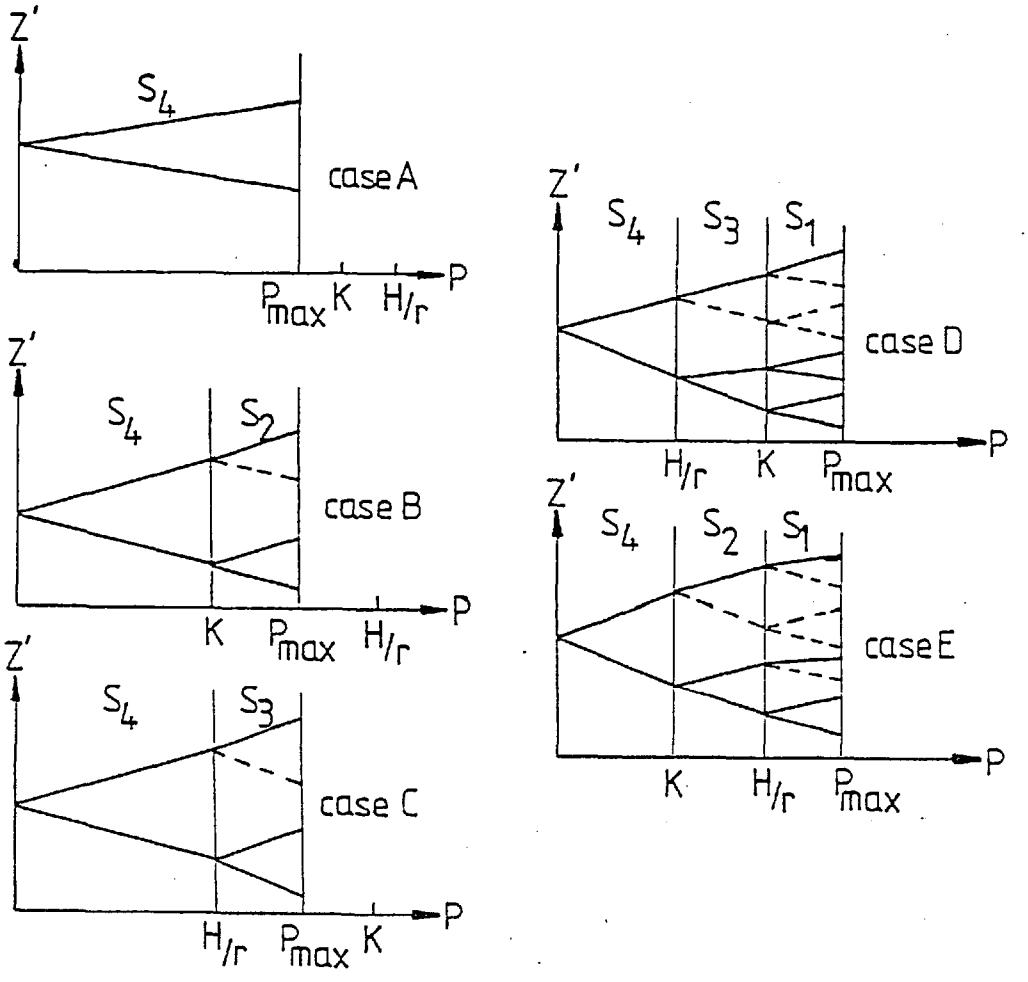

Fig. A3.1 Minimisation of Cost Function (Linear Model)

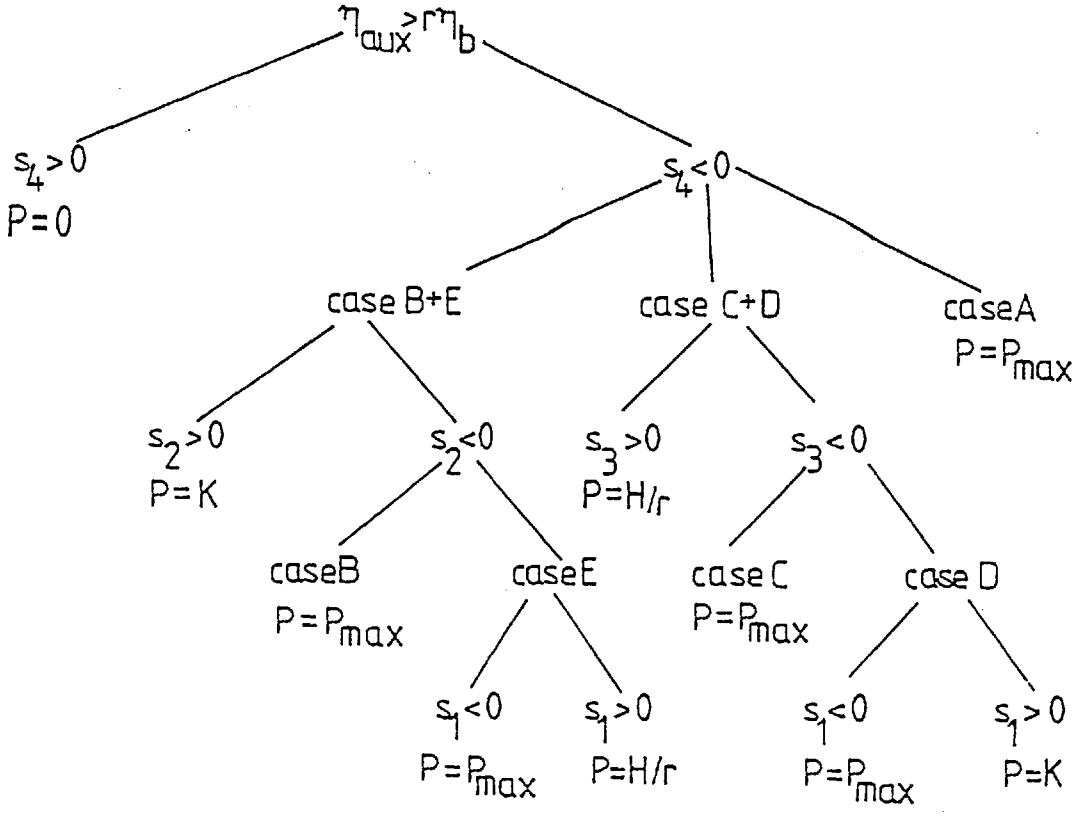

Fig. A3.2 Decision Process for Cost Function Minimisation (Linear Model)

cases are shown, depending on the relative magnitudes of P_{max}, K and H/r.

For the reasonable assumptions $C_{e1} \geq C_{e2}$ and $\eta_{aux} > r\eta_b$, $s_4 > 0$ implies that s_1, s_2, $s_3 > 0$ and $s_2 > 0$ implies that $s_1 > 0$. The non viable paths are shown dashed in figure A3.1. A decision figure can be constructed (fig. A3.2). It is a relatively simple matter to program this decision process for a computer, in order to automate the calculation of site operation. The calculation may be extended to include afterfiring (Ref.5).

The limitations of this model have been discussed in chapter 5.

The Variable Recuperation Gas Turbine Site Model

The variable recuperation gas turbine is designed to give a variable recoverable heat to power ratio, and hence cannot be represented by a linear model. The turbine is illustrated in figure A3.3 and is described more fully in reference 52. The aim is to vary the recoverable heat to power ratio by providing variable preheating of the combustion air from the turbine exhaust. The model is such that the unrecuperated or fixed recuperation gas turbine becomes a special case.

The theory will be described first for the operation of 1 turbine and then extended to the case of N turbines.

The turbine characteristic representation is based on data provided by R. Lowder of the GEC Mechanical Engineering Laboratory. The turbine operating regime is illustrated in figure A3.4, which shows it to be a quadrilateral bounded by the lines:

a where $E/P = a_1 (Q/P) + a_2 - a_3$

b " $E/P = a_1 (Q/P) + a_2 - a_3 \left[\frac{P_{min}}{P_{max}}\right]^{2/3}$

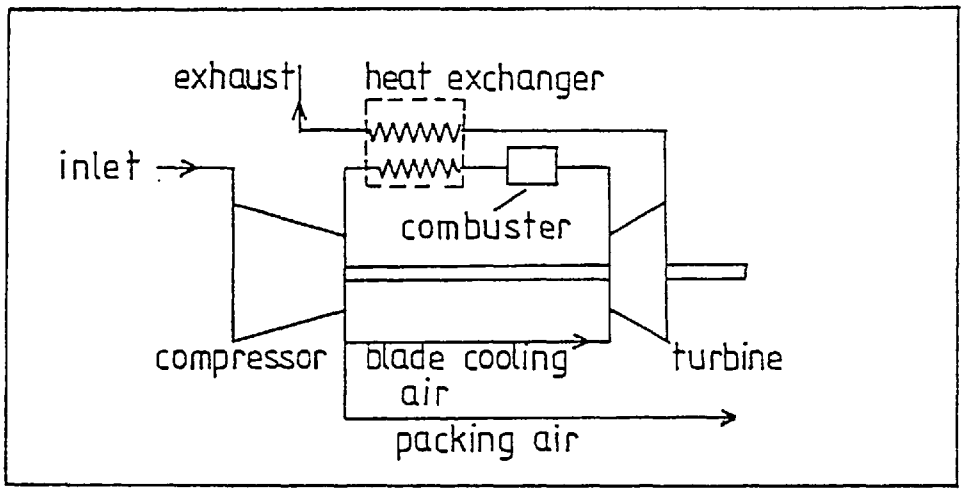

Fig. A3.3 Variable Recuperation Gas Turbine (Ref. 52)

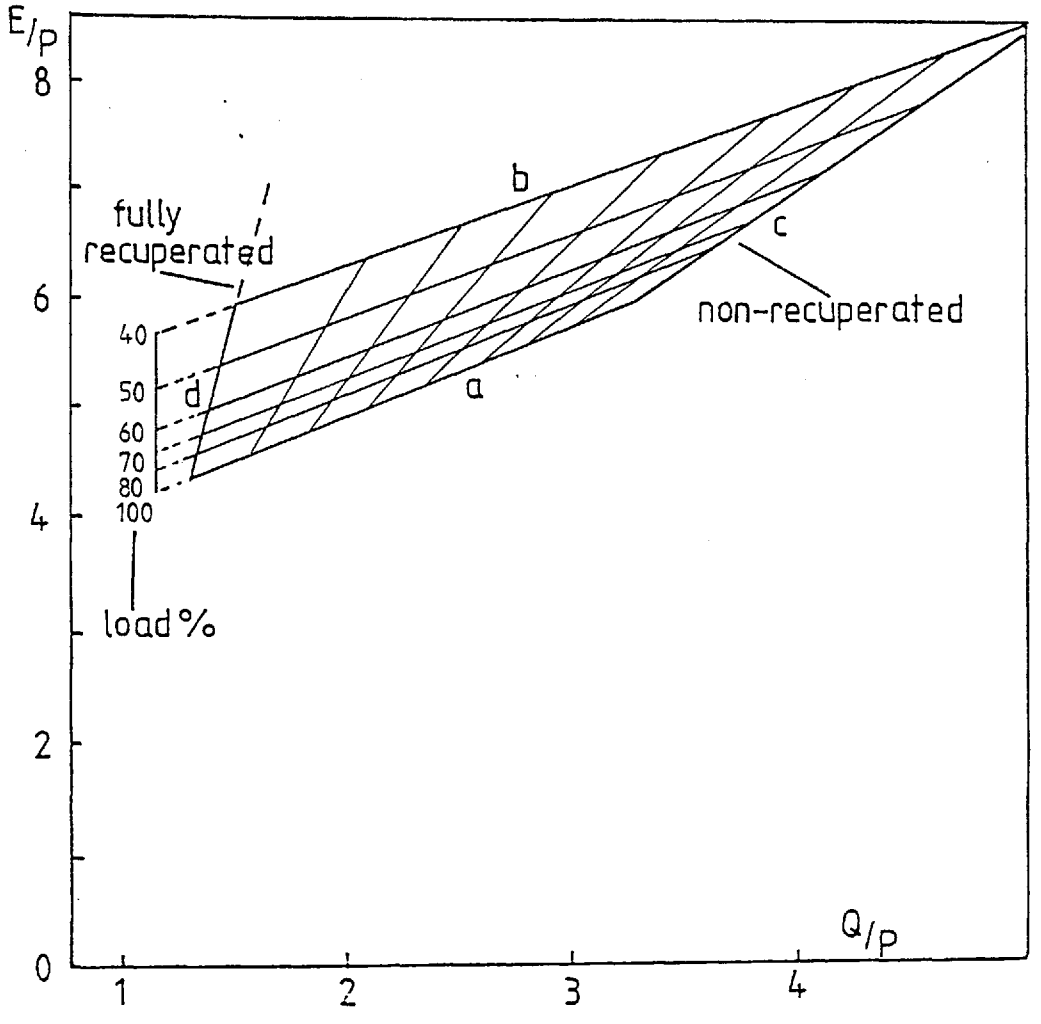

Fig. A3.4 Variable Recuperation Gas Turbine Operation Regime (Ref. 52)

c where $E/P = b_1 (Q/P) + b_2$ representing the unrecuperated characteristic.

d " $E/P = b_3 (Q/P) + b_4$ representing the fully recuperated characteristic.

Within these boundaries $E/P = a_1 (Q/P) + a_2 - a_3 (P/P_{max})^{2/3}$

Q = heat recovered from prime mover

E = energy flow in fuel input to turbine

$a_{1,2,3}$ and $b_{1,2,3,4}$ are constants for a particular turbine.

The part load operation is represented by the $(P/P_{max})^{2/3}$ factor i.e. specific fuel consumption = $A - Bp^{2/3}$, where A and B are constants. P_{max} does in fact slowly decrease (approximately linearly) with increasing recuperator thermal ratio, due to the back pressure imposed by the recuperator on the turbine.

The cost function (including the cost of meeting the site electricity demand) is given by:

(i) $$\begin{cases} z = c_f E + \begin{cases} C_{el}(K-P) & k > P \\ C_{e2}(K-P) & k \leq P \end{cases} + \begin{cases} \dfrac{C_f(H-Q)}{\eta_a} & Q \leq H \\ 0 & Q > H \end{cases} & \text{for } P>0 \\ z = c_{el}K + \dfrac{C_f H}{\eta_{aux}} & \text{for } P = 0 \end{cases}$$

where η_a = afterfiring efficiency

Permissible values of P are within the operating regime shown in fig. A3.4.

It is assumed that if afterfiring is used (if not $\eta_a = \eta_{aux}$), the balance of heat load (H-Q) may be met by afterfiring unless the turbine is turned off. This is a reasonable assumption unless required heat to power ratios are very high, as the excess oxygen level in the turbine exhaust is high, and it simplifies the analysis. The cost function for 3rd party ownership is as above but with the constant term $C_e.K$ missing; it does not therefore change the optimisation process.

Substituting the engine characteristic into (i) gives:

(ii)
$$z = C_f\left\{a_2P - a_3\left\{\frac{P}{P_{max}}\right\}^{5/3}\right\} + \left\{\begin{matrix} C_{e1}(K-P) & K>P \\ C_{e2}(K-P) & K\leq P \end{matrix}\right\} + a_1Q + \left\{\begin{matrix} C_f\left(\frac{H-Q}{\eta_a}\right) & Q\leq H \\ 0 & Q>H \end{matrix}\right\} \quad \text{for } P>0$$

$$z = C_{e1}K + \frac{C_fH}{\eta_{aux}} \quad \text{for } P = 0$$

Subject to boundaries $E/_P = b_1\left\{Q/_P\right\} + b_2$

$$E/_P = b_3\left\{Q/_P\right\} + b_4$$

and $P = 0$ or $P_{min} \leq P \leq P_{max}$

Equation (ii) has 2 useful properties:

1. $z = f_1(Q) + f_2(P)$ therefore the P and Q dependences can be treated separately.
2. $f_2(P)$ is of the form $y = A_1P - A_2P^{5/3}$ where $A_1, A_2 > 0$ hence $\frac{d^2y}{dP^2} < 0$, and any turning point within the acceptable field of P values is a maximum.

The operating regime is illustrated for axes P and Q in figure A3.5, and the cost function is shown in figure A3.6. The optimisation proceeds within the two dimensional area bounded by the Q_{max}, Q_{min}, P_{max} and P_{min} lines; there being discontinuities in the first derivative of z at Q=H and P=K.

The properties of the cost function enable it to be evaluated at a limited number of well defined, specific points in order to find the minimum. Five cases are defined depending upon the relative positions of the Q=H line, and the engine operating regime. The points for which z is evaluated for the 5 cases are as follows (see fig. A3.5 for location of some of the points):

Case 1 Evaluate at $(P_{min\,1}, Q_{max\,2})$

$(K, Q_k) \Leftrightarrow P_{min1} \leq K \leq P_{max1}$ ie. intersect of P=K and Q_{max} lines

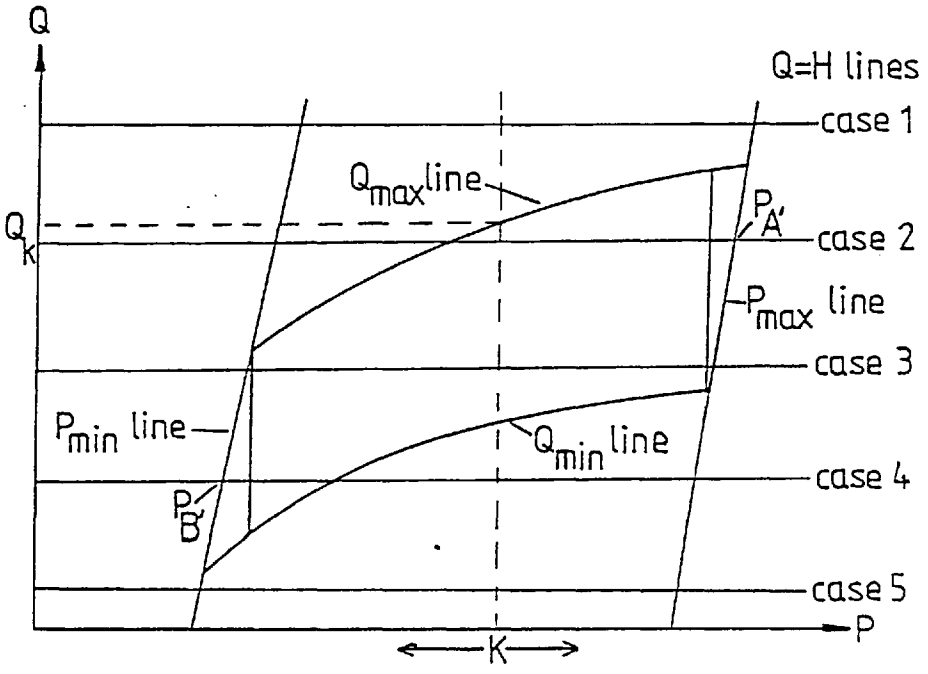

Fig. A3.5 Gas Turbine Operating Regime
:P and Q Dependance

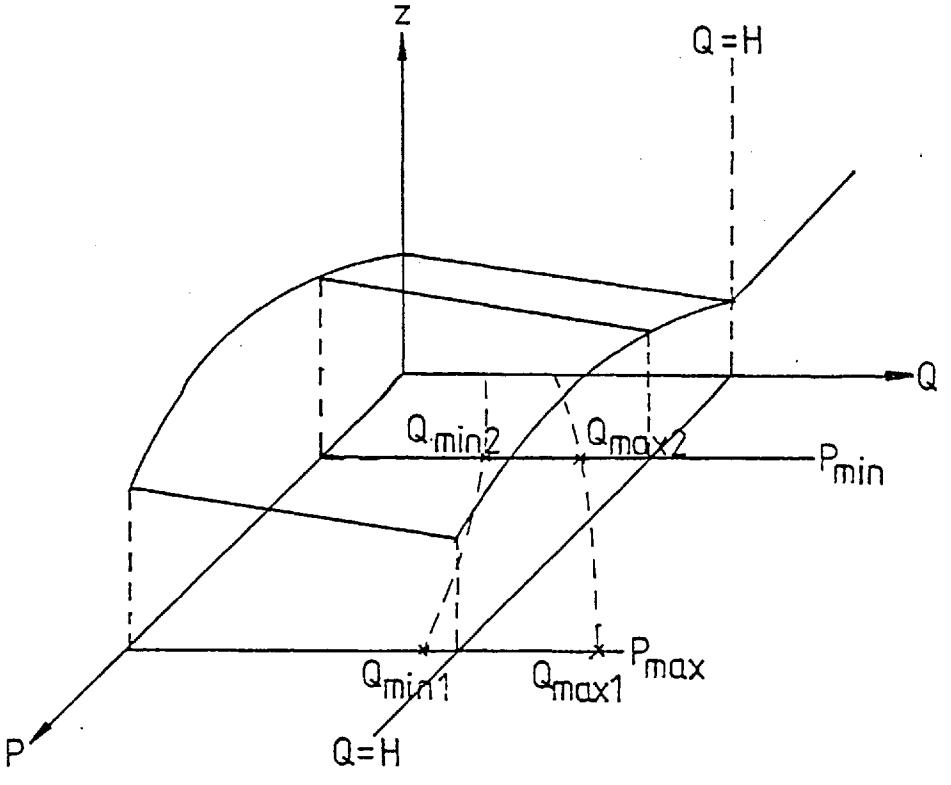

Fig. A3.6 Variable Recuperation Gas Turbine Cost Function

(P_{max1}, Q_{max1})

Case 2 Evaluate at (P_{min1}, Q_{max2})

(P_i,H) i.e. the intersect of the Q=H and Q_{max} lines

$$(P_A',H) \text{ where } P_A' = P_{max1} - \left\{ \frac{P_{max1} - P_{max2}}{Q_{max1} - Q_{min1}} \right\} (Q_{max1} - H)$$

(K,Q_k) where $Q_k = H \Leftrightarrow P_A' \geq K \geq P_i$

or Q_k = intersect P=K and Q_{max} lines $\Leftrightarrow P_{min1} \leq K < P_i$

Case 3. $$(P_B',H) \text{ where } P_B' = P_{min1} - \left\{ \frac{P_{min1} - P_{min2}}{Q_{max2} - Q_{min2}} \right\} (Q_{max2} - H)$$

$(K,H) \Leftrightarrow P_B' \leq K \leq P_A'$

(P_A',H)

Case 4. (P_B',H)

(P_i,H) ie. intersect Q=H and Q_{min} lines

(P_{max2},Q_{min1})

(K,Q_k) where $Q_k = H \Leftrightarrow P_B' \leq K \leq P_i$

Q_k = intersect P=K and Q_{min} lines $\Leftrightarrow P_i \leq K \leq P_{max2}$

Case 5. (P_{min2},Q_{min2})

$(K,Q_k) \Leftrightarrow P_{min2} \leq K \leq P_{max2}$, Q_k = intersect P=K and Q_{min} lines

(P_{max2},Q_{min1})

In addition the option of turning the turbine off by evaluating at (0,0) is included in each case.

The above method has been for one prime move in the scheme, but it can be extended with little modification to several prime movers as described below. The analysis is much simplified by the fact that for

$m \leqslant N$ identical turbines operational, the fuel cost minimum will be achieved when they all run at the same power level. The proof is as follows (it is an extended version of that given in Ref. 48):

For a desired total power output = P_R, heat output = Q_R, the constraints are $(\sum_{n=o}^{N} P_n) - P_R = 0$ and $(\sum_{n=o}^{N} Q_n) - Q_R = 0$ where P_n, Q_n = power and heat outputs of n'th turbine.

For a minimum of F_t(= total fuel cost to the turbines), by Lagrange multipliers (λ_1, λ_2)

$$\frac{\partial}{\partial P_n}\left\{ F_t - \lambda_1 \left(\sum_{n=o}^{N} P_n - P_R\right) - \lambda_2 \left(\sum_{n=o}^{N} Q_n - Q_R\right) \right\} = 0$$

and $$\frac{\partial}{\partial Q_n}\left\{ F_t - \lambda_1 \left(\sum_{n=0}^{N} P_n - P_R\right) - \lambda_2 \left(\sum_{n=o}^{N} Q_n - Q_R\right) \right\} = 0$$

Q_n is independent of P_n within the operational envelope and hence the above equations reduce to:

$$\frac{\partial F_t}{\partial P_n} - \lambda_1 = 0 \quad \text{and} \quad \frac{\partial F_t}{\partial Q_n} - \lambda_2 = 0$$

$$\Rightarrow \quad \frac{\partial F_n}{\partial P_n} = \lambda_1 \quad \text{and} \quad \frac{\partial F_n}{\partial Q_n} = \lambda_2 \qquad n = 0, 1, \ldots, N$$

Hence each turbine operates at the same load.

The discontinuity at $P=P_{min}$ means that the minima must be evaluated for m = 0,1,...,N and the minimum of these values chosen.

If N turbines of same type and size are installed, then the minimisation of the cost function is performed as for one turbine, but with H and K divided by m, the number of turbines operating, for m = 1, ...,N. For each value of m, the minimum of the cost function found is multiplied by m, before finally the minimum value of the cost function over the values of m is chosen.

This analysis, together with appropriate input and output routines, was programmed in Fortran IV. Input data includes the electricity import/export tariffs, heat and power demands, fuel cost and equipment characteristics. Maintenance periods may also be specified. Output includes totals of fuel used, traded electricity, profits and fuel savings, efficiencies, etc. In addition a subroutine is included at the end, to formulate the probability density functions of the scheme's electricity output for each hour of the typical days. Running times depend on the time period considered and the number of turbines, but are typically around 25 seconds central processing time on a CDC 6600 computer, for 1 turbine and hourly optimisations for 1 year.

The Diesel Engine Site Model

In many respects the diesel engine site model is very similar to that of the gas turbine; particularly the input and output routines. The characteristic representation and optimisation method are however somewhat different and are described below.

The characteristics of engine and afterfirer are represented by 3 quadratic equations:

$$E/_P = f_{e1}P^2 + f_{e2}P + f_{e3}$$

$$Q/_P = f_{q1}P^2 + f_{q2}P + f_{q3}$$

$$H_{et}/_P = f_{t1}P^2 + f_{t2}P + f_{t3}$$

where H_{et} = heat recovered from the fuel burnt in the engine (Q) + Heat afterfired (H_{at}). f_{ei}, f_{qi} and f_{ti} are parameters determined by the engine, heat recovery equipment and afterfiring rig.

These equations were found to be capable of giving a good fit to experimentally determined and computer simulated operating characteristics,

the form of which are shown in fig. A3.7. The limitation on after-firing is included because the potential is not as great as for gas turbines, and may have a bearing on the operating requirements experienced. The important simplification of aggregation of all heat recovery should be noted. Although on large heavy fuel oil burning engines the heat to power ratio is fairly constant over the normal operating range, the non-linear approach becomes more important for dual fuel or spark ignition engines.

The cost function (including the cost of meeting the site power demand) is:

$$z = k_m C_f E + \begin{cases} C_{e1}(K-P) & K > P \\ C_{e2}(K-P) & K \leq P \end{cases} + \begin{cases} C_f \dfrac{(H_{et} - Q)}{\eta_a} + \dfrac{C_f(H-H_{et})}{\eta_{aux}} & H > H_{et} \\ C_f \dfrac{(H - Q)}{\eta_a} & Q \leq H \leq H_{et} \\ 0 & Q > H \end{cases}$$

The symbols are as for the gas turbine, and k_m is a multiplication factor to allow for maintenance costs. Maintenance cost is included in this way, as it is higher for diesel engines than gas turbines, and is assumed approximately proportional to the fuel consumed.

Figure A3.7 shows possible site heat and power demands (H and K) in relation to engine operating regimes. In a similar way to that used for the gas turbine, 6 cases depending on the value of H can be defined. For each of these the cost function is evaluated at each point of discontinuity of $\frac{dz}{dp}$, and at the minima between these points if they exist. There are at most 9 points, from which the minimum must be found. Evaluation at P = 0 is included in each case. The extension to the case of several engines is the same as that for the gas turbine.

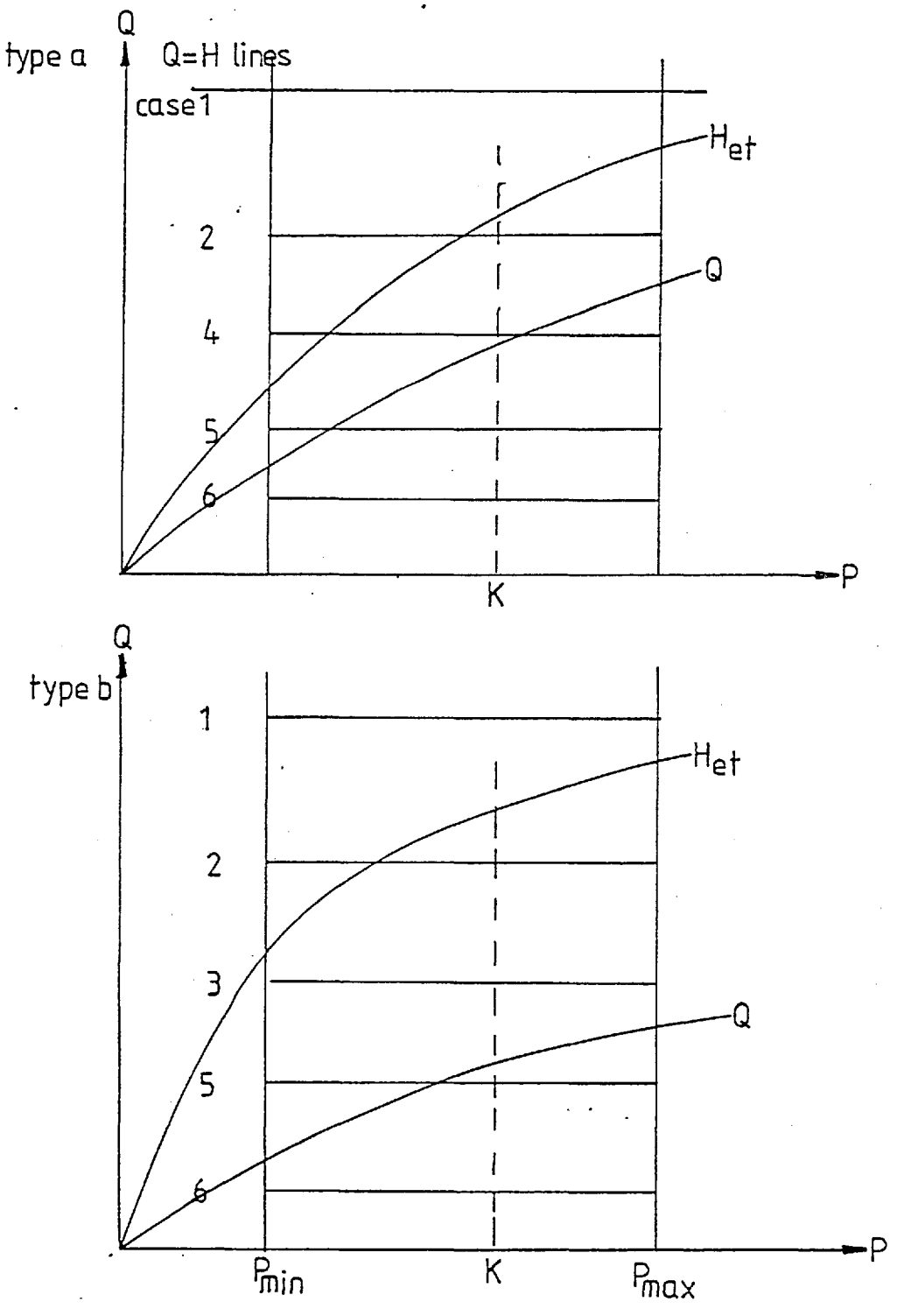

Fig. A3.7 Diesel Operating Regime

Variables local to Appendix 3

C_{e1} = Electricity import price

C_{e2} = Electricity export price

C_f = Cost of fuel

E = Energy flow to turbine/engine

H = Site heat demand

H_{at} = Heat recovered from afterfiring

H_{et} = Heat recovered from fuel burnt in engine

K = Site power demand

k_m = Multiplication factor for maintenance costs

P = Power produced by prime mover

P_{max} = Maximum power output

$P_{max1,2}$ = Points on locus of P_{max}

P_{min} = Minimum operating power output

$P_{min1,2}$ = Points on locus of P_{min}

Q = Heat recovered from Turbine/Engine

Q_K = Intersect of P=K and Q_{min} lines

Q_{max} = Maximum heat recoverable from prime mover

$Q_{max1,2}$ = Points on Q_{max} line

Q_{min} = Minimum heat recovered from operating prime mover

$Q_{min1,2}$ = Points on Q_{min} line

r = Ratio recoverable heat to power

$s_{1,2,3,4}$ = Slope

Z = Cost function

Z' = Modified cost function

η_a = Afterfiring efficiency

η_{aux} = Boiler efficiency

η_b = Brake efficiency

APPENDIX 4

THEORY OF THE SYSTEM RELIABILITY PROGRAM

The program calculates the MW/MW capacity credit of a CHP scheme, by simulating the effects of power output from the scheme on system reliability. The program was developed by A.P. Rockingham and details are not as yet released. The theory however, has been published (Refs. 71 and 72), and a brief summary will be given in this appendix. The method is presented in a stepwise manner corresponding to the sequence of calculations.

1. From a year's hour-by-hour electricity demand data, probabilistic load density functions are formed for each hour of days typical of selected time periods of the year (fig. A4.1a):

   $P_D(L_D).\Delta L_D$ = probability load (l) is in the range $L_D \leqslant l \leqslant L_D + \Delta L_D$

   From these the probabilistic load duration functions, represented as $F_D(L_D)$ (fig. A4.1b), are formed for each hour as follows:

   $$F_D(L_D) = \text{Probability load} \geqslant L_D = \int_{\infty}^{L_D} P_D(l)dl$$

2. The plant outage density function $P_{N,O}(L_o)$ represents the probability that for a system with N plants, the forced outage capacity is L_o. It is assumed constant hour-by-hour, and is formed as follows:

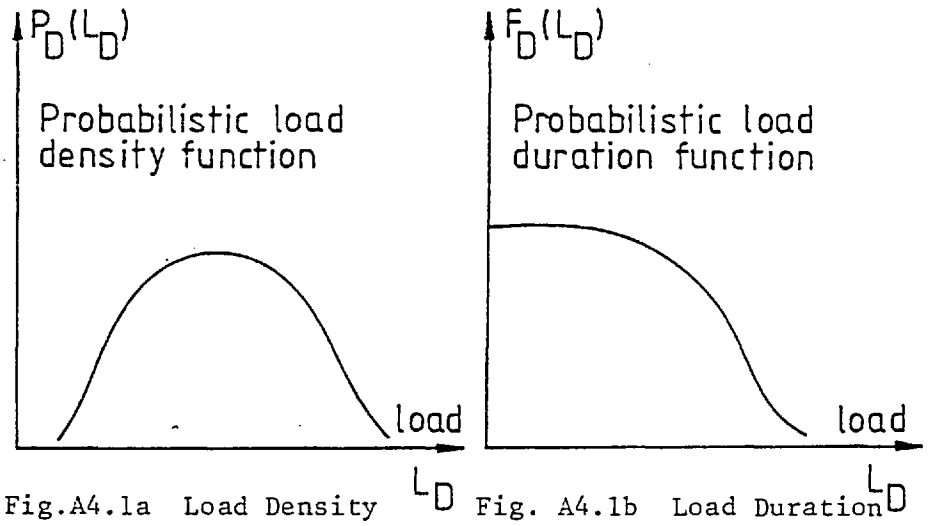

Fig.A4.1a Load Density Function

Fig. A4.1b Load Duration Function

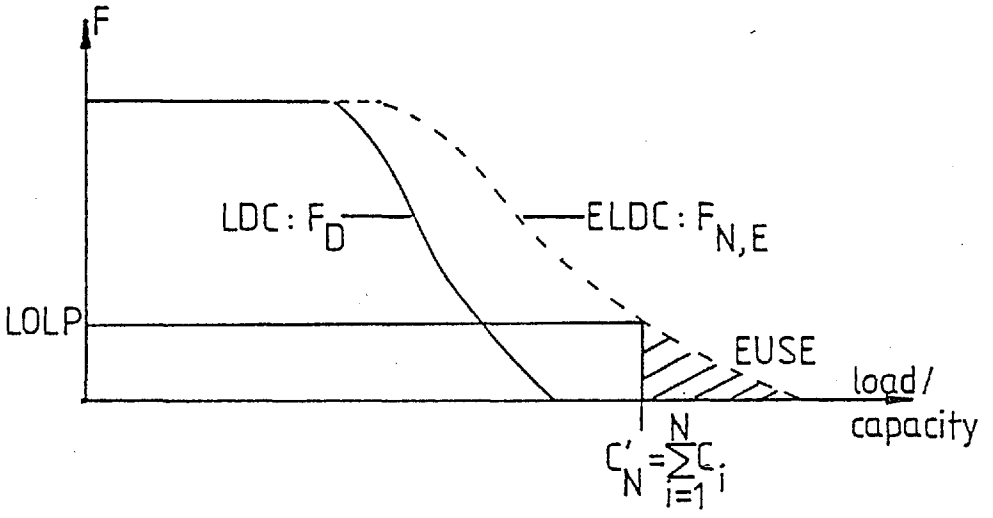

Fig. A4.2 Some System Parameters

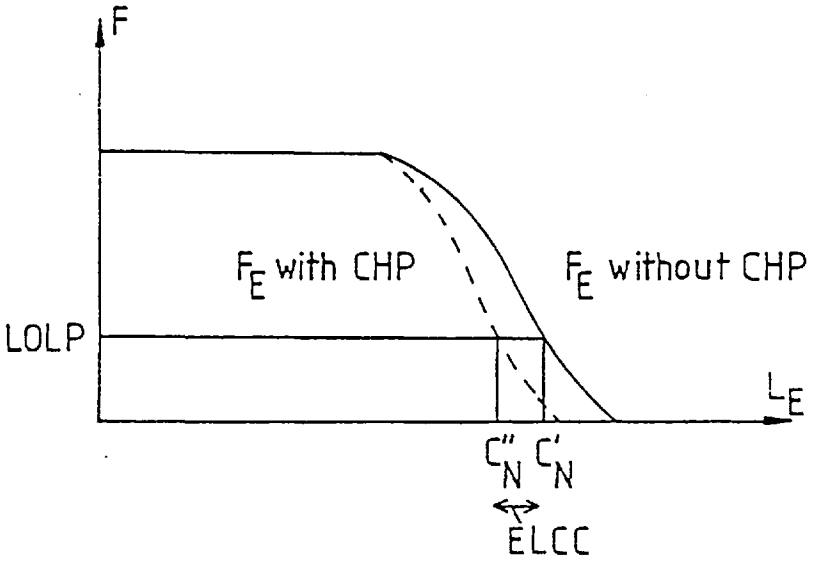

Fig. A4.3 ELCC of CHP Scheme

For a system containing N plants, these plants are committed to load according to a merit order, and are labelled i = 1,2...,N. The probability, for a system with j plants, that the plant outage l_o is in the range $L_o \leq l_o \leq L_o + \Delta L_o$, is $P_{j,o}(L_o).\Delta L_o$, and is calculated from the recursion relation (Ref.46):

$$P_{j,o}(L_o) = P_{j-1,o}(L_o).a_j + P_{j-i,o}(L_o-C_j).q_j \text{ for } L_o \geq C_j$$

$$P_{j,o}(L_o) = P_{j-1,o}(L_o).a_j \text{ for } L_o < C_j$$

where q_j = forced outage rate of plant j

a_j = availability of plant j: $a_j + q_j = 1$

C_j = capacity of plant j.

3. In order to include the effects of forced outage on the system an equivalent load (L_E) is defined: $L_E = L_D + L_o$. P_D and $P_{j,o}$ are stochastically independent and hence the equivalent load density function for a system with j plants, $P_{j,E}(L_E)$ is given by:

$$P_{j,E}(L_E) = \int_o^\infty P_D(L_E - y)\, P_{j,o}(y)dy$$ i.e. it is the convolution of P_D and P_o.

The equivalent load duration curve $F_{j,E}(L_E)$ is calculated as:

$$F_{j,E}(L_E) = \int_\infty^{L_E} P_{j,E}(y)dy$$

or can be formed directly: $$F_{j,E}(L_E) = \int_o^{L_E} F_D(L_E-y)\, P_{j,o}(y)dy$$

4. It is now possible to define some important parameters of the existing system (fig. A4.2):

(i) The probability that the system load exceeds the installed capacity (LOLP) equals $F_{N,E}(C_N')$ where

C_N' = installed capacity = $\sum_{i=1}^{N} C_i$

(ii) The expectation value of the energy unserved by the system (EUSE) is the area under the equivalent load duration curve to the right of C_N'.

Hence EUSE = $\tau \int_{C_N'}^{\infty} F_{N,E}(x)dx$, where τ = time period considered

(iii) The expected energy production of the j'th plant

$$\bar{E}_j = \tau\left\{\int_{c'_{j-1}}^{\infty} F_{j-1,E}(x)dx - \int_{c'_j}^{\infty} F_{j,E}(x)dx\right\} = a_j\tau \int_{c'_{j-1}}^{c'_j} F_{j-1,E}(x)dx$$

(iv) The expected system running cost = $\sum_{i=1}^{N} B_{fi}\bar{E}_i$ where

B_{fi} = running cost/kWh of set i

Note: no cost penalty has been assigned to EUSE.

5. Steps 1 to 4 are first performed to establish the parameters given in step 4. The analysis of the change in system operation upon the introduction of the CHP scheme's contribution, proceeds via the formation of an intermediate load duration curve, as described next.

By operating the site model on the site heat and power demands, with an import/export electricity tariff, probabilistic density functions of the CHP electricity output, P_{CHP}, are formed for each hour of the 'typical' days. The intermediate load duration curve $F_I(L_I)$ is formed for each hour by:

$$F_I(L_I) = \int_0^{L_I} F_D(L_I+y)\, P_{CHP}(y)dy \quad L_I \geq C_{CHP}$$

$$F_I(L_I) = 1 \quad L_I < C_{CHP}$$

$L_I = L_D - L_{CHP}$ where C_{CHP} = CHP capacity

L_{CHP} = CHP power output.

The hourly intermediate load duration curves are then combined to form an intermediate load duration curve for the day: the analysis then

proceeds as before with the formation of the equivalent load duration curve. The change in system expected running cost is the saving attributable to the CHP scheme. If units are traded at system expected marginal cost, the amount paid to the CHP scheme is equal to the change in system expected running cost.

The definition of the effective load carrying capability (ELCC) of the CHP scheme is illustrated in fig. A4.3. It is the change in required installed system capacity to meet a given LOLP.

i.e. ELCC = $C_N' - C_N''$ where superscripts ' and '' indicate required system capacities before and after CHP.

The MW/MW capacity credit therefore = $\frac{C_N' - C_N''}{C_{CHP}} = \frac{ELCC}{C_{CHP}}$

The ELCC may alternatively be defined as the change required to installed system capacity to maintain a given EUSE.

The program is written in FORTRAN IV. Running times are very sensitive to the complexity of the system description and the relative sizes of the CHP scheme and system. Data input must include a breakdown of plants giving capacities and availabilities, but some aggregation is usually needed to reduce running times to acceptable levels.

APPENDIX 5

SYMBOLS AND ABBREVIATIONS

Global Symbols

A_{min} = Minimum Flow Area

C_{al} = Calorific Value of Fuel

$C_{e_{ma}}$ = Average ESI marginal unit generating cost (running costs)

C_f = Cost of Fuel

C_{marg} = ESI marginal unit generating cost (running costs)

d_o = Tube outside diameter

f = fuel/air ratio

f_s = stoichiometric fuel/air ratio

FOR = Forced Outage Rate

H = Heat Demand

H_c = Fraction of Fuel Input Energy to Coolant

k_m = Multiplicative Factor for Maintenance Costs

L = Load Factor

N_u = Nusselt Number

P = Power (general)

P_a = Air Pressure

P_b = Back Pressure imposed on Turbocharger Outlet.

P_{max} = Maximum power output

Q = Heat (general)

r = Recoverable heat to power ratio

R_e = Reynolds number

R_m = Boost pressure ratio (ratio inlet manifold to ambient pressures)

R_T = Trapped air fuel ratio

s_l = Longitudinal tube spacing

s_t = Transverse tube spacing

T_e = Exhaust manifold temperature

T_o = Turbine outlet temperature

T_g = Gas temperature

T_w = Water temperature

W_a = Airflow through the engine

W_f = Rate of fuel flow to the engine

W_T = Trapped airflow

Δx = Change in x

η_a = Afterfiring Efficiency

η_{aux} = Auxiliary Boiler Efficiency

η_b = Fraction of fuel input energy to brake power

η_e = Fraction of fuel input energy recoverable as exhaust heat (usually based on a boiler exit temp. of 200^{o}C)

η_i = Fraction of fuel input energy to intercooler

γ = Operating cost per unit of electricity generated

λ = Scavenge Ratio (ratio of total mass of airflow through engine to trapped airflow)

μ = mean of a normal distribution

$\emptyset$ = Annual charge per installed kW of a generating plant

σ = standard deviation of a normal distribution.

Abbreviations

AGR	Advanced Gas Reactor
bmep	Brake Mean Effective Pressure
BST	Bulk Supply Tariff
^{o}CA	Degrees Crank Angle
CEGB	Central Electricity Generating Board
CHP	Combined Heat and Power
ELCC	Effective Load Carrying Capability
ESI	Electricity Supply Industry
EUSE	Expected Unserved Energy
evc	Exhaust Valve Closing
evo	Exhaust Valve Opening
FOR	Forced Outage Rate
HFO	Heavy Fuel Oil
IRR	Internal Rate of Return
ivc	Inlet Valve Closing
ivo	Inlet Valve Opening
LRMC	Long Run Marginal Cost
NCB	National Coal Board
NESC	Net Effective System Cost
NPW	Net Present Worth
rpm	Revolutions Per Minute
SMD	Simultaneous Maximum Demand
SRMC	Short Run Marginal Cost
tdc	Top Dead Centre
toe	Ton of Oil Equivalent

REFERENCES

1. ARNOTT, P. and GOLDSMITH, K. 'Supplying to the Total Energy Demands of Industrial Complexes'. Proceedings of the 1st International Total Energy Congress 1976.

2. BARTOLIC, R. 'Crosshead and Medium Speed Diesel Engines for Large Power Stations'. Diesel Engineers and Users Association Publication 333. Jan. 1970.

3. BENSON, R.S. and SVETNICKA, F.V. '2-stage turbocharging of diesel engines: a matching procedure and an experimental investigation'. Trans. of Society of Automotive Engineers 1974. Paper 740740.

4. BERRIE, T.W. 'Economics of System Planning' Electrical Review, 15-29th Sept. 1967.

5. BLEAY, J.A., DOBBS, I.M. and FELLS, I. 'Combined Heat and Power Schemes and the Public Supply'. Dept. of Chemical Engineering, University of Newcastle-upon-Tyne, Dec. 1978. Project funded by Science Research Council contract B/RG/75355.

6. BOOTH, R.R. 'Power Systems Simulation Model Based on Probability analysis'. I.E.E.E. Paper 71C 26-PWR-II-C Presented at P.I.C.A. Conference, Boston, May 1971.

7. BOWNS, D.E., CAVE, P.R., HARGREAVES, M.R.O. and WALLACE, F.J., 'Transient Characteristics of Turbocharged Diesel Engines'. Proc. I. Mech.E. CP15 1973.

8. BURCHNALL, J.A. 'The Supply Industry and Private Generation', Electricity Council Monograph 1976.

9. CENTRAL ELECTRICITY GENERATING BOARD 'Annual Report and Accounts 1978/79'.

10. CENTRAL ELECTRICITY GENERATING BOARD 'Bulk Supply Tariff for 1977/78'.

11. CENTRAL ELECTRICITY GENERATING BOARD 'Statistical Yearbook 1977/78'.

12. CENTRAL POLICY REVIEW STAFF 'Energy Conservation'.

13. CHESSHIRE, J. and ROBSON, M. 'Survey of the Industrial Boiler Stock in the UK: A Progress Report'. Science Policy Research Unit, University of Sussex, January 1979.

14. CONFEDERATION OF BRITISH INDUSTRY 'A Statistical Survey of Industrial Fuel and Energy Use'. CBI 1974.

15. CRAWLEY, E.F. 'The Application of the Medium Speed Diesel Engine for Generation of Electrical Power' Diesel Engineers and Users Association Publication 373, Jan. 1976.

16. CURTIL, R. and MAGNET, J.L. 'Exhaust Pipe Systems for High Pressure Charging'. Proc. I. Mech. E. 1978, Paper C50/78.

17. DEPARTMENT OF ENERGY 'Combined Heat and Electrical Power Generation in the United Kingdom'. Energy Paper 35 HMSO 1979.

18. DEPARTMENT OF ENERGY 'Digest of UK Energy Statistics 1979'.HMSO 1979.

19. DEPARTMENT OF ENERGY 'District Heating Combined with Electricity Generation in the United Kingdom'. Energy Paper 20 HMSO 1977.

20. DEPARTMENT OF ENERGY 'Energy Commission Paper Number 6: Coal and

Nuclear Power Station Costs'. Dept. of Energy, Jan. 1978.

21. DEPARTMENT OF ENERGY 'Energy Policy - A Consultative Document' HMSO 1978.

22. DIESEL AND GAS TURBINE PROGRESS WORLDWIDE. October 1978.

23. DIESEL ENGINEERS AND USERS ASSOCIATION 'Working Costs and Operational Reports 1977'.

24. DITTUS, F.W. and BOELTER, L.M.K. Univ. Calif. (Berkeley) Pub. Eng. Vol.2, p.443, 1930.

25. EBERLE, M.K. 'Anticipated Changes in the Fuel Oil Qualities for Marine Diesel Engines'. Sulzer Publication, October 1977.

26. ECE SECRETARIAT 'Combined Production of Heat and Electricity: Present Situation and Future Prospects in the Economic Commission for Europe'. Proceedings of the 1st International Total Energy Congress 1976.

27. ENERGY TECHNOLOGY SUPPORT UNIT 'Industrial Uses of Energy' ETSU publication SG(78)1, November 1978.

28. FISHENDEN, M., SAUNDERS, O.A. and SPALDING, D.B., 'Heat Transfer'. Proc. 2nd Conference on Waste Heat Recovery, Institute of Fuel, 1961.

29. FREEMAN, P.F. and WALSHAM, B.E. 'A Guide to some Analytical Turbo-charger Matching Techniques'. Proc. I. Mech. E. 1978, Paper C59/78.

30. FRENCH, C.C.J. 'Taking the Heat off the Highly Boosted Diesel Engine'. Trans. of Society of Automotive Engineers 1969. Paper 690463.

31. FROY, R.K. 'Lubricants and Fuels for Medium Speed Trunk Piston Engines'. Diesel Engineers and Users Association Publication 344. September 1971.

32. GALLOIS, J. 'Operational and Development Experience with the Pielstick Engine'. Diesel Engineers and Users Association Publication 367, 1975.

33. GHUMAN, A.S., IWAMURO, M.A. and WEBER, H.G. 'Turbocharged Diesel Engine Simulation to Predict Steady-State and Transient Performance'. American Society of Mechanical Engineers 1977. Paper 77-DGP-5.

34. GRIMISON, D. 'Correlation and Utilization of New Data on Flow Resistance and Heat Transfer for Crossflow of Gases over Tube Banks'. Trans. American Society of Mechanical Engineers Vol.59, pp.583-594, 1937.

35. GURNEY, J.D. 'Industrial Combined Heat and Power - A Case History', National Energy Managers Conference, Birmingham, Oct. 10-11, 1978.

36. HANEEF, M. 'Corrosion Tests on Materials Exposed in Flue Gases from Oil Firing'. Journal of the Institute of Fuel. June 1960.

37. HELLEMANS, J. 'European Practice on Self-Generation of Electricity (Commercial Obstacles)'. Local Energy Centres Conference, Imperial College 1977.

38. HILL, B.J. 'Fluidised Bed Combustion as Applied to the Gas Turbine Cycle'. Proceedings of the 1st International Total Energy Congress 1976.

39. HOLLER, H.G. 'The Influence of Induction and Exhaust System Design on Power Producing Characteristics of Diesel Engines'. Trans. of Society of Automotive Engineers 1970. Paper 700535.

40. HOLMAN, J.P. 'Heat Transfer', 4th Ed. McGraw-Hill, 1976.

41. HUNT, H. and BETTERIDGE, G.E. 'The Economics of Nuclear Power'. United Kingdom Atomic Energy Authority, October 1978.

42. INSTITUTION OF MECHANICAL ENGINEERS 'Computers in Internal Combustion Engine Design'. Proceedings 1967-68, Volume 182, Part 3L.

43. JAKOB, M. Contribution to Discussion. Trans. American Society of Mechanical Engineers, Vol.60, p.384, 1938.

44. JANOTA, M.S. 'Opening Address to Conference on Turbocharging and Turbochargers'. Proc. I. Mech. E. 1978, Paper C49/78.

45. JENKIN, F.P. 'Power System Planning in England and Wales' Presented at I.E.E.E. Conference, New York 1977.

46. JOY, D.S. and JENKINS, R.T. 'Probabilistic Model for Estimating the Operating Cost of an Electric Power Generating System'. Nuclear Utilities Planning Methods Symposium, Chattanooga, Tennesee Jan. 1974, ORNL DWG 71-9483.

47. KENDALL, M. 'Small Combined Heat and Power Plant in the United Kingdom'. Churchill College, Cambridge, Nov. 1977. Carried out under SRC grant GR/A/3505.1.

48. KIRCHMAYER, L.K. 'Economic Operation of Power Systems'. J. Wiley 1958.

49. LARJOLA, J. 'Further Savings Available with Afterburning' Total Energy - Combined Heat and Power Seminar, APE-Crossley Ltd., September 1978.

50. LEACH, G. et al, 'A Low Energy Strategy for the United Kingdom' Science Reviews Ltd. 1979.

51. LONNROTH, M., STEEN, P. and JOHANSSON, T.B. 'Energy in Transition'. Secretariat for Future Studies, Sweden 1977.

52. LOWDER, J.R.A. 'Aspects of Meeting Complex Industrial Energy Demand Patterns using Recuperated Gas Turbines'. Proc. Future Energy Concepts Conference, I.E.E., London 1979. pp.334-344.

53. LUCAS, N.J.D. 'An Alternative Appraisal of District Heating in Glasgow'. Applied Energy, 2, p.309.

54. LUCAS, N.J.D. 'CHP and the Fuel Industries'. Whole City Heating - Combined Heat and Power Conference, London, November 21st and 22nd, 1979.

55. LUCAS, N.J.D. 'The Case for Combined Heat and Power in the UK'. Energy Research Vol.2, pp.29-42 (1978).

56. LUCAS, N.J.D. 'The National Case for Local Production of Heat and Power in Parallel with the Public Supply of Electricity'. Applied Energy, 2, p.225.

57. LUCAS, N.J.D. and MINASS, S. 'The Prospects for a Nuclear Steam Supply Utility in the United Kingdom - a Study of Merseyside'. Proceedings of the 2nd International Total Energy Congress, Copenhagen 1979.

58. LUTON, P. and SINHA, S.K. 'Development of Analytical Aspects of Diesel Engine Design'. Proceedings of 12th International Congress on Combustion Engines. Tokyo 1977.

59. LUSTGARTEN, G. 'Latest State of Development for Medium Speed Diesel Engines'. Sulzer Technical Review 2/1977.

60. LUSTGARTEN, G. and ECKERT, B.O. 'Recent Developments and Service Experience with Sulzer Medium Speed Diesel Engines', Proceedings of 12th International Congress on Combustion Engines, Tokyo, 1977.

61. M.A.N. 'Cogeneration Plants with Diesel and Gas Engines'. MAN Publication.

62. McLELLAN and PARTNERS 'Combined Power and Space Heating in Industry'. March 1979, Dept. of Energy Pubn.

63. MERZ and McLELLAN 'Study of Combined Heat and Electricity Generation in Industry'. Available from Confederation of British Industry (1976).

64. MIRRLEES BLACKSTONE 'Heavy Fuel and the Diesel Engine', Mirrlees Blackstone Publication No. 4500/3.

65. NATIONAL ECONOMIC DEVELOPMENT OFFICE 'Energy Conservation in the United Kingdom', HMSO 1974.

66. PARMANTIER, J. 'Optimal Heat and Power Systems Planning' Presented TIMS-ORSA joint meeting New Orleans, April 30 - May 2, 1979.

67. PHILLIPS, JENKIN et al, 'A Mathematical Model for Determining Generating Plant Mix'. Power System Computation Conference, Rome 1969.

68. PIETRO, W. de. 'Experience in Service with Exhaust Gas Turbochargers of the VTR Series', Brown Boveri Review 4, 1977.

69. RAYMOND, R.J. et al, 'Cost and Application of Coal Burning Diesel Power Plants: A Preliminary Assessment', Thermo Electron Corp., Waltham, Mass., Aug. 1975.

70. RITCHIE, J.S. 'Engines other than Gas Turbines'. Proceedings of Total Energy Conference, Brighton 1971.

71. ROCKINGHAM, A.P. 'A Probabilistic Simulation Model for the Calculation of the Value of Wind Energy to Electric Utilities'.

Proceedings of British Wind Energy Association Conference, April 1979.

72. ROCKINGHAM, A.P. 'Some Aspects of Work on the Evaluation of the Worth of Renewable Energy Sources to Large Electrical Power Systems', Presented CNRS - SRC Symposium, Toulouse, July 1978.

73. RYTI, M. and MEIER, E. 'On Selecting the Method of Turbocharging 4-Stroke Diesel Engines'. Brown Boveri Review, 1969.

74. SAGER, M.A., RINGLEE, R.J. and WOOD, A.J. 'A New Generation Production Cost Program to Recognise Forced Outages' I.E.E.E. Paper T72 159-7. Presented at IEEE Winter Meeting, New York, January 30 - February 4, 1972.

75. SCHNURBEIN, E. 'Constant-Pressure Turbocharging for Medium-Speed Four-Stroke Engines' Proc. I. Mech. E. 1978, Paper C51/78.

76. SHEPHERD, G. 'Total Energy Projects'. Electrical Power Engineer, March 1979.

77. SIEDER, E.N. and TATE, C.E. 'Heat Transfer and Pressure Drop of Liquids in Tubes'. Ind. Eng. Chem. Vol.28, p.1429, 1936.

78. SIMONETTI, G. 'Laboratory Research on Turbine Blade Materials Corrosion'. Proceedings of International Congress on Combustion Engines, London 1965.

79. SITKEI, G. 'Heat Transfer and Thermal Loading in Internal Combustion Engines'. Budapest, Akademini Kiado, 1974.

80. SMIT, J.A. and WELLE, M. 'A New Concept in Waste-Heat Utilization from Slow and Medium-Speed Diesel Engines', Proceedings of the 2nd International Total Energy Congress, Copenhagen 1979.

81. SMITH, E. and AICHER, W. 'Heat-Recovery Boilers for Total Energy Systems'. Proceedings of Total Energy Conference, Brighton 1971. Institute of Fuel.

82. SOEHNGEN, E.E. 'Development of Coal Burning Diesel Engines in Germany'. Soehngen E. and Associates, Fairborn, Ohio, August 1976.

83. SUKOV, S., IGI, T., and NOZAKI, Y. 'Experience and Investigation on the Performance of a Power Plant with a Large-Size Medium Speed Diesel Engine'. Proceedings of 12th International Congress on Combustion Engines. Tokyo 1977.

84. TATCHELL, J. 'Economic Assessment of Local Generation by Industry'. Local Energy Centres Conference, July 6th and 7th 1977, Imperial College, London.

85. WALLACE, F.J. 'Performance of 2-stroke Compression Ignition Engines in Combination with Compressors and Turbines'. Proc. I. Mech. E. Vol. 177, No.2, 1963.

86. WALLACE, F.J. and CAVE, P.R. 'A General Approach to the Computer Solution of Single and 2-Stage Turbocharged Diesel Engine Matching'. Proc. I. Mech. E., Vol.187, 48/73.

87. WALLACE, F.J. and WAY, R.J.B. 'Engine Performance Analysis', M.Sc. Course Notes, School of Engineering, Univ. of Bath.

88. WATSON, N. 'Charge Cooling, the Intake and Exhaust Systems', Presented at the Fluid Dynamics Institute, Dartmouth College, New Hampshire, August 1977.

89. WATSON, N. and MARZOUK, M. 'A Non-Linear Digital Simulation of Turbocharged Diesel Engines under Transient Conditions', Trans. of Society of Automotive Engineers 1977, Paper 770123.

90. WESSELO, J.H. 'The Stork-Werkspoor TM410 Engine for Industrial Application'. Diesel Engineers and Users Association Publication 357, (1973).

91. WHITEHOUSE, N.D., STOTTER, A., GOUDIE, G.O. and PRENTICE, B.W., 'Method of Predicting Some Aspects of Performance of a Diesel Engine Using a Digital Computer'. Proc. I. Mech. E., Vol.176, No.9, (1962).

92. WILLIAMS, R.H. 'Industrial Cogeneration', Ann. Rev. Energy 1978, 3: 313-56.

93. WOLF, G., BITTERLI, A. and MARTI, A. 'Bore Cooled Combustion Chamber Components on Sulzer Diesel Engines'. Sulzer Technical Review 1/1979.

94. WOSCHNI, G. 'Electronic Calculation of the Time Curve of Pressure, Temperature and Mass Flow Rate in the Cylinder of a Diesel Engine'. Proc. I. Mech. E. 1967-68, Vol. 182, Part 3L.